TARGETING EPIGENETICS AND NRF2-PATHWAY BY DIETARY PHYTOCHEMICALS: PROMISING CANCER PREVENTION APPROACH

By

YUQING YANG

A dissertation submitted to the

School of Graduate Studies

Rutgers, The State University of New Jersey

In partial fulfillment of the requirements

For the degree of

Doctor of Philosophy

Graduate Program in Pharmaceutical Science

Written under the direction of

Ah-Ng Tony Kong

And approved by

_____

_____

_____

_____

New Brunswick, New Jersey

October 2017

ABSTRACT OF THE DISSERTATION

TARGETING EPIGENETICS AND NRF2-PATHWAY BY DIETARY PHYTOCHEMICALS: PROMISING CANCER PREVENTION APPROACH

by YUQING YANG

Dissertation Director:

Ah-Ng Tony Kong

The induction of nuclear factor (erythroid-derived 2)-like 2 (Nrf2)- antioxidant response elements (ARE)-mediated antioxidant enzymes provides a cellular defense against oxidative stress, a major drive of human diseases such as the tumor. Phytochemicals in folk medicine are widely being used as natural sources to develop novel therapeutics. Astaxanthin (AST) with potent antioxidant activity in combination with omega-3 fatty acid docosahexaenoic acid (DHA) or eicosapentaenoic acid (EPA) at low concentration showed synergistic defense against oxidative stress via Nrf2-ARE pathway. The three natural chemicals alone and in combination elevated cellular GSH level, increased total antioxidant activity, induced mRNA expression of Nrf2 and its downstream genes in human HepG2-C8

cells. In addition, AST significantly decreased the methylation of *GSTP1* promoter region and restored the expression of *GSTP1*, which is involved in detoxification and metabolism to prevent genome damage and cancer initiation. It suggests a correlation between the DNA methylation and *GSTP1* expression in human prostate LNCaP cells. AST reduced protein expression and enzyme activity of the DNA methyltransferases (DNMTs). Moreover, we demonstrated that Nrf2 shows protective role in epidermis against inflammation and extracellular matrix (ECM) damage induced by the UVB-irradiation. As compared with the wildt-ype (WT) mice, Nrf2 knockout (KO) mice showed the increased protein expression of inflammatory markers, including P53, macrophage inflammatory protein-2 (MIP-2), and pro-matrix metalloproteinase-9 (pro-MMP-9). The protective effects of Nrf2 in response to the UVB-irradiation were mediated by increased HO-1 protein expression. Moreover, we conducted genome-wide analysis of DNA methylation in UVB- and DMBA-TPA induced mouse skin tumor models to identify genes and pathways with significant changes. The top-ranked genes and pathways will provide insight into the discovery of key genes in skin tumor initiation and progression so as to provide potential preventive biomarkers. Furthermore, we demonstrated that ursolic acid (UA), and sulforaphane (SFN) reduced *in vivo* skin carcinogenesis induced by UVB-irradiation. In conclusion, dietary natural chemicals alone or in combination attenuate oxidative stress, inflammation and even carcinogenesis

through modulation of genetic and epigenetic events, and provide promising insights into cancer prevention.

PREFACE

This thesis is for the Degree of Doctor of Philosophy in Pharmaceutical Science at Rutgers, The State University of New Jersey. It serves as documentation of my research work carried out between January 2013 and October 2017 under the supervision of Dr. Ah-Ng Tony Kong in the Department of Pharmaceutics. This work is original, except where suitable references are made to previous work.

The thesis consists of seven chapters. These seven chapters contain papers that are published or intended to be submitted to a journal indexed by PubMed Central. Chapter 1 is published in *Current Topics Medicinal Chemistry* as a review article. Chapter 2 is published as a research article in *Food Chemical Toxicology*. Chapter 3 is published as a research article in *AAPS J*. Chapter 4 is published as a research article in *Cell Biosciences*. Chapter 5 is published as a research article in *Life Sciences*. Chapter 6 is intended to be submitted as part of research articles.

Chapter 1 summarized recent studies focusing on the importance of natural compound-derived epigenetic regulators targeting epigenetic readers, writers, and erasers, which provides more insights into the potential application of phytochemicals for further development of the preventive and therapeutic strategy. Chapter 2 illustrated synergistic antioxidant effects of astaxanthin with omega-3 fatty acids in the nuclear factor (erythroid-derived 2)-like 2 (Nrf2)- antioxidant response elements (ARE) pathway. Chapter 3 investigated the epigenetic modifying effects of AST on the methylation status of *GSTP1* and Nrf2 in human prostate

LNCaP cells. Chapter 4 investigated the role of Nrf2 in protecting against UVB-irradiation related to the inhibition of extracellular matrix (ECM) degradation. Chapter 5 focused on the genome-wide DNA methylation profiles of skin cancers induced by UVB-irradiation or DMBA/TPA using methylated DNA immunoprecipitation (MeDIP) followed by next-generation sequencing. Chapter 6 focuses on the effects of ursolic acid and sulforaphane on the epigenetic alterations in *in vivo* UVB-induced inflammation and carcinogenesis.

These chapters covered various aspects of the pharmaceutical effects of key dietary phytochemicals with a focus astaxanthin, sulforaphane, and ursolic acid in cancer prevention, Nrf2 activation, anti-inflammatory and pro-apoptotic effects, epigenetic modulation and future directions in cancer research.

Yuqing Yang

October 2017

ACKNOWLEDGEMENT

First of all, I would like to express my sincere gratitude to my advisor Dr. Ah-Ng Tony Kong for his kind support, encouragement and guidance. I would not be able to complete this work without his valuable guidance during the past six years.

I would also offer my sincere thanks to my committee members, Dr. Suzie Chen, Dr. Li Cai and Dr. Leonid Kagan for their guidance, critical review and valuable comments of this dissertation.

It is my great pleasure to acknowledge all the current and previous colleagues in Dr. Ah-Ng Tony Kong's laboratory, especially Dr. Constance Lay Lay Saw, Dr. Tin Oo Khor, Dr. Francisco Fuentes, Dr, Limin Shu, Dr. Zhengyuan Su, Dr. Jonghun Lee, Dr. Wenji Li, Dr. Renyi Wu, Dr. Chao Wang, Dr. Ran Yin, Dr. Linbo Gao, and Dr. Shan Su. I would like to thank my fellow students Dr. Sarandeep Boyanapalli, Dr. Ximena Paredes-Gonzalez, Dr. Ying Huang, Dr. Chengyue Zhang, Dr. Yue Guo, Dr. Mingnan Cao, Dr. David Cheng, Ms. Christina Ramirez, Mr. Doug Pung, and Ms. Irene Yang to make my greaudate study much pleasurable.

My special thanks also go to Ms. Hui Pung for her administrative efforts during the past six years of my PhD studies in the program and also, to Dr. Yaoping Lu, Dr. Yong Lin, Ms Tao Li, Ms. Sarah Peng, Ms. Anna Liu and Ms. Yue Liu for their invaluable collaboration and support. The projects described were carried out with their help and collaboration. I acknowledge the financial support from Department

of Pharmaceutics, Mario School of Pharmacy and Division of Life Sciences during the entire graduate study.

Finally, I owe my deepest gratitude to my family and friends who offered me their unconditional love, support, and understanding throughout all this time. First and foremost to my parents Xianmei and Jing Yang. Your years of love and inspiration make who I am today and assist me to be the best person I can. To my parents-in-law Yeong-Jye and I-Chieh Chen, for your continuous support through words and actions. Finally, to my husband Po-Fu, for your love, inspiration and support. I deeply appreciate the love and support from my whole family and friends in achieving this endeavor.

DICTATION

This dissertation is delicated to my family for their unconditional love and support.

TABLE OF CONTENTS

LIST OF TABLES

TABLE OF FIGURES

1 Introduction of natural compound-derived epigenetic regulators[1][2][3]

1.1 Introduction

The classical definition of epigenetics was initially proposed by Conrad Waddington as heritable changes of a phenotype without alterations in the DNA sequence [1]. Recently, epigenetic studies have been frequently applied to chromatin biology. These types of epigenetic alterations have been identified during the stages of carcinogenesis by specific patterns and characteristics [2]. Heritable epigenetic changes in gene expression are transmitted through both mitosis and meiosis without any change in the nucleotide sequence of the DNA [3]; however, this concept remains contentious. In addition, abnormal epigenetic modifications have been

[1] Part of this chapter has been published in *Current Topics in Medicinal Chemistry* as a review paper: **Yang, A. Y**., Kim, H., Li, W., & Kong, A. N. (2016). Natural compound-derived epigenetic regulators targeting epigenetic readers, writers and erasers. *Curr Top Med Chem*, 16(7), 697-713.

[2] Keywords: Epigenetics, post-translational modification, histone modifications, readers, writers, erasers.

[3] Abbreviations: AM, allyl mercaptan; AML, acute myeloid leukaemia; BA, boswellic acid; BET, bromodomain and extraterminal family of proteins; BRD, bromodomain-containing protein; BRDT, bromodomain testis-specific protein; CDDO, 2-cyano-3, 12-dioxooleana-1, 9(11)-dien-28-oic acid; DADS, Diallyl disulfide; DNMT, DNA methyltransferase; DOT1L, DOT1-like histone H3K79 methyltransferases; EZH2, enhancer of zeste homolog 2; FDA, Food and Drug Administration; FoxO1, forkhead box O1; HAT, histone acetyltransferase; GSTP1, glutathione S-transferase Pi 1; GNATs, Gcn5-related N-acetyltransferases; HDAC, histone deacetylase; HDM, histone demethylases; HMT, histone methyltransferase; KMT, lysine methyltransferase; HSP, heat shock proteins; LSD1, lysine-specific demethylase 1; MR, mineralocorticoid receptor; MBD, methyl CpG-binding domain; MeCP2, methyl CpG binding protein 2; OA, Oleanolic acid; PEITC, Phenethyl isothiocyanate; PHD, plant homeodomain; PRMTs, protein arginine methyltransferases; PTM, post-translational modification; PRC2, polycomb repressive complex 2; PDCD4, programmed cell death 4; SCFAs, short-chain fatty acids; VPA, valproic acid; SAM, S-adenosylmethionine; SAMC, S-allylmercaptocysteine; SFN, Sulforaphane; TSA, trichostatin A; TET, Ten-eleven translocation enzymes; UA, ursolic acid.

identified in various diseases, including different types of cancers. It is important to understand the epigenetic mechanisms underlying states from tumor initiation to heritability to define epigenetic transmission and understand how the misreading, miswriting and mis-erasing of chromatin contribute to oncogenesis and progression [4, 5]. In this review, we will focus on the link between oncogenesis and epigenetic aberrations. We will also discuss natural compound-derived epigenetic regulators as potentially novel pharmaceutical candidates targeting epigenetic readers, writers, and erasers with the current preclinical and clinical uses of these compounds (Figure 1.1).

1.2 Epigenetics and chromatin biology

Generally, epigenetic changes can be categorized into several major biochemical mechanisms, including changes in DNA methylation, histone tail modification and non-coding RNA functions. In this review, we will focus on DNA methylation and histone tail modification.

1.2.1 DNA methylation

DNA methylation is a heritable modification of the DNA structure that involves adding a methyl group to the carbon 5 of cytosine (5mC) within the CpG dinucleotide. Regions of CpGs undergo methylation singularly or in clusters, so-called CpG islands [6]. Gene silencing is usually due to the methylation of the promoter regions of the silenced genes [7]. The hypermethylation of the CpG islands in gene promoter regions has been commonly identified in cancer cells, resulting in

the silencing of tumor suppressor genes [8, 9]. However, the overall hypomethylation of DNA has been reported in association with tumor progression. A balance of widespread hypomethylation and regional hypermethylation may be the key to human neoplasia [10]. The methylation of DNA is regulated by DNA methyltransferase (DNMT), including DNMT1, DNMT3a, and DNMT3b. The DNMT3 family methylates the CpG dinucleotide through *de novo* pathways [11], and the DNMT1 family is reported to maintain the methylation during replication [8]. Additionally, methylated DNA can recruit members of the methyl CpG-binding domain (MBD) family, including methyl CpG-binding protein 2 (MeCP2) and MBD1 - 4 [12]. The MBD proteins can recruit histone deacetylases (HDACs), which act with DNA methylation to silence gene expression [13]. Discovery of Ten-eleven translocation (TET) enzymes helps to shed light on the mechanism of DNA demethylation. TET enzymes are dioxygenases which are dependent on 2-oxoglutarate (2OG) and Fe(II) to oxidize 5mC into 5-hydroxymethylcytosine (5hmC) [14-16].

1.2.2 Histone modifications

In addition to DNA methylation, epigenetic alterations also include histone modifications [17]. The mechanism by which epigenetic alterations are translated into meaningful biological signals is important; therefore, the identification of factors involved in creating, reading and removing epigenetic modifications has received increasing attention. For example, changes in DNA packaging, which can

result from epigenetic changes, affect gene expression directly [18]. Chromatin is the scaffold for packaging the genome, which contains heritable materials as a macromolecular complex of DNA and histone proteins. One of the primary functions of chromatin is to recruit epigenetic regulators. Chromatin modifications affect non-covalent interactions among histones or between histones and DNA. A histone octamer is composed of an H3/H4 tetramer and two H2A/H2B dimers, which are wrapped with DNA to form the nucleosome. The major histone modifications include acetylation, methylation, phosphorylation, ubiquitination, and sumoylation (addition of small ubiquitin-like modifiers) [19, 20]. In histone modification, there are various histone-modifying enzymes involved, including histone acetyltransferases (HATs), histone methyltransferases (HMTs), HDACs and histone demethylases (HDMs). These enzymes have different functions regarding the histone tails: HATs add acetyl groups; HMTs add methyl groups; HDACs remove acetyl groups; and HDMs remove methyl groups [21, 22]. Those histone modifications can either activate or repress transcription, depending on their location and type. Histone modifications play a key role in maintaining the highly folded chromatin structure, which is closely linked to gene expression [23-25].

1.2.3 microRNA

MicroRNAs (mi-RNAs or miRs) are single-stranded small RNA molecules (~19–22 nucleotides long) involved in posttranscriptional gene regulation by either inhibition of translation or mRNA degradation [26, 27]. miRNAs have created new

opportunities for the development of diagnostics, prognostics and targeted therapeutics in different cancer types including lung cancer [26], melanoma [27], prostate cancer [28] and others. These reviews have summarized recent advances and approaches for identification of candidate miRNAs and their target genes in different types of cancers. For example, increased expression of enhancer of zeste homolog 2 (EZH2), an HMT of increasing importance, was associated with melanoma progression and overall patient survival and miRNA-31 overexpression resulted in down-regulation of EZH2. Down-regulation of miR-31 expression was also a result of epigenetic silencing by DNA methylation, and via EZH2-mediated histone methylation [29]. It appears that studying how epigenetic alterations involving DNA methylation, histone modifications, and miRNA expression could provide a new opportunity for the development of diagnostics, prognostics and targeted therapeutics in different cancer types.

1.3 Epigenetic readers, writers, and erasers in the use of epigenetic modifications as therapeutic targets in cancer

Epigenetic modification is a dynamic process involving “epigenetic readers,” “epigenetic writers” and “epigenetic erasers”. In this review, we will focus on these effectors of epigenetic modification and introduce recent advances regarding their mechanisms of action, as well as their potential as chemopreventive and therapeutic targets of small molecules and natural compound-derived epigenetic regulators (Table 1.1).

1.3.1 Epigenetic readers

Epigenetic readers, also known as “chromatin readers”, possess specialized domains that recognize specific covalent modifications of the nucleosome and respond to upstream signals [30]. Mutations in chromatin reader domains abolish the chromatin-reading capacity of certain epigenetic regulators in various diseases, including cancers [31]. In addition, these epigenetic readers can identify different modified amino acids as well as the same amino acid in various states. For example, as mentioned before, lysine residues can undergo different covalent modifications, including acetylation, methylation and phosphorylation. To add more complexity, the same lysine residue can have several degrees of methylation: monomethylation, dimethylation and trimethylation. Epigenetic readers have several types of methyl-lysine-recognizing motifs, including tumor domains, chromodomains and the plant homeodomain (PHD), within proteins. Each type is in a family of proteins with varying specificities and preferred binding sites. The PHD finger is capable of detecting methylated histones. For instance, the PHD fingers of the proteins BHC80 and DNMT3L detect and bind unmethylated lysine residues [32, 33].

By contrast, if a lysine residue undergoes acetylation, it will dock to proteins with acetyl-lysine-binding residues such as bromodomains [34]. Bromodomains are highly conserved motifs that form a scaffold to facilitate DNA-templated processes. The knockout of particular bromodomain-containing proteins in mice induces embryonic lethality [35]. The bromodomain and extraterminal (BET) family of

proteins includes four members: bromodomain-containing protein 2 (BRD2), BRD3, BRD4, and bromodomain testis-specific protein (BRDT). These proteins regulate transcription and cell growth, and the dysregulation of BET proteins has been demonstrated in cancers. For example, BRD2 is overexpressed in the lymphocytes of B-cell lymphoma patients [36]. BRD3 and BRD4 have been identified as drivers of proliferation in the malignancy NUT midline carcinoma [37]. These reports suggest that BET proteins may be therapeutic targets in certain types of cancers using BET inhibitors, for example, the recently reported small molecules that specifically inhibit the BET family of proteins [37-39].

BET protein inhibitors are designed to block the interaction of the bromodomain with the acetylated residue by assembling a functional protein complex at the gene locus. The BET protein inhibitors developed to date include JQ1, I-BET151, and many others. For example, JQ1 can displace the aberrant fusion protein BRD4-NUT responsible for NUT midline carcinoma [37]. In addition, JQ1 prevents the binding of BRD4 to the upstream region of the MYC promoter region and subsequently reduces the expression of key oncogenes in myeloma cell lines [40, 41].

MBD proteins recognize methylated CpGs and bind to them to trigger methylation of H3K9, resulting in transcriptional repression [42]. Currently, the combination of 5- azacitidine and HDAC inhibitors have been used to treat hematological malignancies [43]. However, 5- azacitidine is a nonspecific demethylating agent, and it may have the potential of demethylating promoter of

silenced oncogenes and activate them to induce global hypomethylation. MBD1 appears to be a better candidate for cancer therapy. MBD1 recognizes methylated DNA and induces chromatin remodeling, regulating transcription by decoding methylated DNA. MBD protein has been reported to be involved in specific genes in different types of cancer. For instance, Imke *et al.* analyzed the involvement of MBDs and histone modifications on the regulation of CD44, Cyclin D2, GLIPR1 and PTEN in the prostate cancer cells DU145 and LNCaP, and the breast cancer cells MCF-7 [44]. Comparison of the different promoters shows that MeCP2 and MBD2a repress promoter-specific Cyclin D2 in all cell lines, whereas in MCF-7 cells MeCP2 repressed cell-specific all methylated promoters [44]. However, the underlying mechanisms remain to be elucidated. If the abnormal DNA methylation cannot be recognized with inhibition of MBD proteins, the aberrant effect of DNA methylation status would be reduced to be less meaningful. Recently, Wyhs *et al.* have developed and compared fluorescence polarization and time-resolved fluorescence resonance energy transfer based high-throughput screening assays to identify small-molecule inhibitors of MBD2 and other DNA-protein interactions [45]. This includes two known DNA intercalators, mitoxantrone and idarubicin, and two other inhibitory compounds, NF449 and aurintricarboxylic acid. They are reported to be nonspecifically inhibited the binding of a transcription factor to a methylated oligonucleotide [45].

1.3.2 Epigenetic writers

Epigenetic writers are proteins that are capable of adding modifications to DNA or histones. These proteins include DNMTs, HATs, HMTs and others. The epigenetic writers operate on the chromatin platform and introduce rapid, dynamic modifications in response to the environment.

DNMTs are actively involved in the modification of cytosines mostly in the context of CpG dinucleotides. It is a potential cancer therapeutic approach by reversing the hypermethylation of DNA promoter and gene silencing. There are two major DNA demethylating drugs, decitabine (DAC) and its analog azacitidine, as irreversible inhibitors of DNMT1 and DNMT3 [46, 47]. Efficacy of azacitidine has been applied in the treatment of higher-risk myelodysplastic syndromes (MDS) as a randomized, open-label, phase III study [48]. Transient exposure of DNA methylation inhibitors decitabine and azacitidine at a low dose decreased genome-wide DNA promoter methylation without immediate cytotoxicity such as DNA damage, apoptosis, and cell-cycle arrest [49].

HATs transfer an acetyl group from acetyl coenzyme A (acetyl-CoA) to the ε-amino group of lysine residues to form ε-N-acetyl-lysine in histones, thereby opening the chromatin. HATs are classified as type A or type B. Type A HATs are located in the nucleus and acetylate histones and chromatin-associated proteins. There are three families of enzymes, including Gcn5-related N-acetyltransferases (GNATs) and MYST (named after the four founding members, Sas3, Sas2,

and Tip60). Type B HATs (comprising only HAT1) operate in the nucleus and cytoplasm to acetylate cytoplasmic histones, facilitating the translocation of these histones to the nucleus and subsequent deposition onto DNA [50]. HATs require the presence of actyl-CoA for catalytic activity. HAT inhibitors include bisubstrate HAT inhibitors, natural product HAT inhibitors, and low-molecular-weight HAT inhibitors [51].

HMTs are classified as protein arginine methyltransferases (PRMTs) and protein lysine methyltransferases (KMTs). These enzymes transfer a methyl group from the cofactor S-adenosylmethionine (SAM) to arginine or lysine residues. The KMTs include DOT1-like histone H3K79 methyltransferase (DOT1L) containing the SET domain, a conserved catalytic domain also present in the PRMTs [52]. DOT1L is a key protein and an increasingly interesting therapeutic target in mixed-lineage leukemia (MLL)-rearranged leukemia. Daigle *et al*. reported that EPZ004777 acts as a selective inhibitor of the DOT1L H3K79 methyltransferase by imitating the cofactor SAM. EPZ004777 has anti-proliferative effects by blocking the expression of leukemogenic genes, with selectivity to kill cells bearing the MLL gene translocation [53]. However, the poor pharmacokinetic properties of this inhibitor limit its further application. Therefore, EPZ-5676, a second-generation DOT1L inhibitor, is undergoing clinical trials (ClincalTrials.gov identifier: NCT01684150) [54].

Another HMT of increasing importance is EZH2. EZH2 is the catalytic component of the polycomb repressive complex 2 (PRC2), and these factors are critically responsible for the methylation of H3K27, silencing various genes and altering biological processes [55]. This HMT is overexpressed in different types of cancers, including prostate, breast, kidney and lung cancers [56-59], which highlights the importance of developing methylation inhibitors targeting H3K27. For example, 3-deazaneplanocin A (DZNep), a molecule derived from SAM, decreases H3K27 methylation and induces apoptosis in cancer cells as an EZH2 inhibitor [60]. DZNep can reactivate silenced genes in cancer cells and selectively inhibit the trimethylation of H3K27me3 and H4K20me3 [61]. Most recently, several EZH2 inhibitors have been discovered with highly potent selectivity for EZH2 *in vivo* and *in vitro*, including EPZ-6438, GSK126 and EPZ005687 [62-64]. EPZ-6438 has already been utilized in clinical trials to treat patients with B-cell lymphoma (ClincalTrials.gov identifier: NCT01897571) and is the first EZH2 inhibitor that has been applied to solid malignant rhabdoid tumors [65].

1.3.3 Epigenetic erasers

Epigenetic erasers are proteins that are capable of removing modifications to DNA or histones that were produced by epigenetic writers to regulate gene expression. Epigenetic erasers include TET enzymes, HKMs and HDACs, targeting histones or other non-histone proteins.

TET family proteins help to uncover the mechanism of DNA demethylation, by limiting DNMT1's recognition to 5-hmc, so DNMT1 will not be able to perform the methylation of the DNA strand to maintain methylation status. The methylation is lost gradually in dividing cells in a passive manner [66]. Abnormal patterns of cytosine methylation have been observed in melanoma in association with tumor progression and downregulation of the TET family genes [67]. However, TET mutation is rare in solid tumors, and acquired mutations are missense mutations without certain consequences on TET protein in many cases [68, 69].

Histone lysine methylation (HKM) is a dynamic modification regulated by the recruitment of methyltransferases and demethylases [70, 71]. Recently, several histone demethylases were identified as being overexpressed in some human tumors. There are two well-studied families, including the lysine-specific demethylase (LSD) [72] and JmjC domain-containing lysine demethylase families [73, 74]. Members of the LSD family of proteins include the histone demethylase LSD1 (KDM1A) and the histone demethylase LSD2 (KDM1B). These proteins have oxidase-like domains, which have catalytic activities to remove the methyl group from histone lysines [75]. The LSD enzymes are highly expressed and could be valuable therapeutic biomarkers in prostate, breast and colorectal cancers [76-78]. Tranylcypromine, an enzyme monoamine oxidase (MAO) inhibitor, also inhibits LSD1 because of the similarity in the sequences of the catalytic domains of the LSD proteins and MAO enzymes [79, 80]. However, this non-selective characteristic reduces the application

of this drug due to notable potential side effects. Therefore, derivatives of tranylcypromine have been developed. For example, ORY-1001 is in clinical trials for the treatment of relapsed or refractory acute leukemia (EudraCT Number: 2013–002447-29). Other studies have investigated a weak but selective LSD1 inhibitor that has *in vitro* and *in vivo* activity [81]. The JmjC domain-containing lysine demethylase family can remove methyl groups from mono-, di- and trimethylated lysines, in contrast to the LSD demethylases [74, 82]. GSK-J1, another promising compound, is an inhibitor of the JMJD3 subfamily. GSK-J1 binds competitively to the 2-oxoglutarate cofactor and chelates the metal in the active site [83].

HDACs are enzymes that remove the acetyl group from lysine residues in histones. Histone deacetylation causes transcription repression in the chromatin. HDACs are categorized as class I (HDAC1, HDAC2, HDAC3, and HDAC8), class IIa (HDAC4, HDAC5, HDAC7, and HDAC9), class IIb (HDAC6 and HDAC10), class III (SIRT1 to SIRT7) or class IV (HDAC11). SIRT1 to SIRT7, the seven sirtuins share a conserved NAD-binding and catalytic core domain but with different N- or C-terminal extensions. They are involved in transcription regulation, metabolic regulation, cell survival and many other biological pathways [84]. SIRT1 to SIRT7 could be promising therapeutic targets to treat cancers because many sirtuin inhibitors have been reported to have anticancer activities [85]. Hu *et al*. have summarized different classes of sirtuin inhibitors based on their structural categories and mechanisms of action [85]. For example, nicotinamide inhibit SIRT1 to SIRT3,

SIRT5 and SIRT6. It has shown that nicotinamide can inhibit growth, promote apoptosis in leukemic cells and human prostate cancer cells [86-89]. Specific SIRT1 inhibitor cambinol can reduce tumorigeneisis in TH-MYCN transgenic mice by suppressing cancer cell proliferation [90].

In addition to histones, these HDACs can deacetylate non-histone proteins as well. For example, the tumor suppressor P53 protein is deacetylated by class I HDACs [91]. Recently, evidence has emerged indicating that HDAC expression has been altered in cancer cells and tumor tissues [92-94]. Therefore, HDACs are important targets for manipulating epigenetic modifications in cancer cells as a novel treatment strategy.

HDAC inhibitors bind to the catalytic site of HDACs and prevent these enzymes from binding to a substrate (histone or DNA). These HDAC inhibitors affect several biological processes, such as cell cycle arrest in the G1 stage, the inhibition of cell growth [95], cell differentiation and apoptosis [96], and HDAC inhibitor LBH589 (Panobinostat) induced sensitivity in combination with chemotherapeutic agents [97, 98].

HDAC inhibitors have been classified into four major classes based on their structures and different specificities for HDACs as follows: cyclic peptides, hydroxamates, short-chain fatty acids (SCFAs) and benzamides. For example, romidepsin (Isodax®) is a cyclic peptide that is isolated as a prodrug from *Chromobacterium violaceum*, a Gram-negative, anaerobic, non-sporing

coccobacillus. Romidepsin is an HDAC-selective inhibitor that binds to the Zn^{2+} in the active site of HDACs. Romidepsin induces cell-cycle arrest and apoptosis, and this drug was approved by the US FDA to treat refractory cutaneous T-cell lymphoma in 2009 [99, 100] and peripheral T-cell lymphoma in 2011 [101, 102]. Cyclic peptides target human cancer cell lines *in vitro* and could be precursors for developing new drugs [103]. Hydroxamic acids are another important structural group, which includes trichostatin A (TSA) and others. TSA was the first compound found to inhibit HDACs [104] and has been reported to have a wide range of anti-cancer effects [105, 106]; however, TSA has been removed from clinical trials due to side effects. In 2006, vorinostat, suberoylanilide hydroxamic acid (SAHA), was approved by the FDA to treat cutaneous T-cell lymphoma [107] as a specific inhibitor of HDAC1, HDAC2, HDAC3 and HDAC6 [108].

Very recently, the HDAC inhibitors LBH589 (Panobinostat) and PXD101 (Belinostat) received FDA approval for patients with multiple myeloma and peripheral T-cell lymphoma, respectively. On July 3, 2014, the FDA granted accelerated approval for belinostat (BELEODAQ®; Spectrum Pharmaceuticals, Inc.), an HDAC inhibitor, for patients with relapsed or refractory peripheral T-cell lymphoma [109]. Novartis has developed oral and intravenous formulations of panobinostat (Farydak®), an HDAC inhibitor, for the treatment of cancer [110].

1.4 Natural compounds alter epigenetic modifications via epigenetic readers, writers, and erasers - therapeutic targets

In this section, we will summarize and discuss certain epigenetic readers, writers, and erasers associated with cancer development and how newly discovered natural compounds and their derivatives could interact with these targets potentially resulting in cancer prevention and or treatment.

1.4.1 Phenolic compounds

There are various dietary polyphenolic phytochemicals with chemopreventive and chemotherapeutic effects due to the anti-oxidant and anti-inflammatory effects of these compounds in immune and cancer cells [111]. Based on their structures, phenolic compounds can be divided into two main classes: flavonoids and nonflavonoids. Phenolic compounds are commonly found in soybeans, spices and other sources. Currently, these natural dietary polyphenols, including curcumin and genistein, have been shown to reverse adverse epigenetic modifications that act on a chromosomal level. Phenolic compounds can reportedly reverse abnormal epigenetic modifications by regulating the activity of HDACs, HATs, HMTs, HDMs and DNMTs in cancer cells.

1.4.1.1 Curcumin

Curcumin is a well-characterized natural HAT inhibitor and a major active component from the rhizome of *Curcuma longa*. Curcumin has shown high efficacy in chemoprevention and as a chemotherapeutic in head, neck and lung cancers [112,

113]. Recently, it has been shown that curcumin decreased the expression of DNMTs and HDAC subtypes (HDAC4, 5, 6, and 8) and upregulated deleted in lung and esophageal cancer 1 (DLEC1), a tumor suppressor gene, in HT29 cells [114]. In leukemia cells, curcumin downregulated HDAC6, a class IIb deacetylase, as well as heat shock proteins (HSPs), and resulting in cell cycle arrest and apoptosis [115]. In addition, treatment with derivatives of the curcumin-like curcumin analog C66 attenuated diabetes-related increases in histone acetylation, HAT activity, and p300/CBP HAT expression [116]. In addition, treatment with derivatives of the curcumin-like curcumin analog C66 attenuated diabetes-related increases in histone acetylation, HAT activity, and p300/CBP HAT expression [116]. Treatment of curcumin significantly inhibited the HAT activity human hepatoma Hep3B cells, but not HDACs, contributing to the histone hypoacetylation [117].

1.4.1.2 EGCG

Epigallocatechin-3-gallate (EGCG) is one of the well-studied green tea polyphenols with many health beneficial biological effects including cancer chemoprevention and chemotherapy in prostate cancers [118], gastroenterological cancers [119] and others. Green tea polyphenols can activate p53 by inhibiting class I HDACs, resulting in acetylated Lys373 and Lys382 residues and inducing cell cycle arrest and apoptosis in LNCaP human prostate cancer cells [120, 121]. In addition, among these green tea polyphenols, EGCG has been identified as an inhibitor of HAT, whereas other polyphenol derivatives have lower HAT inhibitory

effects, including catechin, epicatechin, and epigallocatechin [122]. EGCG is with more specificity for HATs but less specificity for other epigenetic writers, including HMTs; the inhibition of HAT by EGCG reduced NF-κB activity and decreased the binding of p300 to the IL-6 promoter, subsequently suppressing pro-inflammatory response [122]. EGCG treatment decreased global DNA methylation levels, and HDAC activity in human skin cancer A431 cells with reactivation of silenced tumor suppressor genes, Cip1/p21 and p16INK4a [123]. The combination of EGCG with the HDAC inhibitor, TSA, showed a synergistic effect of reactivation of ERα expression in ERα-negative breast cancer cells. EGCG is reported to remodel the chromatin structure of the ERα promoter leading to ERα reactivation [124]. The combination of EGCG with cisplatin significantly inhibited proliferation, and induced cell cycle arrest in G1 phase in non-small-cell lung cancer A549/DDP cells. They are reported to inhibit DNMT activity and HDAC activity, reversal of hypermethylated status and downregulated expression of GAS1, TIMP4, ICAM1 and WISP2 genes [125]. Very recently, EGCG is reported to reverse the expression of various tumor-suppressor genes (TSGs) by inhibiting DNMTs and HDACs in human cervical cancer cells [126].

In addition, EGCG has impacts on Bmi-1 and enhancer of zeste homolog 2 (Ezh2), two key PcG proteins as epigenetic regulators of chromatin. It is reported that EGCG reduced Bmi-1 and Ezh2 level in SCC-13 cells. Also, a global reduction in histone H3 lysine 27 trimethylation was reported to be associated with a reduction in

survival [127]. EGCG with or without 3-deazaneplanocin A (DZNep) co-treatment in skin cancer cells reduce the level of PcG proteins including Ezh2, Bmi-1, and others. In addition, HDAC1 is also reduced, associated with increased tumor suppressor expression and reduced cell survival rates [128]. In a most recent report, green tea polyphenols (GTP) and EGCG induced TIMP-3 mRNA and protein levels by epigenetic silencing mechanism(s) involving increased EZH2 activity and class I HDACs in breast cancer cells [129]. In skin cancer cells, Bmi-1 is observed with increased expression contributing to skin cancer cells survival. EGCG treatment suppressed skin cancer cells survival [130].

1.4.1.3 Genistein

Genistein is a phytoestrogen derived from soybeans and other sources. This compound has been reported to play a major role in the post-translational modification of histones. In LNCaP human prostate cancer cells, genistein inhibited HDAC6, a heat shock protein Hsp90 deacetylase, which in turn decreased the level of the androgen receptor (AR) by regulating the ability of the HDAC6-Hsp chaperone to stabilize the AR protein [131].

Quercetin is a dietary polyphenol derived primarily from buckwheat and citrus. Quercetin inhibited HAT activity and subsequently reduced the recruitment of cofactors to the chromatin associated with pro-inflammatory genes in epithelial cells [132]. In addition, quercetin inhibited the expression of the epigenetic markers

HDAC-1 and DNMT1 to induce cell cycle arrest and apoptosis, thereby blocking invasion and angiogenesis [133].

1.4.1.4 Resveratrol

Resveratrol is a polyphenol derived from plants such as blueberries, cranberries, and grapes. Resveratrol has exhibited anti-inflammatory and other effects via the regulation of pathways such as the cell cycle, apoptosis, angiogenesis and tumor metastases [134]. Recent studies show that resveratrol can downregulate metastasis-associated protein 1 (MTA1), which inactivates PTEN in prostate cancer cells. In addition, resveratrol could also activate the nicotinamide adenine dinucleotide (NAD+)-dependent deacetylase SIRT1 as one of the key features. Resveratrol activates sirtuins, as the class III HDAC. It's reported that resveratrol could induce cell cycle arrest in the G1 phase and it inhibits gastric cancer in an SIRT1-dependent manner [135]. *In silico* docking models were used to study resveratrol's interaction with different types of HDACs [136]. *In vitro* analyses of solid tumor cell lines showed that resveratrol inhibited all eleven human HDACs of class I, II and IV in a dose-dependent manner. Resveratrol promotes acetylation and reactivation of PTEN via inhibition of the MTA1/HDAC complex, resulting in inhibition of cell survival pathway such as the Akt pathway [137].

1.4.2 Organosulfur compounds

Organosulfur compounds are organic compounds that contain a variety of sulfur functional groups, such as C-S double and triple bonds, thioethers, disulfides, polysulfides, sulfonic acids, esters, amides, sulfuranes and persulfuranes [138]. Many organosulfur compounds have been investigated for roles in epigenetic regulation. For example, sulforaphane (SFN) has been widely proven to be involved in global DNA demethylation, HDAC inhibition, and mi-RNA modulation [139-142]; phenethyl isothiocyanate (PEITC) inhibits both HDAC and CpG methylation in various genes [143-145]; and diallyl disulfide (DADS) enhances histone acetylation by inhibiting HDAC [146, 147].

1.4.2.1 SFN

SFN is an organosulfur compound containing an isothiocyanate group and can be found in many cruciferous vegetables. SFN has proapoptotic and antiproliferative properties [148]. Its diverse biological effects also include anticancer effects, cell cycle arrest, and the induction of heme oxygenase and phase-2 detoxifying enzyme [149]. SFN mediates its anticancer effects primarily via epigenetic mechanisms [149], which may include the inhibition of HDAC, which increases global and local histone acetylation [150, 151], the induction of demethylation [139] and the modulation of miRNA [142].

When tested in human embryonic kidney 293 cells, SFN was found to inhibit HDAC activity, increase histone acetylation, and increase the number of acetylated

histones bound to the P21 promoter, thus increasing p21 (Cip1/Waf1) expression [152]. SFN has been demonstrated to prevent the TPA-induced neoplastic transformation of mouse epidermal JB6 (JB6 P+) cells by inhibiting the activity of HDACs, especially HDAC1, HDAC2, HDAC3 and HDAC4 [140]. In a clinical study, after the consumption of 68 g of broccoli sprouts containing approximately 105 mg of SFN, HDAC activity was significantly decreased in the peripheral blood mononuclear cells of all three subjects [153].

SFN has demonstrated DNMT-inhibiting effects. Meeran *et al.* first reported that SFN inhibits DNMT1 and DNMT3A in MCF-7 and MDA-MB-231 human breast cancer cells [154]. SFN was found to regulate the MSTN signaling pathway in porcine satellite cells by significantly inhibiting HDAC activity and DNMT1 expression [155]. SFN was observed to inhibit proliferation in MCF-7 and MDA-MB-231 breast cancer cells and to downregulate DNMT1 by 0.75-fold, DNMT3A by 0.0185-fold, and DNMT3B by 1.174-fold [156].

Recent studies have revealed the role of SFN in modulating miRNA. SFN was found to inhibit DCIS stem cell signaling by increasing exosomal miR-140 and decreasing exosomal miR-21 and miR-29 [142]. By inducing miR-200c, SFN inhibits the epithelial-mesenchymal-transition and metastasis [157]. In a Chip-Seq assay, SFN was found to reduce miR-29B-1 expression [158].

1.4.2.2 PEITC

Similar to SFN, PEITC contains an isothiocyanate functional group and is widely found in a variety of cruciferous vegetables. PEITC exhibits the dual functions of HDAC inhibition and CpG demethylation in various genes [143-145].

Generally, PEITC acts as an HDAC inhibitor. In the LNCaP cell line, PEITC upregulated p21 gene expression by significantly enhancing histone acetylation via the inhibition of HDAC activity and by inducing histone methylation modifications, resulting in chromatin remodeling [159]. Wang LG *et al*. also found that PEITC increases histone acetylation in LNCaP cells by decreasing the activity of HDACs, especially HDAC1 [160].

Moreover, PEITC demethylates the promoter and restores the expression of glutathione S-transferase Pi 1 (GSTP1) in both androgen-dependent and androgen-independent LNCaP cancer cells [160]. PEITC has also been demonstrated to have hypomethylation potential *in vivo*. In TRAMP mice that were given an oral dose of 15 μmol of PEITC daily for 13 weeks, prostate tumorigenesis was significantly retarded due to the demethylation of the MGMT promoter [145].

1.4.2.3 DADS

DADS, a dietary disulfide, is found at high concentrations in garlic. DADS have been shown to enhance histone acetylation [146, 147]. Bioinformatics research suggests that both DADS and SFN have structural features compatible with HDAC inhibition [161].

After metabolic conversion, DADS is gradually converted to its main active metabolites, S-allylmercaptocysteine (SAMC) and allyl mercaptan (AM) [162, 163]. DADS and SAMC were found to induce the differentiation of erythroleukemic cells by enhancing histone acetylation [164]. *In vitro*, AM was a more potent inhibitor of HDAC than the precursor compounds DADS and SAMC, leading to the hyperacetylation of H3 and H4, enhancement of the association of ac-H3 with the p21 promoter and upregulation of p21 [165]. DADS treatment can induce transient histone hyperacetylation, p21 induction and apoptosis in various types of cancer cells [166]. In Caco-2 and HT-29 cells, 200 μM DADS was found to significantly inhibit HDAC activity, inducing histone hyperacetylation and increasing $p21^{waf1/cip1}$ expression [167]. In *in vivo* experiments, the injection of DADS (200 mg/kg b.w.) into male rats was reported to result in increased histone acetylation in normal hepatocytes and colonocytes [168].

1.4.3 Triterpenoids

Triterpenoids, which are synthesized by the cyclization of squalene, are metabolites of isopentenyl pyrophosphate [169]. At least 20,000 triterpenoids exist in nature. To date, many natural fruits and medicinal plants such as apples, ballon flower, bearberry, blueberries, boswellia, cranberries, figs, ginseng, holy basil, lavender, mango, onions, olives, reishi, and rosemary, among others, have been found to be rich natural sources of triterpenoids [170]. Increasing evidence demonstrates that triterpenoids are involved in a variety of biological activities, with

anti-proliferative, pro-apoptotic, anti-oxidative, anti-inflammatory, anti-allergic, anti-microbial, anti-viral, anti-pruritic, anti-angiogenic, anti-invasive, and anti-tumor properties [170-172]. Nonetheless, it is not well understood whether triterpenoids act on epigenetic regulators and/or how triterpenoids interact with epigenetic regulators to exert their biological functions. We herein summarize some studies that illustrate the potential of triterpenoids to produce epigenetic alterations that protect against a variety of human diseases, including cancer.

1.4.3.1 Oleanolic acid

Oleanolic acid (OA, 3β-hydroxyolean-12-en-28-oic acid) is a pentacyclic triterpenoid that can be obtained from approximately 1,600 different plants [173]. Of note, OA is used as the backbone for a new synthetic oleanane triterpenoid, 2-cyano-3, 12-dioxooleana-1, 9(11)-dien-28-oic acid (CDDO) and its derivatives, such as CDDO-methyl ester (CDDO-Me) and CDDO-imidazole (CDDO-Im) [173, 174]. OA is a typical triterpenoid that exerts protective effects on the liver, heart, and stomach and functions as an anti-viral, anti-oxidative, anti-inflammatory, and anti-cancer agent [174, 175]. A very recent report revealed that miR-122 is a potential target in cancer prevention [176]; miR-122 has anti-tumor activity, and its promoter is hypermethylated in liver cancer cells [177, 178]. OA treatment enhanced miR-122 expression, thereby suppressing the growth of lung cancer cells and lung cancer xenografts in mice. OA displays anti-diabetic activity by reducing hyperglycemia [179]. Zhou and his colleagues determined the hypoglycemic

mechanisms of OA in a mouse model of type 2 diabetes [180]. The administration of OA to diabetic mice increased phosphorylation and acetylation at lysines 259, 262, and 271 in Forkhead box O1 (FoxO1). These modifications of FoxO1 were accompanied by an increase of HAT1 and the inhibitory phosphorylation of HDAC4 and HDAC5. Notably, the effect of OA lasted up to 4 weeks after suspending OA treatment.

1.4.3.2 Ursolic acid

As an isomer of OA, ursolic acid (UA; 3b-hydroxy-12-urs-12-en-28-oic acid), is present in a variety of fruits and medicinal herbs, including apple peels, cranberry, bearberry, lavender, peppermint leaves, and holy basil [181]. UA has been used only as an emulsifying agent in pharmaceutics, cosmetics, and food and thus has not historically attracted much attention; however, robust studies have been performed since the discovery that UA protects against inflammation from carrageen-induced paw edema [182]. To date, UA has been found to be useful in treating various pathological conditions, including oxidative stress, DNA damage, hyperlipidemia, and inflammation [181-183]. UA is one of the triterpenoids exhibiting anti-cancer activity through diverse signaling pathways, such as the apoptotic pathway [184]. In a study identifying the effect of UA on human acute myeloid leukemia HL-60 cells, the cytotoxicity of UA was attributed to increased acetylation of histones H3, H3K18, and H3K9 and decreased expression of HDAC 1, 3, 4, 5, and 6 [185]. In human glioma cells, UA induced apoptosis by decreasing levels of miR-21, which is

regulated by DNA methylation [186, 187]. The reduction in miR-21 activated a cell death pathway via caspase-3 and programmed cell death 4 (PDCD4).

1.4.3.3 CDDO and its derivatives

CDDO is a synthetic oleanane triterpenoid (SO) and the most potent triterpenoid with activity in the nanomolar and/or picomolar range. CDDC was developed by the chemical modification of three sites in OA, the C-28 carboxyl group, the C-12-C-13 double bond, and the C-3 hydroxy group [188]. Moreover, additional changes at the C17 of CDDO have yielded several types of derivatives, such as a methyl ester (CDDO-Me), imidazolides (CDDO-Im), amides (methyl amide, CDDO-MA; ethyl amide, CDDO-EA; trifluoroethyl amide, CDDO-TFEA), and a dinitrile (di-CDDO) [188, 189]. In addition to the use of SOs for treating cancer, a growing list of *in vitro* and *in vivo* data demonstrate that they are involved in a broad spectrum of biological mechanisms, including differentiation, proliferation, growth arrest, apoptosis, and inflammation [190]. After SOs were first synthesized in the late 90s [191], the role of SO in epigenetic modulation was quickly discovered. Treatment of acute promyelocytic leukemia ATRA-sensitive NB4 and resistant MR2 cells with CDDO and all-trans-retinoic acid (ATRA) increased H3-Lys9 acetylation in the RARβ2 promoter. This histone acetylation induced expression of the peroxisome proliferator-activated receptor-γ (PPARγ), resulting in enhanced apoptosis and differentiation [192]. CDDO-Me has stronger anti-cancer potency than CDDO [193]. An investigation demonstrated that CDDO-Me inhibits proliferation and induces

apoptosis in human pancreatic cancer cells by downregulating hTERT expression, which was mediated through a decrease in DNMT1 and DNMT3a, the demethylation of CpGs in the hTERT promoter, and a reduction in acetylated H3-Lys9, acetylated H4, dimethyl-H3-Lys4, and trimethyl-H3-Lys9 at the hTERT promoter [194].

1.4.3.4 Boswellic acid

Boswellic acid (BA), the most abundant exudate from the gum resin of *Boswellia serrate*, has been used in India to treat inflammatory disorders such as arthritis and inflammatory bowel disease because of its potent anti-oxidative capacity [195, 196]. Based on these positive effects, clinical trials have been conducted using BA to treat Crohn's disease, chronic colitis, ulcerative colitis, and brain tumors [197]. BA consists of four components, β-boswellic acid (β-BA), acetyl-β-boswellic acid (ABA), 11-keto-boswellic acid (KBA), and 11-keto-β-acetyl-11-keto-β-boswellic acid (AKBA) [198]. KBA and AKBA are among the main compounds responsible for the pharmacologic effects of BA. AKBA has been found to have anti-tumor effects in several forms of cancers in the brain, bone marrow, colon, liver, pancreas, and prostate [199, 200]. The mechanism for AKBA's cytotoxicity to cancer cells seems in part to be epigenetic modulation. Human colorectal cancer SW48 cells that have undergone AKBA-induced growth inhibition and apoptosis exhibit a loss of methylation in a large number of CpG sites [201]. In addition, AKBA treatment caused two tumor suppressor genes, SAMD14 and SMPD3, to be demethylated and

DNMT activities to decrease in SW48 and SW480 cells. The same group also demonstrated that AKBA increased let-7b, let-7i, miR-200b, and miR-200c in human colorectal cells and nude mice transplanted with HCT116 cells, leading to the inhibition of cell growth, proliferation, and migration, as well as the induction of apoptosis in colorectal cancer [202].

1.4.4 Ginsenosides

Ginseng (Panax ginseng C.A. Meyer) is a very common medicinal herb and food supplement in Asia, particularly in China, Japan, and South Korea, and is even currently used in Western countries [203, 204]. Ginseng has long been used to maintain physical health and combat aging and is the main ingredient in traditional medicine. Ginsenosides are triterpenoid saponins, the primary active components of ginseng [205]. Diverse structural modifications classify ginsenosides into three groups: i) the oleanolic acid group (Ro); ii) the 20(S)-protopanaxadiol group (e.g., Ra, Rb, Rc, Rd, Rg3, Rh2 and Rs); and iii) the 20(S)-protopanaxatriol group (e.g., Re, Rf, Rg1, Rg2 and Rh1) (G-6, 7). Each ginsenoside plays a unique role in human disease. As part of a chemopreventive and anti-cancer regimen, ginsenosides have many advantages, including fewer side effects, low rates of recurrence, and a reduction in cancer-related symptoms [206]. As a result, such regimens increase the cure rate in cancer patients.

Rh2 is a member of the 20(S)-protopanaxatriol group of ginsenosides. The treatment of human non-small cell lung cancer A549 cells with Rh2 upregulated 44

miRNAs, including let7 and miR-196, and downregulated 24 miRNAs, such as miR-193 [207]. Because let-7, miR-196, and miR-193 are miRNAs regulated by epigenetic mechanisms, these results suggest that Rh2 may modulate epigenetic alterations in lung cancer cells. Indeed, Rh2 increased HDAC4 expression in human liver carcinoma HepG2 cells [206]. The increased HDAC4 caused the repression of AP-1 and MMP3 expression, leading to reduced survival and migration. Rg2 may affect the epigenetic regulation of genes, as seen from a study of brain tumors. Human glioma cells treated with Rg2 displayed growth inhibition and apoptosis through increased miR-128 expression [208]. The repression of miR-128 induces upregulation of Bim-1, which is highly expressed in cancer cells [209].

Unlike Rh2, the relevance of Rg1 to epigenetic pathways has been confirmed through its effects on angiogenesis. Rg1 is another bioactive member of the 20(S)-protopanaxatriol ginsenosides. In human umbilical vein endothelial cells (HUVECs), Rg1 repressed the expression of miR-214, accelerating eNOS expression and angiogenesis [210]; however, miR-214 is a negative regulator of EZH2, which is elevated in cancers [211]. Lately, it has been proposed that miR-15b inhibits 5-hydroxymethylcytosine (5hmc) by decreasing TET3 [212]. The levels of 5hmc are low [213, 214] during tumor progression but are high in low-grade brain tumors and liver cancer patients with high survival rates and low recurrence rates [215, 216]. Notably, Rg1 downregulated miR-15b, which is involved in angiogenesis in HUVECs [217].

Compound K, a metabolite of 20(S)-protopanaxadiol ginsenosides, impaired the RUNX3 re-expression-induced growth of human colorectal cancer HT-29 cells through the demethylation of RUNX3 promoter, which is known to be hypermethylated in colon cancer cells and patients. The decrease in RUNX3 methylation was associated with the decreased expression and activity of DNMT1. In addition, an IC50 concentration of Compound K acetylated the RUNX3 promoter with diminished HDAC1 expression and HDAC activity, and increased the acetylation of histones H3 and H4, which arrested the cell cycle at the G0/G1 phase [218].

Two stereoisomers of Rg3, 20(S)-Rg3 and 20(R)-Rg3, are members of the protopanaxadiol group [219]. Recently, it was found that Rg3 acts as an HDAC3 inhibitor in melanoma cells [220]. The treatment of human melanoma A375 and C8161 cells with Rg3 produced cell cycle arrest at the G0/G1 phase through decreased HDAC3 expression and increased acetylation of p53 on Lysine-373 and Lysine-382. These epigenetic events led to a reduction in PRB, cyclin E, cyclin D1, CDK2, and CDK4 and the induction of p21 expression. In these studies, Rg3 administration to nude mice inoculated with A375 cells conferred lower expression levels of HDAC3 and higher levels of acetylation of p53 (Lys-373/Lys-382), which resulted in reduced xenograft tumor volume and tumor weight.

1.4.5 Other phytochemicals and their derivatives

1.4.5.1 3, 3'-Diindolylmethane

3, 3'-Diindolylmethane (DIM) is a byproduct of the digestion of indole-3-carbinol (I3C), which is found in cruciferous vegetables, including broccoli, cabbage, kale and Brussels sprouts. DIM acts as an anticancer agent by inducing cell cycle arrest and apoptosis and is undergoing clinical trials [221]. DIM can selectively inhibit class I HDACs by inducing their proteasome-mediated degradation, revealing the potential of DIM as a chemoprevention agent [222]. Both DIM and I3C counteract the effects of enterotoxin B (SEB)-induced activation of T cells in mice as inhibitors of class I HDACs, but not class II HDACs [223]. Notably, DIM, but not I3C, specifically decreases HDAC2 activity in LNCaP and PC-3 prostate cancer cells [224]. Recently, the effects of DIM and SFN on genome-wide promoter methylation have been tested in normal prostate epithelial cells and prostate cancer cells, and the results indicated that DIM reversed abnormal methylation in cancer-associated genes [225]. All of these investigations suggest that DIM can exert cancer preventive and even therapeutic effects via the reversal of abnormal epigenetic alterations.

1.4.5.2 Valproic acid

SCFAs are produced from the fermentation of dietary fiber in the colon [226]. SCFAs can be categorized based on the number of lipids and include butyric and valeric acid. Valproic acid (VPA) was first synthesized in 1882 by Burton as an

analog of valeric acid. VPA has been shown to be an HDAC inhibitor in several clinical studies when used in combination with all-trans retinoic acid to treat acute myeloid leukemia (AML) patients with intensive chemotherapy [227]. VPA has been reported to show anti-leukemic effects in combination with other demethylating agents such as decitabine and 5-azacitidine (5-AZA) [228]. In addition, VPA is in phase III clinical trial as an HDAC inhibitor in solid tumors [229]. Those trials illustrate the emerging importance of targeting epigenetic erasers in the classical standard combination chemotherapy [229]. Recently, VPA has been shown to attenuate cardiac hypertrophy and fibrosis by inhibiting HDACs to acetylate the mineralocorticoid receptor (MR) in spontaneously hypertensive rats [230]. Amide derivatives of valproate are being considered as potential follow-up compounds, including valproyl glycinamide, 3-methylbutanamide or isovaleramide and SPD421 (DP-valproate) [231, 232].

1.4.5.3 Anacardic acid

Anacardic acid, a bioactive phytochemical found in the shell of nuts from *Anacardium occidentale*, is a non-competitive inhibitor of p300, PCAF, and Tip60 [233]. Anacardic acid is structurally related to salicylic acid. Anacardic acid still has limited applications, similar to most natural compounds, because of its low cell permeability [234]. In contrast to anacardic acid, garcinol is a highly permeable but non-specific HAT inhibitor that is extracted from the rinds of the *Garcinia indica* fruit

[235]. This non-specific nature of garcinol increases toxicity; therefore, more specific, less toxic HAT inhibitors, LTK14 and LTK15, were derived from garcinol [236].

1.5 Conclusions and perspectives

Individual phenotypes appear to be a complex record of interactions with the environment, that is, lifelong exposure to stimuli and the consequential reactions of the genome and epigenome. Recently, understanding how epigenetic mechanisms record environmental changes within individuals and contribute to the development of various types of diseases including cancers has gained increasing importance. These studies enhance our understanding and ability to manipulate the epigenome, especially to reverse abnormal epigenetic modifications and restore normal biological function.

Natural compounds in the diet or herbal medicinal phytochemicals are promising epigenome modifiers targeting epigenetic readers, writers and erasers resulting in diseases prevention including cancer chemoprevention or chemotherapeutic treatment. In addition to these characteristics as epigenetic regulators, natural compounds are generally characterized by low toxicity and easy access in daily life. All these advantages have placed bioactive natural compounds as important health beneficial and potential diseases prevention agents including cancer chemoprevention. Our current review provides a brief insight into some selected dietary phytochemicals on their potential epigenetic targets. A summary of these alterations is provided in Table 1.1, which includes accumulating evidence of

dietary chemopreventive compounds' role in preventing and reversing these abnormal epigenetic modifications in cell culture or animal model systems. Understanding the potential differences in different cell types and organs will be crucial in designing future personalized dietary strategy in diseases prevention including cancer. Furthermore, a combination of some of these selective epigenetic regulators with more targeted epigenetic drugs could potentially yield synergistic effects in cancer prevention and therapy. For instance, butyrate, an HDAC inhibitor, in combination with a dietary vitamin A derivative, is used in the treatment of acute promyelocytic leukemias [237]. Some epigenetic drugs are currently used in combination with cancer chemotherapeutic agents in reversing transcriptional resistance mechanisms in cancers [238]. In addition, although miRNA and long non-coding RNA are not the focus of this review, they have been important targets of many natural dietary compounds, including polyphenols [239].

In conclusion, it is important to fully understand the biological functions and detailed mechanisms of action of chromatin proteins. Further exploration of natural compounds alone or in combination is promising to move forward to evidence-based clinical trials using them as modifiers targeting epigenetic readers, writers and erasers resulting in cancer chemoprevention or even chemotherapeutic treatment.

1.6 Figures and Tables

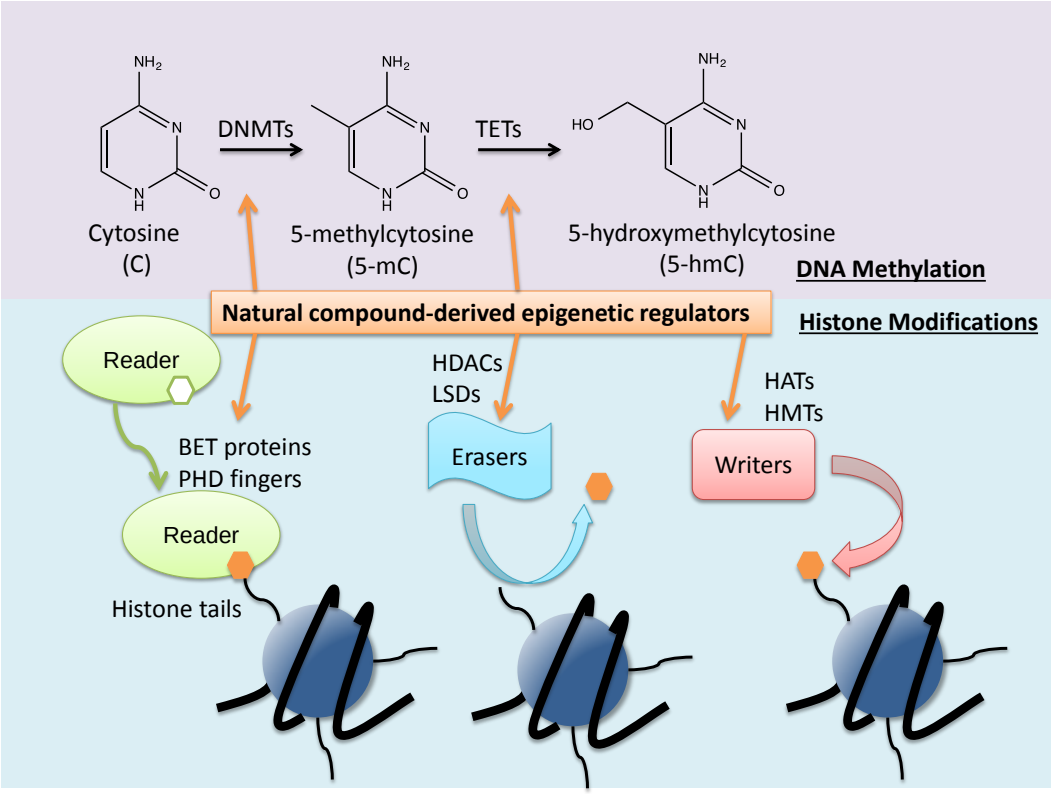

Figure 1.1 Natural compound-derived epigenetic regulators targeting epigenetic readers, writers and erasers

Table 1.1. Natural dietary compounds and derivatives with targets at epigenetic writers, readers, and erasers in cancers.

Compound	Epigenetic targets	Phase	Cancer types	Reference
Curcumin	Decrease expression of DNMTs, HDACs	Preclinical	Colon, leukemia, head, neck and lung	[112-116]
EGCG	Decrease expression of class I HDACs and HATs; decrease EZH2 protein level; decrease DNMT activity	Preclinical	Prostate, skin, breast and cervical cancers	[121, 123-127]
Genistein	Decrease expression HDAC6	Preclinical	Prostate	[131]
Quercetin	Decrease expression of HDAC1 and DNMT1; decrease HAT activity	Preclinical	Prostate	[132, 133]
Resveratrol	Inhibit the MTA1/HDAC complex	Preclinical	Prostate	[134, 137]
Sulforaphane	Decrease HDACs and DNMTs activity	Preclinical	Breast and skin	[140, 153-156]
Phenethyl isothiocyanate	Decrease HDACs and CpG methylation	Preclinical	Prostate, colon,	[143-145, 162-168]
Oleanolic acid	Increase HAT1 activity; decrease phosphorylation of HDAC4 and HDAC5	Preclinical	*type 2 Diabetes*	[180]
Ursolic acid	Decrease expression of HDAC 1, 3, 4, 5, and 6	Preclinical	human acute myeloid leukemia	[185]
Boswellic acid	Loss of methylation in lots of CpG sites; decrease DNMTs activities	Preclinical	human colorectal cancer	[201, 202]
Ginsenosides Rh2	Rh2 increased HDAC4 expression	Preclinical	human liver carcinoma HepG2 cells	[206]
Ginsenosides Rg1	Rg1 repressed expression of miR-214 and miR-214 is a negative regulator of EZH2	Preclinical	human umbilical vein endothelial cells	[210, 211]
Compound K	Decrease HDAC1 and DNMT1 activities	Preclinical	human colorectal cancer cells	[218, 230]
3,3’-Diindolyl methane	Decrease HDACs activities	Preclinical	Prostate cancers cells	[222]
Valproic acid	Decrease HDACs activities	Phase III clinical trial	solid tumors	[229]
Anacardic acid	Inhibit p300, PCAF, and Tip60	Preclinical	Breast	[233]
Garcinol	Decrease HAT activities	Preclinical	Hepatocellular carcinoma	[240]
LTK14, LTK 15	Decrease HAT activities	Preclinical		[236]

2 Astaxanthin and omega-3 fatty acids individually and in combination protect against oxidative stress via the Nrf2–ARE pathway[4][5][6]

2.1 Introduction

Oxidative stress is involved in the pathogenesis of many diseases, including cancer. The biochemical processes involved in the chemoprotective effects of agents against oxidative stress have not been completely discovered; however, part of the beneficial action results from the induction of phase II detoxifying/antioxidant enzymes [241, 242]. These enzymes detoxify many harmful substances by converting them into hydrophilic metabolites that are readily excreted. Phase II detoxifying/antioxidant enzymes, such as glutathione S-transferase (GST), heme oxygenase-1 (HO-1), and NAD(P)H dehydrogenase, quinone 1 (NQO1), are highly inducible in animals and humans [243], and there is a strong inverse relationship between their tissue levels and the susceptibility of tissue to chemical-induced carcinogenesis [241, 244]. The coordinated induction of phase II

[4] Part of this chapter has been published as an original research paper: Saw, C. L. [1], **Yang, A. Y.** [1], Guo, Y., & Kong, A. N. (2013). Astaxanthin and omega-3 fatty acids individually and in combination protect against oxidative stress via the Nrf2-ARE pathway. *Food Chem Toxicol*, 62, 869-875. ([1] These authors contributed equally in this publication.)

[5] Keywords: astaxanthin, docosahexaenoic acid, eicosapentaenoic acid, oxidative stress, antioxidant response element, nuclear factor (erythroid-derived 2)-like 2

[6] Abbreviations: ARE, antioxidant response element; AST, astaxanthin; CI, combination index; DHA, docosahexaenoic acid; DPPH, 2, 2-diphenyl-1-picrylhydrazyl; DMSO, dimethyl sulfoxide; EPA, eicosapentaenoic acid; FBS, fetal bovine serum; GSH, glutathione; GSTM2, glutathione S-transferase M2; HO-1, heme oxygenase-1; NQO1, NAD(P)H: quinone oxydoreductase 1; Nrf2, nuclear factor (erythroid-derived 2)-like 2; OD, optical density; PUFAs, polyunsaturated fatty acids; qRT-PCR, quantitative reverse-transcriptase polymerase chain reaction; RSA, radical scavenging activity; SFN, sulforaphane

detoxifying/antioxidant enzymes is mediated by *cis*-regulatory DNA sequences located in promoter and enhancer regions known as antioxidant response elements (AREs). The ARE transcription factor nuclear factor (erythroid-derived 2)-like 2 (Nrf2) plays a central role in the induction of detoxifying/antioxidant genes [241].

Astaxanthin (AST; Figure 2.1), a red dietary carotenoid, is found in microalgae, such as *Haematococcus pluvialis* and *Chlorella zofingiensis* [245], and aquatic animals. AST possesses various pharmacological activities, including antioxidative activity [245-248], antitumor effects [249-251], hepatoprotective effects [252], and antidiabetic [253] and anti-inflammatory properties [254]; the antioxidant properties of AST could explain its health-promoting activities. AST has beneficial effects both *in vivo* and *in vitro*, suggesting its potential use in the prevention of various diseases, including cancer [255] and Parkinson's disease [256]. Thus far, few studies have specifically investigated the role of Nrf2 in mediating the antioxidant effects of AST, excluding recent reports on cyclophosphamide-induced oxidative stress in rats [257] and K562 human immortalized myelogenous leukemia cells [258] and on MPP+-induced oxidative stress in PC12 cells [256]. Recently, the beneficial effects of AST in improving oxidative stress biomarker levels in overweight and obese adults have been reported [259]. Interestingly, it has also been recently reported that an AST-related compound, fucoxanthin, was more effective at attenuating weight gain in mice in combination with fish oil than as a single agent [260]. Moreover, the combinations of AST or fucoxanthin with docosahexaenoic acid (DHA) or

eicosapentaenoic acid (EPA), two active components in fish oil, are sold over the counter as dietary supplements. It has been reported that AST in combination with fish oil enhances the immune response by improving the glutathione-based redox balance in rat plasma and neutrophils [261]. However, whether synergism occurs between AST and DHA or EPA (Figure 2.1) and the involvement of the Nrf2/ARE pathway in this potential synergism have not been confirmed. Therefore, it is of scientific interest and clinical significance to examine the antioxidant effects of AST alone and in combination with DHA or EPA.

DHA and EPA are omega-3 polyunsaturated fatty acids (PUFAs); they are important nutritional essentials found in fish oil. They possess benefits in terms of cardiovascular protection [262, 263] and anti-inflammatory effects [264, 265]. They have potential as potent anti-inflammatory agents because they decrease the production of inflammatory eicosanoids, cytokines, and reactive oxygen species [266]. The benefits of PUFAs have been demonstrated in clinical trials in patients with advanced lung cancer [267] and colorectal cancer [268]. Our group previously reported that Nrf2 plays a role in the anti-inflammatory activities of DHA and EPA by comparing Nrf2-knockout and wild-type macrophages [265]. The inhibition of lipopolysaccharide-induced cyclooxygenase 2, inducible nitric oxide synthase, interleukin 1-beta, interleukin 6, and tumor necrosis factor alpha was attenuated in Nrf2-knockout macrophages compared with the inhibition in Nrf2 wild-type macrophages. Potential crosstalk between Nrf2 and anti-inflammatory pathways has

been reported [241, 269, 270]. Taken together, these studies suggest a possible link between the Nrf2 signaling pathway and the activity of AST, DHA, and EPA. Therefore, we hypothesized that the induction of Nrf2 involves the activation of the ARE transcription system. We also hypothesized that AST would synergize with DHA and EPA. In this study, we demonstrated the synergistic antioxidant effects of AST, DHA, and EPA at low concentrations. The Nrf2/ARE pathway was involved in the antioxidant effects induced by AST, DHA, and EPA in HepG2-C8 cells that stably expressed an ARE-luciferase reporter gene [271]. These findings provide valuable information for the development of novel therapeutics with beneficial antioxidant activities.

2.2 Materials and Methods

2.2.1 Chemicals

AST was obtained from Santa Cruz Biotechnology, Inc. (catalog no. sc-202473, Lot #C1810; Santa Cruz, CA, USA). *cis*-4,7,10,13,16,19-Docosahexaenoic acid (DHA, catalog no. D2534, ≥98%), *cis*-5,8,11,14,17-eicosapentaenoic acid (EPA, catalog no. E2011, ≥99%), and 2′,1,1-diphenyl-2-picrylhydrazyl radical (DPPH, catalog no. D913-2) were purchased from Sigma-Aldrich (St. Louis, MO, USA). Quercetin was used as the standard in the DPPH scavenging assay (catalog no. 152003; MP Biomedicals Inc., Solon, OH, USA). Sulforaphane (SFN, catalog no. S8044) was purchased from LKT Laboratories, Inc. (St. Paul, MN, USA).

2.2.2 Cell culture

The HepG2 immortalized human hepatoma cell line was purchased from American Type Culture Collection and transfected with pARE-TI-luciferase (provided by Dr. William Fahl, University of Wisconsin) using FuGENE 6 [272]. Twenty-four hours after the transfection, the cells were incubated in fresh medium containing 0.8 mg/mL G418. Clonal cells were selected for growth in the presence of G418 by limiting dilution, and the induction of the ARE-reporter gene by SFN was confirmed [273, 274]. The selected cell line, HepG2-C8, was used in our studies. HepG2-C8 cells were maintained in Dulbecco's Modified Eagle's Medium supplemented with 10% fetal bovine serum (FBS) and antibiotics (10 U/mL penicillin G and 100 μg/mL streptomycin) at 37°C in a humidified 5% CO_2/95% air incubator. To treat the cells, AST, DHA, and EPA were prepared in medium supplemented with 1% FBS.

2.2.3 Free radical scavenging activity (RSA): The DPPH method

The DPPH RSAs of AST, EPA, and DHA were determined according to the method reported by Chan et al. [275] with certain modifications to perform the assay in a microplate. Different concentrations of the three compounds (5–200 μM) were prepared in a 96-well plate. The samples were mixed with 5 μL of a 2 mM methanolic DPPH solution and adjusted to a final volume of 200 μL with methanol. Methanol was used for the baseline correction. The control was 50 μM methanolic DPPH solution. The absorbance was measured at 517 nm at different time points,

including 5, 10, 15, 20, 30, 40, 50 and 60 min. Changes in the optical density (OD) of the samples were measured, and these changes indicated the percent inhibition of DPPH radical formation. The results were expressed as a percentage using the following equation 2:

$$\% \text{ RSA} = [(\text{Control OD} - \text{Sample OD})/\text{control OD}] \times 100 \quad (2)$$

where sample OD is the absorbance of the solution containing AST, DHA, or EPA and the control OD is the absorbance of the control DPPH solution. The background absorbance of methanol was subtracted from the absorbance of both the control and the sample ODs. A minimum of three independent experiments was performed. As the standard in the DPPH scavenging assay, quercetin was tested at the same concentrations as AST, DHA, and EPA.

2.2.4 Cell viability test MTS assay

The cell viability assay was based on the ability of cells to convert a tetrazolium compound (MTS) into a colored formazan product. The bioconversion is presumably accomplished by NADPH or NADH, which is produced by dehydrogenase enzymes in metabolically active cells. The cells were seeded in 96-well plates overnight at the density of 1×10^4 cells/well in 100 µL of medium containing 1% FBS and allowed to adhere to the plates. CellTiter 96® AQueous One Solution (20 µL; Promega, Madison, WI, USA) was added to the cells 24 h after the cells were treated with the test compounds (3.13–100 µM). The negative control cells were treated with 0.1% dimethyl sulfoxide (DMSO). The 96-well plate was

incubated for 3 h at 37°C in a humidified 5% CO_2 atmosphere. The absorbance was monitored at 490 nm using a spectrophotometer (μQuant Biomolecular Spectrophotometer, Bio-Tek Instruments Inc., Winooski, VT, USA). The cell viability was calculated as a percentage based on the following equation: (absorbance in treated sample/absorbance in control) × 100%.

2.2.5 Intracellular glutathione (GSH) measurement

HepG2-C8 cells were seeded in a 96-well plate at a density of 1×10^4 cells/well in 100 μL of medium containing 1% FBS and allowed to adhere to the plate overnight. The cells were treated with various concentrations of AST, DHA, or EPA alone or with the combination of 12.5 μM AST and 12.5 μM DHA or EPA for 24 h. The intracellular GSH concentration was measured using a Glutathione Assay Kit (Oxford Biomedical Research, Inc., Oxford, MI, USA). All of the procedures were performed according to the manufacturer's instructions with modifications for the use of a 96-well plate.

2.2.6 Total antioxidant power colorimetric assay

HepG2-C8 cells were seeded in 12-well plates at a density of 1×10^5 cells/well in 1 mL of medium containing 1% FBS overnight. The cells were treated with different concentrations of AST, DHA, or EPA alone or with the combination of 12.5 μM AST and 12.5 μM DHA or EPA for 24 h. The antioxidant capacity was measured using the Colorimetric Assay for Total Antioxidant Power Kit (Oxford Biomedical

Research, Inc.). All of the procedures were performed according to the manufacturer's instructions with modifications for the use of a 96-well plate.

2.2.7 Luciferase reporter activity assay

HepG2-C8 cells were plated in 12-well plates at a density of 1×10^5 cells/well in 1 mL of medium containing 1% FBS overnight. The cells were treated with the test agents individually or in combination following the same treatment procedures described for the MTS assay. The luciferase activity was determined according to the manufacturer's protocol (Promega). After treatment, the cells were washed once with ice-cold phosphate-buffered saline and then harvested in reporter lysis buffer. The homogenates were centrifuged at 13,400 × g for 1 min at 4°C. A 10-µL aliquot of supernatant was used to measure the luciferase activity using a Berthold luminometer (Berthold Detection System GmbH, Pforzheim, Germany). The luciferase activity was normalized to the protein concentration and expressed as the fold induction relative to 0.1% DMSO.

2.2.8 Investigating the synergistic effects of AST and DHA or EPA using the combination index (CI)

Investigating the synergism between AST and DHA or EPA involved plotting the dose responses for AST, DHA, and EPA individually and for the different drug combinations. Combination drug effect analysis based on the Loewe additivity model, which was first introduced by Chou et al. [276], was used to examine the

drug-drug interactions. The CI, which characterizes the drug-drug interaction, is defined in Equation 1 as follows:

Equation 1

$$CI = \frac{d_1}{D_{x,1}} + \frac{d_2}{D_{x,2}} \qquad (1)$$

where d_1 and d_2 represent the concentrations of drug 1 (AST) and drug 2 (DHA or EPA), respectively, in the combination treatment that produce an effect x, whereas $D_{x,1}$ and $D_{x,2}$ represent the concentrations of drug 1 (AST) and drug 2 (EPA or DHA), respectively, which produce the same effect x when administered individually. When the CI is equal to, less than, or greater than 1, the combination is additive, synergistic, or antagonistic, respectively. The Loewe additivity model is one of the best general reference models for evaluating potential drug interactions [277]; therefore, we used it in previous studies of chemopreventive compounds, including DHA and EPA, and successfully identified various combinations that exhibited synergism [264, 278].

2.2.9 RNA isolation and quantitative reverse-transcriptase polymerase chain reaction (qRT-PCR)

HepG2-C8 cells were treated with particular concentrations of the test compounds alone or in combination. The cells were treated with AST, DHA, or EPA alone at concentrations of 3.13, 6.25, and 12.5 µM as well as with the combination of 12.5 µM AST and 12.5 µM DHA or EPA. After 6 h, total RNA was extracted using an RNeasy Micro Kit (Qiagen, Valencia, CA, USA). RNA concentrations

were determined using a NanoDrop 2000 (Thermo Scientific, Rockford, IL, USA). For each sample, 2 mg of total RNA was reverse-transcribed to single-stranded cDNA using TaqMan1 Reverse Transcription reagents (catalog no. N808-0234, Applied Biosystems Inc., Foster City, CA, USA). qRT-PCR was performed on the cDNA aliquots using SYBR Green PCR Master Mix (catalog no. 4309155, Applied Biosystems Inc.) to quantitatively detect the gene expression of Nrf2, HO-1, NQO1, GSTm2, and glyceraldehyde 3-phosphate dehydrogenase (the internal standard) on an Applied Biosystems 7900HT Fast Real-Time PCR System (Applied Biosystems Inc.). The primer pairs were designed using the Primer Quest Oligo Design and Analysis Tool (Integrated DNA Technologies Inc., Coralville, IA, USA), and the sequences have been previously reported [278]. All of the assays were subjected to melt curve analysis to confirm the presence of a single PCR product.

2.2.10 Data presentation and statistical analysis

At least three independent experiments were performed for each analysis. The results are presented as the mean ± standard error of the mean (SEM) for each group, unless otherwise specified. The differences between the controls and the treated groups were evaluated using Student's t-test.

2.3 Results

2.3.1 Free RSA using the DPPH Method

Figure 2.2 depicts the dose-response (Figure 2.2A) and temporal-response (Figure 2.2B) curves for the free RSAs of AST, DHA, EPA and the standard

quercetin. The results are expressed as a percentage of the ratio of the decrease in absorbance at 517 nm to the absorbance of DPPH at 517 nm. Typically, at equal concentrations, all compounds had greater RSA at 60 min than at 30 min, and excluding quercetin concentrations exceeding 5 μM, there was a linear increase in the RSA from 30 to 60 min (Figure 2.2A & B). At 160 μM, AST exhibited greater than 75% RSA for the stable DPPH free radical at 60 min (Figure 2.2B). Under the same conditions, DHA and EPA displayed 23 and 46% activity, respectively. The RSA of AST was superior to those of DHA and EPA at equal concentrations; the scavenging effect of AST at 60 min ranged from 30 to 75% at a concentration of 5–200 μM (Figure 2.2B). However, quercetin was the best DHHP scavenger; at the lowest tested concentration of 5 μM, quercetin effectively scavenged 70–80% of the DHHP at 30 and 60 min.

2.3.2 Non-toxic effects of AST, DHA, and EPA in HepG2-C8 cells

To determine the effects of AST, DHA, and EPA alone and the combination of 12.5 μM AST and 12.5 μM DHA or EPA on cell viability, HepG2-C8 cells were plated in 96-well plates overnight and treated with the compounds. Figure 2.3 presents the percent cell viability after 24 h of drug treatment. AST was relatively non-toxic at a concentration of 100 μM compared with the toxicity of DHA and EPA. The cell viability in the presence of DHA or EPA decreased with increasing compound concentrations, resulting in 55.3 (DHA) and 56.0% (EPA) cell death at 100 μM. Excluding the highest concentration of DHA or EPA (100 μM), all other

concentrations were non-toxic compared with the toxicity of 0.1% DMSO. Therefore, non-toxic concentrations of AST, DHA, and EPA were selected for further studies to determine the chemopreventive antioxidant properties of each compound.

2.3.3 Antioxidant capacity based on the GSH and total antioxidant power assays

To test our hypothesis that there is synergism between AST and DHA or EPA, cells were treated with 12.5 μM AST in combination with 12.5 μM DHA or EPA, and the GSH and total antioxidant power assay results were compared with those obtained from single-compound treatments.

Non-toxic concentrations of each compound were utilized to determine cellular GSH levels (Figure 2.4). The GSH levels in HepG2-C8 cells treated with AST at non-toxic concentrations exhibited a dose response from 3.13 to 100 μM. DHA at 50 μM induced a 170% increase in the GSH concentration compared with the effects of 0.1% DMSO. EPA at 50 μM resulted in a 1.42-fold increase in the GSH concentration compared with the effects of 0.1% DMSO. These data clearly indicated that AST significantly increased the cellular GSH levels compared with DHA or EPA. The combination treatments did not have stronger effects on the GSH concentration than 12.5 μM AST alone; however, the combinations were superior to 12.5 μM DHA or EPA alone.

It has been hypothesized that the concentrations of drugs used in combinations affect synergism and that drugs are more likely to display synergism at lower

concentrations. Therefore, low concentrations of AST, EPA, and DHA (3.13, 6.25, and 12.5 μM) and the combination of 12.5 μM AST and 12.5 μM DHA or EPA were tested in the total antioxidant power assay. The total antioxidant capacity of the combination of 12.5 μM AST and DHA or EPA was not significantly different from that of 12.5 μM AST, DHA, or EPA alone (Figure 2.5). However, some enhancements of total antioxidant capacity were observed compared with the effects of 12.5 μM AST, DHA, or EPA alone.

2.3.4 Concentration-dependent induction of an ARE by AST, DHA, and EPA alone as well as synergism with the drug combinations

HepG2-C8 cells were incubated with different concentrations of AST, DHA, or EPA alone or with the combination of 12.5 μM AST and 12.5 μM DHA or EPA for 24 h. The luciferase activity increased in a concentration-dependent manner in response to each compound. The maximum fold induction (4.5-fold) occurred in cells treated with 100 μM AST (Figure 2.6). The DHA and EPA concentrations ranged from 3.13 to 50 μM, which were relatively non-toxic concentrations as determined by the MTS assay (Figure 2.3). At 50 μM, DHA more strongly induced the ARE than EPA (Figure 2.6). The combination of 12.5 μM AST and 12.5 μM DHA or EPA was synergistic as evidenced by the increased fold induction (Figure 2.6).

2.3.5 Synergism identified by the CI

The CI was calculated using equation 1 in the Materials and Methods. Table 2.1 presents the CI data for the combination of 12.5 μM AST and 12.5 μM DHA or EPA, which synergistically induced the ARE (Figure 2.6). Three independent studies of the CI were performed. When the CI equals 1.00, the combination is additive. If the CI is greater than 1.00, then the combination is antagonistic. The CI values of the combination of 12.5 μM AST and 12.5 μM DHA or EPA were less than 1.00, indicating that these combinations were synergistic. Statistical analyses revealed that the CI values were both significantly less than 1 ($P < 0.05$).

2.3.6 Modulation of Nrf2, HO-1, NQO1, and GSTm2 mRNA expression by AST, DHA, or EPA alone or in combination

The mRNA expression levels of Nrf2, HO-1, NQO1, and GSTm2 were quantified by qRT-PCR in cells treated with the compounds alone or in combination (Figure 2.7). AST, DHA, and EPA alone induced Nrf2 expression (Figure 2.7A). The expression levels of HO-1 (Figure 2.7B) and NQO1 (Figure 2.7C) in EPA-treated cells increased in a concentration-dependent manner, with maximal induction observed with 12.5 μM EPA. Cells treated with AST, DHA, or EPA exhibited the highest Nrf2 mRNA expression at the concentration of 6.25 μM; the expression levels were slightly lower at 12.5 μM. The same expression pattern was observed for HO-1 in response to AST or DHA and for NQO1 in response to AST. In all cases, treatment with 12.5 μM AST in combination with 12.5 μM DHA or

EPA resulted in a greater fold induction in the mRNA expression of Nrf2, HO-1, NQO1, and GSTm2 compared with the effects of 12.5 μM AST, DHA, or EPA alone.

2.4 Discussion and Conclusions

We hypothesized that AST, DHA, and EPA would activate the ARE transcription system and that the combination of AST and DHA or EPA would be synergistic. The concentration of drugs used in combination can affect whether the drug-drug interaction is additive, synergistic, or antagonistic. Synergism is usually observed at low concentrations of drugs in combination. Synergism is clinically significant when low concentrations of drugs produce better efficacy with less toxicity than either drug alone. The concentrations of AST, DHA, and EPA reflected the dietary consumption levels as potential chemoprevention supplements. The daily intake of 5 or 20 mg of AST for 3 weeks resulted in final plasma concentrations of 0.34 or 0.67 μM, respectively, without adverse effects [259]. In a recent pharmacokinetic study of DHA in 48 subjects consuming fish once or twice a month, the plasma concentrations of DHA and EPA were determined to be approximately 60 (182 μM) and 10 μg/mL (33 μM), respectively [279]. The concentrations of DHA and EPA utilized in the combination treatments in the present study were lower than those used in the aforementioned pharmacokinetic clinical study [279]. The low AST concentration used in combination with DHA or EPA in the present study provided promising evidence for the potential for synergistic antioxidant

effects in human trials. Synergism was observed for the combination of AST and DHA or EPA in various antioxidant models in the current study, including synergistic effects on the GSH concentration (Figure 2.4), total antioxidant power (Figure 2.5), ARE induction (Figure 2.6), CI calculations (**Error! Reference source not found.**), and the mRNA expression of Nrf2 and related genes (Figure 2.7).

Antioxidant activity involves a complex process that is regulated by several mechanisms. Because of its complexity, more than one assay must be performed when evaluating the antioxidant activity of pure compounds or extracts [280]. In this work, excluding the DPPH assay performed in a test tube, GSH levels, and total antioxidant power were assayed *in vitro* to determine the antioxidant capacity. The DPPH assay provided information regarding the ability of the tested compounds to scavenge DPPH free radicals. The GSH levels indicated that AST, DHA, and EPA alone and the combination of 12.5 μM AST and 12.5 μM DHA or EPA have antioxidant power. Radical scavengers protect cells and tissues from free radicals, thereby preventing diseases such as cancer. Although it is unclear whether AST, DHA, and EPA are active against free radicals after being absorbed and metabolized, radical-scavenging assays have gained acceptance for their ability to rapidly screen materials of interest.

Our current study demonstrates that AST, DHA, and EPA alone and in combination protected cells by inducing antioxidant activity via the Nrf2 signaling pathway in HepG2-C8 cells. The Nrf2 signaling pathway has been reported to

mediate the anti-oxidative stress protection induced by AST in the cyclophosphamide-induced oxidative stress model [257]. Without an oxidative insult, we confirmed the involvement of Nrf2 and its related genes in HepG2-C8 cells (Figure 2.7). The induction of NQO1 and HO-1 has been established as a strong cellular defense against oxidative stress; our findings agree with this observation. We also observed increased intracellular GSH levels (Figure 2.4) and total antioxidant power (Figure 2.5) in response to AST treatment.

Low concentrations of AST, DHA, and EPA alone and in combination (12.5 μM AST and 12.5 μM DHA or EPA) are potentially physiologically attainable according to the clinical trials of AST, DHA, and EPA. Therefore, it is conceivable that lower concentrations of AST, DHA, and EPA alone and in combination may achieve optimal Nrf2-mediated anti-oxidative protection. In conclusion, we demonstrated that the combination of low-concentration AST and DHA or EPA synergize as antioxidants. The Nrf2/ARE pathway was involved in mediating the antioxidant effects of AST, DHA, and EPA alone and in combination in HepG2-C8 cells.

2.5 Figures and Tables

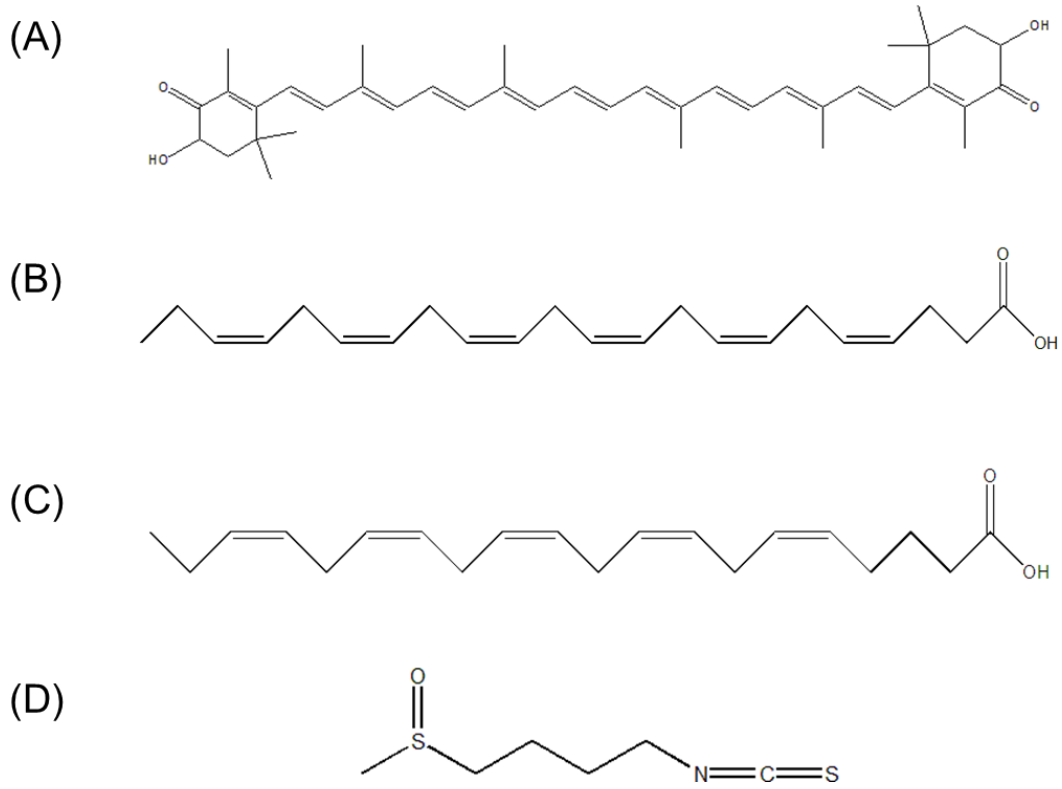

Figure 2.1. The chemical structures of (A) astaxanthin (AST), (B) docosahexaenoic acid (DHA), (C) eicosapentaenoic acid (EPA), and (D) sulforaphane (SFN).

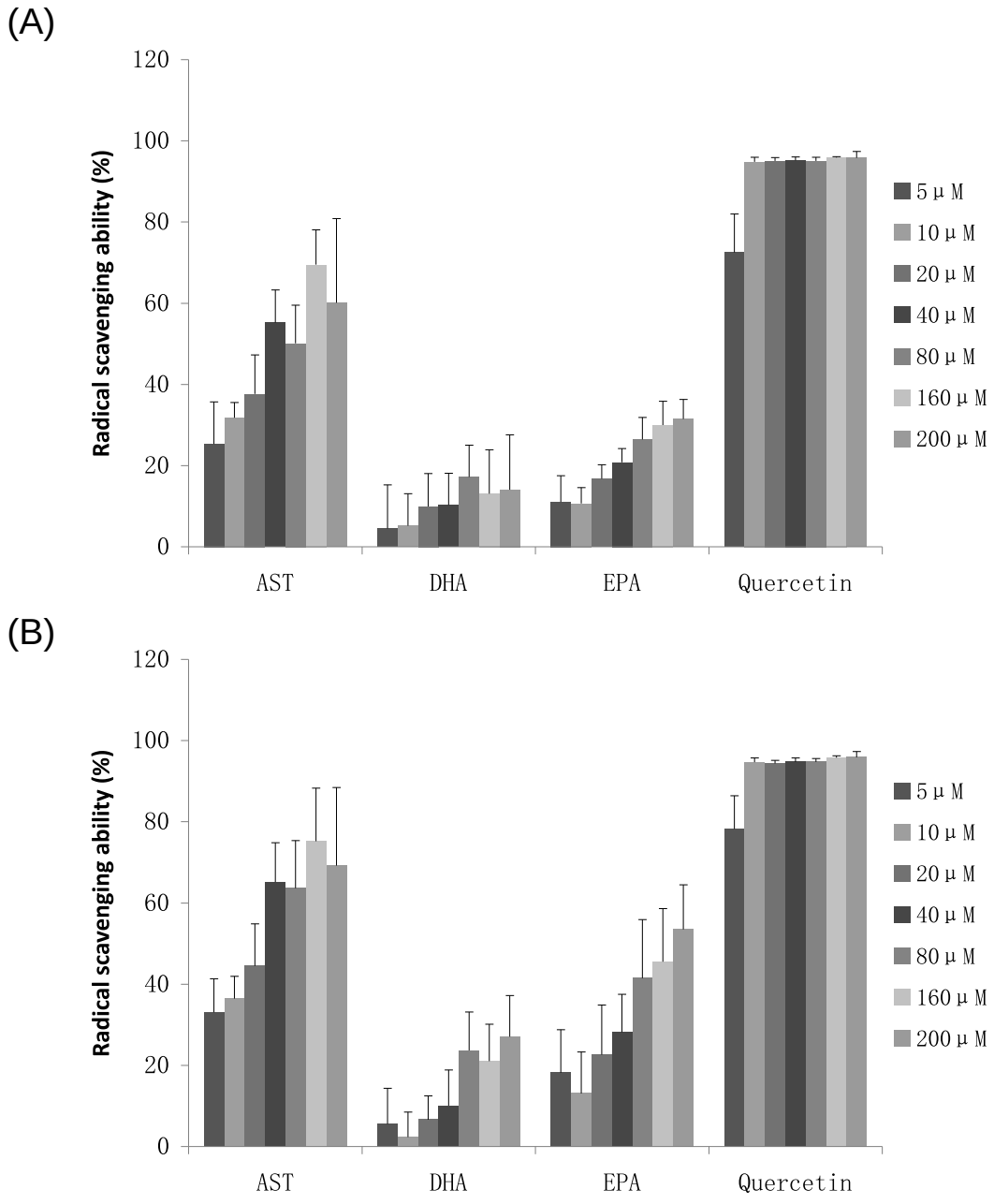

Figure 2.2. The free radical scavenging activity of AST, DHA, EPA, and quercetin at different concentrations using the DPPH method at (A) 30 min and (B) 60 min. Quercetin was included as the positive control. The results are expressed as the mean ± SEM of three independent assays.

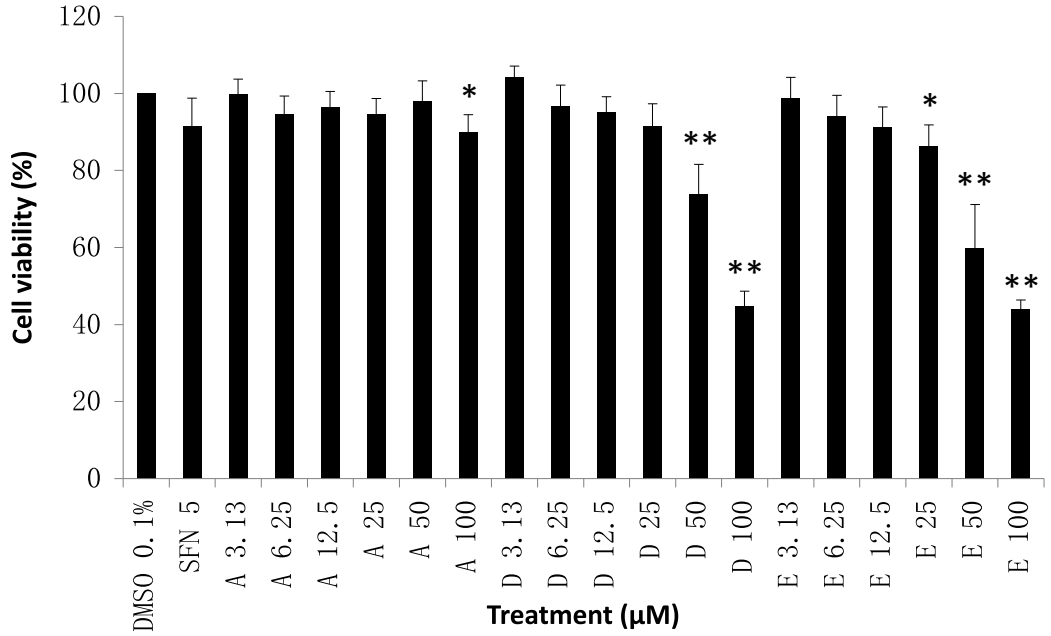

Figure 2.3. Cell viability measured by MTS assay.

HepG2-C8 cells treated with different concentrations of AST, DHA, or EPA for 24 h. The results are expressed as the mean ± SEM. * $P < 0.05$, ** $P < 0.01$ compared with cells treated with 0.1% DMSO (negative control). A, AST; D, DHA; E, EPA.

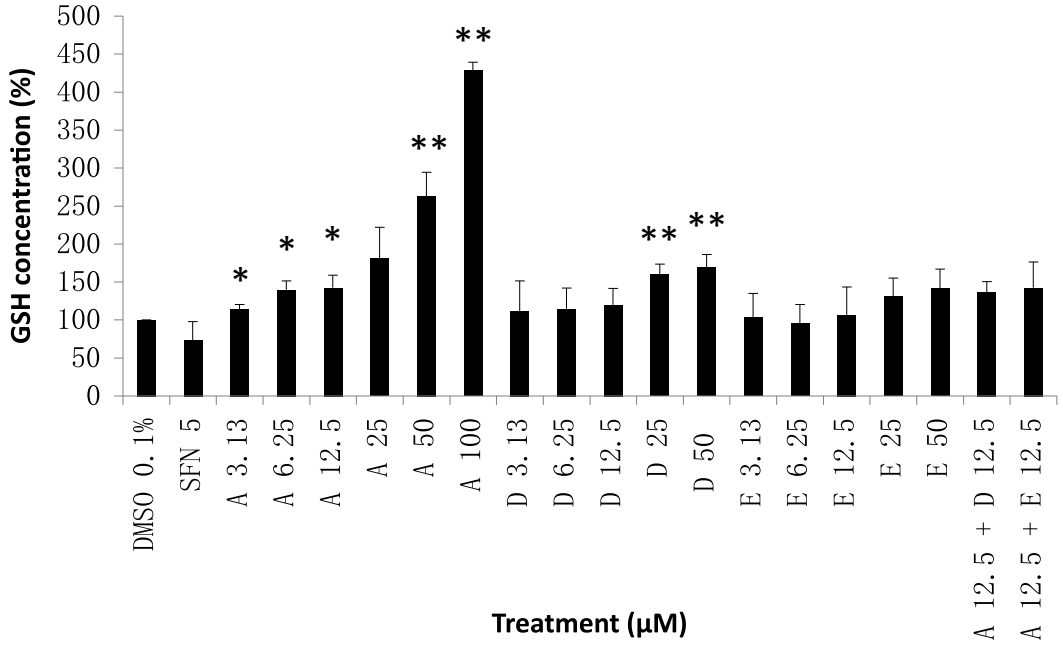

Figure 2.4. Antioxidant activity by cellular GSH concentration.

HepG2-C8 cells treated with AST, DHA, EPA or 12.5 μM AST in combination with 12.5 μM DHA or EPA for 24 h. The GSH concentration in HepG2-C8 cells was normalized to that in cells treated with 0.1% DMSO (negative control). Each value represents the mean ± SEM. * $P < 0.05$, ** $P < 0.01$ compared with cells treated with 0.1% DMSO. SFN (5 μM) was used as the positive control. A, AST; D, DHA; E, EPA.

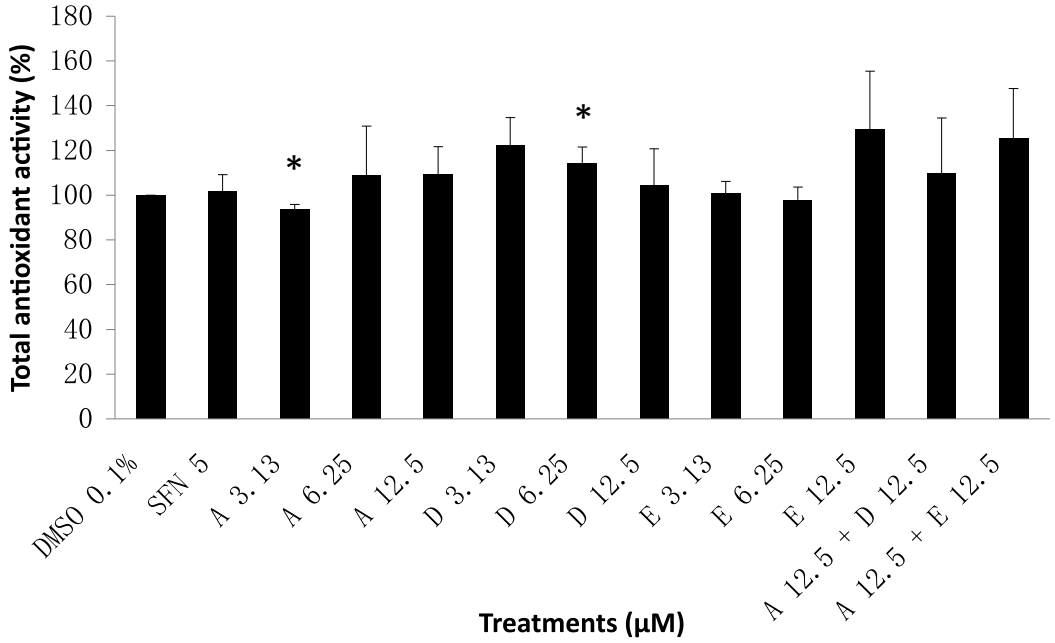

Figure 2.5. Total antioxidant activity.

HepG2-C8 cells treated for 24 h with AST, DHA, EPA or AST in combination with DHA or EPA at different concentrations. The total antioxidant activity in HepG2-C8 cells was normalized to cells treated with 0.1% DMSO (negative control). Each value represents the mean ± SEM. * $P < 0.05$ compared with cells treated with 0.1% DMSO. A, AST; D, DHA; E, EPA.

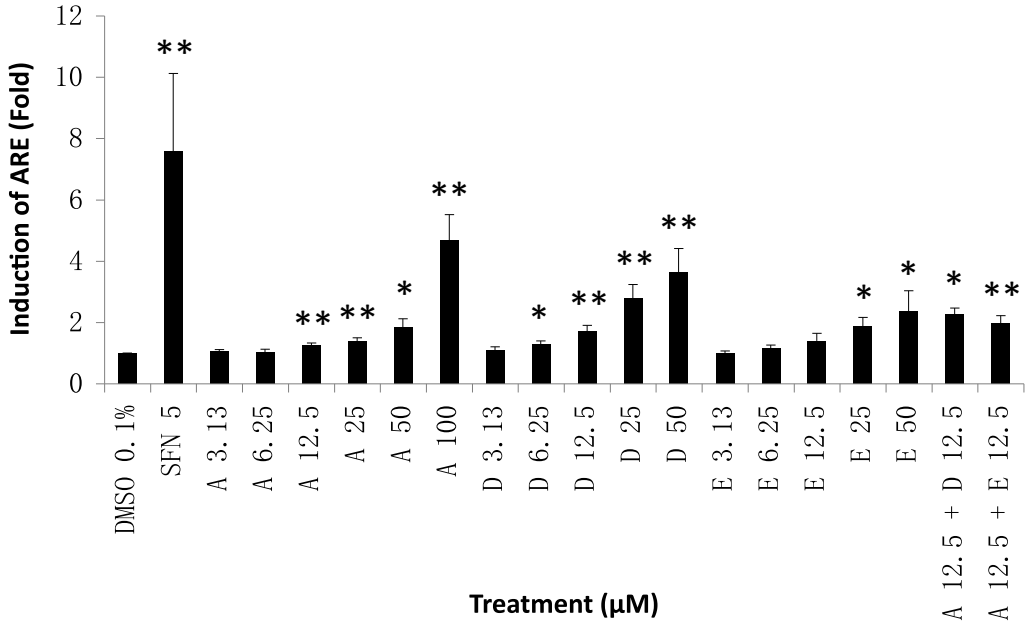

Figure 2.6. ARE induction measured by luciferase reporter assay.

The concentration-dependent induction of luciferase reporter activity by AST, EPA, DHA, or 12.5 μM AST in combination with 12.5 μM DHA or EPA after 24 h in HepG2-C8 cells. HepG2 cells stably transfected with an ARE-luciferase construct were selected as described in the Materials and Methods. The synergism of the combination of 12.5 μM AST and 12.5 μM DHA or EPA was confirmed by calculating the CI for the ARE assays (please refer to Table 1). The luciferase activity was determined 24 h after treatment and normalized to the protein concentration. The luciferase activity induced by each treatment was normalized to the activity in HepG2-C8 cells treated with 0.1% DMSO and expressed as the fold induction. Each value represents the mean ± SEM. * $P < 0.05$, ** $P < 0.01$ compared with the cells treated with 0.1% DMSO. A, AST; D, DHA; E, EPA.

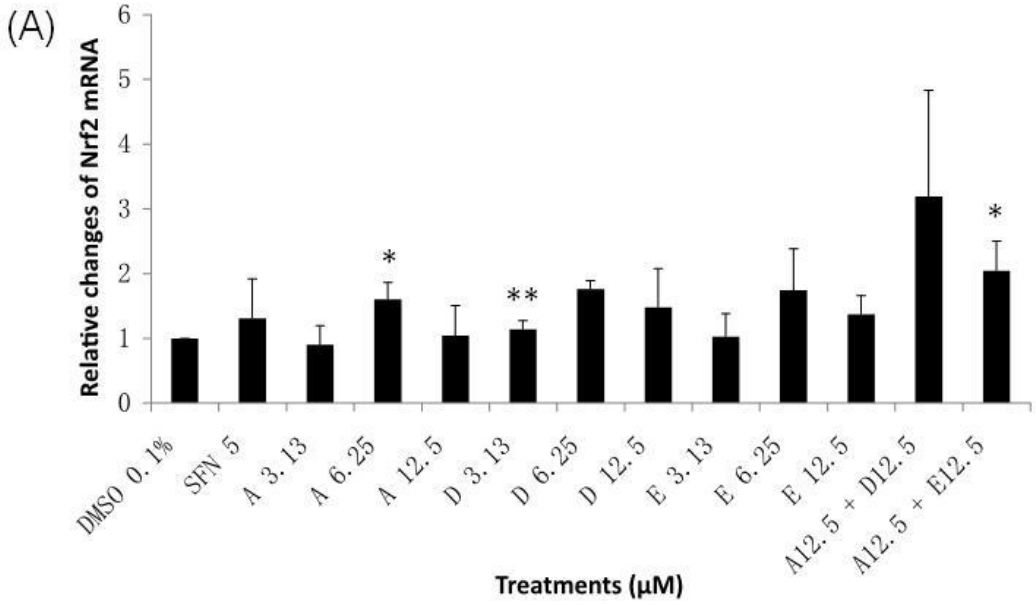
(A)
Relative changes of Nrf2 mRNA
0
1
2
3
4
5
6
*
**
*
DMSO 0.1%
SFN 5
A 3.13
A 6.25
A 12.5
D 3.13
D 6.25
D 12.5
E 3.13
E 6.25
E 12.5
A12.5 + D12.5
A12.5 + E12.5
Treatments (μM)

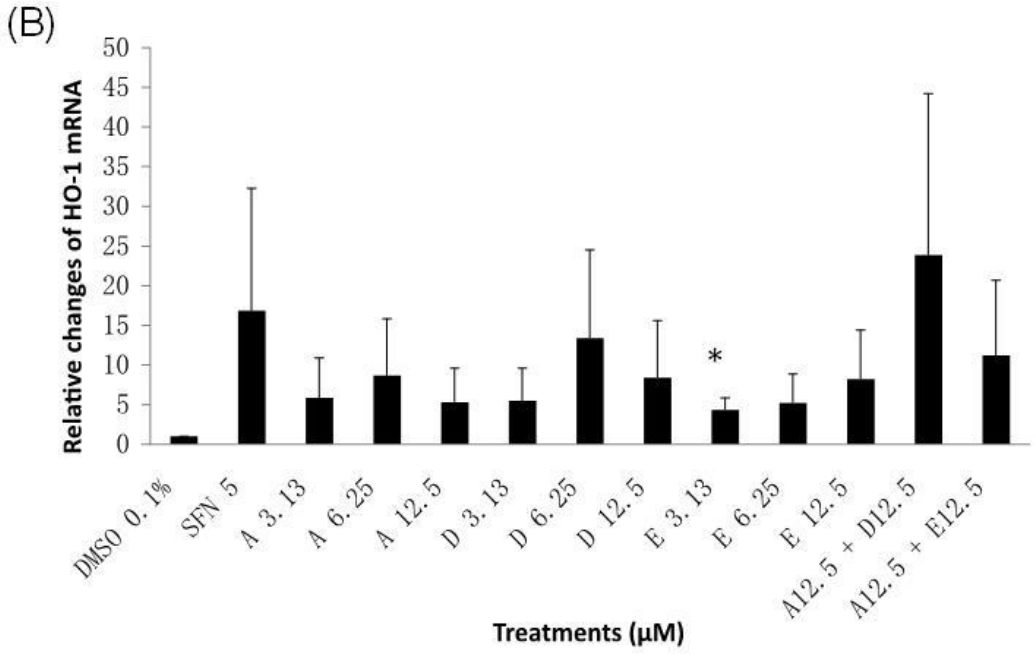
(B)
Relative changes of HO-1 mRNA
0
5
10
15
20
25
30
35
40
45
50
*
DMSO 0.1%
SFN 5
A 3.13
A 6.25
A 12.5
D 3.13
D 6.25
D 12.5
E 3.13
E 6.25
E 12.5
A12.5 + D12.5
A12.5 + E12.5
Treatments (μM)

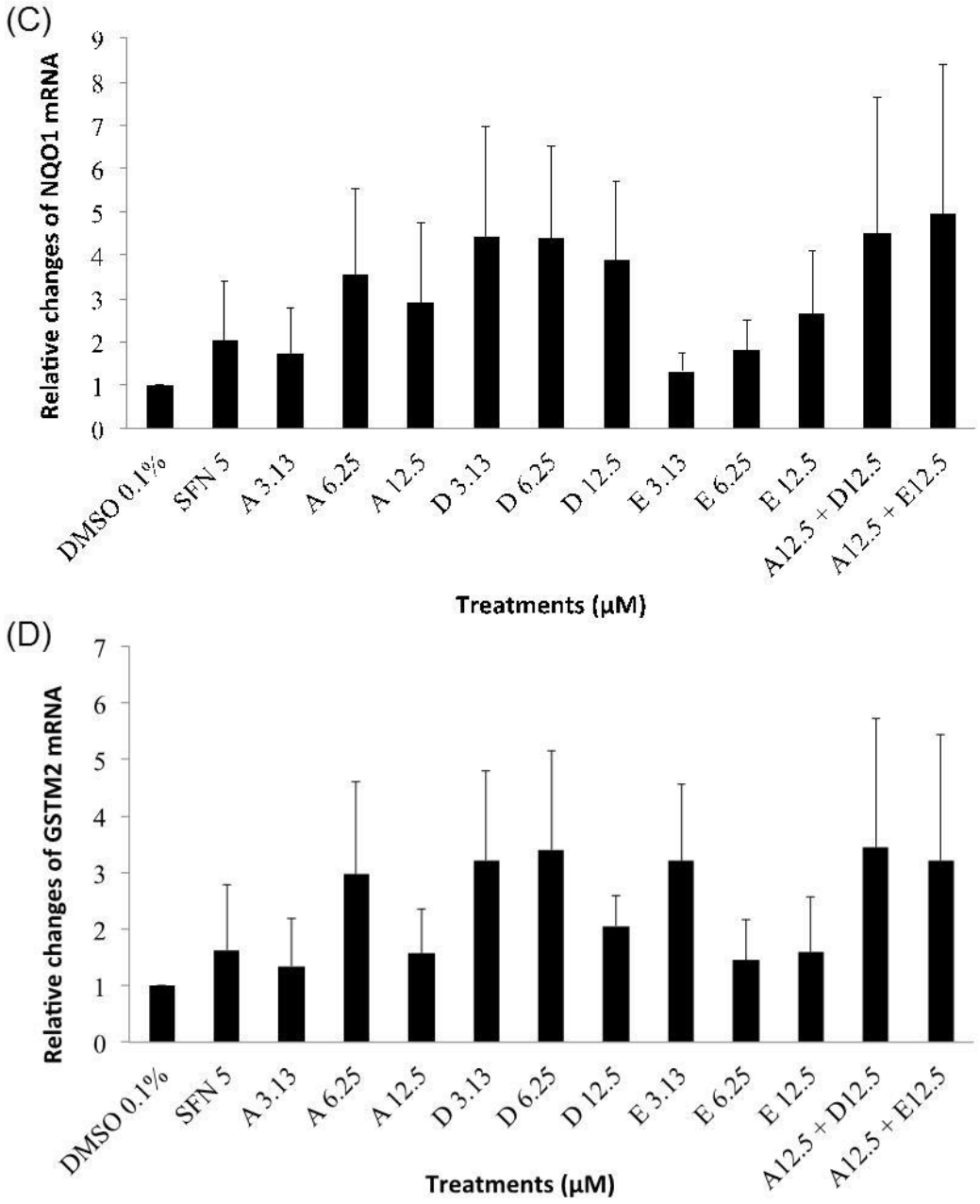

Figure 2.7. Expression of Nrf2 targeted genes at mRNA level.

HepG2-C8 cells treated for 6 h with AST, DHA, EPA, or the combination of 12.5 μM AST and 12.5 μM DHA or EPA. The induction of Nrf2 (A), HO-1 (B), NQO1 (C), and GSTM2 (D) was normalized to the negative control (0.1% DMSO) and expressed as the fold induction. Each value represents the mean ± SEM. * $P < 0.05$,

** $P < 0.01$ compared with cells treated with 0.1% DMSO. A, AST; D, DHA; E, EPA.

Table 2.1. The Combination Index (CI) calculated from the combination treatments that induced ARE activity in HepG2-C8 cells.

The data are presented as the mean ± SEM. * $P < 0.05$, ** $P < 0.01$ compared with cells treated with 0.1% DMSO. A, AST; D, DHA; E, EPA.

	A 12.5 + D 12.5	**A 12.5 + E 12.5**
CI	0.78 ± 0.09*	0.68 ± 0.06**

3 Epigenetic CpG methylation of the promoter and reactivation of the expression of GSTP1 by astaxanthin in human prostate LNCaP cells[7][8][9]

3.1 Introduction

Prostate cancer (PCa) is the most prevalent type of cancer in men; there are more than 3.3 million men living with prostate cancer, with an additional 180,000 cases expected to be diagnosed in 2016 [281]. Age is one of the major risk factors because the majority of prostate cancer survivors (64%) are age 70 years or older [281]. In addition to age, abnormal epigenetic changes have been correlated with an increasing incidence of prostate cancer. DNA methylation is one of the most investigated epigenetic alterations in PCa. DNA methylation-based gene silencing is common in stages of prostate carcinogenesis and tumor progression from normal cells to pre-initiated cells. Glutathione-S-transferases (GSTs) are a family of polymorphic phase II metabolic enzymes that are involved in the detoxification of carcinogenic and cytotoxic substances by catalyzing their conjugation with reduced

[7] Part of this chapter has been published as an original research paper: **Yang, Y.**, Fuentes, F., Shu, L., Wang, C., Pung, D., Li, W., Zhang, C., Guo, Y., & Kong, A. N. (2017). Epigenetic CpG Methylation of the Promoter and Reactivation of the Expression of GSTP1 by Astaxanthin in Human Prostate LNCaP Cells. *AAPS J*, 19(2), 421-430.

[8] Keywords: astaxanthin, GSTP1, prostate cancer, epigenetics, DNA methylation

[9] Abbreviations: ARE, antioxidant response element; AST, astaxanthin; 5-aza, 5-Aza-deoxycytidine; TSA, trichostatin A; DMSO, dimethyl sulfoxide; DNMT, DNA methyltransferases; HDAC, histone deacetylase; EPA, eicosapentaenoic acid; FBS, fetal bovine serum; GAPDH, Glyceraldehyde-3-Phosphate Dehydrogenase; GSTs, Glutathione-S-transferases; GSTP1, glutathione S-transferase pi 1; GSH, glutathione; GSTM2, glutathione S-transferase M2; PCa, Prostate cancer; HO-1, heme oxygenase-1; NQO1, NAD(P)H: quinone oxydoreductase 1; Nrf2 or NFE2L2, nuclear factor (erythroid-derived 2)-like 2; qRT-PCR, quantitative reverse-transcriptase polymerase chain reaction; RSA, radical scavenging activity; SFN, sulforaphane; SETD7, SET Domain Containing Lysine Methyltransferase 7.

glutathione [282, 283]. There are four major classes of GSTs: alpha, mu, pi, and theta. The glutathione S-transferase pi 1 gene (*GSTP1*), a polymorphic gene encoding *GSTP1* variant proteins, is reported to repress the expression of antioxidant and detoxifying enzymes. *GSTP1* has been implicated in a large variety of detoxification and metabolism reactions and is involved in the prevention of genome damage and cancer initiation [284, 285]. The *GSTP1* gene is characterized as a tumor suppressor gene and is located on chromosome 11q13 [286]. An aberrant methylation pattern of *GSTP1* has been noticed in different cancer types, including those of the liver, prostate, and breast cancers [287, 288]. GSTP1 is commonly down-regulated in prostate tumor progression and is correlated with the DNA methylation status [289, 290]. However, the exact biological trigger of *GSTP1* gene silencing in prostate cancer remains to be elucidated.

Erythroid 2p45 (NF-E2)–related factor 2 (NFE2L2 or Nrf2) is a basic-region leucine zipper (bZIP) transcription factor that regulates the expression of many phase II detoxifying enzymes, including GSTs. Thus, Nrf2 protects against oxidative stress and electrophilic challenges to maintain cellular chemical homeostasis [291]. An *in vivo* study showed that Nrf2-deficient mice exhibit significantly lower expression levels of cellular defense-related genes in various tissues, as summarized in reviews [292, 293], and they are at greater risk of developing colorectal [294] and skin cancers [295-298]. Nrf2 and members of the GST family have been reported to be decreased in human prostate cancer [299]. The absence of *GSTP1* gene

expression has been reported in high-grade prostate intraepithelial neoplasias, and the methylation of its promoter region has been identified in 90% of cancer samples and 70% of prostate intraepithelial neoplasia samples [300].

DNA hypermethylation represents increased CpG island methylation in normally unmethylated promoter regions of cancer-associated genes, and *GSTP1* hypermethylation is the most intensely investigated gene-specific hypermethylation in PCa [301]. In a meta-analysis, *GSTP1* was methylated in 82% of PCa cases and 5% of controls [301] making it a promising PCa marker. *GSTP1* methylation alterations can also be detected in histologically negative biopsy samples and can be used to improve the sensitivity of the standard histology workup for prostate cancer detection [302]. These findings suggest that epigenetic alterations in histologically negative biopsy samples may serve as potential markers of PCa diagnosis after a biopsy [303].

To date, as efforts are made to target tumor-specific abnormal DNA methylation, natural dietary compounds have shown beneficial effects in reversing these abnormal epigenetic changes. Astaxanthin (AST, Astaxanthin; Figure 3.1) is a red dietary carotenoid that is commonly found in microalgae, such as *Haematococcus pluvialis* and *Chlorella zofingiensis* [245], and aquatic animals. AST possesses various pharmacological activities, including antioxidative activity [245-248], antitumor effects [249-251], hepatoprotective effects [252], antidiabetic effects [253] and anti-inflammatory properties [254]. *In vivo* and *in vitro* results suggest that AST

has health-promoting activities, suggesting its potential use in the prevention of various diseases, including cancers [255] and Parkinson's disease [277]. Our lab previously reported that astaxanthin shows synergistic antioxidant effects with polyunsaturated fatty acids at low concentrations via the Nrf2/ARE pathway, producing anti-oxidative effects [304]. Recently, it was reported that AST increased chromosomal stability and normalized the epigenetic modifications in oocyte maturation [305]. Therefore, the aim of this study is to investigate the role of AST in restoring the expression of Nrf2 and *GSTP1* through epigenetic modification in human prostate LNCaP cells.

3.2 Materials and methods

3.2.1 Chemicals and reagents

Astaxanthin (AST) was purchased from Sigma-Aldrich, Inc. (Catalog No., SML0982, St. Louis, MO, USA). The MTS [3-(4,5-dimethylthiazol-2-yl)-5-(3-carboxymethoxyphenyl)-2-(4-sulfophenyl)-2H-te trazolium, inner salt)] test using CellTiter 96® AQueous One Solution was purchased from Promega (Madison, WI, USA). 5-Aza-deoxycytidine (5-aza) and trichostatin A (TSA) were obtained from Sigma-Aldrich, Inc. (St. Louis, MO, USA). Fetal bovine serum (FBS), Roswell Park Memorial Institute (RPMI) 1640 medium, and trypsin-EDTA solution were purchased from Gibco Laboratories (Waltham, MA, USA).

3.2.2 Cell culture and treatment

LNCaP (androgen-dependent prostate cancer cell line from the American Type Culture Collection VA, USA) cells were maintained in RPMI-1640 with 10% FBS and grown at 37°C in a humidified 5% CO_2 atmosphere. LNCaP cells were plated on 10 cm plates for 24 hours and then treated with either 0.1% dimethylsulfoxide (DMSO), 2.5 μM 5-aza, or different concentrations of AST in 1% FBS-containing RPMI 1640 medium for a total of five days. The medium was changed every two days. On the fourth day, 500 nM TSA was added to the medium with the 5-aza at 2.5 μM for another 18 hours before the cell harvest. Cells were then harvested for the extraction of DNA, RNA, and protein.

3.2.3 Cell viability test: MTS assay

The cell viability assay was based on the ability of cells to convert a tetrazolium compound (MTS) into a colored formazan product. This bioconversion is presumably accomplished by NADPH or NADH, which are produced by dehydrogenase enzymes in metabolically active cells. Cells were seeded in 96-well plates overnight at the density of 1×10^4 cells/well in 100 μL of medium containing 10% FBS and allowed to adhere to the plates. CellTiter 96® AQueous One Solution (20 μL; Promega, Madison, WI, USA) was added to the cells after the cells were treated with AST at 3.13–100 μM in 1% FBS medium for three days or five days. The negative control cells were treated with 0.1% DMSO. The 96-well plate was incubated for 2 h at 37ºC in a humidified 5% CO_2 atmosphere. The absorbance was

monitored at 490 nm using a spectrophotometer (Infinite® 200 PRO series, Tecan Systems, Inc., USA). The cell viability was calculated as a percentage compared to the 0.1% DMSO group as the control.

3.2.4 DNA extraction and bisulfite genomic sequencing

Genomic DNA was isolated from the treated cells using the QIAamp DNA Mini Kit (Qiagen, Valencia, CA). Bisulfite conversion of genomic DNA was performed using the EZ DNA Methylation Gold Kit (Zymo Research Corp, Irvine, CA) according to the manufacturer's instructions, as previously described [306]. Genomic DNA and sodium bisulfite-converted genomic DNA were obtained from 0.1% DMSO-, 5-aza+TSA- or AST-treated LNCaP cells using the same procedures as described above. The converted DNA was amplified by PCR using Platinum PCR SuperMix (Invitrogen, Carlsbad, CA) with bisulfite genomic sequencing primers for the Nrf2 gene promoter region spanning methylated CpG sites from −1530 to −1143, with the translational start site (TSS) referenced as +1, as previously described [307]. For the *GSTP1* gene (*Homo sapiens* chromosome 11, GRCh37.p13), bisulfite genomic sequencing primers covered the CpG island region spanning methylated CpG sites from +882 to +1116, with the TSS referenced as +1. The primers were designed using the MethPrimer program [308]. The sequences of the primers used were: *GSTP1* sense 5’ GGA GTA TGT GTT TGG TAG GGA A 3’ and anti-sense 5’ TCC TTC CAA CTC TAA CCC TAA T 3’. The following PCR amplification conditions were used: 3 minutes at 94°C; 30 seconds at 94°C, 45 seconds at 70/55°C

and 1 minute at 72°C for 15 cycles; 30 seconds at 94°C, 45 seconds at 60°C and 1 minute at 72°C for 25 cycles; and 5 minutes at 72°C for 1 cycle. The PCR products were cloned into the pCR4 TOPO vector using a TOPO TA Cloning Kit (Invitrogen, Carlsbad, CA). Plasmid DNA from at least 10 colonies from each treatment was prepared using the QIAprep Spin Miniprep Kit (Qiagen, Valencia, CA) and sequenced by Genwiz® [309].

3.2.5 RNA isolation and reverse transcription PCR

Total RNA was extracted from treated LNCaP cells using the RNeasy Mini Kit (Qiagen, Valencia, CA). First-strand cDNA was synthesized from 1 µg of total RNA using the SuperScript III First-Strand Synthesis System for RT-PCR (Invitrogen, Carlsbad, CA) according to the manufacturer's instructions. The cDNA was used as the template for real-time PCR (Applied Biosystems ViiA 7 Real-Time PCR System). GAPDH was used as an internal loading control. The sequences of the primers used for cDNA amplification are shown in Table 3.1.

3.2.6 SETD7 knockdown in LNCaP cells

Lentivirus-mediated short hairpin RNAs were used to establish stable mock (scramble control, sh-Mock) and SET Domain Containing Lysine Methyltransferase 7 (SETD7) knockdown (sh-SETD7) LNCaP cells. The shRNA clone sets were obtained from Genecopoeia (Rockville, MD, USA), and lentiviral transduction was performed according to the manufacturer’s manual. After selection in RPMI 1640 medium supplemented with 10% FBS and 2 mg/mL puromycin for 3 weeks, the

sh-Mock and sh-SETD7 cells were further used to evaluate the functional role of SETD7. Total RNA was extracted from the cells treated with 0.1% DMSO or AST for 24 hours using the RNeasy Mini Kit (Qiagen, Valencia, CA). First-strand cDNA was synthesized from 1 μg of total RNA using the SuperScript III First-Strand Synthesis System for RT-PCR (Invitrogen, Carlsbad, CA) according to the manufacturer's instructions. The cDNA was used as the template for real-time PCR (Applied Biosystems ViiA 7 Real-Time PCR System). GAPDH was used as an internal loading control. The sequences of the primers used for cDNA amplification are shown in Table 3.1.

3.2.7 Preparation of protein lysates and western blotting

The treated cells were harvested using radioimmunoprecipitation assay (RIPA) buffer supplemented with a protein inhibitor cocktail (Sigma). The protein concentrations of the cleared lysates were determined using the bicinchoninic acid (BCA) method (Pierce, Rockford, IL), and 25 μg of the total protein was resolved by 4% to 15% sodium dodecyl sulfate-polyacrylamide gel electrophoresis (SDS-PAGE) (Bio-Rad, Hercules, CA). After electrophoresis, the proteins were electrotransferred to a polyvinylidene difluoride (PVDF) membrane (Millipore, Bedford, MA). The PVDF membrane was then blocked with 5% bovine serum albumin (BSA) in phosphate buffered saline (PBS)-0.1% Tween 20 and then sequentially incubated with specific primary antibodies and horseradish peroxidase (HRP)-conjugated secondary antibodies. The blots were visualized with the Super Signal enhanced

chemiluminescence detection system and documented using the Gel Documentation 2000 system (Bio-Rad, Hercules, CA). The antibodies were purchased from the following sources: anti-Nrf2 from Epitomics Inc.; anti-NQO1, anti-GSTP1, and anti-β-actin from Santa Cruz Biotechnology; antibodies of DNA methyltransferases (DNMTs) including anti-DNMT1, anti-DNMT3a, and anti-DNMT3b from IMGENEX (San Diego, CA, USA).

3.2.8 DNMT and HDAC activity assays

DNMT activity and histone deacetylase (HDAC) activity assays were conducted using a DNMT activity/inhibition assay kit (Epigentek, Farmingdale, NY) and an HDAC activity/inhibition direct assay kit (Epigentek, Farmingdale, NY), respectively, following the manufacturer's protocol. The nuclear protein fraction was extracted by the NEPER Nuclear and Cytoplasmic Protein Extraction Kit (Thermo Scientific, Pittsburgh, PA), and the relative DNMT activity was calculated based on the ratio of the AST treatment group to the control after normalization to the protein amount.

3.2.9 Data presentation and statistical analysis

At least three independent experiments were performed for each analysis. The results are presented as the mean ± standard error of the mean (SEM) for each group unless otherwise specified. The differences between the controls and the treated groups were evaluated using Student's *t*-test.

3.3 Results

3.3.1 AST is cytotoxic to LNCaP cells

The MTS assay was used to examine the cytotoxicity of AST. AST treatment decreased the cell viability in dose- and time-dependent manners from 3-day to 5-day treatment (Figure 3.2). Three-day treatment with AST was less toxic compared to 5-day treatment. AST (< 25 μM) resulted in viability greater than 70%. These doses were selected for further studies of AST's effects on epigenetic modifications and the expression of the *GSTP1* and Nrf2 genes. AST increased Nrf2 and *GSTP1* mRNA expression but did not affect the protein expression significantly in LNCaP cells

To examine whether AST has any effect on the expression of Nrf2 and GSTP1, the mRNA and protein levels of Nrf2 and *GSTP1* were determined, as shown in Figure 3.3. The combination of 5-Aza (2.5 μM) and TSA (500 nM) increased the mRNA expression levels of Nrf2 and *GSTP1*. AST treatment increased the Nrf2 mRNA expression level at 6.25 μM but not at 12.5 μM. Compared to Nrf2 mRNA expression, AST treatment increased the *GSTP1* mRNA expression level at 12.5 μM but not at 6.25 μM. Then, western blotting was conducted to analyze the protein expression of Nrf2, NQO1, and GSTP1. As shown in Figure 3.4, treatment with AST slightly increased the protein expression of Nrf2, NQO1, and GSTP1, but the increase was not significant.

3.3.2 AST decreased the methylation status of the *GSTP1* gene promoter region but had no effect on the methylation status of the Nrf2 gene promoter region

Bisulfite sequencing was performed to determine the methylation status of the *GSTP1* gene and Nrf2 promoter regions (Figure 3.5 and Figure 3.6). We previously reported that 5-aza and TSA in combination decreased the CpG methylation levels of the Nrf2 gene promoter region in murine prostate cancer TRAMP C1 cells and in human prostate cancer LNCaP cells [306, 307]. As shown in Figure 3.5, 5-aza and TSA combination treatment over 5 days in LNCaP cells significantly ($P = 0.008$) reduced the methylation level of these selected CpG sites (- 1530 to -1143) from 58% to 38%. However, AST treatment at 6.25 µM and 12.5 µM did not significantly reduce the CpG methylation level of the Nrf2 gene promoter region, as in shown in Figure 3.5.

In Figure 3.6, LNCaP cells treated with 0.1% DMSO showed hypermethylation of *GSTP1* at twenty-one CpG sites with 88% methylation. The methylation level was decreased to 81% with the co-treatment of 5-aza (2.5 µM) and TSA (500 nM) (Figure 3.6A). AST at 12.5 µM reduced the methylation level to 82% of twenty-one CpG sites, as shown in Figure 3.6. AST at 12.5 µM and 5-aza+TSA significantly decreased the methylation ratio of 21 CpG sites of the *GSTP1* gene (Figure 3.6B).

3.3.3 AST significantly affected the mRNA expression of DNMT3a

DNMTs are the major enzymes that transfer and maintain a methyl group at the fifth carbon of cytosine residues within CpG islands in DNA [310]. DNA

methylation, as one of the key epigenetic modifications, regulates gene expression in eukaryotes. AST at 12.5 μM decreased the mRNA expression of DNMT1, DNMT3a**,** and DNMT3b with 5-day treatment. However, AST at 6.25 μM significantly increased the mRNA expression of DNMT3a ($P < 0.05$) in Figure 3.7A.

The histone-lysine N-methyltransferase SETD7 was initially described to modulate the monomethylation of histone H3 at lysine 4 [311]. For now, numerous non-histone targets have been reported for SETD7, including DNMT1 [312]. Lentivirus-mediated short hairpin RNAs were used to establish stable mock (scramble control, sh-Mock) and SETD7 (SETD7) knockdown (sh-SETD7) LNCaP cells. Total RNA was extracted from treated sh-Mock and sh-SETD7 cells with 0.1% DMSO or AST for 24 hours to study the effects of AST with or without SETD7. As shown in Figure 3.7B, mRNA expression of *SETD7* was reduced in sh-SETD7 LNCaP cells compared to the scramble control, sh-Mock LNCaP cells. AST (6.25–25 μM) increased the mRNA expression of *NQO1* in sh-mock LNCaP cells but not in sh-SETD7 LNCaP cells (Figure 3.7B).

3.3.4 AST reduced protein expression and activity of the DNMT enzymes in LNCaP cells

We then carried out western blotting to analyze the protein expression levels of DNMTs in LNCaP cells. In Figure 3.8, AST at 6.25 μM and 12.5 μM could reduce the protein expression levels of DNMT3b but not DNMT1 or DNMT3b. The combination of 5-aza (2.5 μM) and TSA (500 nM) significantly reduced the protein

expression levels of DNMT1, DNMT3a, and DNMT3b. In addition, treatment with AST significantly inhibited DNMTs activity; AST at 25 μM significantly reduced DNMT activity to 65.2% (Figure 3.9). Another key epigenetic modification is histone modification, which can affect chromatin structure [313]. There were no significant differences in the protein expression of HDAC1–HDAC5 or HDAC8 when comparing the control and AST treatment (data not shown). Interestingly, AST at a low dose (6.25 μM) significantly increased the HDAC activity to 104.0% compared to the control; However, AST at higher doses (12.5 μM and 25 μM) significantly decreased HDAC activity to 87.4% and 83.4%, respectively.

3.4 Discussion and conclusions

AST, a red dietary carotenoid, has been reported to possess anti-oxidative activity [245-248], anti-cancer effects [249-251] and anti-inflammatory properties [254]. These beneficial effects occur both *in vivo* and *in vitro*, suggesting AST's potential use in the prevention of various diseases, especially in cancer [255]. Recently, AST was reported to increase chromosomal stability and normalize the epigenetic modifications in oocyte maturation [305]. In addition, we previously reported that AST shows synergistic antioxidant effects with polyunsaturated fatty acids at low concentrations via the Nrf2/ARE pathway [304]. However, there is a lack of experimental evidence that shows the epigenetic effects of AST in prostate cancer cells. Therefore, the aim of this study was to further elucidate the molecular mechanism of AST in epigenetic regulation by investigating the role of AST in

restoring the expression of Nrf2 and *GSTP1* through epigenetic modification in human prostate LNCaP cells.

Previous findings have demonstrated that Nrf2 regulates the expression of antioxidant and phase II detoxifying enzymes, including NQO1, HO-1, and GSTs, to induce cytoprotective effects [269]. In addition, deficiency in Nrf2 is correlated to increased susceptibility to carcinogenesis; the induction of cytoprotective enzymes is one important approach to preventing cancers [314]. Therefore, the control of the transcriptional activation of Nrf2 and its target genes appears to be involved in an important mechanism that protects against cellular injuries from oxidative stress, especially via GSTs [269]. The down-regulation of Nrf2 appears to be responsible for the reduced GST expression, elevated oxidative stress and DNA damage in prostate tumorigenesis [299]. GST genes are down-regulated in primary tumors but not in metastatic tumors; *GSTP1* silencing is mediated by promoter DNA hypermethylation in TRAMP tumors [315]. However, the 5' regions of GST genes showed no significant differences between normal prostatic epithelial cells and prostate tumors in TRAMP mice by MassARRAY Quantitative DNA Methylation Analysis (MAQMA) [315]. In our previous study, we showed that the epigenetic reactivation of Nrf2 results in the inhibition of the transformation of JB6 P+ cells [140]. Nrf2 and members of the GST family are decreased in human prostate cancer [299]. The absence of *GSTP1* gene expression has been reported in high-grade prostate intraepithelial neoplasia, and the methylation of its promoter region has

been identified in 90% of cancer samples and 70% of prostate intraepithelial neoplasia samples [300]. Among extensively studied mechanisms, epigenetic changes, including DNA methylation and chromatin modifications, have been found to play an important role in tumorigenesis [316]. Dietary phytochemicals with chemopreventive effects, including curcumin [317] and genistein [318], have been demonstrated to regulate epigenetic activity. Natural dietary compounds have shown beneficial effects in reversing these abnormal epigenetic changes to target tumor-specific abnormal DNA methylation.

In this study, we investigated the effects of AST on epigenetic modification enzymes and whether AST could restore the abnormal epigenetic changes of Nrf2 and *GSTP1* genes. AST treatment increased Nrf2 and *GSTP1* expression at the mRNA level (Figure 3.3). Treatment with AST did not affect the protein expression levels of Nrf2, NQO1 or GSTP1 significantly in LNCaP cells (Figure 3.4). Bisulfite sequencing is more specific in identifying the CpG methylation status of Nrf2 and *GSTP1*. The role of CpG methylation in the suppression of Nrf2 and *GSTP1* expression and activation was tested by treatment with 5-aza and TSA in LNCaP cells. AST significantly decreased the methylation of twenty-one CpG sites of *GSTP1,* suggesting a correlation between methylation and increased GSTP1 expression.

In conclusion, this study shows for the first time that AST demethylated the hypermethylation of CpG sites in *GSTP1* but not the Nrf2 CpG island region *in vitro*

and reactivate their mRNA expression levels in human LNCaP prostate cancer cells. Epigenetic regulation is considered to be more amenable than restoring genetic mutations [319]. Further studies of the methylation profiles from a large number of primary tumor samples will provide important information on the role of the methylation of the CpG islands of Nrf2 and *GSTP1*, which could be used as preventive and therapeutic targets to treat prostate cancer in future clinical trials. In addition, our current study suggests that AST can demethylate some promoters of specific genes and may promote the stability of the entire chromatin structure; it will be interesting to study AST's effects on the methylation status of the whole genome.

3.5 Figures and Tables

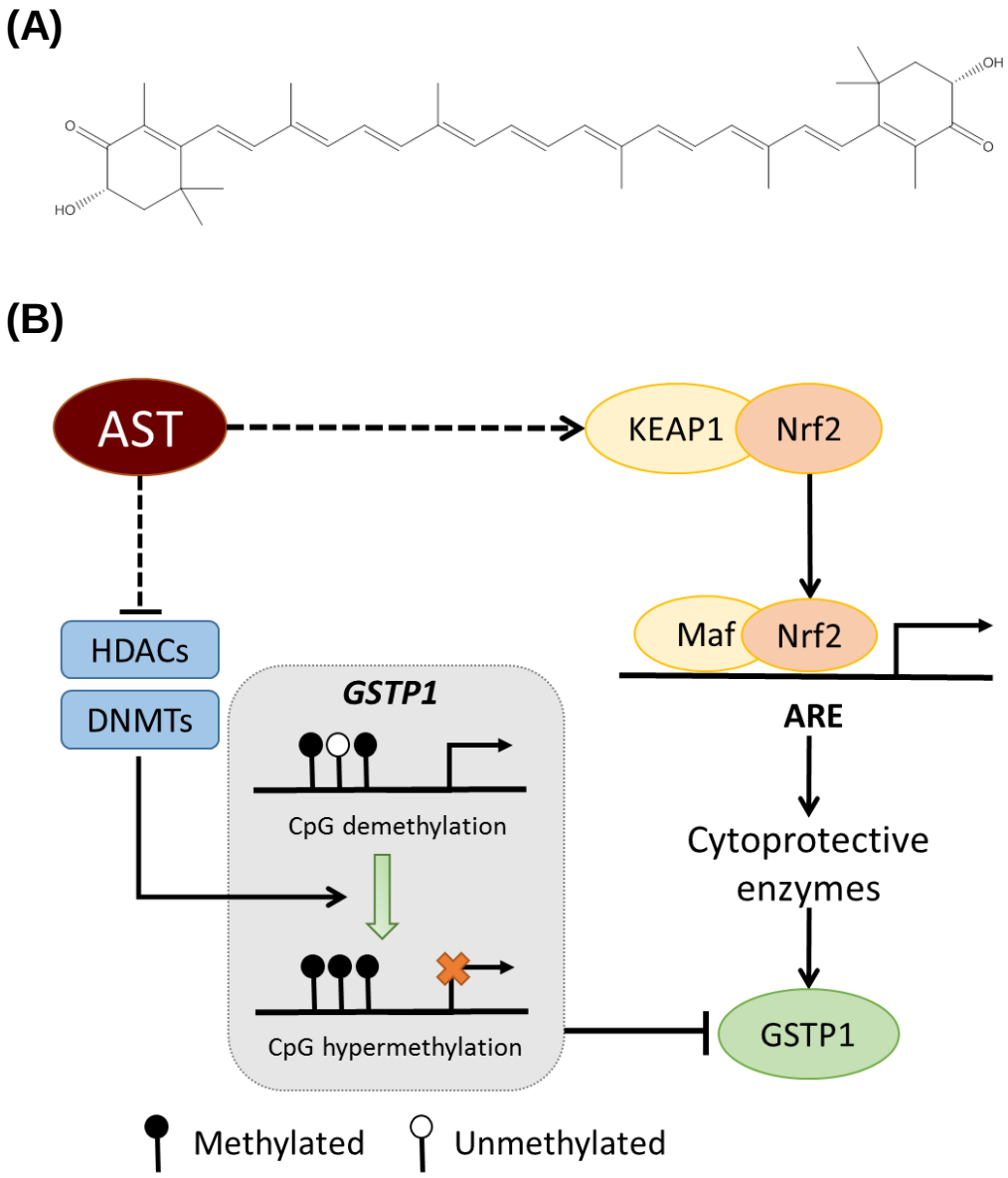

Figure 3.1. Schematic diagram of the structure of AST and its mechanism of action.

(A) Chemical structure of AST. (B) Effects of AST on DNA methylation and activation of Nrf2/ARE pathway.

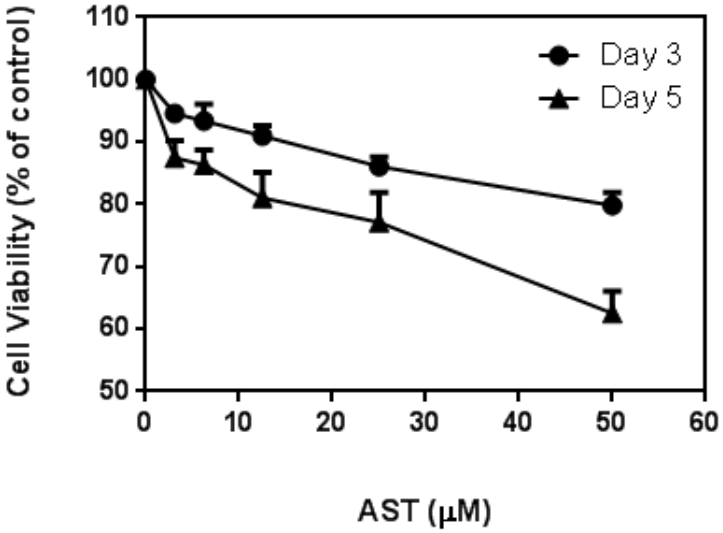

Figure 3.2. Cell viability of LNCaP cells after treatment with AST.

Cells were treated with various concentrations of AST for three or five days as described in the *Materials and Methods* section. Cell viability was determined by the MTS assay. The data are presented as the mean ± SEM.

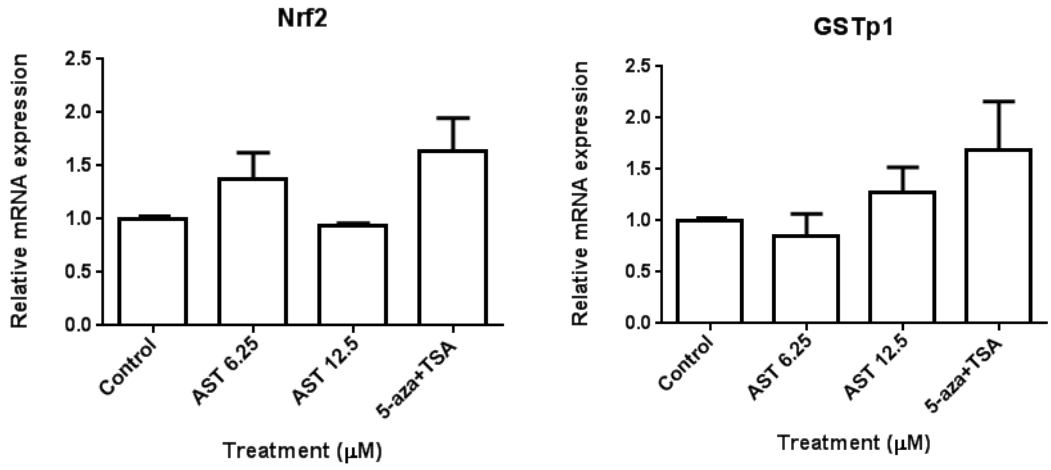

Figure 3.3. Effects of AST on the mRNA expression of Nrf2 and GSTp1 in LNCaP cells.

Cells were treated with various concentrations of AST (6.25 μM and 12.5 μM) or 5-aza (2.5 μM) in combination with TSA (500 nM) for five days. The data are expressed as the mean ± SEM. GAPDH was used as an endogenous housekeeping gene.

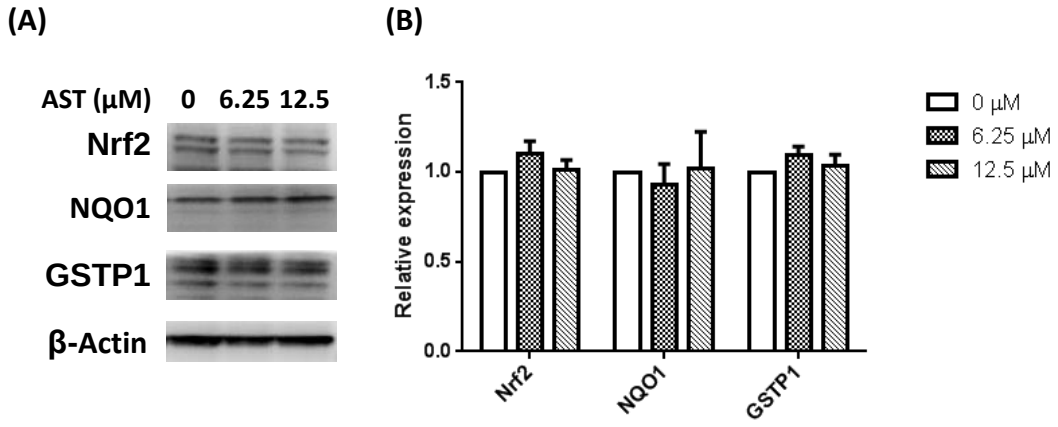

Figure 3.4. Effects of AST on the decreased protein expression of Nrf2 and the downstream proteins NQO1 and GSTP1.

LNCaP cells were treated with various concentrations of AST or 5-aza + TSA for five days as described in the Materials and Methods section. (A) Representative figure of the protein expression levels of Nrf2, NQO1 and GSTP1 determined by western blotting, with β-actin as a loading control. (B) Quantification by densitometry from at least three independent experiments. The results are presented as the mean ± SEM.

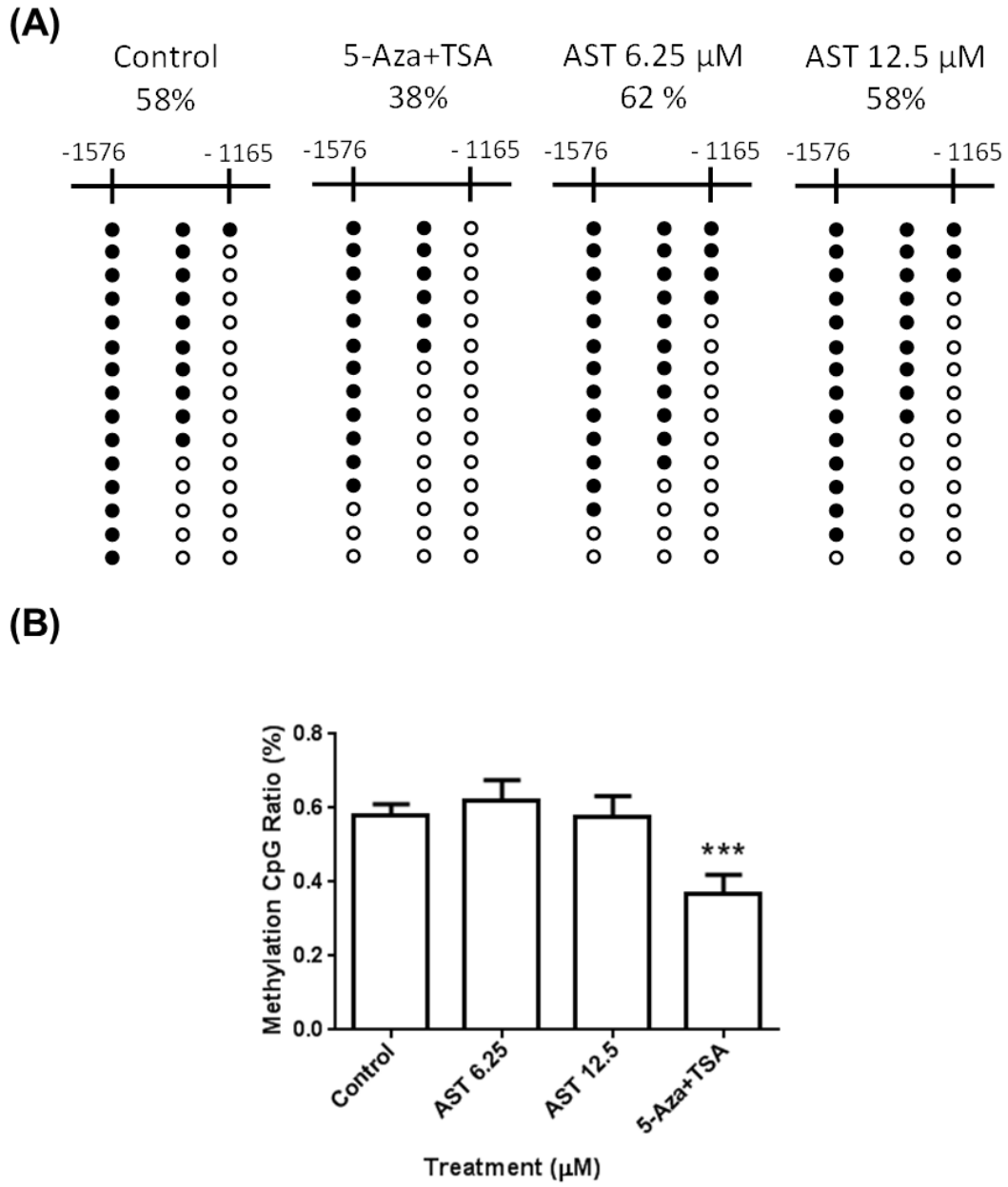

Figure 3.5. Effects of AST on the methylation status of the Nrf2 promoter region in LNCaP cells.

Genomic DNA was extracted from cells treated with various concentrations of AST or 5-aza in combination with TSA for 5 days. The methylation patterns of the three CpG sites located at positions –1576 to –1165 from the TSS (defined as position 1) in the Nrf2 promoter, were determined by bisulfite genomic sequencing, as

described in the Materials and Methods section. (A) A representative figure of 15 clones to show the methylation profile of these three CpG sites. Filled dots represent methylated CpGs, and open circles represent unmethylated CpGs. (B) To estimate the total percentage of methylated CpG sites, the number of methylated dots was counted and divided by the total number of dots. At least 10 clones from each replicate and at least three independent replicates were analyzed. The data are expressed as the mean ± SEM. ***, $P < 0.001$ compared to the control group. Student's t-test was used to calculate the significance of differences compared to the control.

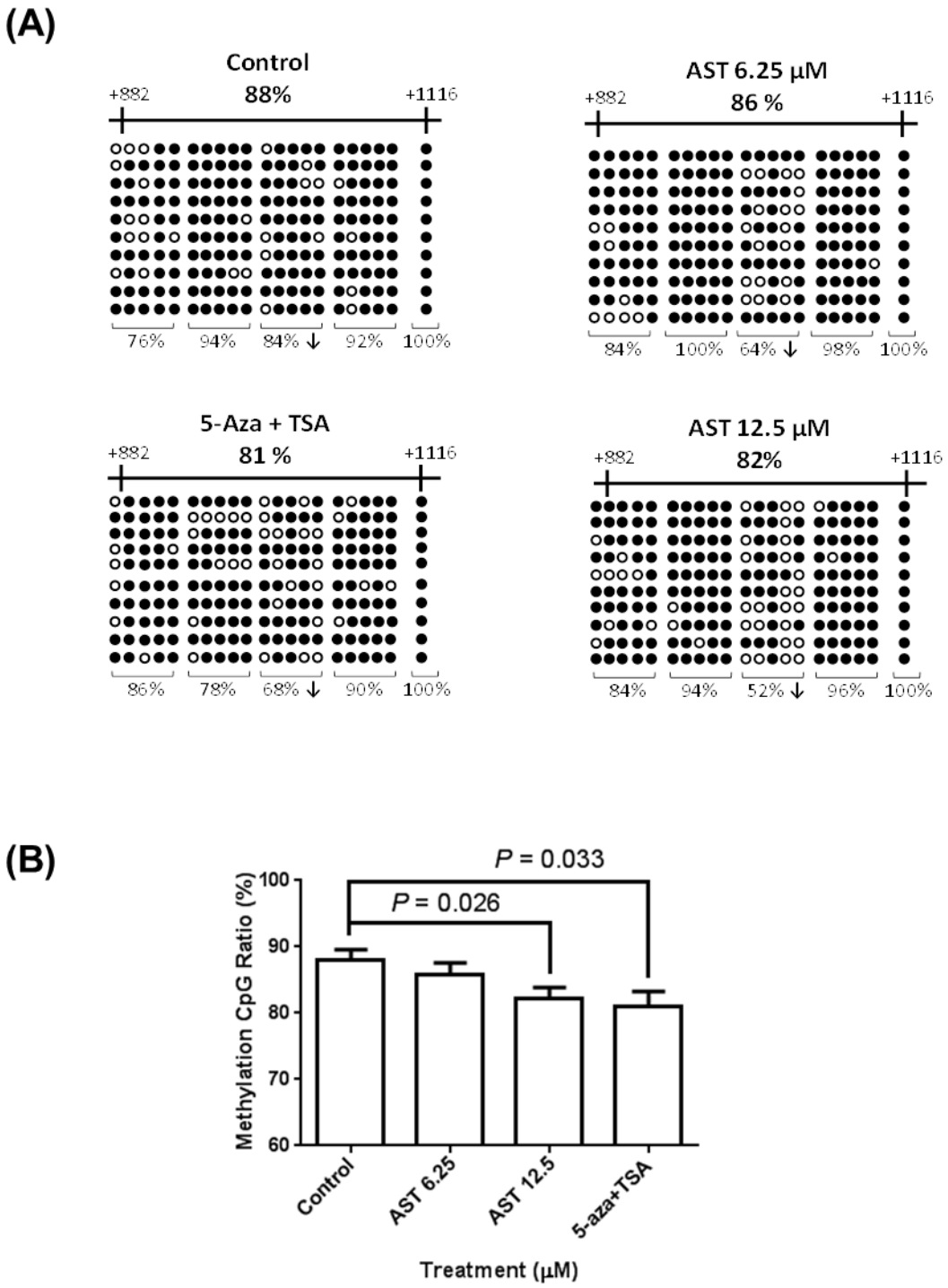

Figure 3.6. Effects of AST on the methylation of *GSTP1* in LNCaP cells.

Genomic DNA was extracted from cells treated with various concentrations of AST or 5-aza in combination with TSA for 5 days. The methylation patterns of the 21 CpG sites located at positions +882 to +1116 from the TSS (defined as position 1) in

the GSTp1 promoter were determined by bisulfite genomic sequencing as described in the *Materials and Methods* section. (A) A representative figure of 10 clones to show the methylation profile of these 21 CpG sites. Filled dots represent methylated CpGs, and open circles represent unmethylated CpGs. To estimate the percentage of methylated CpGs, the number of methylated CpGs from these ten representative sequences was counted and divided by the total number of dots for five CpG sites. (B) To estimate the total percentage of methylated CpG sites, the number of methylated dots was counted and divided by the total number of dots. At least 10 clones from each replicate and at least three independent replicates were analyzed. The data are expressed as the mean ± SEM. Student's *t*-test was used to calculate the significance of differences compared to the control.

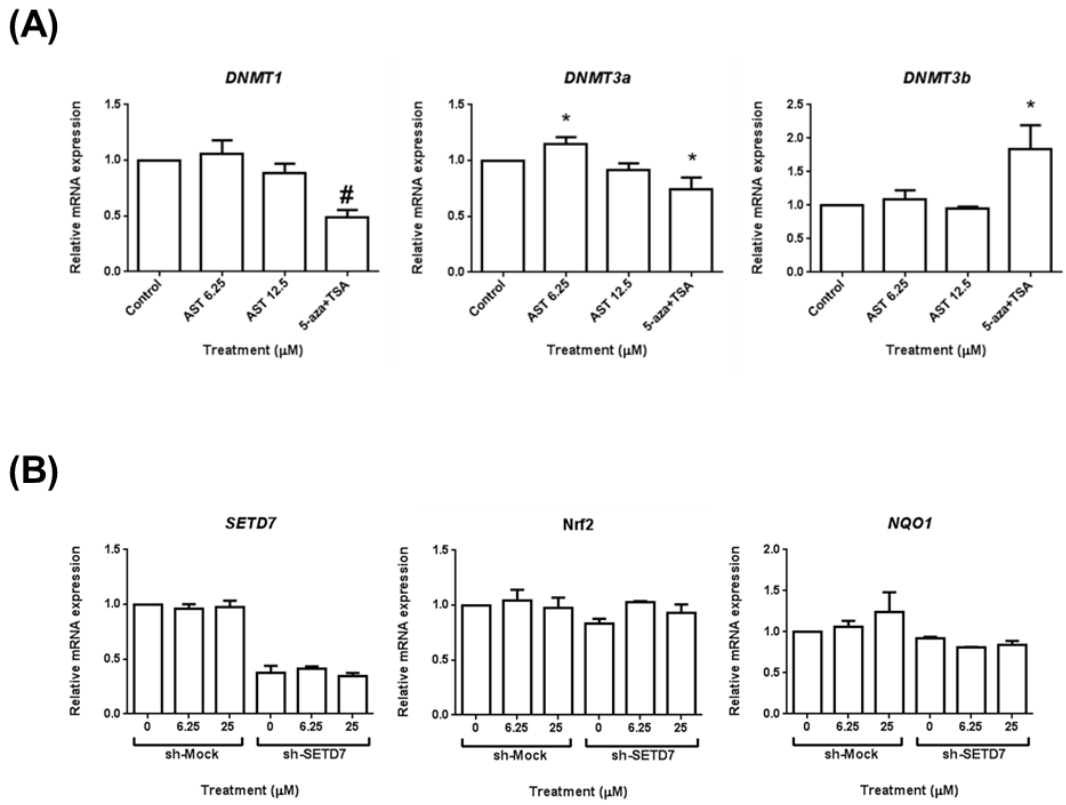

Figure 3.7. Effects of AST on the relative endogenous mRNA expression of DNMTs, SETD7, Nrf2 and NQO1 in LNCaP cells.

(A) RNA was extracted from cells treated for 5 days with various concentrations of AST or 5-aza in combination with TSA for five days in LNCaP cells, as described in the *Materials and Methods* section. (B) Lentivirus-mediated short hairpin RNAs were used to establish stable mock (scramble control, sh-Mock) and SETD7 (SETD7) knockdown (sh-SETD7) LNCaP cells. Total RNA was extracted from treated sh-Mock and sh-SETD7 cells with 0.1% DMSO or AST for 24 hours. The data are expressed as the mean ± SEM. GAPDH was used as an endogenous housekeeping gene.

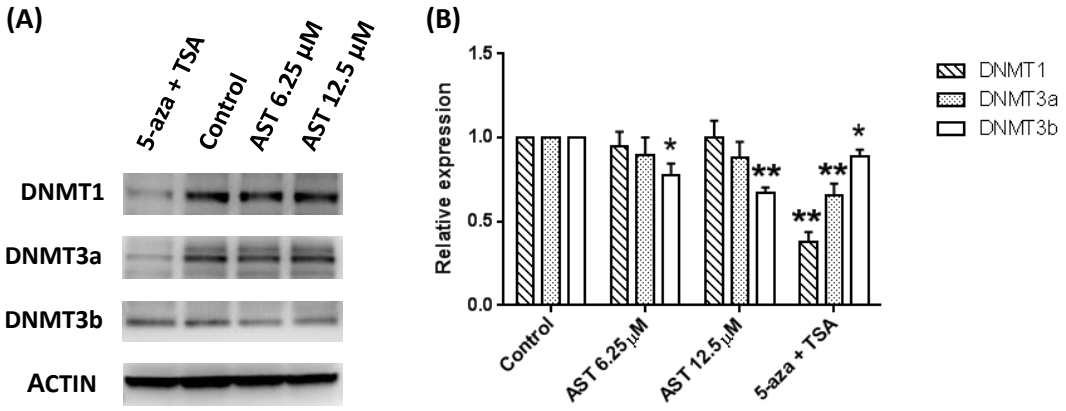

Figure 3.8. Effects of AST on decreasing the protein expression of DNMTs.

LNCaP cells were treated with various concentrations of AST or 5-aza+TSA for 5 days. (A) Representative figure of the protein expression levels of DNMT1, DNMT3a and DNMT3b determined by western blotting, with *β*-actin as a loading control. (B) Quantification by densitometry from at least three independent experiments. The results are presented as the means ± SEM. Student's *t*-test was used to calculate the significance of difference compared to the control. *, $P < 0.05$; **, $P < 0.01$.

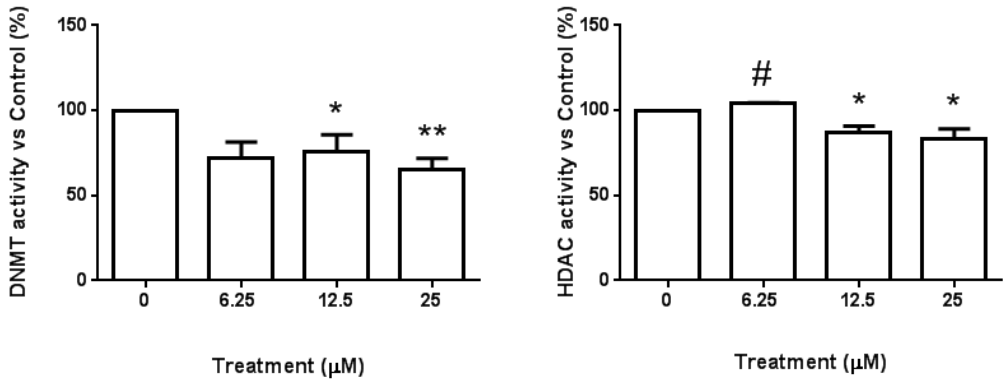

Figure 3.9. Effects of AST on decreasing the activity of DNMTs and HDACs.

The DNMT and HDAC activities were calculated following the manufacturer's protocol and were based on the ratio of the AST treatment group to the control. The results are presented as the mean ± SEM. Student's *t*-test was used to calculate the significance of differences compared to the control. *, $P < 0.05$; **, $P < 0.01$; #, $P < 0.001$.

Table 3.1. The primer set for qPCR

Primer	Sequence (5'→ 3')
NRF2 F	CAAAAGGAGCAAGAGAAAGCC
NRF2 R	TCTGATTTGGGAATGTGGGC
SETD7 F	TCACGGAGAAAAGAACGGACG
SETD7 R	ATCATCCACATAATACCCCTCCA
NQO1 F	TCACCGAGAGCCTAGTTCC
NQO1 R	TCATGGCATAGTTGAAGGAACG
GSTP1 F	CCCTACACCGTGGTCTATTTCC
GSTP1 R	CAGGAGGCTTTGAGTGAGC
DNMT1 F	AGGCGGCTCAAAGATTTGGAA
DNMT1 R	GCAGAAATTCGTGCAAGAGATTC
DNMT3a F	CCGATGCTGGGGACAAGAAT
DNMT3a R	CCCGTCATCCACCAAGACAC
DNMT3b F	AGGGAAGACTCGATCCTCGTC
DNMT3b R	GTGTGTAGCTTAGCAGACTGG
GAPDH F	ACATCGCTCAGACACCATG
GAPDH R	TGTAGTTGAGGTCAATGAAGGG

4 Nrf2 null enhances UVB-induced skin inflammation and extracellular matrix damages in C57/BL6 mice[10][11][12]

4.1 Introduction

The incidence of non-melanoma skin cancer has steadily increased, and ultraviolet (UV) light is one of the major causes of non-melanoma skin cancer. In fact, UV-induced non-melanoma skin cancer is the most common type of cancer in the US and worldwide [320, 321]. UVB is the most potent form of UV radiation; exposure to UVB radiation both burns the skin and drives the initiation, promotion, and progression of skin carcinogenesis [322]. UV irradiation induces the delayed expression of UV-responsive genes such as matrix metalloproteinases (MMPs), which degrade macromolecular components of the extracellular matrix (ECM), and these changes represent a hallmark of carcinogenesis and aging [323]. Moreover, altered ECM metabolism has been implicated in various diseases [324]. Oxidative stress, such as that caused by excessive reactive oxygen species (ROS), is caused by UVB damage to DNA, protein, and lipids and can lead to inflammation, gene mutation, and immunosuppression [292, 325]. Due to the critical role of ROS in

[10] Part of this chapter has been published as an original research paper: Saw, C. L., **Yang, A. Y.**, Huang, M. T., Liu, Y., Lee, J. H., Khor, T. O., Su, Z. Y., Shu, L., Lu, Y., Conney, A. H., & Kong, A. N. (2014). Nrf2 null enhances UVB-induced skin inflammation and extracellular matrix damages. *Cell Biosci*, 4(1), 39.

[11] Keywords: Nuclear factor (erythroid-derived 2)-like 2 (NFE2L2 or Nrf2), Ultraviolet, Inflammation, p53, pro-MMP-9, MIP-2, ECM

[12] Abbreviations: DMBA, 7,12-dimethylbenz(a)anthracene; ECM, extracellular matrix; HO-1, heme oxygenase-1; MMP, matrix metalloproteinases; MIP-2, macrophage inflammatory protein-2; NFE2L2 or Nrf2, nuclear factor erythroid-2 (NF-E2)-related factor 2; NF-κB, nuclear factor kappa B; ROS, reactive oxygen species; TPA, 12-O-tetradecanoylphorbol-13-acetate; UV, ultraviolet.

UVB-induced photo-carcinogenesis, ROS detoxification mechanisms have emerged as effective approaches for cancer prevention [326]. Nuclear factor erythroid-2 (NF-E2)-related factor 2 (Nrf2), a member of the cap ‘n’ collar family of redox-sensitive bZIP (basic leucine zipper) proteins, is the major transcriptional regulator of the expression of genes encoding phase II detoxifying/antioxidant enzymes, including heme oxygenase-1 (HO-1) [292]. HO-1 exhibits broad cytoprotective effects in various inflammatory diseases [327] and was shown to play a critical protective role in limiting oxidative damage in a UVB-induced model [328]. MMP-9 was reported to be upregulated in angiogenic dysplasias and invasive cancers of the epidermis in a mouse model of multistage tumorigenesis. Notably, MMP-9 is predominantly expressed in neutrophils, macrophages, and mast cells rather than oncogene-positive neoplastic cells [329]. It has also been reported that the disruption of Nrf2 enhanced the up-regulation of key inflammatory transcription factors, such as nuclear factor kappa B (NF-κB) and MMP-9 [330], and increased expression of macrophage inflammatory protein-2 (MIP-2), a neutrophil chemotactic factor, was observed in response to 12-O-tetradecanoylphorbol-13-acetate (TPA)-induced epidermal hyperplasia in mice [331]. The p53 tumor suppressor gene plays an important role in protecting cells against DNA damage and strand breaks [332], and the impact of UVB on p53 has been experimentally verified [333]. Moreover, p53 is known to be activated by DNA damage [332], oxidative stress [334], and inflammation [335, 336].

We previously reported the critical role of nuclear Nrf2 in the classical 2-stage model of skin carcinogenesis induced by the chemical carcinogen 7,12-dimethylbenz(a)anthracene (DMBA) and the tumor promoter TPA in Nrf2 knockout (Nrf2 KO) and wild-type (WT) mice [297]. We also recently reported that Nrf2 plays an important role in the SFN-mediated protective effects against UVB-induced inflammation [296]. To explore the potential impact of Nrf2 on UVB-induced inflammatory ECM damage in the skin, we studied the potential biomarkers involved in ECM degradation and inflammation in Nrf2 KO and WT mice, as these markers may be relevant to human skin carcinogenesis and photoaging [326, 337-340]. Based on this context, our current study aimed to ascertain the role of Nrf2 in UVB-induced ECM damage by focusing on inflammation and DNA repair in Nrf2 KO and Nrf2 WT mice.

4.2 Materials and Methods

4.2.1 Animals

Male and female Nrf2 KO and WT C57BL/6 mice were obtained as previously described [297]. The offspring of the eighth generation of Nrf2 KO mice on the C57BL/6 background were used in this study. The genotype of each animal was confirmed using DNA extracted from the tail and analyzed by PCR. Nrf2 WT mice were purchased from The Jackson Laboratory (Bar Harbor, ME, USA). Mice were housed at the Rutgers Animal Facility, maintained under 12-h light/dark cycles, and

provided *ad libitum* access to food and water. All animal procedures were approved by the Institutional Animal Care and Use Committee.

4.2.2 UV lamps

To induce skin inflammation, animals received a single dose of UVB light (300 mJ/cm^2) as previously described [296, 341]. These UV lamps (FS72T12-UVB-HO; National Biological Corp., Twinsburg, OH, USA) emit little or no radiation < 280 nm and > 375 nm. The lamps emit UVB (280-320 nm; 75-80% of total energy) and UVA (320-375 nm; 20-25% of total energy), as described in our previous studies [296, 341]. The dose of UVB was quantified using a UVB Spectra 305 dosimeter (Daavlin Co., Bryan, OH, USA). The radiation was calibrated with an IL-1700 research radiometer/photometer (International Light Inc., Newburyport, MA, USA).

4.2.3 Experimental design

Experiments were performed in Nrf2 WT and KO mice to determine whether a single dose of 300 mJ/cm^2 UVB irradiation would be sufficient to induce inflammatory reactions in the skin. Seven days after UVB irradiation, ear punches (6 mm in diameter) were obtained and weighed. Two sets of experiments were conducted in Nrf2 WT and KO mice after UVB exposure (at 8 h and 8 days). For each experiment, 4 groups of mice were evaluated: (1) no UVB in Nrf2 WT mice; (2) UVB in Nrf2 WT mice; (3) no UVB in Nrf2 KO mice; and (4) UVB in Nrf2 KO mice. A minimum of three animals was included in each group. The hair on the dorsal region of each mouse was removed 2 days before UVB irradiation, as

previously described [296]. At the end of the experiment, the mice were sacrificed by cervical dislocation, and the skin samples were frozen in liquid nitrogen and stored at -80ºC.

4.2.4 Preparation of skin specimens and histological examination

Skin samples were obtained from the dorsal area of the mouse and were placed in 10% phosphate-buffered formalin at room temperature overnight. The samples were then dehydrated in increasing concentrations (80, 95, and 100%) of ethanol, cleared in xylene, and embedded in Paraplast Plus (Fisher Scientific, Pittsburgh, PA, USA). Four-micrometer serial sections were cut from the skin block, deparaffinized, rehydrated, and stained with hematoxylin and eosin (H&E). The H&E sections were examined under a light microscope (Nikon Eclipse E600, Japan).

4.2.5 ELISA for pro-inflammatory proteins and p53

The protein levels of pro-inflammatory cytokines and p53 were determined using two-site sandwich enzyme-linked immunosorbent assays (ELISAs). Dorsal skin tissues were homogenized in phosphate-buffered saline (PBS) containing 0.4 M NaCl, 0.05% Tween-20, 0.5% bovine serum albumin, 0.1 mM phenylmethylsulphonyl fluoride, 0.1 mM benzethonium chloride, 10 mM EDTA, and 200 KIU aprotinin per mL. The homogenates were centrifuged at 12,000 ×g for 15 min at 4ºC. The supernatant was used for the determination of cytokines levels. Pro-matrix metalloproteinase-9 (pro-MMP-9; DY909), macrophage inflammatory

protein-2 (MIP-2; DY452), and p53 (DYC1746-2) kits were purchased from R&D Systems, Inc. (Minneapolis, MN, USA).

4.2.6 Western blotting

The protein samples were prepared as described above for the ELISAs. The protein concentration was measured using Bio-Rad protein assay reagent (Hercules, CA, USA). Equal amounts of protein (20 μg) from each sample were loaded onto a homemade 10% Tris/glycine SDS-polyacrylamide gel containing 0.1% SDS and run at 200 V for 1 h. The proteins were transferred to a nitrocellulose membrane by electroblotting using a Bio-Rad semidry transfer blotting apparatus over 1.5 h at 90 V (Bio-Rad, Hercules, CA, USA). The membrane was blocked with blocking buffer (Odyssey system, LI-COR Biosciences, Lincoln, NE, USA) for 1 h at room temperature. The primary antibodies were diluted in the same blocking buffer and were added to detect the target proteins. After an overnight incubation at 4ºC, the membrane was washed with TBST (Tris-buffered saline and 0.05% Tween-20) and then incubated with the secondary antibody. Finally, the target protein bands were visualized with an Odyssey infrared imager. Antibodies against β-actin and HO-1 were purchased from Santa Cruz Biotechnology, Inc. (CA, USA). Densitometry was performed using the Image J software (version 1.44, National Institute of Health, USA). The relative protein expression was obtained by first calculating the relative intensity compared to the control (no UVB treatment) sample on the same blot and then normalizing this value to the intensity of β-actin from the same sample.

4.2.7 Data presentation and statistical analysis

The data are presented as the mean ± standard error of the mean (SEM), except as otherwise stated. Student's *t*-test was used to determine statistically significant differences between groups. A p value < 0.05 was considered statistically significant.

4.3 Results

4.3.1 A single dose of 300 mJ/cm^2 UVB significantly increased the ear biopsy weight, and Nrf2 KO mice were more susceptible to UVB-induced skin edema

To determine the effect of Nrf2 on UVB-induced trauma to mouse skin, we irritated mouse skin with a single dose of UVB (300 mJ/cm^2) and measured the ear biopsy weight 1 week after exposure. In the untreated group, the average ear weights of the Nrf2 WT and KO mice were 7.28 ± 0.23 mg and 6.57 ± 0.36 mg, respectively. In the UVB-treated group, these weights increased to 8.45 ± 0.48 mg in Nrf2 WT mice and to 13.13 ± 0.08 mg in Nrf2 KO mice (Figure 4.1A). UVB exposure significantly increased the ear biopsy weight in Nrf2 KO mice by nearly 100%, whereas there was only a 16% increase observed in Nrf2 WT mice. The ear biopsy weight ratio indicated that Nrf2 KO mice were more susceptible to UVB-induced skin edema (Figure 4.1B). These data demonstrated that a single dose of UVB (300 mJ/cm^2) was sufficient to cause UVB-induced inflammatory damage to mouse skin, especially in Nrf2 KO mice. This single dose of UVB was used in all the following experiments.

4.3.2 The absence of Nrf2 gene expression increased the UVB-induced skin thickness

To determine the effect of Nrf2 in mouse skin exposed to UVB irritation, we treated the dorsal skin area with a single dose of UVB (300 mJ/cm^2) and took a skin biopsy 8 days later. Nrf2 KO mice exhibited a significant increase in skin thickness 8 days after UVB irradiation (Figure 4.2), and a single dose of UVB (300 mJ/cm^2) led to a greater increase in skin thickness in Nrf2 KO mice compared to Nrf2 WT mice (Figure 4.2).

4.3.3 Nrf2 KO mice were significantly more susceptible to UVB-induced inflammation and ECM degradation

To characterize the UVB-induced inflammatory damage to the ECM, we measured the expression of biomarkers related to inflammation (MIP-2) and ECM degradation (pro-MMP-9) 8 h after UVB exposure. A single dose of UVB (300 mJ/cm^2) significantly upregulated the protein expression of MIP-2 and pro-MMP-9 in both Nrf2 WT and KO mice (Figure 4.3A and C). However, after UVB irradiation, these biomarkers were more significantly upregulated in Nrf2 KO mice compared to WT mice (Figure 4.3B and D).

4.3.4 Nrf2 KO mice were more susceptible to UVB-induced upregulation of p53

To evaluate sustained DNA damage, we examined p53 protein expression 8 h after UVB irradiation. In both Nrf2 WT and KO mice, a single dose of UVB (300 mJ/cm^2) significantly increased p53 protein expression compared to untreated skin

(Figure 4.4). However, there was a greater increase in p53 expression in Nrf2 KO mice compared to Nrf2 WT mice.

4.3.5 UVB increased expression of the Nrf2 target HO-1, an antioxidant biomarker, in Nrf2 WT mice compared to Nrf2 KO mice

To elucidate the mechanism responsible for the photo-protective effect of Nrf2 in UVB-exposed mice, Nrf2 WT and KO mice were exposed to UVB irradiation and sacrificed 8 h later. We measured the expression of HO-1, an anti-oxidative enzyme downstream of Nrf2, in Nrf2 WT and KO mice and compared these levels to those observed in untreated control Nrf2 WT and KO mice. Compared to untreated WT mice, HO-1 protein expression was significantly increased in UVB-treated Nrf2 WT mice ($P < 0.05$), whereas HO-1 expression was not significantly altered in Nrf2 KO mice (Figure 4.5). In particular, UVB exposure increased HO-1 expression by 43% in Nrf2 WT mice, which was much higher than the 24% increase observed in Nrf2 KO mice.

4.4 Discussion and Conclusions

In the present study, we investigated the photo-protective role of Nrf2 in inflammation-mediated ECM damage induced by UV, and our results indicated that Nrf2 KO mice were more susceptible to UVB radiation. Erythema has long been used as an indicator of UV-induced inflammation [342] and has been characterized as a reliable, reproducible and quantitative measurement of the degree of UV-induced inflammation [343]. Thus, measuring the weight or thickness of

irritated skin is a reliable indicator of inflammation [296, 344]. The results presented here demonstrated that UVB exposure significantly increased the ear biopsy weight in Nrf2 KO mice by almost 100%, whereas the ear biopsy weight only increased by 16% in Nrf2 WT mice. Moreover, the ratio of ear biopsy weights suggested that Nrf2 KO mice were more susceptible to UVB-induced skin edema (Figure 4.1). In addition, Nrf2 KO mice exhibited a greater increase in skin thickness after UVB exposure (Figure 4.2), which suggested that the loss of Nrf2 resulted in increased sensitivity to UVB radiation, thereby implying that there was more active inflammation in Nrf2-deficient mice. Therefore, we performed various biological assays to demonstrate that the observed UVB-induced responses were related to inflammation, ECM stability, and DNA damage. It has been reported in *in vivo* studies of human skin that UV irradiation significantly affects the coordinated regulation of various MMPs; after a single exposure to UV, MMP-9 activity increased 4-fold compared to non-UV irradiated human skin in a time-dependent manner [345]. MIP-2, a key mediator of neutrophil recruitment, is involved in the early infiltration of neutrophils into UVB-exposed skin [346]. In our study, UVB irradiation significantly enhanced the expression of MIP-2 in both Nrf2 WT and KO mice (Figure 4.3A). However, the increase in MIP-2 expression was much greater in Nrf2 KO mice compared to WT mice (Figure 4.3B). These MIP-2 findings correlate with those of a previous study in which MIP-2 expression was increased in mice after UVB irradiation [346]. Photoaged skin displays prominent alterations in the

collagenous ECM of connective tissue [345], and the detrimental effects of ECM degradation include diminished structural integrity, impaired wound healing, loss of cell viability, and cancer metastasis [347]. There is growing interest in understanding the role of aberrant ECM modifications, especially regarding the "cancer stem cell niche" and the "metastatic niche" during key stages of cancer progression [292, 348]. Pro-MMP-9 expression was increased significantly in Nrf2 KO mice compared to WT mice (Figure 4.3C and D), and these results indicated that the absence of Nrf2 augmented the expression of matrix-degrading proteinases, including pro-MMP-9, in response to UVB irradiation. Furthermore, many ECM fragments that are created via degradation by various MMPs act as chemotactic factors that cause endothelial and inflammatory cells to migrate into areas of active tumor cell proliferation and growth [349]. Thus, the photo-protective effect of Nrf2 was mediated by a reduction in MMP-9 expression. The p53 tumor suppressor gene is typically activated by DNA damage [332], oxidative stress [334], and/or inflammation [335, 336], and we observed that both of Nrf2 WT and KO mice exhibited increased p53 expression in response to UVB exposure, although the p53 expression was higher in KO mice. Regarding the role of p53 in DNA repair, increased p53 expression correlates with increased DNA damage, suggesting that the loss of Nrf2 may fail to protect DNA but could enable abundant p53 to repair the DNA damage. Indeed, a previous study showed that the extent of DNA damage correlates with the amount of UV exposure in various skin cells and models [350].

In our study, the higher p53 expression observed in Nrf2 KO mice after UVB exposure could be an indicator of more sustained DNA damage in need of repair. HO-1 is a downstream antioxidant enzyme that is regulated by Nrf2 and has a broad cytoprotective effect in various inflammatory diseases and UVB irradiation [327, 328]. In our study, UVB exposure enhanced HO-1 expression by 43% in Nrf2 WT mice and by 24% in Nrf2 KO mice (Figure 4.5), which indicated that the photo-protective effect of Nrf2 was mediated by HO-1.

UVB irradiation induces aberrant biological responses, such as increased skin erythema and thickness, up-regulated expression of inflammatory and ECM-degrading enzymes, and augmented DNA damage. According to our results, these biological responses were milder in WT mice compared to Nrf2 KO mice. In addition, our UVB-induced mechanistic study revealed that the protective effect of Nrf2 was mediated by HO-1, and these findings suggest that Nrf2 plays a key role in protecting against UVB irradiation. Moreover, our study is the first to demonstrate that the photo-protective effect of Nrf2 is closely related to the inhibition of ECM degradation and inflammation through the overexpression of HO-1.

4.5 Figures and Tables

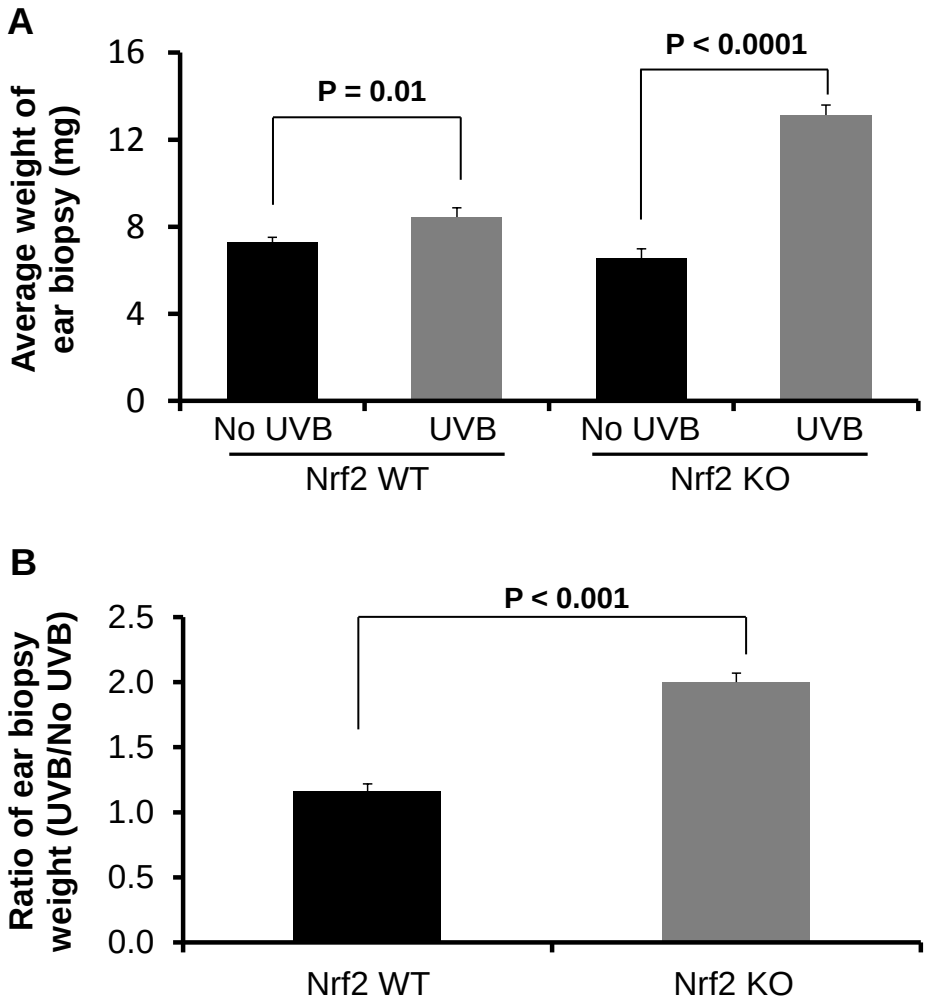

Figure 4.1. Ear biopsy weights in Nrf2 WT and KO mice after UVB exposure.

Nrf2 WT and KO mice were treated with or without a single dose of UVB (300 mJ/cm^2). The mice were sacrificed 1 week after UVB irradiation. Ear punches (6 mm in diameter) were taken and weighed. (B) The ratio of the ear punch weight in UVB-treated versus control skin suggested that Nrf2 significantly protected against the UVB-induced increase in ear punch weight ($P < 0.05$). The data are presented as the mean ± SEM.

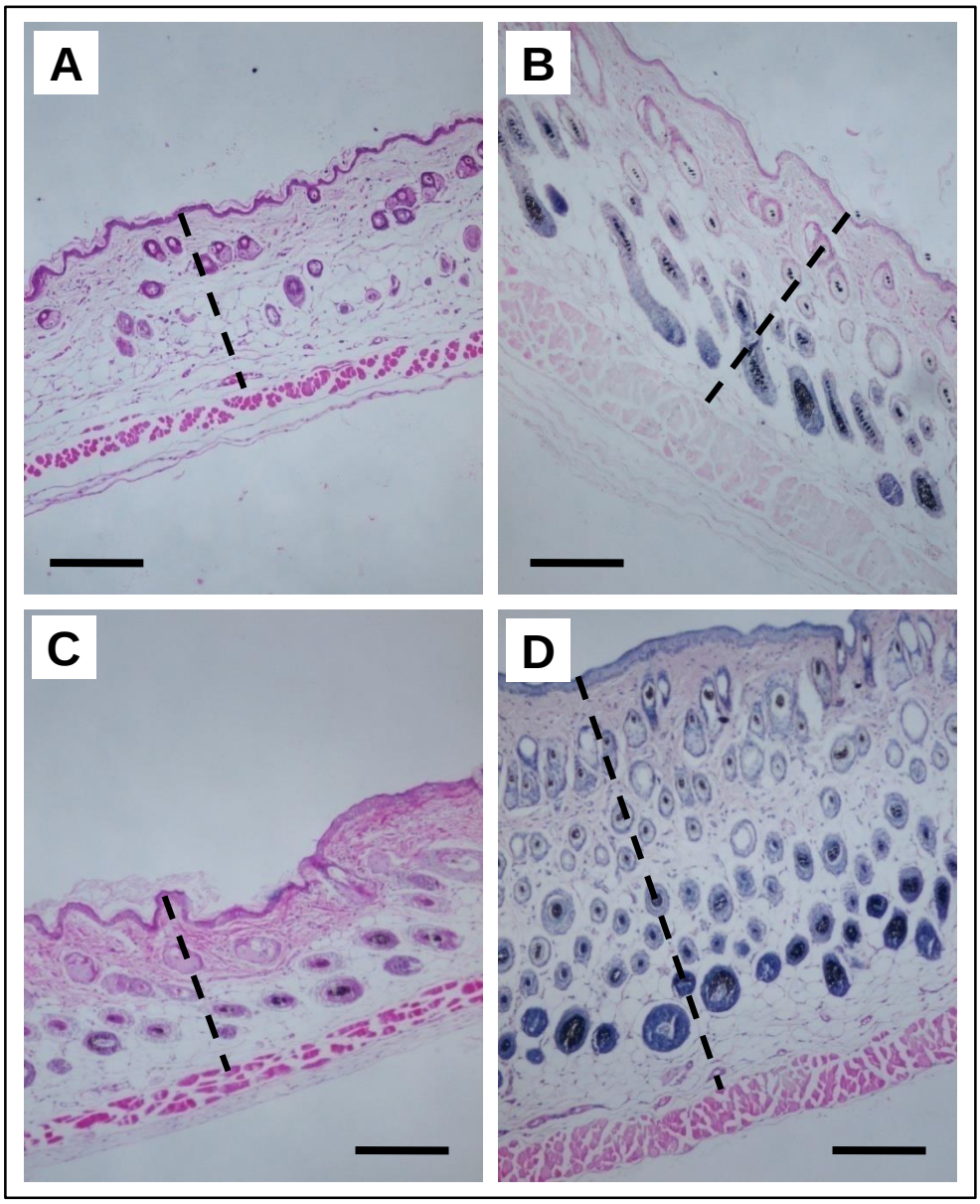

Figure 4.2 Skin thickness in Nrf2 WT versus Nrf2 KO mice after UVB exposure.

H&E staining was performed in skin samples 8 days after treatment with a single dose of UVB (300 mJ/cm^2). WT mice were treated (A) without UVB or (B) with UVB. KO mice were treated (C) without UVB or (D) with UVB. The horizontal line represents 200 μm, and the broken lines indicate the skin thickness. Original magnification, ×400. The Nrf2 KO mice exhibited more edema and inflammatory changes, such as increased skin thickness, whereas the Nrf2 WT mice demonstrated

fewer changes; these data correlated with the ear punch weights (Figure 4.1) and other biomarkers (Figure 4.3, Figure 4.4 and Figure 4.5).

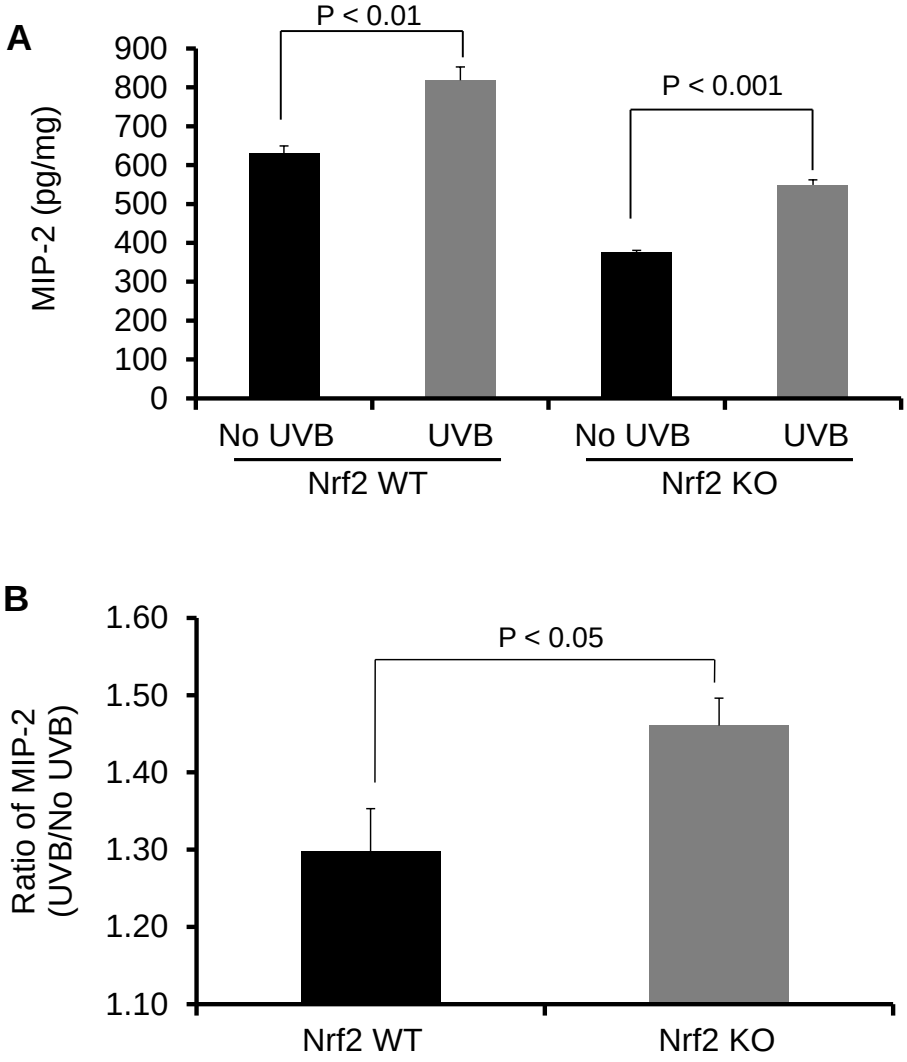
A
P < 0.01
P < 0.001
MIP-2 (pg/mg)
900
800
700
600
500
400
300
200
100
0
No UVB
UVB
No UVB
UVB
Nrf2 WT
Nrf2 KO
B
P < 0.05
Ratio of MIP-2 (UVB/No UVB)
1.60
1.50
1.40
1.30
1.20
1.10
Nrf2 WT
Nrf2 KO

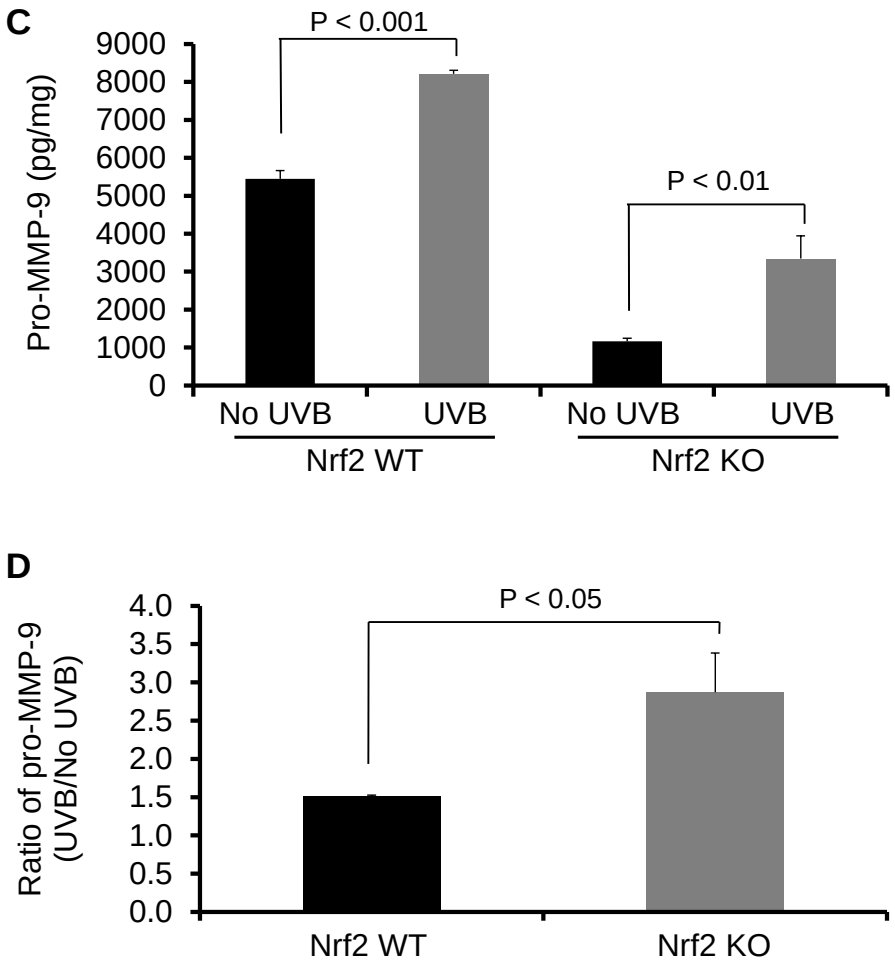

Figure 4.3. MIP-2 and Pro-MMP-9 expression in Nrf2 WT versus Nrf2 KO mice after UVB exposure.

Nrf2 WT and KO mice were irradiated with a single dose of UVB (300 mJ/cm2). After 8 h, (A) the MIP-2 expression and (B) the Pro-MMP-9 expression in WT and Nrf2 KO mice; (C) the ratios of MIP-2 protein levels and (D) the ratios of Pro-MMP-9 protein levels in UVB-treated versus control skin (No UVB-treated) were determined; Nrf2 significantly protected against UVB-induced the MIP-2 and pro-MMP-9 expression ($P < 0.05$). The data are presented as the mean ± SEM.

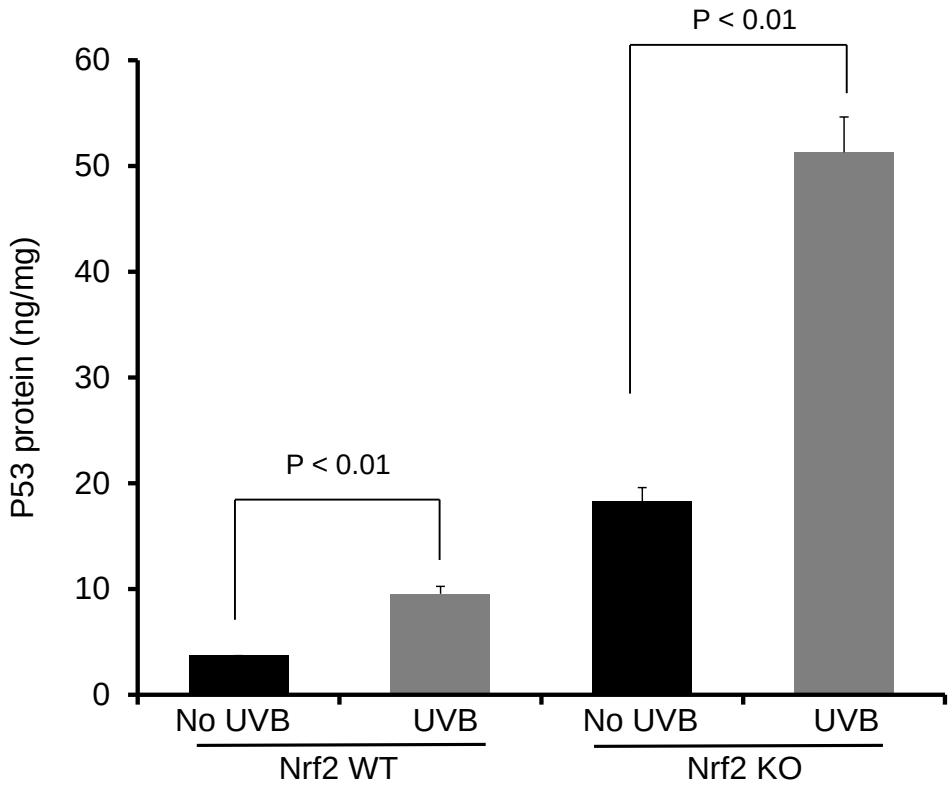

Figure 4.4. p53 expression in Nrf2 WT versus KO mice after UVB exposure.

Nrf2 WT and KO mice were irradiated with a single dose of UVB (300 mJ/cm^2). p53 protein levels increased in WT and KO mice 8 h after UVB irradiation; however, there was a greater increase in p53 expression in Nrf2 KO compared to WT mice. The data are presented as the mean ± SEM.

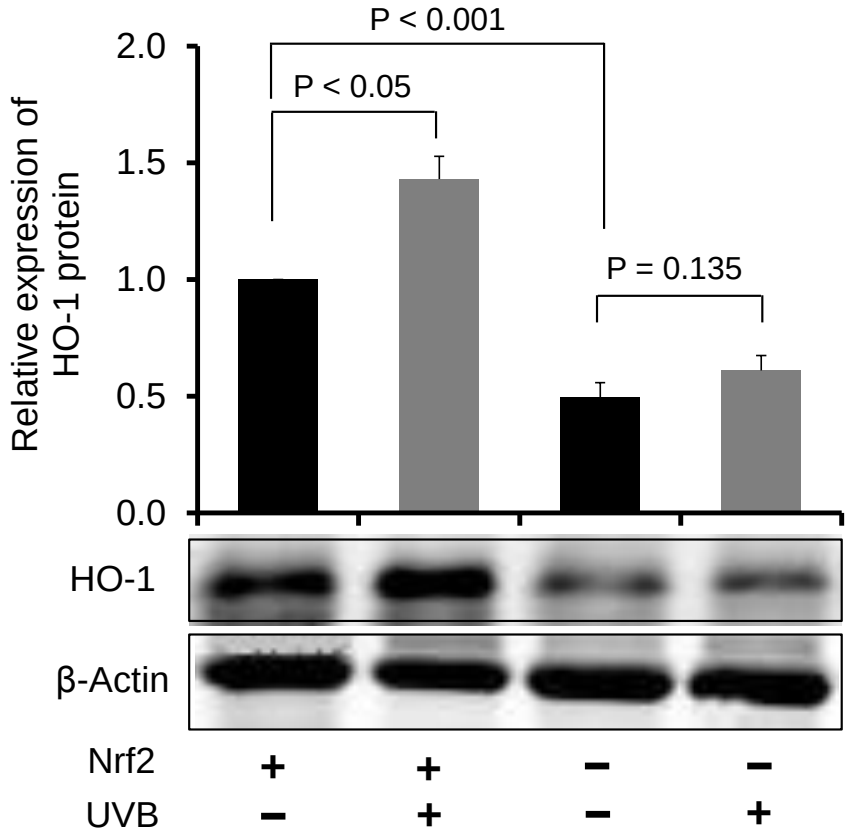

Figure 4.5. Nrf2-targeted antioxidant biomarkers in Nrf2 WT versus KO mice after UVB exposure.

Nrf2 WT and KO mice were irradiated with a single dose of UVB (300 mJ/cm^2). Expression of the Nrf2-regulated antioxidant protein HO-1 was measured in the skin. β-Actin served as the endogenous housekeeping protein. Protein samples (50 μg) were subjected to western blotting, and the relative intensity was calculated by dividing the intensity of the protein band in the control sample by that in the UVB-treated sample and then normalizing against the intensity of β-actin on the same membrane. After UVB irradiation, HO-1 expression was increased in WT mice but decreased in KO mice.

5 Genome-wide analysis of DNAmethylation in UVB- and DMBA/TPA-induced mouse skin cancer models [13][14][15]

5.1 Introduction

Accumulating evidence suggests that epigenetic DNA alterations play a crucial role in cancer initiation and development. Specifically, aberrant DNA methylation at the 5′-position of cytosine in CG dinucleotides in the cancer genome is postulated to be the most relevant epigenetic change in cancer [351]. DNA methylation affects gene expression and therefore regulates a wide range of biological processes, including proliferation, cell death, mutation and cancer initiation/promotion/progression [352, 353]. Both global hypomethylation and regional hypermethylation are characteristics of tumorigenesis [354, 355]. DNA hypermethylation at promoter regions is a predominant epigenetic mechanism for reducing the expression of tumor suppressor genes. Epigenetic silencing of tumor suppressor genes has been reported in mouse models of malignant tumors [356, 357]. Thus, the present study aimed to profile the global DNA methylation changes that occur during carcinogenesis. To address this aim, we conducted global profiling of

[13] Part of this chapter has been published as an original research paper: **Yang, A. Y.** [1], Lee, J. H. [1], Shu, L., Zhang, C., Su, Z. Y., Lu, Y., Huang, M. T., Ramirez, C., Pung, D., Huang, Y., Verzi, M., Hart, R. P., & Kong, A. N. (2014). Genome-wide analysis of DNA methylation in UVB- and DMBA/TPA-induced mouse skin cancer models. *Life Sci*, 113(1-2), 45-54. ([1] These authors contributed equally in this publication.)

[14] Keywords: DNA methylation, epigenetics, MeDIP-Seq, UVB, DMBA/TPA

[15] Abbreviations: MeDIP - Methylated DNA immunoprecipitation; UVB - Ultraviolet B; DMBA - 7,12-dimethylbenz(a)anthracene; TPA - 12-O-tetradecanoylphorbol-1,3-acetate; IPA - Ingenuity® pathway analysis; IL – Interleukin.

DNA methylation changes in two representative skin carcinogenesis models, ultraviolet B (UVB)-exposed SKH-1 hairless mice and DMBA/TPA-induced carcinogenesis in CD-1 mice.

Ultraviolet irradiation has been reported to induce epigenetic alterations, which may contribute to the development of skin cancer [358]. However, the precise mechanism by which UV irradiation is related to melanomagenesis remains unclear. In addition, a method for screening epigenetically modified genes in melanoma patients needs to be established [359, 360]. Mutations in oncogenes and tumor suppressor genes have been reported in melanoma. However, most of these mutations are not present in non-melanoma skin cancer [361], suggesting a specific role for UV irradiation in melanomagenesis. In skin tumors, UV irradiation has been reported to induce epigenetic modifications and may contribute to the development of skin cancer. Epigenetic changes, such as DNA methylation and histone modification, may play a crucial role in the initiation and development of certain types of cancer [362]. Epigenetic alterations generally represent the interface between the environment and the genome [363].

The multistage skin carcinogenesis model is established by applying a sub-threshold dose of the carcinogen DMBA followed by repetitive treatments with the tumor promoter TPA. With three well-defined stages—initiation, promotion, and progression—this model is similar to natural human tumor development. This model has been widely used to investigate the anti-tumor efficacy of chemicals and the

molecular events that occur during each stage of tumor development. Several genetic alterations identified in human skin cancer patients have also been described in the mouse multistage skin carcinogenesis model, such as changes in cyclin D1 [364], TP53 [365], CDKN21 [366] and PTEN [367]. The underlying similarity in the biology of cancer between mice and humans implies that genes related to mouse tumor development may also be relevant to human tumor development.

In the present study, we used methylated DNA immunoprecipitation (MeDIP) coupled with next-generation sequencing to profile the whole genome DNA methylation patterns from the UVB and DMBA/TPA models. The MeDIP-Seq results were evaluated by Ingenuity® Pathway Analysis (IPA) to investigate genetic crosstalk and signal/function overlap. The present study included an initial assessment of genes with a modified methylation profile and the identification of interacting molecular networks in skin carcinogenesis models.

5.2 Materials and methods

5.2.1 Chemicals and antibodies

The chemicals used in the current study were as follows: 7,12-dimethylbenz(a)anthracene (DMBA; Sigma-Aldrich, MO, USA) and 12-O-tetradecanoylphorbol-1,3-acetate (TPA; Alexis Co., CA, USA). The 5-methylcytidine monoclonal antibody was purchased from Eurogentec., Belgium.

5.2.2 Mice and skin cancer induction

Two representative skin carcinogenesis models were utilized in the present study. SKH-1 hairless female mice, 7-8 weeks old, were treated with UVB (30 mJ/cm^2) twice a week for 36 weeks. The UV lamps (FS72T12-UVB-HO; National Biological, Twinsburg, OH) emitted UVB (280-320 nm; 70-80% of the total energy) and ultraviolet A (320-375 nm; 20-75% of the total energy). The dose of UVB was quantified using a UVB Spectra 305 dosimeter (The Daavlin Company, Bryan, OH). The radiation was further calibrated using a research radiometer/photometer (model IL-1700; International Light Inc., Newburyport, MA). The mice were assessed twice weekly for the appearance of papillomas and carcinomas. Skin papilloma and carcinoma samples were collected, frozen in liquid nitrogen and stored at −80 °C. The epidermises of age-matched untreated mice were isolated from fresh skin as a control group.

Six-week-old female CD-1 mice were used for the DMBA/TPA-induced multistage carcinogenesis model. One day before treatment, the backs of the mice were shaved. For tumor initiation, 200 nmol DMBA in 200 μL of acetone was injected into the back skin of the mice. Three days after DMBA treatment, 5 nmol TPA in 200 μL of acetone was applied three times a week for 11 weeks to induce tumor promotion and progression.

5.2.3 Global analysis of methylated DNA

Genomic DNA (gDNA) was extracted from UV irradiation-induced tumor

samples from 3 female mice and from non-irradiated epidermis samples from 3 female age-matched SKH-1 mice; from female CD-1 mice in the DMBA/TPA-induced carcinogenesis model for the MeDIP-Seq assay. gDNA was extracted using a DNeasy Kit (Qiagen, Valencia, CA) according to the manufacturer's protocol. The gDNA was electrophoresed on an agarose gel, and the OD ratios were determined to confirm the purity and concentration of the gDNA prior to fragmentation by Covaris (Covaris, Inc., Woburn, MA USA). Fragmented gDNA was evaluated for size distribution and concentration using an Agilent Bioanalyzer 2100 and a NanoDrop spectrophotometer.

5.2.4 MeDIP-Seq

MeDIP was performed to analyze genome-wide methylation. MeDIP was performed using a MagMeDIP Kit from Diagenode according to the manufacturer's instructions. Methylated DNA was recovered by immunoprecipitation with antibodies specific to methylated cytosine used to separate methylated DNA fragments from unmethylated fragments, and Illumina libraries were created from the captured gDNA using NEBNext reagents (catalog# E6040; New England Biolabs, Ipswich, MA, USA). Enriched libraries were evaluated for size distribution and concentration using an Agilent Bioanalyzer 2100. The samples were then sequenced on an Illumina HiSeq2000 machine, which generated paired-end reads of 90 or 100 nucleotides (nt). The results were analyzed for data quality and exome coverage using the platform provided by DNAnexus (DNAnexus, Inc., Mountain

View, CA, USA). Samples were sent to Otogenetics Corporation (Norcross, GA) for Illumina sequencing and alignment with the genome. The resulting BAM files were downloaded for analysis.

MeDIP alignments were compared with control samples using Cuffdiff 2.0.2 with no length correction [368]. Briefly, a list of overlapping regions of sequence alignment common to both the immunoprecipitated and the control samples was created and used to judge the quantitative enrichment in MeDIP samples over control samples using Cuffdiff; statistically significant peaks at 5% FDR and a minimum 4-fold difference using the Cummerbund package in R were selected [368]. Peaks were matched with adjacent annotated genes using ChIPpeakAnno [369].

5.2.5 Functional and pathway analysis by Ingenuity Pathway Analysis

We analyzed lists of genes with significant fold changes (based on the *P* values; UV-induced tumor vs. control and DMBA/TPA treatment vs. control) in the methylation pattern (increases and decreases) ascertained in the MeDIP-Seq experiment using Ingenuity® Pathways Analysis 4.0 (IPA 4.0, Ingenuity Systems, www.ingenuity.com). IPA utilized gene symbols that were identified as neighboring enriched methylation peaks by ChIPpeakAnno used for all of the analyses. IPA mapped 6,003 genes in the UVB group and 5,424 genes in the DMBA/TPA group with a $\geq$ 2-fold change compared with the control correspondingly. Based on these fold change data, IPA identified biological functions and canonical pathways related

to UVB-induced cancer. The list of genes within canonical pathways was ranked using the ratio of the number of genes mapped to each pathway to the total number of genes in the corresponding pathway, which is presented as observations/total in Table 5.6.

5.3 Results

5.3.1 MeDIP-Seq results

Skin samples were collected from the UVB- and DMBA/TPA-induced mouse skin cancer models, and gDNA was isolated from each sample. A whole-genome DNA methylation analysis was performed on the DNA samples using the described MeDIP-Seq method. The results were analyzed in a paired manner comparing the tumor to the normal skin tissue samples for each model.

In the UVB group, 6,003 genes were identified in the two samples with a ≥ 2-fold change in methylation and an increase or decrease in gene expression. Compared with the control, 4,140 genes exhibited increased methylation, and methylation was decreased in 1,863 genes (Figure 5.1). However, in the DMBA/TPA treatment group, 5,424 genes were identified with a ≥ 2-fold change in peak reads between the tumor and the normal skin samples. Among these 5,424 genes, the methylation pattern was up-regulated in 3,781 genes and down-regulated in 1,643 genes. To prioritize those changes, we ranked the top 50 up-regulated (+, Table 5.1 and Table 5.2) and down-regulated (−, Table 5.3 and Table 5.4) genes based on the $\log_2$ fold change from highest to lowest, all with *P* values less than 0.05.

5.3.2 Pathway analysis by IPA

To ascertain the significance of the methylation changes, 6,003 genes in the UVB group and 5,424 genes in the DMBA/TPA group with a greater than 2-fold change in methylation were analyzed using the Ingenuity® Pathway Analysis (IPA) software package. The top 5 canonical signaling pathways were categorized (Table 5.5) based on the ratio of the number of input genes to the total number of genes in the corresponding pathway in the Ingenuity® Pathway Analysis software. Fisher's exact test was used to calculate *P* values to determine the significance of the associations of the input genes with the canonical pathways.

IPA identified more than 50 signaling pathways containing genes with significantly up-regulated and down-regulated methylation. The interleukin-6 (IL-6)-related signaling pathway was mapped by IPA to the UVB group (Figure 5.1); the methylation profile is presented in red (up-regulation) and green (down-regulation). Figure 5.2 and Table 5.7 lists the genes involved in the IL-6 signaling pathway that exhibited altered methylation (14 up-regulated and 30 down-regulated) as mapped by IPA. It has been reported that IL-6 protein expression is induced by UV irradiation [370]. Correspondingly, the MeDIP-Seq data revealed that IL-6 up-regulated methylation by 3.252-fold ($\log_2$). Based on the IPA functional pathways, skin cancer belongs to the category of the mechanism of cancer. The top 5 genes related to skin cancer based on IPA are ranked by fold

change in Table 5.6. This list includes genes with increased methylation and genes with decreased methylation that are related to skin cancer pathways by IPA.

5.4 Discussion and Conclusions

It was previously reported that hypermethylation of CpG islands in tumor suppressor genes occurs in human squamous cell carcinoma cell lines and primary skin tumor tissues. Similar changes in DNA methylation patterns were observed in the multistage mouse skin cancer model. In addition, loss of global genomic methylation has been shown to be associated with increased aggressiveness of mouse skin cancer cell lines. However, the precise mechanism by which UV irradiation promotes melanoma remains unclear. Furthermore, there is no method for screening potential epigenetically modified genes involved in promoting skin cancers [360, 371-373]. Long-term exposure to UV irradiation is considered a major etiologic risk factor for the development of melanoma and non-melanoma skin cancers. Epigenetic alterations are generally considered to represent the interface between the environment and the genome [363]. Ultraviolet irradiation has been reported to induce epigenetic alterations, which may contribute to the development of skin cancer. In the present study, we performed global genome methylation screening using MeDIP-Seq to identify genomic loci with aberrant methylation patterns in cancer tissues.

One of the adverse effects of UV irradiation that has been observed in skin tumor development is a chronic and sustained inflammatory response. The

relationship between inflammation and epigenetic modifications in cancer is under active investigation [374-376]. In this study, a UV irradiation-induced abnormal inflammatory response was suggested based on the IPA mapped IL-6 pathways, which included the methylation profiles of pro-inflammatory cytokines, receptors and mitogen-activated protein kinases. Higher levels of pro-inflammatory cytokines are associated with tumor development and progression [377, 378]. Interleukins (ILs) have different systemic functions and are involved in inflammation. Nile *et al*. reported that the methylation of CpGs in the promoter region of *IL-6* affected the mRNA levels in mononuclear cells [374]. Tekpli *et al*. reported that the methylation of CpGs near the IL-6 transcriptional start site is significantly higher in non-small cell lung cancer cells and is associated with lower IL-6 mRNA expression [375]. Our study demonstrated that IL-6 gene methylation was significantly higher in UV irradiation-induced skin tumors.

IL-6-Jak-Stat3 inflammatory signaling is also involved in cell survival and provides a proliferative advantage in the two-stage chemical carcinogenesis model using DMBA as the tumor initiator and TPA as the promoter. Phosphorylated-Stat3 overexpression in a papilloma cell line leads to enhanced cell migration and invasion [379]. Transgenic mice with constitutive Stat3 expression have a shorter latency period and increased tumor incidence compared with non-transgenic littermates after DMBA/TPA treatment [380]. Moreover, mice with constitutively activated Stat3 bypassed the premalignant stage and were initially diagnosed with carcinoma in situ,

which rapidly progressed to squamous cell carcinoma. In our present study, we found 34 genes with altered DNA methylation in total 124 genes involved in the IL-6 pathway in the UV group. Among these genes with altered methylation, the SOCS1 (suppressor of cytokine signaling 1) gene, which encodes a suppressor in the IL-6-Jak-Stat3 loop, was hypermethylated in the tumor samples.

The top-ranked hypermethylated and hypomethylated genes could enable the discovery of key genes in skin cancer development. For example, RBFOX1 is the top up-regulated gene in terms of methylation status change in UV-irradiated tumors compared with normal epidermis by IPA (Figure 5.1). RBFOX1 is an RNA-binding protein that is highly expressed in the cytoplasm. RBFOX1 mutations were identified in colorectal cancer cell lines (CRC), and RBFOX1 deletion was observed in a significant proportion of CRC cases (106/419) [381, 382]. However, the role of RBFOX1 in skin cancer development is unclear. Surprisingly, tumor tissues from the DMBA/TPA group exhibited a unique profile in terms of the top 50 genes with up- or down-regulated methylation compared with the profile in the UVB group. Cell adhesion molecule 2 (CADM2) was one of the top methylated genes in DMBA/TPA tumors. CADM2 belongs to a protein family that participates in maintaining cell polarity and that has been considered to be a novel category of tumor suppressors [383]. Clinically, low CADM2 expression predicts a high risk of recurrence in patients with hepatocellular carcinoma after hepatectomy [384]. It has also been reported that aberrant promoter hypermethylation and loss of CADM2

expression are associated with human renal cell carcinoma tumor progression [385]. Our study is the first report to suggest that CADM2 methylation is involved in skin carcinogenesis. Moreover, we identified changes in the methylation patterns of several genes encoding microRNAs, which are also involved in epigenetic regulation. This observation indicates that epigenetic changes may occur at multiple levels with complex crosstalk in skin cancer development and progression.

The genes identified in this study demonstrated significant alterations in response to UV irradiation-induced inflammation and skin cancer development. Although IPA revealed some overlapping signaling changes in response to both UV irradiation and DMBA-TPA treatment and certain highly affected targets were common (including, GRIA1 and TNS1), the top-ranked genes based on fold change differed markedly between the two treatments, indicating that distinct epigenetic mechanisms trigger cancer after exposure to UV or the DMBA carcinogen.

In this study, a comprehensive analysis of the DNA methylation patterns in the UVB or DMBA/TPA induced tumors compared with age-matched normal skin was completed. Genes coding for inflammatory cytokines were identified by IPA to exhibit altered methylation profiles and may be associated with increased susceptibility to tumor development. Specifically, based on changes in methylation, molecular networks were identified that included genes encoding inflammatory cytokines. Additional studies with a particular emphasis on epigenetic alterations,

such as DNA methylation, may lead to the development of new strategies for the prevention of skin cancer and inflammation-related skin disease.

5.5 Figures and Tables

Table 5.1. Top 50 annotated genes with up-regulated methylation ranked by log_2 fold change in the UVB group. (B) DMBA/TPA group.

Rank	Symbol	Gene Name	Log_2 Fold Change (UVB/ Control)	Location	Type(s)
1	RBFOX1	RNA binding protein, fox-1 homolog (C. elegans) 1	5.457	Cytoplasm	other
2	IMPG2	interphotoreceptor matrix proteoglycan 2	5.367	Extracellular Space	other
3	DGKK	diacylglycerol kinase, kappa	5.31	Cytoplasm	kinase
4	MAD1L1	MAD1 mitotic arrest deficient-like 1 (yeast)	5.252	Nucleus	other
5	EVX2	even-skipped homeobox 2	5.19	Nucleus	transcription regulator
6	PAN3	PAN3 poly(A) specific ribonuclease subunit homolog (S. cerevisiae)	4.989	Cytoplasm	other
7	AAMP	angio-associated, migratory cell protein	4.837	Plasma Membrane	other
8	ARHGAP18	Rho GTPase activating protein 18	4.837	Cytoplasm	other
9	ACAA2	acetyl-CoA acyltransferase 2	4.574	Cytoplasm	enzyme
10	OLFM1	olfactomedin 1	4.574	Cytoplasm	other
11	TGS1	trimethylguanosine synthase 1	4.574	Nucleus	enzyme
12	DYM	dymeclin	4.525	Cytoplasm	other
13	Hspg2	heparan sulfate proteoglycan 2	4.474	Extracellular Space	other
14	Kcnip2	Kv channel-interacting protein 2	4.474	Plasma Membrane	other
15	TNS1	tensin 1	4.474	Plasma Membrane	other

16	AGAP1	ArfGAP with GTPase domain, ankyrin repeat and PH domain 1	4.367	Cytoplasm	enzyme
17	CCDC180	coiled-coil domain containing 180	4.367	Other	other
18	EDN1	endothelin 1	4.367	Extracellular Space	cytokine
19	FOXE1	forkhead box E1 (thyroid transcription factor 2)	4.367	Nucleus	transcription regulator
20	KCNN4	potassium intermediate/small conductance calcium-activated channel, subfamily N, member 4	4.367	Plasma Membrane	ion channel
21	LOXHD1	lipoxygenase homology domains 1	4.367	Extracellular Space	other
22	DCP2	decapping mRNA 2	4.252	Nucleus	enzyme
23	DET1	de-etiolated homolog 1 (Arabidopsis)	4.252	Nucleus	other
24	DSC3	desmocollin 3	4.252	Plasma Membrane	other
25	HOXD11	homeobox D11	4.252	Nucleus	transcription regulator
26	MAML2	mastermind-like 2 (Drosophila)	4.252	Nucleus	transcription regulator
27	MYO1E	myosin IE	4.252	Cytoplasm	enzyme
28	PCBD1	pterin-4 alpha-carbinolamine dehydratase/dimerization cofactor of hepatocyte nuclear factor 1 alpha	4.252	Nucleus	transcription regulator
29	WNT3	wingless-type MMTV integration site family, member 3	4.252	Extracellular Space	other
30	CENPF	centromere protein F, 350/400kDa	4.126	Nucleus	other
31	Dos	downstream of Stk11	4.126	Other	other
32	FBXO11	F-box protein 11	4.126	Cytoplasm	enzyme
33	GPR37	G protein-coupled	4.126	Plasma	G-protein

		receptor 37 (endothelin receptor type B-like)		Membrane	coupled receptor
34	HPCA	hippocalcin	4.126	Cytoplasm	other
35	LIMS2	LIM and senescent cell antigen-like domains 2	4.126	Cytoplasm	other
36	LRRC8B	leucine rich repeat containing 8 family, member B	4.126	Other	other
37	LTA4H	leukotriene A4 hydrolase	4.126	Cytoplasm	enzyme
38	MEMO1	mediator of cell motility 1	4.126	Cytoplasm	other
39	mir-221	microRNA 221	4.126	Cytoplasm	microRNA
40	mir-802	microRNA 802	4.126	Cytoplasm	microRNA
41	Olfr1323	olfactory receptor 1323	4.126	Plasma Membrane	G-protein coupled receptor
42	PLN	phospholamban	4.126	Cytoplasm	transporter
43	PTPN23	protein tyrosine phosphatase, non-receptor type 23	4.126	Cytoplasm	phosphatase
44	SLC7A9	solute carrier family 7 (amino acid transporter light chain, bo,+ system), member 9	4.126	Plasma Membrane	transporter
45	VRK1	vaccinia related kinase 1	4.126	Nucleus	kinase
46	ZBTB34	zinc finger and BTB domain containing 34	4.126	Nucleus	other
47	ZNF622	zinc finger protein 622	4.126	Nucleus	other
48	SMYD2	SET and MYND domain containing 2	4.082	Cytoplasm	enzyme
49	DYSF	dysferlin, limb girdle muscular dystrophy 2B (autosomal recessive)	3.989	Plasma Membrane	other
50	Ear2 (includes others)	eosinophil-associated, ribonuclease A family, member 2	3.989	Cytoplasm	enzyme

Table 5.2. Top 50 annotated genes with up-regulated methylation ranked by log_2 fold change in the DMBA/TPA group.

Rank	Symbol	Gene Name	Log_2 Fold Change (DMBA-TPA / Control)	Location	Type(s)
1	FAM135A	family with sequence similarity 135, member A	5.974	Other	enzyme
2	CADM2	cell adhesion molecule 2	5.231	Plasma Membrane	other
3	VWC2L	von Willebrand factor C domain containing protein 2-like	4.877	Extracellular Space	other
4	PTH2R	parathyroid hormone 2 receptor	4.708	Plasma Membrane	G-protein coupled receptor
5	NPY	neuropeptide Y	4.515	Extracellular Space	other
6	TNS1	tensin 1	4.408	Plasma Membrane	other
7	PHYHIPL	phytanoyl-CoA 2-hydroxylase interacting protein-like	4.408	Cytoplasm	other
8	COX7C	cytochrome c oxidase subunit VIIc	4.408	Cytoplasm	enzyme
9	CMYA5	cardiomyopathy associated 5	4.408	Plasma Membrane	other
10	HELB	helicase (DNA) B	4.351	Nucleus	enzyme

11	WDR63	WD repeat domain 63	4.292	Other	other
12	SIPA1L2	signal-induced proliferation-associated 1 like 2	4.292	Other	other
13	let-7	microRNA let-7a-1	4.292	Cytoplasm	microRNA
14	DSEL	dermatan sulfate epimerase-like	4.292	Extracellular Space	enzyme
15	ZNF521	zinc finger protein 521	4.167	Nucleus	other
16	TMTC2	transmembrane and tetratricopeptide repeat containing 2	4.167	Cytoplasm	other
17	OTOL1	otolin 1	4.167	Other	other
18	METTL21A	methyltransferase like 21A	4.167	Other	enzyme
19	INTU	inturned planar cell polarity protein	4.167	Cytoplasm	other
20	DHCR7	7-dehydrocholesterol reductase	4.167	Cytoplasm	enzyme
21	Cyp2a12/Cyp2a22	cytochrome P450, family 2, subfamily a, polypeptide 12	4.167	Cytoplasm	enzyme
22	CTSC	cathepsin C	4.167	Cytoplasm	peptidase
23	CHORDC1	cysteine and histidine-rich domain (CHORD) containing 1	4.167	Other	other
24	CBLN1	cerebellin 1 precursor	4.167	Cytoplasm	other
25	THAP1	THAP domain containing, apoptosis associated	4.029	Nucleus	other

		protein 1			
26	RYBP	RING1 and YY1 binding protein	4.029	Nucleus	transcription regulator
27	NDUFA12	NADH dehydrogenase (ubiquinone) 1 alpha subcomplex, 12	4.029	Cytoplasm	enzyme
28	Mug1/Mug2	murinoglobulin 1	4.029	Extracellular Space	transporter
29	MFSD10	major facilitator superfamily domain containing 10	4.029	Other	transporter
30	KIF16B	kinesin family member 16B	4.029	Cytoplasm	enzyme
31	GRID2	glutamate receptor, ionotropic, delta 2	4.029	Plasma Membrane	ion channel
32	Gm4836 (includes others)	predicted gene 4836	4.029	Cytoplasm	other
33	FOXN3	forkhead box N3	4.029	Nucleus	transcription regulator
34	Cyp4f16/Gm9705	cytochrome P450, family 4, subfamily f, polypeptide 16	4.029	Cytoplasm	enzyme
35	CXorf22	chromosome X open reading frame 22	4.029	Other	other
36	Pag1	phosphoprotein associated with glycosphingolipid microdomains 1	3.955	Plasma Membrane	other
37	MSH6	mutS homolog 6	3.923	Nucleus	enzyme

38	ZFAT	zinc finger and AT hook domain containing	3.877	Nucleus	other
39	Vmn1r188 (includes others)	vomeronasal 1 receptor 217	3.877	Plasma Membrane	G-protein coupled receptor
40	TYW3	tRNA-yW synthesizing protein 3 homolog (S. cerevisiae)	3.877	Other	other
41	TPO	thyroid peroxidase	3.877	Plasma Membrane	enzyme
42	TLR4	toll-like receptor 4	3.877	Plasma Membrane	transmembrane receptor
43	THSD7B	thrombospondin, type I, domain containing 7B	3.877	Other	other
44	SPINK5	serine peptidase inhibitor, Kazal type 5	3.877	Extracellular Space	other
45	SLC9A8	solute carrier family 9, subfamily A (NHE8, cation proton antiporter 8), member 8	3.877	Cytoplasm	transporter
46	SEC23A	Sec23 homolog A (S. cerevisiae)	3.877	Cytoplasm	transporter
47	RPS4Y1	ribosomal protein S4, Y-linked 1	3.877	Cytoplasm	other
48	PPP1R1C	protein phosphatase 1, regulatory (inhibitor) subunit 1C	3.877	Cytoplasm	phosphatase
49	PARP8	poly (ADP-ribose) polymerase family, member 8	3.877	Other	other

50	NLRP4	NLR family, pyrin domain containing 4	3.877	Cytoplasm	other

Table 5.3. Top 50 annotated genes with down-regulated methylation ranked by log_2 fold change in the UVB group.

	Symbol	Gene Name	Log_2 Fold Change (UVB/ Control)	Location	Type(s)
1	Nrxn3	neurexin III	-4.543	Plasma Membrane	other
2	SYN2	synapsin II	-4.378	Plasma Membrane	other
3	Mup1 (includes others)	major urinary protein 1	-4.333	Extracellular Space	other
4	KRT86	keratin 86	-4.24	Cytoplasm	other
5	SULT1C3	sulfotransferase family, cytosolic, 1C, member 3	-4.24	Cytoplasm	enzyme
6	ATP1A3	ATPase, Na+/K+ transporting, alpha 3 polypeptide	-4.191	Plasma Membrane	transporter
7	CHORDC1	cysteine and histidine-rich domain (CHORD) containing 1	-4.191	Other	other
8	NRXN1	neurexin 1	-4.191	Plasma Membrane	transporter
9	Htr6	5-hydroxytryptamine (serotonin) receptor 6, G protein-coupled	-4.141	Plasma Membrane	G-protein coupled receptor
10	PAM	peptidylglycine alpha-amidating monooxygenase	-4.141	Plasma Membrane	enzyme
11	SERPINB3	serpin peptidase inhibitor, clade B (ovalbumin), member 3	-4.141	Cytoplasm	other
12	TDRD3	tudor domain containing 3	-4.141	Nucleus	transcriptio n regulator
13	Olfr1153	olfactory receptor 1153	-4.088	Plasma Membrane	G-protein coupled receptor
14	WFIKKN2	WAP, follistatin/kazal, immunoglobulin, kunitz	-4.088	Other	other

		and netrin domain containing 2			
15	ABAT	4-aminobutyrate aminotransferase	-4.034	Cytoplasm	enzyme
16	ARHGAP6	Rho GTPase activating protein 6	-4.034	Cytoplasm	other
17	AUH	AU RNA binding protein/enoyl-CoA hydratase	-4.034	Cytoplasm	enzyme
18	CEP70	centrosomal protein 70kDa	-4.034	Cytoplasm	other
19	DGKH	diacylglycerol kinase, eta	-4.034	Cytoplasm	kinase
20	GRIA1	glutamate receptor, ionotropic, AMPA 1	-4.034	Plasma Membrane	ion channel
21	SLC4A7	solute carrier family 4, sodium bicarbonate cotransporter, member 7	-4.034	Plasma Membrane	transporter
22	SLITRK1	SLIT and NTRK-like family, member 1	-4.034	Other	other
23	Speer4a (includes others)	spermatogenesis associated glutamate (E)-rich protein 4a	-4.034	Nucleus	other
24	CETN1	centrin, EF-hand protein, 1	-3.977	Nucleus	enzyme
25	CYLC1	cylicin, basic protein of sperm head cytoskeleton 1	-3.977	Cytoplasm	other
26	HS3ST5	heparan sulfate (glucosamine) 3-O-sulfotransferase 5	-3.977	Cytoplasm	enzyme
27	Ott (includes others)	ovary testis transcribed	-3.977	Other	other
28	Scg5	secretogranin V	-3.977	Cytoplasm	other
29	CHM	choroideremia (Rab escort protein 1)	-3.918	Cytoplasm	enzyme
30	Clvs2	clavesin 2	-3.918	Cytoplasm	other
31	MRPS30	mitochondrial ribosomal protein S30	-3.918	Cytoplasm	enzyme
32	Olfr1010	olfactory receptor 1010	-3.918	Plasma Membrane	G-protein coupled receptor

33	PPP1R12A	protein phosphatase 1, regulatory subunit 12A	-3.918	Cytoplasm	phosphatase
34	ZMYND11	zinc finger, MYND-type containing 11	-3.918	Nucleus	other
35	ADCY10	adenylate cyclase 10 (soluble)	-3.857	Cytoplasm	enzyme
36	Agtr1b	angiotensin II receptor, type 1b	-3.857	Plasma Membrane	G-protein coupled receptor
37	APAF1	apoptotic peptidase activating factor 1	-3.857	Cytoplasm	other
38	AQP1	aquaporin 1	-3.857	Plasma Membrane	transporter
39	CDH10	cadherin 10, type 2 (T2-cadherin)	-3.857	Plasma Membrane	other
40	CHRM3	cholinergic receptor, muscarinic 3	-3.857	Plasma Membrane	G-protein coupled receptor
41	GCNT2	glucosaminyl (N-acetyl) transferase 2, I-branching enzyme (I blood group)	-3.857	Cytoplasm	enzyme
42	GNAI1	guanine nucleotide binding protein (G protein), alpha inhibiting activity polypeptide 1	-3.857	Plasma Membrane	enzyme
43	SELENBP1	selenium binding protein 1	-3.857	Cytoplasm	other
44	SP110	SP110 nuclear body protein	-3.857	Nucleus	other
45	TMEM5	transmembrane protein 5	-3.857	Plasma Membrane	other
46	XIRP2	xin actin-binding repeat containing 2	-3.857	Other	other
47	ZKSCAN2	zinc finger with KRAB and SCAN domains 2	-3.857	Nucleus	transcription regulator
48	1700009N14Rik	RIKEN cDNA 1700009N14 gene	-3.793	Other	transporter
49	AGPAT9	1-acylglycerol-3-phosphate O-acyltransferase 9	-3.793	Cytoplasm	enzyme
50	ASCL1	achaete-scute complex homolog 1 (Drosophila)	-3.793	Nucleus	transcription regulator

Table 5.4. Top 50 annotated genes with down-regulated methylation ranked by log_2 fold change in the DMBA/TPA group.

Rank	Symbol	Gene Name	Log_2 Fold Change (DMBA-TPA/ Control)	Location	Type(s)
1	EBPL	emopamil binding protein-like	-5.292	Cytoplasm	enzyme
2	PANX1	pannexin 1	-5.247	Plasma Membrane	transporter
3	HES5	hairy and enhancer of split 5 (Drosophila)	-4.632	Nucleus	other
4	LHX4	LIM homeobox 4	-4.247	Nucleus	transcription regulator
5	GSG1L	GSG1-like	-4.247	Plasma Membrane	other
6	PBX1	pre-B-cell leukemia homeobox 1	-4.199	Nucleus	transcription regulator
7	LRRC8B	leucine rich repeat containing 8 family, member B	-4.199	Other	other
8	ASAH2	N-acylsphingosine amidohydrolase (non-lysosomal ceramidase) 2	-4.199	Cytoplasm	enzyme
9	ALKBH3	alkB, alkylation repair homolog 3 (E. coli)	-4.199	Nucleus	enzyme
10	ZNF518	zinc finger protein 518B	-4.100	Other	other

	B				
11	MAN1A1	mannosidase, alpha, class 1A, member 1	-4.100	Cytoplasm	enzyme
12	TOX3	TOX high mobility group box family member 3	-3.993	Other	other
13	LSM11	LSM11, U7 small nuclear RNA associated	-3.936	Nucleus	other
14	TCEA3	transcription elongation factor A (SII), 3	-3.877	Nucleus	transcription regulator
15	OR7D2	olfactory receptor, family 7, subfamily D, member 2	-3.877	Plasma Membrane	G-protein coupled receptor
16	KIAA0947	KIAA0947	-3.877	Other	other
17	CBLB	Cbl proto-oncogene B, E3 ubiquitin protein ligase	-3.877	Nucleus	other
18	NOS1AP	nitric oxide synthase 1 (neuronal) adaptor protein	-3.816	Cytoplasm	other
19	MACC1	metastasis associated in colon cancer 1	-3.816	Nucleus	other
20	ZNF277	zinc finger protein 277	-3.752	Nucleus	transcription regulator
21	Sp100	nuclear antigen Sp100	-3.752	Nucleus	transcription regulator
22	KCNA6	potassium voltage-gated channel, shaker-related subfamily, member 6	-3.752	Plasma Membrane	ion channel
23	C19orf10	chromosome 19 open reading frame 10	-3.752	Extracellular Space	cytokine

24	TMEM 17	transmembrane protein 17	-3.685	Extracellular Space	other
25	FAM92 B	family with sequence similarity 92, member B	-3.650	Other	other
26	TBC1D 5	TBC1 domain family, member 5	-3.646	Extracellular Space	other
27	Nrg1	neuregulin 1	-3.614	Extracellular Space	growth factor
28	GORAS P1	golgi reassembly stacking protein 1, 65kDa	-3.614	Cytoplasm	other
29	AHRR	aryl-hydrocarbon receptor repressor	-3.614	Nucleus	other
30	ADOR A2A	adenosine A2a receptor	-3.614	Plasma Membrane	G-protein coupled receptor
31	RAB11 A	RAB11A, member RAS oncogene family	-3.540	Cytoplasm	enzyme
32	ISY1-R AB43	ISY1-RAB43 readthrough	-3.540	Nucleus	other
33	GNE	glucosamine (UDP-N-acetyl)-2-epimeras e/N-acetylmannosamine kinase	-3.540	Cytoplasm	kinase
34	FAM98 A	family with sequence similarity 98, member A	-3.540	Other	other
35	ENPP4	ectonucleotide pyrophosphatase/phosphodi esterase 4 (putative)	-3.540	Other	enzyme
36	CCDC4	coiled-coil domain	-3.540	Other	other

	3	containing 43			
37	ARHGEF10	Rho guanine nucleotide exchange factor (GEF) 10	-3.540	Cytoplasm	enzyme
38	TARSL2	threonyl-tRNA synthetase-like 2	-3.462	Other	enzyme
39	SCARB1	scavenger receptor class B, member 1	-3.462	Plasma Membrane	transporter
40	RAB27A	RAB27A, member RAS oncogene family	-3.462	Cytoplasm	enzyme
41	L3MBTL3	l(3)mbt-like 3 (Drosophila)	-3.462	Nucleus	other
42	Higd1a	HIG1 domain family, member 1A	-3.462	Cytoplasm	other
43	GRIA1	glutamate receptor, ionotropic, AMPA 1	-3.462	Plasma Membrane	ion channel
44	GPC5	glypican 5	-3.462	Plasma Membrane	other
45	CLGN	calmegin	-3.462	Cytoplasm	peptidase
46	CHKA	choline kinase alpha	-3.462	Cytoplasm	kinase
47	ASGR1	asialoglycoprotein receptor 1	-3.462	Plasma Membrane	transmembrane receptor
48	AMY2A	amylase, alpha 2A (pancreatic)	-3.462	Extracellular Space	enzyme
49	C1orf109	chromosome 1 open reading frame 109	-3.444	Other	other
50	CADPS	Ca^{++}-dependent secretion activator	-3.430	Plasma Membrane	other

Table 5.5. Top 5 altered canonical pathways determined using Ingenuity Pathways Software in the UVB and DMBA/TPA groups. The shared pathways are shown in bold.

Rank	Name	Ratio	Observation /Total	p-value
UVB/Control				
1	cAMP-mediated signaling	0.478	108/226	1.27E-09
2	G-Protein Coupled Receptor Signaling	0.442	122/276	5.24E-09
3	**Molecular Mechanisms of Cancer**	**0.371**	**144/388**	**9.86E-07**
4	PTEN Signaling	0.42	58/138	5.21E-06
5	Role of Osteoblasts, Osteoclasts and Chondrocytes in Rheumatoid Arthritis	0.388	97/250	5.58E-06
DMBA-TPA/ Control				
1	Protein Kinase A Signaling	0.352	144/409	5.5E-06
2	**Molecular Mechanisms of Cancer**	**0.325**	**126/338**	**4.57E-05**
3	Xenobiotic Metabolism Signaling	0.351	101/288	7.59E-05
4	Regulation of the Epithelial-Mesenchymal Transition Pathway	0.342	67/196	0.0011
5	Mouse Embryonic Stem Cell Pluripotency	0.394	39/99	0.0013

Table 5.6. Top 5 genes with altered methylation in skin cancers.

These up-regulated or down-regulated genes are related to skin cancer using IPA Software Functional and Diseases analysis module in the UVB and the DMBA/TPA groups. Shared genes are shown in bold.

Rank	Mapped Genes	Log_2 Fold Change
UVB/Control		
Up-regulated		
1	RBFOX1	5.457
2	LOXHD1	4.367
3	EDN1	4.367
4	DYSF	3.989
5	NPSR1	3.837
Down-regulated		
1	SULT1C3	-4.24
2	ABAT	-4.034
3	**GRIA1**	**-4.034**
4	PCSK1	-3.726
5	SCN2A	-3.655
DMBA-TPA/Control		
Up-regulated		
1	GRID2	4.029
2	NLRP4	3.877
3	EMR1	3.877
4	IL15	3.877
5	PCDH18	3.708
Down-regulated		
1	**GRIA1**	**-3.462**
2	CADPS	-3.43
3	BCL2L11	-3.292
4	ACVR1C	-3.292
5	GRM3	-3.292

Table 5.7. List of genes mapped to the IL-6 pathway by IPA.

	Log_2 Fold Change (UVB/Control)	**Symbol**	**Gene Name**
Down-regulated			
1	-3.421	IL1RAPL2	interleukin 1 receptor accessory protein-like 2
2	-3.24	HSPB3	heat shock 27kDa protein 3
3	-3.141	MAPK10	mitogen-activated protein kinase 10
4	-3.141	PIK3C2G	phosphatidylinositol-4-phosphate 3-kinase, catalytic subunit type 2 gamma
5	-3.141	SOCS1	suppressor of cytokine signaling 1
6	-2.918	PIK3R1	phosphoinositide-3-kinase, regulatory subunit 1 (alpha)
7	-2.793	IL1RL1	interleukin 1 receptor-like 1
8	-2.793	MAP3K7	mitogen-activated protein kinase kinase kinase 7
9	-2.655	CRP	C-reactive protein, pentraxin-related
10	-2.503	ABCB1	ATP-binding cassette, sub-family B (MDR/TAP), member 1
11	-2.503	IL1R2	interleukin 1 receptor, type II
12	-2.333	IL36B	interleukin 36, beta
13	-2.141	MAP2K1	mitogen-activated protein kinase kinase 1
14	-2.034	PIK3R4	phosphoinositide-3-kinase, regulatory subunit 4
Up-regulated			
1	3.667	AKT3	v-akt murine thymoma viral oncogene homolog 3
2	3.667	PIK3CG	phosphatidylinositol-4,5-bisphosphate 3-kinase, catalytic subunit gamma
3	3.667	PTPN11	protein tyrosine phosphatase, non-receptor type 11
4	3.474	PIK3C3	phosphatidylinositol 3-kinase, catalytic subunit type 3
5	3.252	COL1A1	collagen, type I, alpha 1

6	3.252	IL6	interleukin 6 (interferon, beta 2)
7	3.252	RELA	v-rel avian reticuloendotheliosis viral oncogene homolog A
8	3.169	IL1RL2	interleukin 1 receptor-like 2
9	2.989	IL1RAP	interleukin 1 receptor accessory protein
10	2.989	MAP2K6	mitogen-activated protein kinase kinase 6
11	2.989	RRAS2	related RAS viral (r-ras) oncogene homolog 2
12	2.989	SRF	serum response factor (c-fos serum response element-binding transcription factor)
13	2.915	NFKB2	nuclear factor of kappa light polypeptide gene enhancer in B-cells 2 (p49/p100)
14	2.667	A2M	alpha-2-macroglobulin
15	2.667	AKT1	v-akt murine thymoma viral oncogene homolog 1
16	2.667	CSNK2A1	casein kinase 2, alpha 1 polypeptide
17	2.667	HSPB1	heat shock 27kDa protein 1
18	2.667	IL6ST	interleukin 6 signal transducer (gp130, oncostatin M receptor)
19	2.667	MAP2K4	mitogen-activated protein kinase kinase 4
20	2.667	NFKBIA	nuclear factor of kappa light polypeptide gene enhancer in B-cells inhibitor, alpha
21	2.474	PIK3C2A	phosphatidylinositol-4-phosphate 3-kinase, catalytic subunit type 2 alpha
22	2.252	FOS	FBJ murine osteosarcoma viral oncogene homolog
23	2.252	IL1R1	interleukin 1 receptor, type I
24	2.252	LBP	lipopolysaccharide binding protein
25	2.252	MAPK1	mitogen-activated protein kinase 1
26	2.252	MAPK8	mitogen-activated protein kinase 8
27	2.252	MAPK13	mitogen-activated protein kinase 13
28	2.252	NFKB1	nuclear factor of kappa light polypeptide gene enhancer in B-cells 1
29	2.252	SOS1	son of sevenless homolog 1

30	2.252	SOS2	son of sevenless homolog 2

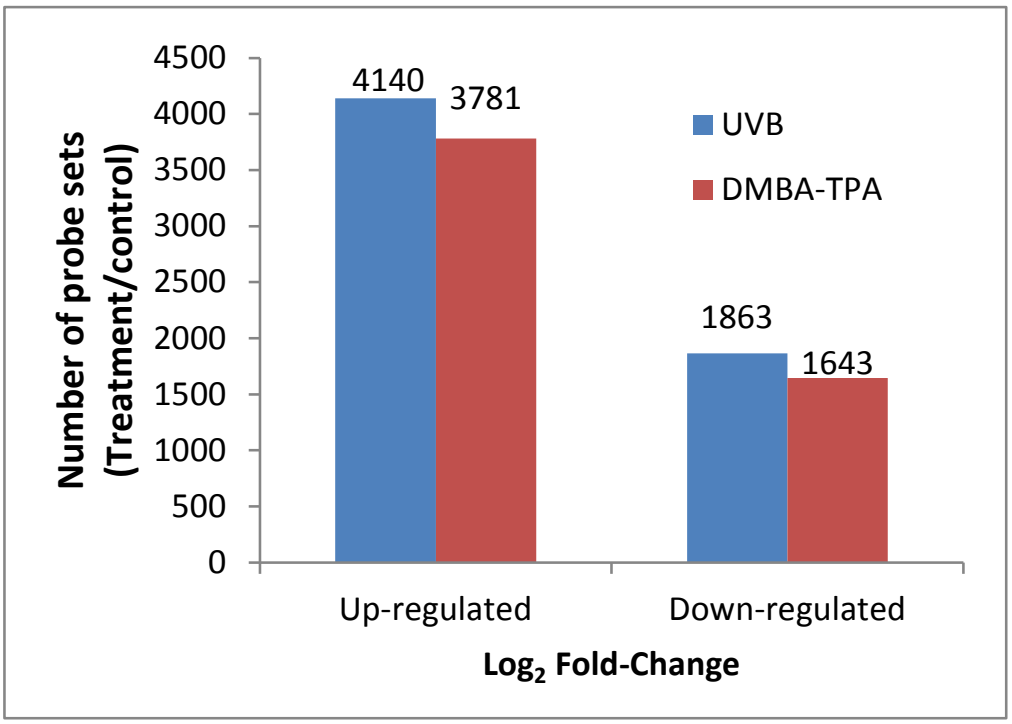

Figure 5.1. Total number of significantly up-regulated and down-regulated genes based on the changes in methylation (≥ 2-fold change) in the UVB and DMBA/TPA groups.

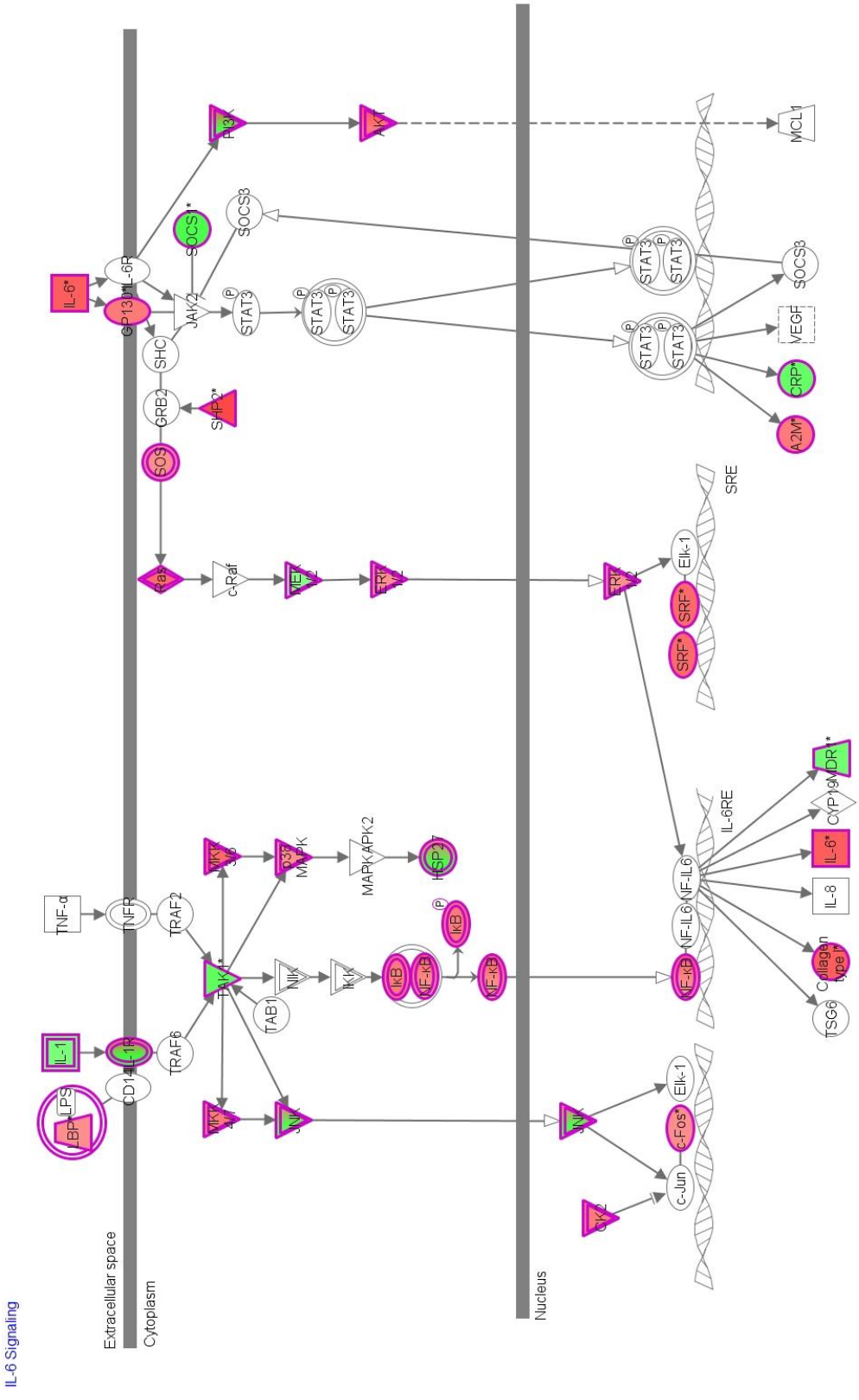
IL-6 Signaling
Extracellular space
Cytoplasm
Nucleus
IL-6*
IL-6R
gp130
JAK2
STAT3
SOCS1*
SOCS3
PI3K
AKT
MCL1
SHC
GRB2
SOS
SHP2*
Ras
c-Raf
MEK
ERK
SRE
Elk-1
SRF*
IL-6RE
NF-IL6
NF-κB
IκB
TAK1
TAB1
MKK
p38 MAPK
MAPKAPK2
HSP27
JNK
c-Fos*
c-Jun
GYZ
VEGF
CRP*
A2M*
IL-8
TSG6
Collagen type I*
CYP1B1*
MDR1*
TNF-α
TNFR
TRAF2
TRAF6
IL-1
CD14
LBP
LPS
© 2000-2014 Ingenuity Systems, Inc. All rights reserved.

Figure 5.2. Genes mapped to the IL-6 pathway by IPA Software. Red, increased methylation; green, decreased methylation; UVB irradiated vs. control.

6 Effects of ursolic acid and sulforaphane on the epigenetic alterations in UVB-induced inflammation and carcinogenesis *in vivo*[16]

6.1 Introduction

There are 1 million skin cancer cases increasing annually in the United States including basal cells carcinomas (BCCs), squamous cell carcinomas (SCCs), and melanomas. BCCs and SCCs are non-melanoma skin cancers (NMSCs), which are 96% of all skin cancers. Surgical management is the traditional treatment strategy for NMSCs, but it is disfiguring and costly. Hence, it is important to develop a safe and effective strategy to prevent initiation and progression of NMSCs.

Exposure to ultraviolet B (UVB) is one of the major causative factors for NMSCs. Long-term exposure to UVB radiation induces inflammation, oxidative stress, DNA mutation, and damage, which are involved in initiation, promotion and progression of NMSCs [386]. The early UV-exposure induces inflammatory responses with the increased blood flow, vascular permeability, expression of cyclooxygenases-2 (COX-2), and production of prostaglandin (PG) metabolites [377]. UVB-induced inflammation is an important event in all three stages of NMSCs [377], showing the importance of controlling the UVB-induced inflammation to prevent the skin cancer risk.

Oxidative stress coupled with chronic inflammation was found to drive carcinogenesis. Nuclear factor (erythroid-derived 2)-like 2 (NFE2L2 or Nrf2) is a

[16] Part of this chapter is intended to be submitted as a research article.

critical transcription factor that regulates the anti-oxidative stress and inflammation responses [241, 387]. It is involved in the protection against the development and progression of various types of skin cancers [388]. Our previous study has demonstrated that Nrf2 knockout mice (Nrf2 -/-) mice are more susceptible to 7, 12-Dimethylbenz(a)anthracene (DMBA) - induced skin tumorigenesis, with decreased cellular defense system against oxidative stress and inflammation [297].

Epigenetic deregulation has emerging importance as a hallmark of cancers, although cancer research has been focusing on genetic alterations in carcinogenesis for many years, but [389, 390]. Epigenetic alterations are recognized to be associated with cancer development and provide novel therapeutic targets. Recently, FDA has approved drugs inhibiting histone deacetylase (HDACs) and DNA methyltransferase (DNMTs) as chemotherapeutics with limited usage due to the toxicity [391, 392]. Aberrant epigenetic alterations have been observed in the development and progression of skin cancers [393-395]. We recently identified extensive gene methylation profiles in skin carcinogenesis by conducting global genome-wide epigenome analysis of ultraviolet B (UVB)-irradiated SKH-1 hairless mice and DMBA/TPA-treated CD-1 mice [396].

Many phytochemicals possess chemopreventive effects by modifications of epigenetic processes, including triterpenoids (TTPs) and crucifers isothiocyanates (ITCs) [397]. Ursolic acid (UA) is a natural pentacyclic TTP enriched in blueberries, cranberries, and medicinal plants such as *Rosmarinus officinalis*. UA induces phase

2 enzymes with involvement Nrf2, anti-inflammatory and anti-cancer activities [398-401]. Also, UA increased acetylation of histone H3 and inhibition of HDAC activity *in vitro* [402].

Sulforaphane (SFN) is an important cancer prevention agent and also a Nrf2 activator with no known side effects. SFN inhibits Nrf2 proteasomal degradation and enhances Nrf2 transcriptional activation of ARE genes. SFN suppressed Bmi-1 and Ezh2 level leading to the reduced H3K27me4 formation in SCC-13, A431, and HaCaT cells, and suppress tumor formation in the epidermis [403, 404]. Recently, we reported that SFN inhibited TPA-induced JB6 cellular transformation, and decreased the methylation level of the CpG sites of Nrf2, and enhanced the translocation of Nrf2 into the nucleus. In addition, SFN reduced the protein expression of some epigenetic modifying proteins such as DNA methyltransferase and histone deacetylases [140]. It has been shown that SFN reduced tumor growth in A375 melanoma cell – derived melanoma cancer stem cells in immune-compromised mice by reducing Ezh2 level and H3K27me3 formation [405].

Epidemiological studies suggested that these dietary compounds could protect against skin cancer, although there is no direct clinical trial of SFN or UA in skin cancers. Forte *et al.* reported that cruciferous-and-leafy-vegetables-rich Mediterranean diet protects against cutaneous melanoma [406]. Similarly, the high intake of cruciferous vegetables and triterpenoids enriched beans fight against

non-melanocytic skin cancer in a case-control study conducted in Melbourne, Australia [407]. Hence, it is important to develop a safe and effective strategy using phytochemicals to prevent initiation and progression of NMSCs by targeting at potential epigenetic and epigenomic biomarkers in skin carcinogenesis.

In this study, we used the UVB-induced skin cancer mouse models to examine the epigenetic and epigenomic changes during different stages of skin cancer from imitation, promotion, to later progression. Furthermore, we investigated the roles of SFN and UA in reversing the epigenetic changes resulting in the cancer prevention. These studies contributed to the development of a safe and efficient strategy using natural phytochemicals chemopreventive compounds to prevent skin cancers and to identify potential epigenetic and epigenomic biomarkers during skin carcinogenesis to provide novel therapeutic strategies.

6.2 Materials and methods

6.2.1 Chemicals and reagents

D, L - Sulforaphane (SFN) was purchased from LKT Laboratories, Inc. (S8044; St. Paul, MN, USA) and Toronto Research Chemicals (S699115; Toronto, Ontario, Canada). Ursolic acid (UA) was purchased from Sigma-Aldrich (U6753; St. Louis, MO, USA). Acetone (HPLC grade) and 10% phosphate-buffered formalin were obtained from Fisher Scientific (Hampton, NH, USA). Anti-Nrf2 antibody (ab62352) was purchased from Abcam Inc. (Cambridge, MA, USA). Skin Tissue Microarray was purchased from Biomax Inc. (SK721 and SK208; Rockville, MD, USA).

6.2.2 Animals

Female Nrf2 knockout mice were obtained as previously described [297]. The offspring of the eighth generation of Nrf2 KO mice on the C57BL/6 background were used in this study. The genotype of each animal was confirmed using DNA extracted from the tail and analyzed by PCR. Nrf2 WT mice were purchased from The Jackson Laboratory (Bar Harbor, ME, USA). Female SKH-1 hairless mice were purchased from Charles River Laboratories (Wilmington, MA, USA), as described in previous studies [408]. Mice were housed at the Rutgers Animal Facility, maintained under 12 hours light and dark cycles, and provided ad libitum access to food and water. These mice were housed in the animal facility for at least one week before experiments. All animal procedures were approved by the Institutional Animal Care and Use Committee (IACUCs).

6.2.3 Experimental design

6.2.3.1 Short-term effects of UA on UVB-induced inflammation in Nrf2 wild-type and knock-out C57BL/6J mice

Experiments were performed in Nrf2 WT and KO female C57BL/6 mice (6-8 weeks old) to determine effects of a single dose of 180 mJ/cm^2 UVB-irradiation. Mice were randomly divided into four groups including (1) no UVB in Nrf2 WT mice; (2) UVB in Nrf2 WT mice; (3) no UVB in Nrf2 KO mice; and (4) UVB in Nrf2 KO mice. Mice were sacrificed at two time-points of one-day and seven-day after the last UVB exposure. There were four mice per group per time point. The

hair on the dorsal region of each mouse was removed two days before UVB irradiation as previously described [296]. At the end of the experiment, mice were euthanized and the collected skin samples were frozen in liquid nitrogen immediately and then stored at -80ºC, or placed in 10% phosphate-buffered formalin at room temperature for 24 hours for further analysis.

6.2.3.2 Dose-dependent effects of UA and SFN on UVB-induced apoptotic sunburn cells in the epidermis from SKH-1 mice

Female SKH-1 mice (6 weeks old) were used to study the effects of UA and SFN at various concentrations in response to one-time UVB irradiation at different strengths ranging from 30 to 180 mJ/cm^2. UA or SFN was prepared in 200 µl acetone with various amounts from 0.1 to 2 µmol.

There were two pilot experiments, including compound (UA or SFN) dose-response experiment (Experiment 1) and UVB-dose dependent response experiment (Experiment 2). In experiment 1, there were 10 groups (n = 3, per group), including (1) Vehicle control without UVB with 200 µL acetone only, (2) UVB 30 mJ/cm^2, (3) UA 0.1 µmol with UVB-irradiation, (4) UA 0.5 µmol with UVB-irradiation, (5) UA 2 µmol with UVB-irradiation, (6) UA 2 µmol, (7) SFN 0.1 µmol with UVB-irradiation, (8) UA 0.5 µmol with UVB-irradiation, (9) UA 2 µmol with UVB-irradiation, and (10) SFN 2 µmol. Experiment 2, there were 9 groups (n = 3, per group), including (1) UVB 30 mJ/cm^2, (2) UA 2 µmol with 30 mJ/cm^2 UVB-irradiation, (3) SFN 2 µmol with 30 mJ/cm^2 UVB-irradiation, (4) UVB 90

mJ/cm^2, (5) UA 2 µmol with 90 mJ/cm^2 UVB-irradiation, (6) SFN 2 µmol with 90 mJ/cm^2 UVB-irradiation, (7) UVB 180 mJ/cm^2, (8) UA 2 µmol with 180 mJ/cm^2 UVB-irradiation, and (9) SFN 2 µmol with 180 mJ/cm^2 UVB-irradiation.

6.2.3.3 Long-term chemopreventive effects of UA and SFN on UVB-induced skin carcinogenesis in SKH-1 mice

The long-term experiment was to examine the effects of UA and SFN on UVB-induced skin carcinogenesis in SKH-1 mice. An intermediate UVB dose at 60 mJ/cm^2 was used to induce the skin tumor in SKH-1 hairless mice, with topical application of UA and SFN (2 µmol in 200 µL acetone) once a day for four days a week, and twice UVB-irradiation per week for up to 25 weeks. Skin epidermis, dermis, and tumors will be collected to study the molecular mechanis. In this experiment, mice were randomly divided into six groups including (1) Vehicle control with 200 µL acetone without UVB, (2) 2 µmol UA, (3) 2 µmol SFN, (4) UVB + Acetone, (5) UVB + 2 µmol UA, and (6) UVB + 2 µmol SFN. There were six time-points, including 2-week, 5-week, 10-week, 15-week, 20-week, and 25-week. Tumor growth was monitored daily and measured biweekly using a digital caliper. Tumor volumes were determined and calculated using the formula $V = \pi/6 \times$ Height × Length × Width. Body weight was monitored biweekly to assess the health of animals. Mice with more than 15% weight loss were euthanized and removed from the study.

6.2.4 Exposure of mice to UV lamps

Female SKH-1 hairless mice or C57BL/6 mice at the age of 6 to 8 weeks old were irradiated with UV lamps that emit UVB (280 – 320 nm; 75-80% of total energy) and UVA (320-375 nm; 20-25% of total energy), as described in previous studies [409]. These UV lamps (FS72T12-UVB-HO; National Biological Corp., Twinsburg, OH, USA) emit little or no radiation < 280 nm and > 375 nm. The lamps emit UVB (280-320 nm; 75-80% of total energy) and UVA (320-375 nm; 20-25% of total energy), as described in our previous studies [296, 341]. The dose of UVB was quantified using a UVB Spectra 305 dosimeter (Daavlin Co., Bryan, OH, USA). The radiation was calibrated with an IL-1700 research radiometer/photometer from International Light Inc. (Newburyport, MA, USA).

6.2.5 Preparation of skin specimens and histological examination

Skin samples (25 mm length and 5 mm width) were obtained from the dorsal region of mice, and then placed in 10% phosphate-buffered formalin at room temperature for 24 hours. These samples were transferred to increasing concentrations of ethanol ranging from 70%, 80%, 95% and 100% ethanol, cleared in xylene, and then embedded in Paraplast Plus (Fisher Scientific, Pittsburgh, PA, USA). Four-μm serial sections were made for hematoxylin and eosin (H&E) staining or immunohistological staining. These sections were used for the measurement of morphological identification of apoptotic sunburn cells and other histological changes. In addition, the number of epidermal cells and the epidermal

thickness were measured in the H&E stained skin sections. All histological identifications were performed with 200-fold magnification. The H&E sections were examined under a light microscope (Nikon Eclipse E600, Japan). Effects of UVB were evaluated by the morphological methods after histological H&E staining. This method allowed multiple measurements on serial sections. Apoptotic sunburns cells were pointed out by the arrows. The number of apoptotic sunburn cells in the epidermis was counted in two serial sections per sample to obtain a mean value per mouse. The number of apoptotic sunburn cells was normalized by the length of each specimen. A minimum of three specimens were counted per group to determine the average number per group.

6.2.6 Tissue Microarray

Skin Tissue Microarray (TMA) was purchased from Biomax Inc. (Rockville, MD, USA). This immunohistochemical (IHC) staining and identification of section was performed as published previously [408].

6.2.7 Data presentation and statistical analysis

The data are presented as the mean ± standard error of the mean (SEM), except as otherwise stated. Student's *t*-test was used to determine statistically significant differences between groups. A p-value < 0.05 was considered statistically significant.

6.3 Results

6.3.1 Short-term effects of UA in UVB-induced inflammation in Nrf2 wild-type and Nrf2 knockout C57BL/6J mice

To evaluate the effects of UA on Nrf2, we first used the Nrf2 WT and KO mice in response to UVB-irradiation induced an inflammatory response. Treatment with a single dose of UVB at 180 mJ/cm^2 increased the number of apoptotic sunburn cells after 24 hours (Figure 6.2C). Apoptotic sunburn cells in the epidermis were determined morphologically after H&E staining, identified by their intense eosinophilia cytoplasm and small, dense nuclei. (Figure 6.2B). Importantly, the formation of apoptotic sunburn cells was induced by the four times of topical application of UA before the UVB-irradiation in WT mice (Figure 6.2C). However, there were no significant differences between the UVB-irradiated groups and the UA-treated group with UVB-irradiation in the Nrf2 KO mice (Figure 6.2C). It suggested that UA caused a dose-dependent increase in UVB-induced apoptosis through Nrf2-dependent mechanism.

6.3.2 Dose-dependent effects of UA and SFN on UVB-induced apoptotic sunburn cells in the epidermis of SKH-1 mice

Next, we tested effects of UA and SFN in immunocompetent hairless SKH-1 mice on UVB-induced apoptotic sunburn cells. As shown in Figure 6.3, topical application of UA for four consecutive days before the UVB-irradiation did not increase the apoptotic sunburn cells in the epidermis in SKH-1 mice. Representative

figures of H&E staining are shown in Figure 6.3A and quantification of apoptotic sunburn cells was shown in Figure 6.3B. Compared with UA, SFN at 0.1 μmol in 200 μL acetone significantly inhibited UVB-induced apoptosis, but SFN at 0.5 μmol and 2.0 μmol did not significantly influence the apoptosis.

Conversely, one-time topical application of UA at the dorsal region before UVB-irradiation enhanced UVB-induced apoptotic sunburn cells in the epidermis of SKH-1 hairless mice (Figure 6.4). That topical application of SFN before the UVB-irradiation from 30 mJ/cm^2 to 180 mJ/cm^2 showed inhibitory effects on UVB-induced increase in the number of apoptotic sunburn cells was likely due to the absorption of the UVB-wavelength by SFN (Figure 6.4). Compared to SFN, UA at 2 μmol enhanced 30 mJ/cm^2 UVB-induced apoptosis significantly, but there was no significant difference in the topical application before 60 mJ/cm^2 UVB-irradiation. In contrast, UA significantly reduced the UVB-induced apoptotic sunburn cells when the strength of UVB was increased to 180 mJ/cm^2 (Figure 6.4).

6.3.3 Effects of UA and SFN on UVB-induced inflammation and carcinogenesis in hairless SKH-1 mice

These pilot studies provided references such as the doses of UA, SFN and UVB-irradiation for our proposed long-term chemoprevention studies (Figure 6.5A). SKH-1 hairless mice at the age of 6-week were randomly divided into five groups and the tattoo of mouse ID number was placed on a tail of each mouse. UVB-irradiation and topical application started at the mouse age of eight week.

Topical application of acetone (vehicle), UA or SFN at the dorsal region was right after a single dose of UVB-irradiation at the strength of 60 mJ/cm^2, and at every following day. This topical application after UVB-irradiation avoided the potential sunscreen effects of UA and SFN. Two times of UVB-irradiation per weeks worked as both a tumor initiator and promoter [410, 411]. The body weight of mice was monitored biweekly, and we found that it increased steadily with or without UVB-irradiation (Figure 6.5B). The health condition was monitored every three days, especially the skin condition including UVB-induced epidermal hyperplasia, and the actinic keratosis as pre-cancers [412]. The topical application of UA or SFN without UVB-irradiation was used as the control to show that the selected dose of SFN or UA was safe with mice. Topical application of SFN reduced tumor incidence (percentage of tumor bearing mice), average tumor volume, and tumor multiplicity (tumor number per mouse) after 24-week treatment (Figure 6.5). Compared to SFN, all mice treated with UA were with tumors at the end of 24-week. Treatment with UA or SFN reduced the average tumor volume per mouse and average tumor number per mouse compared to the groups with topical application of acetone with UVB-irradiation (Figure 6.5C-E).

6.3.4 Nrf2 protein expression is lower in squamous cell carcinoma tissues as compared to cancer adjacent normal tissues

IHC staining of human skin cancer tissue microarray (TMA) shows Nrf2 expression was reduced in squamous cell carcinomas (SCCs; Figure 6.6A, B and C)

as compared to cancer adjacent normal skin tissue (Figure 6.6D, E and F). All samples are shown at 400 × magnification. Weak distributed staining of Nrf2 in SCCs showed reduced expression of Nrf2 (Figure 6.6A, B and C) as compared to scattered cells with stronger staining in the epidermis from the cancer adjacent normal skin tissues (Figure 6.6D, E and F).

6.4 Discussion and conclusions

UVB-irradiation is critical for the production of Vitamin D. However, it is also one of the major environmental causes for the initiation and development of skin cancers. We aimed to explore the beneficial effects of phytochemicals which can counter the UVB-induced harmful effects such as carcinogenesis but keep the benefits of Vitamin D production. The beneficial functions of skin require a complex cooperation of molecular signaling pathways. One of the key mechanisms is dependent on Nrf2 against oxidative stress. Nrf2 enhances the cell resistance to the oxidative stress and inflammation induced by the UVB-irradiation and chemical carcinogens, and further reduces malignant transformation and tumor growth [297]. Activation of Nrf2 in keratinocytes and melanocytes shows protective role against mutations induced by environmental stimulation including UVB and chemicals in both genetics and epigenetics.

This present study will provide unique new insights into epigenetic and genetic alterations induced by UVB in initiation, promotion, and progression stages of skin inflammation and carcinogenesis. Importantly, we will identify the anti-oxidative

stress, anti-inflammation and epigenetic modifying effects of UA and SFN resulting in prevention of skin carcinogenesis.

In these pilot studies, we demonstrated that topical application of UA may enhance one dose of UVB-induced apoptosis by a Nrf2-dependent mechanism in female Nrf2 KO and WT C57BL/6 mice. However, in another strain SKH-1 hairless mice, topical application of UA or SFN before UVB-irradiation reduced the UVB-induced apoptotic sunburn cells. This may be caused by the difference of the mouse strain, the one-time topical application of UA and SFN before the UVB-irradiation, or the sunscreen effects of these compounds. Furthermore, we designed a long-term carcinogenesis model induced by the UVB-irradiation to study the effects of UA and SFN. We will further examine the global epigenomic alterations in different stages of skin carcinogenesis and global epigenetic epigenomic response of UA and SFN with the advent of Next Generation Sequencing (NGS) technology. These studies contribute to identify potential epigenetic and epigenomic biomarkers during skin carcinogenesis to provide novel therapeutic strategies.

6.5 Figures and Tables

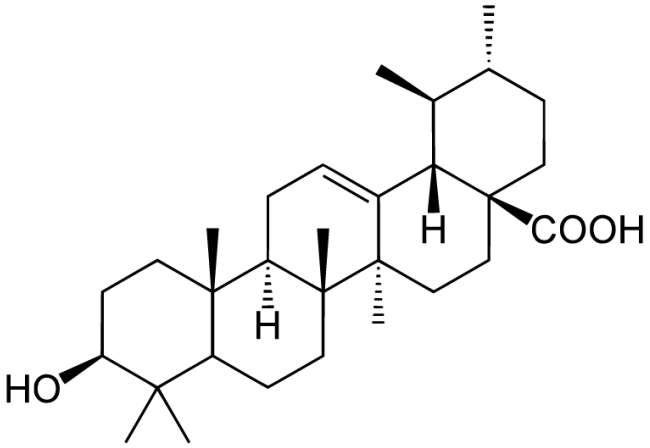

Ursolic Acid (UA)

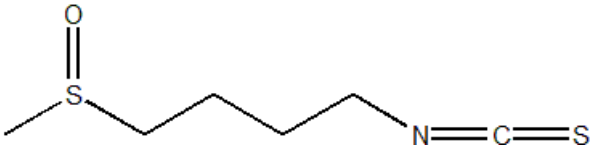

Sulforaphane (SFN)

Figure 6.1. Chemical Structures of ursolic acid (UA) and sulforaphane (SFN).

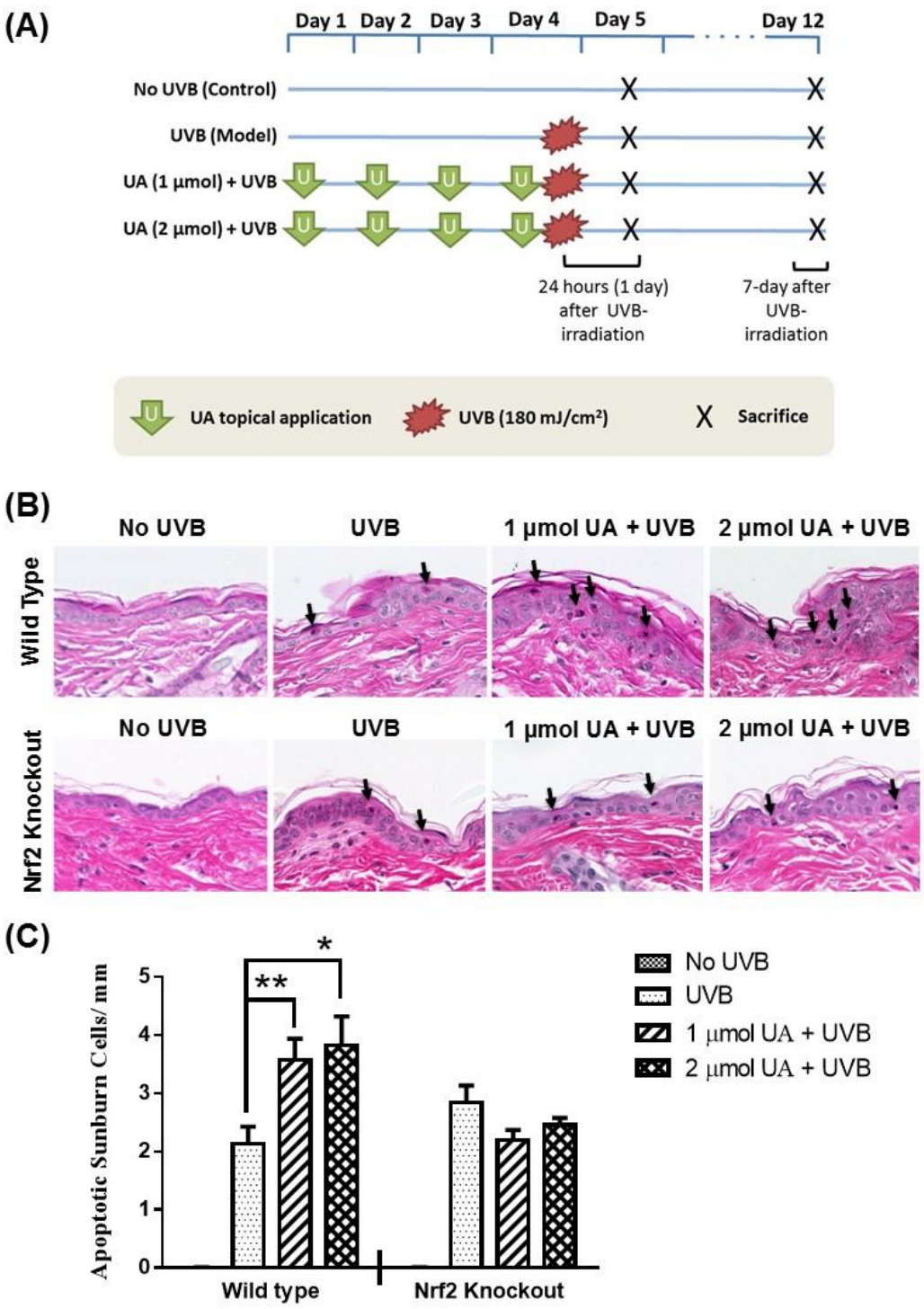

Figure 6.2. Effects of topical application of ursolic acid (UA) on UVB-induced apoptotic sunburn cells from the epidermis of wild-type and Nrf2 knockout C57BL/6J mice at 24 hours after UVB-irradiation.

Shaved female C57/BL6 wild-type (WT) and knockout (KO) mice (6-8 weeks old, four mice per group) were given 100 µl acetone (vehicle control), 1 µmol or 2 µmol ursolic acid in 100 µl acetone topically at the dorsal region once a day for four consecutive days. On the fourth day, 0.5 hours after topical application, mice were treated with a single dose of UVB (180 mJ/cm^2) when is the peak of UVB-induced apoptosis. The group of mice without UVB-irradiation was served as the negative control. All mice were sacrificed at 24 hours after UVB-irradiation. (A) Experimental deign. (B) Representative figures of apoptotic sunburn cells were identified by their intense eosinophilia cytoplasm and small, dense nuclei, which was observed in H&E-stained histological sections of the skin by using light microscopy (Magnification 400×). (C) Quantification of apoptotic sunburn cells in 25 mm length of epidermis. Each value is the mean ± SEM. Student t-test was used to compare the treatment group to the UVB group; *$P < 0.05$, ** $P < 0.01$.

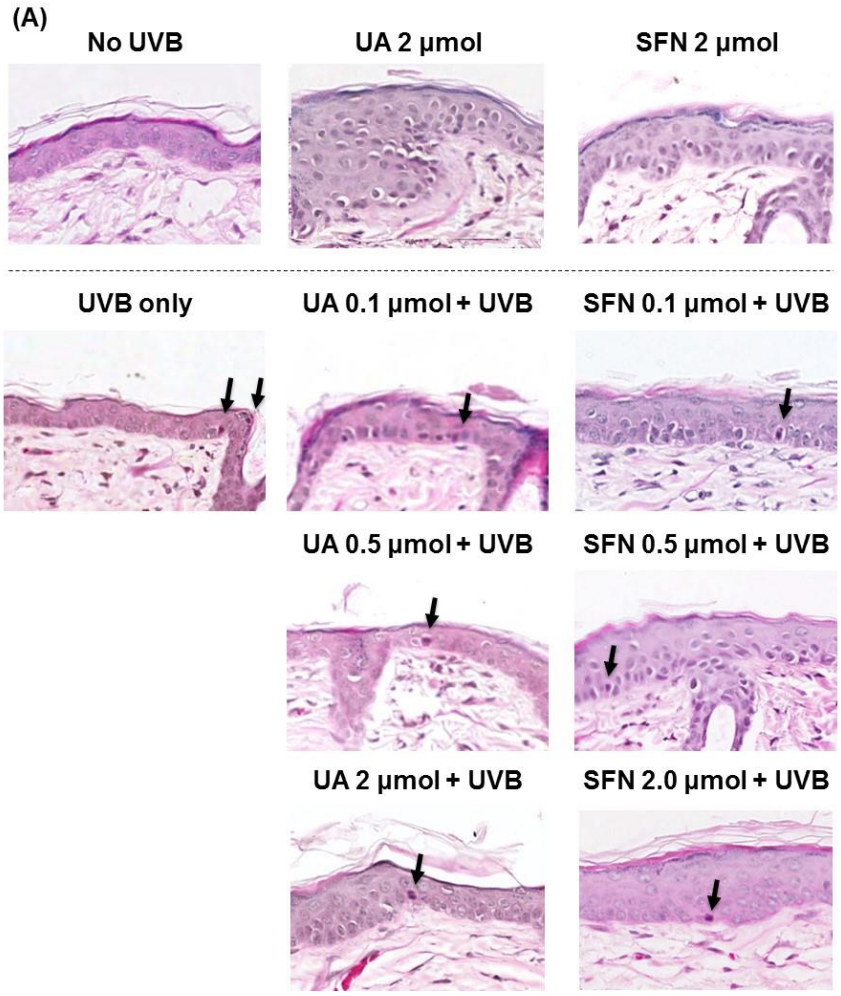
(A)
No UVB
UA 2 µmol
SFN 2 µmol
UVB only
UA 0.1 µmol + UVB
SFN 0.1 µmol + UVB
UA 0.5 µmol + UVB
SFN 0.5 µmol + UVB
UA 2 µmol + UVB
SFN 2.0 µmol + UVB

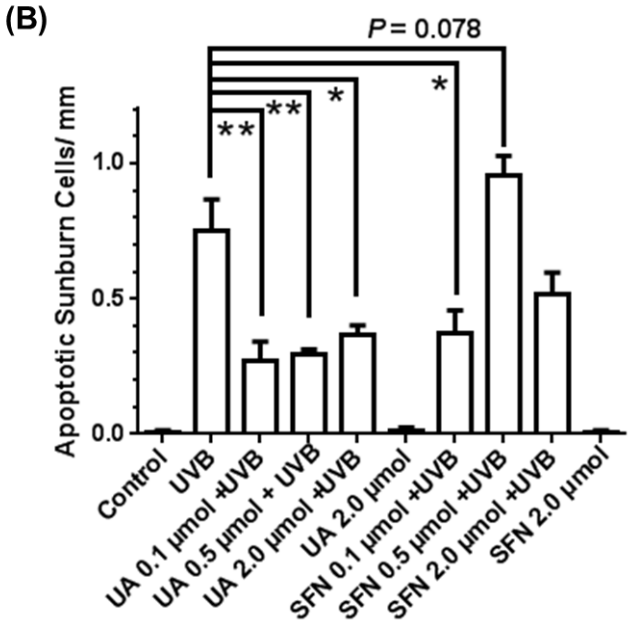
(B)
P = 0.078
**
**
*
*
Apoptotic Sunburn Cells/ mm
1.0
0.5
0.0
Control
UVB
UA 0.1 µmol +UVB
UA 0.5 µmol + UVB
UA 2.0 µmol +UVB
UA 2.0 µmol
SFN 0.1 µmol +UVB
SFN 0.5 µmol +UVB
SFN 2.0 µmol +UVB
SFN 2.0 µmol

Figure 6.3 Effects of topical application of ursolic acid (UA) and sulforaphane (SFN) on UVB-induced apoptotic sunburn cells in the epidermis from wild-type SKH-1 mice at 6 hours after UVB-irradiation.

Female SKH-1 mice (6-8 weeks old, three mice per group) were given 200 µl acetone (vehicle control), various concentrations of UA or SFN in 200 µl acetone topically once a day for four consecutive days. On the fourth day, 0.5 hours after topical application, mice were treated with a single dose of UVB (30 mJ/cm^2) after 6 hours, when is the peak of UVB-induced apoptosis. Mice without UVB-irradiation were served as the controls. All mice were sacrificed at 6 hours after UVB-irradiation. The number of apoptotic sunburn cells in 25mm length of epidermis was counted and determined as described in "Materials and Methods". **(A)** Representative figures of apoptotic sunburn cells were identified by their intense eosinophilia cytoplasm and small, dense nuclei, which was observed in H&E-stained histological sections of the skin by using light microscopy (Magnification 400×). **(B)** Quantification of apoptotic sunburn cells. Each value is the mean ± SEM. Student t-test was used to compare the treatment group to the UVB group; *$P < 0.05$, ** $P < 0.01$.

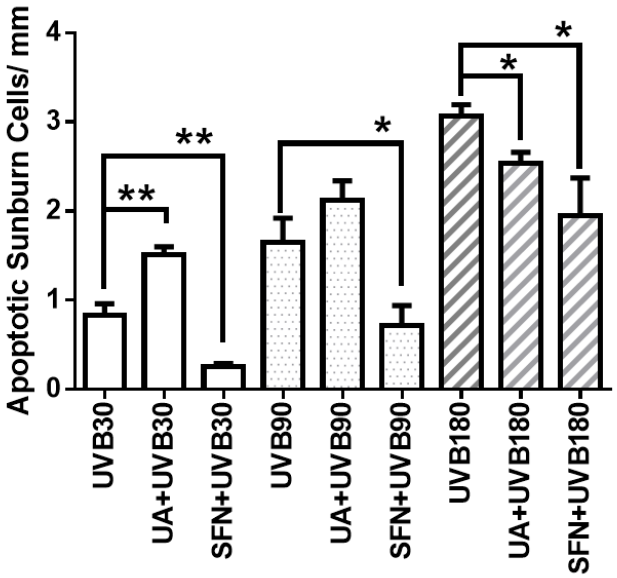

Figure 6.4. Quantification of apoptotic sunburn cells by UVB-irradiation at 30, 90 or 180 mJ/cm^2 after topical application of ursolic acid (UA) or sulforaphane (SFN) at the dorsal region of wild-type SKH-1 mice.

Female SKH-1 mice (6-8 weeks old) were given twice topical application of 200 µl acetone (vehicle control), UA (2 µmol) or SFN (2 µmol) in 200 µl acetone to mice were before a single dose of UVB-irradiation at the strength of 30, 90 or 180 mJ/cm^2. Mice were sacrificed at 6-8 hours after UVB-irradiation, when is the peak of UVB-induced apoptosis. The number of apoptotic sunburn cells in the epidermis was counted and determined as described in "Materials and Methods". Each value is the mean ± SEM (n = 3). Student t-test was used to compare the treatment group to the UVB alone group; *$P < 0.05$, ** $P < 0.01$.

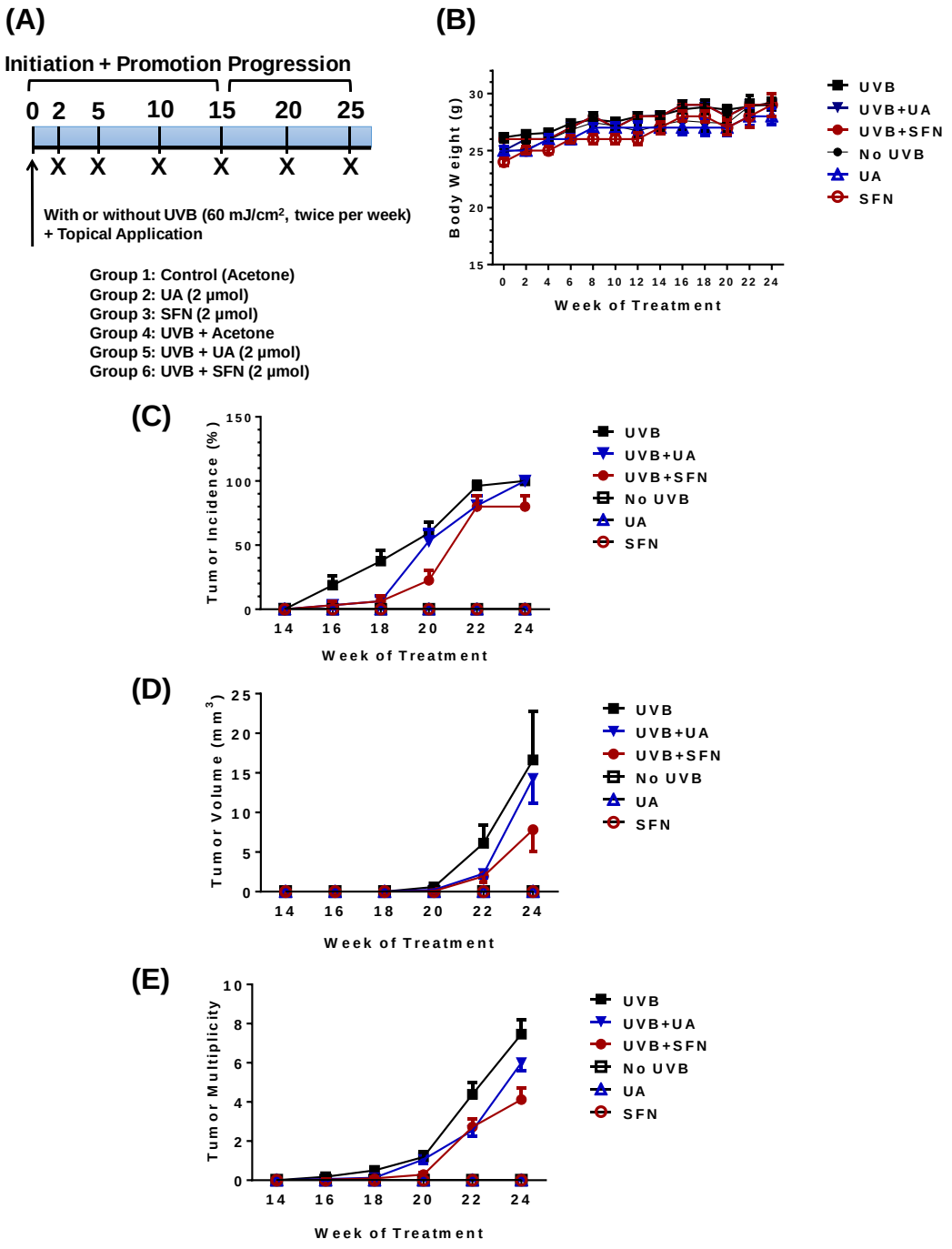

Figure 6.5. UA and SFN suppresses UVB-induced carcinogenesis.

Long-term chemoprevention studies to examine the epigenome/epigenetics during *in vivo* skin cancer development and progression with UVB-induced skin carcinogenesis in SKH-1 mice, to examine the cancer preventive efficacy of UA and

SFN. (A) Graphic of experimental design. (B) Steady increasing in body weight. (C) Percentage of tumor incidence (percentage of tumor-bearing mice). (D) Avearge tumor volume per mouse. (E) Tumor multiplicity to show the average number of tumors per mouse.

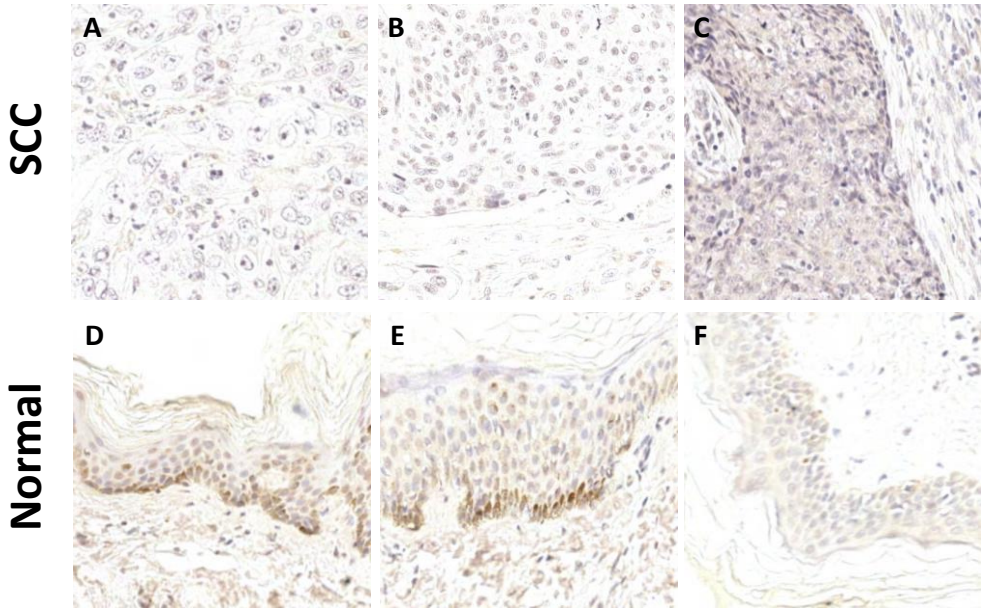

Figure 6.6. Immunihistochemical (IHC) staining of Nrf2 in squamous cell carcinoma (SCC) and cancer adjacent normal tissues.

Representative images of in SCCs from three patients (A, B and C) and cancer adjacent normal skin from another three subjects (D, E and F). (A, B and C) weak distributed staining of Nrf2 in SCCs. (D, E and F) scattered cells with stronger staining in the epidermis. All samples are shown at 400 × magnification.

7 Summary

We first reviewed the roles of phytochemicals in cancer chemoprevention through the Nrf2-ARE pathway and epigenetic modification. We then demonstrated that AST alone and in combination with DHA and EPA showed antioxidant effects via the Nrf2-ARE pathway in human HepG2-C8 cells. To further elucidate the molecular mechanism, we discovered that astaxanthin induced mRNA expression of Nrf2 and its downstream genes including HO-1, NQO1, and GSTM2. In addition, we demonstrated that astaxanthin significantly decreased the methylation of twenty-one CpG sites of *GSTP1* and restored the mRNA expression of *GSTP1*, suggesting a correlation between methylation and *GSTP1* expression. Furthermore, astaxanthin significantly reduced the protein expression of DNMT3b, and enzyme activity of DNMTs and HDACs in human LNCaP cells. In summary, dietary phytochemicals attenuate oxidative stress and abnormal epigenetic modification as promising drug candidates for cancer prevention.

The other major part of our studies is on non-melanoma skin cancers. The incidence of non-melanoma skin cancer has steadily increased per year, and UVB is one of the major courses of non-melanoma skin cancer from the environment. One in five Americans will develop skin cancers in a lifetime. Nrf2 shows protective role against inflammation-mediated extracellular matrix (ECM) damage induced by the UVB-irradiation. Our studies focused on the skin inflammation and epigenetic events in initiation and development of skin cancers. We demonstrated that Nrf2

together with HO-1 played a vital role in protection against UVB-irradiation via the inhibition of ECM damage degradation and inflammation. As compared with the WT mice, Nrf2 KO mice showed the increased protein expression of inflammatory markers including P53, macrophage inflammatory protein-2 (MIP-2), and pro-matrix metalloproteinase-9 (pro-MMP-9). These data suggested that the protective effects of Nrf2 in response to the UVB-irradiation were mediated by the increased HO-1 protein expression and the inhibition of inflammation-mediated extracellular matrix degradation.

In addition, accumulating evidence suggests that epigenetic DNA alteration plays a crucial role in cancer initiation and development. Our genome-wide study revealed lists of genes and cell signaling pathways which were altered in response to UVB-irradiation or the chemical carcinogen. In this study, we used methylated DNA immunoprecipitation (MeDIP) coupled with next-generation sequencing to profile the whole genome DNA methylation patterns from the two representative skin carcinogenesis models including the UVB-exposed SKH-1 hairless mice and multistage skin carcinogenesis DMBA/ TPA model in CD-1 mice. We have used the Ingenuity Pathway Analysis (IPA) software to analyze the MeDIP-Seq data to identify genes and gene interactions with significant changes in the databases of a wide range of biological processes. 6,003 genes in the UVB -induced tumor tissues and 5,424 genes in the DMBA/TPA-induced tumor tissues were identified by the IPA software with either significantly up-regulated or down-regulated methylation

status. These genes and cellular pathways could be applied in diagnosis, prevention of inflammation and oxidative stress in cosmetics, even prevention of initiation and development of skin cancers.

In the present study, we demonstrated that targeting epigenetic modification and Nrf2-pathway by natural dietary compounds such as astaxanthin is a promising approach in cancer prevention. Future study aims to identify the novel inhibitors of HDACs, DNMTs and Nrf2-pathway in cancer prevention by virtual screening combined with experimental validation.

REFERENCES

[1] Berger, S.L., Kouzarides, T., Shiekhattar, R., and Shilatifard, A., An operational definition of epigenetics. *Genes Dev*, **2009**. 23(7): p. 781-783.

[2] Gal-Yam, E.N., Saito, Y., Egger, G., and Jones, P.A., Cancer epigenetics: modifications, screening, and therapy. *Annu Rev Med*, **2008**. 59: p. 267-280.

[3] Graff, J. and Mansuy, I.M., Epigenetic codes in cognition and behaviour. *Behav Brain Res*, **2008**. 192(1): p. 70-87.

[4] Wang, G.G., Allis, C.D., and Chi, P., Chromatin remodeling and cancer, Part II: ATP-dependent chromatin remodeling. *Trends Mol Med*, **2007**. 13(9): p. 373-380.

[5] Wang, G.G., Allis, C.D., and Chi, P., Chromatin remodeling and cancer, Part I: Covalent histone modifications. *Trends Mol Med*, **2007**. 13(9): p. 363-372.

[6] de Groote, M.L., Verschure, P.J., and Rots, M.G., Epigenetic Editing: targeted rewriting of epigenetic marks to modulate expression of selected target genes. *Nucleic Acids Res*, **2012**. 40(21): p. 10596-10613.

[7] Maunakea, A.K., Nagarajan, R.P., Bilenky, M., Ballinger, T.J., D'Souza, C., Fouse, S.D., Johnson, B.E., Hong, C., Nielsen, C., Zhao, Y., Turecki, G., Delaney, A., Varhol, R., Thiessen, N., Shchors, K., Heine, V.M., Rowitch, D.H., Xing, X., Fiore, C., Schillebeeckx, M., Jones, S.J., Haussler, D., Marra, M.A., Hirst, M., Wang, T., and Costello, J.F., Conserved role of intragenic DNA methylation in regulating alternative promoters. *Nature*, **2010**. 466(7303): p. 253-257.

[8] De Smet, C., Lurquin, C., Lethe, B., Martelange, V., and Boon, T., DNA methylation is the primary silencing mechanism for a set of germ line- and tumor-specific genes with a CpG-rich promoter. *Mol Cell Biol*, **1999**. 19(11): p. 7327-7335.

[9] Jones, P.A. and Baylin, S.B., The fundamental role of epigenetic events in cancer. *Nat Rev Genet*, **2002**. 3(6): p. 415-428.

[10] Baylin, S.B., Makos, M., Wu, J.J., Yen, R.W., de Bustros, A., Vertino, P., and Nelkin, B.D., Abnormal patterns of DNA methylation in human neoplasia: potential consequences for tumor progression. *Cancer Cells*, **1991**. 3(10): p. 383-390.

[11] Chen, T. and Li, E., Establishment and maintenance of DNA methylation patterns in mammals. *Curr Top Microbiol Immunol*, **2006**. 301: p. 179-201.

[12] Jones, P.L., Veenstra, G.J., Wade, P.A., Vermaak, D., Kass, S.U., Landsberger, N., Strouboulis, J., and Wolffe, A.P., Methylated DNA and MeCP2 recruit histone deacetylase to repress transcription. *Nat Genet*, **1998**. 19(2): p. 187-191.

[13] Bird, A., DNA methylation patterns and epigenetic memory. *Genes Dev*, **2002**. 16(1): p. 6-21.

[14] Tahiliani, M., Koh, K.P., Shen, Y., Pastor, W.A., Bandukwala, H., Brudno, Y., Agarwal, S., Iyer, L.M., Liu, D.R., Aravind, L., and Rao, A., Conversion of 5-methylcytosine to 5-hydroxymethylcytosine in mammalian DNA by MLL partner TET1. *Science*, **2009**. 324(5929): p. 930-935.

[15] Ito, S., D'Alessio, A.C., Taranova, O.V., Hong, K., Sowers, L.C., and Zhang, Y., Role of Tet proteins in 5mC to 5hmC conversion, ES-cell self-renewal and inner cell mass specification. *Nature*, **2010**. 466(7310): p. 1129-1133.

[16] Kriaucionis, S. and Heintz, N., The nuclear DNA base 5-hydroxymethylcytosine is present in Purkinje neurons and the brain. *Science*, **2009**. 324(5929): p. 929-930.

[17] Khorasanizadeh, S., The nucleosome: from genomic organization to genomic regulation. *Cell*, **2004**. 116(2): p. 259-272.

[18] Dillon, N., Gene regulation and large-scale chromatin organization in the nucleus. *Chromosome Res*, **2006**. 14(1): p. 117-126.

[19] Kouzarides, T., Chromatin modifications and their function. *Cell*, **2007**. 128(4): p. 693-705.

[20] Tan, M., Luo, H., Lee, S., Jin, F., Yang, J.S., Montellier, E., Buchou, T., Cheng, Z., Rousseaux, S., Rajagopal, N., Lu, Z., Ye, Z., Zhu, Q., Wysocka, J., Ye, Y., Khochbin, S., Ren, B., and Zhao, Y., Identification of 67 histone marks and histone lysine crotonylation as a new type of histone modification. *Cell*, **2011**. 146(6): p. 1016-1028.

[21] Haberland, M., Montgomery, R.L., and Olson, E.N., The many roles of histone deacetylases in development and physiology: implications for disease and therapy. *Nat Rev Genet*, **2009**. 10(1): p. 32-42.

[22] Lan, F., Bayliss, P.E., Rinn, J.L., Whetstine, J.R., Wang, J.K., Chen, S., Iwase, S., Alpatov, R., Issaeva, I., Canaani, E., Roberts, T.M., Chang, H.Y., and Shi, Y., A histone H3 lysine 27 demethylase regulates animal posterior development. *Nature*, **2007**. 449(7163): p. 689-694.

[23] Berlowitz, L. and Pallotta, D., Acetylation of nuclear protein in the heterochromatin and euchromatin of mealy bugs. *Exp Cell Res*, **1972**. 71(1): p. 45-48.

[24] Luger, K., Mader, A.W., Richmond, R.K., Sargent, D.F., and Richmond, T.J., Crystal structure of the nucleosome core particle at 2.8 A resolution. *Nature*, **1997**. 389(6648): p. 251-260.

[25] Tremethick, D.J., Higher-order structures of chromatin: the elusive 30 nm fiber. *Cell*, **2007**. 128(4): p. 651-654.

[26] Barger, J.F. and Nana-Sinkam, S.P., MicroRNA as tools and therapeutics in lung cancer. *Respir Med*, **2015**.

[27] Luo, C., Weber, C.E., Osen, W., Bosserhoff, A.K., and Eichmuller, S.B., The role of microRNAs in melanoma. *Eur J Cell Biol*, **2014**. 93(1-2): p. 11-22.

[28] Wang, Y.L., Wu, S., Jiang, B., Yin, F.F., Zheng, S.S., and Hou, S.C., Role of MicroRNAs in Prostate Cancer Pathogenesis. *Clin Genitourin Cancer*, **2015**.

[29] Asangani, I.A., Harms, P.W., Dodson, L., Pandhi, M., Kunju, L.P., Maher, C.A., Fullen, D.R., Johnson, T.M., Giordano, T.J., Palanisamy, N., and Chinnaiyan, A.M., Genetic and epigenetic loss of microRNA-31 leads to feed-forward expression of EZH2 in melanoma. *Oncotarget*, **2012**. 3(9): p. 1011-1025.

[30] Taverna, S.D., Li, H., Ruthenburg, A.J., Allis, C.D., and Patel, D.J., How chromatin-binding modules interpret histone modifications: lessons from professional pocket pickers. *Nat Struct Mol Biol*, **2007**. 14(11): p. 1025-1040.

[31] Chi, P., Allis, C.D., and Wang, G.G., Covalent histone modifications--miswritten, misinterpreted and mis-erased in human cancers. *Nat Rev Cancer*, **2010**. 10(7): p. 457-469.

[32] Lan, F., Collins, R.E., De Cegli, R., Alpatov, R., Horton, J.R., Shi, X., Gozani, O., Cheng, X., and Shi, Y., Recognition of unmethylated histone H3 lysine 4 links BHC80 to LSD1-mediated gene repression. *Nature*, **2007**. 448(7154): p. 718-722.

[33] Ooi, S.K., Qiu, C., Bernstein, E., Li, K., Jia, D., Yang, Z., Erdjument-Bromage, H., Tempst, P., Lin, S.P., Allis, C.D., Cheng, X., and Bestor, T.H., DNMT3L connects unmethylated lysine 4 of histone H3 to de novo methylation of DNA. *Nature*, **2007**. 448(7154): p. 714-717.

[34] Jacobson, R.H., Ladurner, A.G., King, D.S., and Tjian, R., Structure and function of a human TAFII250 double bromodomain module. *Science*, **2000**. 288(5470): p. 1422-1425.

[35] Gyuris, A., Donovan, D.J., Seymour, K.A., Lovasco, L.A., Smilowitz, N.R., Halperin, A.L., Klysik, J.E., and Freiman, R.N., The chromatin-targeting protein Brd2 is required for neural tube closure and embryogenesis. *Biochim Biophys Acta*, **2009**. 1789(5): p. 413-421.

[36] Greenwald, R.J., Tumang, J.R., Sinha, A., Currier, N., Cardiff, R.D., Rothstein, T.L., Faller, D.V., and Denis, G.V., E mu-BRD2 transgenic mice develop B-cell lymphoma and leukemia. *Blood*, **2004**. 103(4): p. 1475-1484.

[37] Filippakopoulos, P., Qi, J., Picaud, S., Shen, Y., Smith, W.B., Fedorov, O., Morse, E.M., Keates, T., Hickman, T.T., Felletar, I., Philpott, M., Munro, S., McKeown, M.R., Wang, Y., Christie, A.L., West, N., Cameron, M.J., Schwartz, B., Heightman, T.D., La Thangue, N., French, C.A., Wiest, O., Kung, A.L., Knapp, S., and Bradner, J.E., Selective inhibition of BET bromodomains. *Nature*, **2010**. 468(7327): p. 1067-1073.

[38] Dawson, M.A., Prinjha, R.K., Dittmann, A., Giotopoulos, G., Bantscheff, M., Chan, W.I., Robson, S.C., Chung, C.W., Hopf, C., Savitski, M.M., Huthmacher, C., Gudgin, E., Lugo, D., Beinke, S., Chapman, T.D., Roberts, E.J., Soden, P.E., Auger, K.R., Mirguet, O., Doehner, K., Delwel, R., Burnett, A.K., Jeffrey, P., Drewes, G., Lee, K., Huntly, B.J., and Kouzarides, T.,

Inhibition of BET recruitment to chromatin as an effective treatment for MLL-fusion leukaemia. *Nature*, **2011**. 478(7370): p. 529-533.

[39] Nicodeme, E., Jeffrey, K.L., Schaefer, U., Beinke, S., Dewell, S., Chung, C.W., Chandwani, R., Marazzi, I., Wilson, P., Coste, H., White, J., Kirilovsky, J., Rice, C.M., Lora, J.M., Prinjha, R.K., Lee, K., and Tarakhovsky, A., Suppression of inflammation by a synthetic histone mimic. *Nature*, **2010**. 468(7327): p. 1119-1123.

[40] Delmore, J.E., Issa, G.C., Lemieux, M.E., Rahl, P.B., Shi, J., Jacobs, H.M., Kastritis, E., Gilpatrick, T., Paranal, R.M., Qi, J., Chesi, M., Schinzel, A.C., McKeown, M.R., Heffernan, T.P., Vakoc, C.R., Bergsagel, P.L., Ghobrial, I.M., Richardson, P.G., Young, R.A., Hahn, W.C., Anderson, K.C., Kung, A.L., Bradner, J.E., and Mitsiades, C.S., BET bromodomain inhibition as a therapeutic strategy to target c-Myc. *Cell*, **2011**. 146(6): p. 904-917.

[41] Mertz, J.A., Conery, A.R., Bryant, B.M., Sandy, P., Balasubramanian, S., Mele, D.A., Bergeron, L., and Sims, R.J., 3rd, Targeting MYC dependence in cancer by inhibiting BET bromodomains. *Proc Natl Acad Sci U S A*, **2011**. 108(40): p. 16669-16674.

[42] Parry, L. and Clarke, A.R., The Roles of the Methyl-CpG Binding Proteins in Cancer. *Genes Cancer*, **2011**. 2(6): p. 618-630.

[43] Lopez-Serra, L. and Esteller, M., Proteins that bind methylated DNA and human cancer: reading the wrong words. *Br J Cancer*, **2008**. 98(12): p. 1881-1885.

[44] Muller, I., Wischnewski, F., Pantel, K., and Schwarzenbach, H., Promoter- and cell-specific epigenetic regulation of CD44, Cyclin D2, GLIPR1 and PTEN by methyl-CpG binding proteins and histone modifications. *BMC Cancer*, **2010**. 10: p. 297.

[45] Wyhs, N., Walker, D., Giovinazzo, H., Yegnasubramanian, S., and Nelson, W.G., Time-Resolved Fluorescence Resonance Energy Transfer Assay for Discovery of Small-Molecule Inhibitors of Methyl-CpG Binding Domain Protein 2. *J Biomol Screen*, **2014**. 19(7): p. 1060-1069.

[46] Yang, X., Lay, F., Han, H., and Jones, P.A., Targeting DNA methylation for epigenetic therapy. *Trends Pharmacol Sci*, **2010**. 31(11): p. 536-546.

[47] Jones, P.A. and Taylor, S.M., Cellular differentiation, cytidine analogs and DNA methylation. *Cell*, **1980**. 20(1): p. 85-93.

[48] Fenaux, P., Mufti, G.J., Hellstrom-Lindberg, E., Santini, V., Finelli, C., Giagounidis, A., Schoch, R., Gattermann, N., Sanz, G., List, A., Gore, S.D., Seymour, J.F., Bennett, J.M., Byrd, J., Backstrom, J., Zimmerman, L., McKenzie, D., Beach, C., Silverman, L.R., and International Vidaza High-Risk, M.D.S.S.S.G., Efficacy of azacitidine compared with that of conventional care regimens in the treatment of higher-risk myelodysplastic syndromes: a randomised, open-label, phase III study. *Lancet Oncol*, **2009**. 10(3): p. 223-232.

[49] Tsai, H.C., Li, H., Van Neste, L., Cai, Y., Robert, C., Rassool, F.V., Shin, J.J., Harbom, K.M., Beaty, R., Pappou, E., Harris, J., Yen, R.W., Ahuja, N., Brock, M.V., Stearns, V., Feller-Kopman, D., Yarmus, L.B., Lin, Y.C., Welm, A.L., Issa, J.P., Minn, I., Matsui, W., Jang, Y.Y., Sharkis, S.J., Baylin, S.B., and Zahnow, C.A., Transient low doses of DNA-demethylating agents exert durable antitumor effects on hematological and epithelial tumor cells. *Cancer Cell*, **2012**. 21(3): p. 430-446.

[50] Ruiz-Carrillo, A., Wangh, L.J., and Allfrey, V.G., Processing of newly synthesized histone molecules. *Science*, **1975**. 190(4210): p. 117-128.

[51] Lau, O.D., Kundu, T.K., Soccio, R.E., Ait-Si-Ali, S., Khalil, E.M., Vassilev, A., Wolffe, A.P., Nakatani, Y., Roeder, R.G., and Cole, P.A., HATs off: selective synthetic inhibitors of the histone acetyltransferases p300 and PCAF. *Mol Cell*, **2000**. 5(3): p. 589-595.

[52] Richon, V.M., Johnston, D., Sneeringer, C.J., Jin, L., Majer, C.R., Elliston, K., Jerva, L.F., Scott, M.P., and Copeland, R.A., Chemogenetic analysis of human protein methyltransferases. *Chem Biol Drug Des*, **2011**. 78(2): p. 199-210.

[53] Daigle, S.R., Olhava, E.J., Therkelsen, C.A., Majer, C.R., Sneeringer, C.J., Song, J., Johnston, L.D., Scott, M.P., Smith, J.J., Xiao, Y., Jin, L., Kuntz, K.W., Chesworth, R., Moyer, M.P., Bernt, K.M., Tseng, J.C., Kung, A.L., Armstrong, S.A., Copeland, R.A., Richon, V.M., and Pollock, R.M., Selective killing of mixed lineage leukemia cells by a potent small-molecule DOT1L inhibitor. *Cancer Cell*, **2011**. 20(1): p. 53-65.

[54] Daigle, S.R., Olhava, E.J., Therkelsen, C.A., Basavapathruni, A., Jin, L., Boriack-Sjodin, P.A., Allain, C.J., Klaus, C.R., Raimondi, A., Scott, M.P., Waters, N.J., Chesworth, R., Moyer, M.P., Copeland, R.A., Richon, V.M., and Pollock, R.M., Potent inhibition of DOT1L as treatment of MLL-fusion leukemia. *Blood*, **2013**. 122(6): p. 1017-1025.

[55] Morey, L. and Helin, K., Polycomb group protein-mediated repression of transcription. *Trends Biochem Sci*, **2010**. 35(6): p. 323-332.

[56] Varambally, S., Dhanasekaran, S.M., Zhou, M., Barrette, T.R., Kumar-Sinha, C., Sanda, M.G., Ghosh, D., Pienta, K.J., Sewalt, R.G., Otte, A.P., Rubin, M.A., and Chinnaiyan, A.M., The polycomb group protein EZH2 is involved in progression of prostate cancer. *Nature*, **2002**. 419(6907): p. 624-629.

[57] Kleer, C.G., Cao, Q., Varambally, S., Shen, R., Ota, I., Tomlins, S.A., Ghosh, D., Sewalt, R.G., Otte, A.P., Hayes, D.F., Sabel, M.S., Livant, D., Weiss, S.J., Rubin, M.A., and Chinnaiyan, A.M., EZH2 is a marker of aggressive breast cancer and promotes neoplastic transformation of breast epithelial cells. *Proc Natl Acad Sci U S A*, **2003**. 100(20): p. 11606-11611.

[58] Wagener, N., Macher-Goeppinger, S., Pritsch, M., Husing, J., Hoppe-Seyler, K., Schirmacher, P., Pfitzenmaier, J., Haferkamp, A., Hoppe-Seyler, F., and Hohenfellner, M., Enhancer of zeste homolog 2 (EZH2) expression is an

independent prognostic factor in renal cell carcinoma. *BMC Cancer*, **2010**. 10: p. 524.

[59] Takawa, M., Masuda, K., Kunizaki, M., Daigo, Y., Takagi, K., Iwai, Y., Cho, H.S., Toyokawa, G., Yamane, Y., Maejima, K., Field, H.I., Kobayashi, T., Akasu, T., Sugiyama, M., Tsuchiya, E., Atomi, Y., Ponder, B.A., Nakamura, Y., and Hamamoto, R., Validation of the histone methyltransferase EZH2 as a therapeutic target for various types of human cancer and as a prognostic marker. *Cancer Sci*, **2011**. 102(7): p. 1298-1305.

[60] Tan, J., Yang, X., Zhuang, L., Jiang, X., Chen, W., Lee, P.L., Karuturi, R.K., Tan, P.B., Liu, E.T., and Yu, Q., Pharmacologic disruption of Polycomb-repressive complex 2-mediated gene repression selectively induces apoptosis in cancer cells. *Genes Dev*, **2007**. 21(9): p. 1050-1063.

[61] Miranda, T.B., Cortez, C.C., Yoo, C.B., Liang, G., Abe, M., Kelly, T.K., Marquez, V.E., and Jones, P.A., DZNep is a global histone methylation inhibitor that reactivates developmental genes not silenced by DNA methylation. *Mol Cancer Ther*, **2009**. 8(6): p. 1579-1588.

[62] Knutson, S.K., Wigle, T.J., Warholic, N.M., Sneeringer, C.J., Allain, C.J., Klaus, C.R., Sacks, J.D., Raimondi, A., Majer, C.R., Song, J., Scott, M.P., Jin, L., Smith, J.J., Olhava, E.J., Chesworth, R., Moyer, M.P., Richon, V.M., Copeland, R.A., Keilhack, H., Pollock, R.M., and Kuntz, K.W., A selective inhibitor of EZH2 blocks H3K27 methylation and kills mutant lymphoma cells. *Nat Chem Biol*, **2012**. 8(11): p. 890-896.

[63] McCabe, M.T., Ott, H.M., Ganji, G., Korenchuk, S., Thompson, C., Van Aller, G.S., Liu, Y., Graves, A.P., Della Pietra, A., 3rd, Diaz, E., LaFrance, L.V., Mellinger, M., Duquenne, C., Tian, X., Kruger, R.G., McHugh, C.F., Brandt, M., Miller, W.H., Dhanak, D., Verma, S.K., Tummino, P.J., and Creasy, C.L., EZH2 inhibition as a therapeutic strategy for lymphoma with EZH2-activating mutations. *Nature*, **2012**. 492(7427): p. 108-112.

[64] Qi, W., Chan, H., Teng, L., Li, L., Chuai, S., Zhang, R., Zeng, J., Li, M., Fan, H., Lin, Y., Gu, J., Ardayfio, O., Zhang, J.H., Yan, X., Fang, J., Mi, Y., Zhang, M., Zhou, T., Feng, G., Chen, Z., Li, G., Yang, T., Zhao, K., Liu, X., Yu, Z., Lu, C.X., Atadja, P., and Li, E., Selective inhibition of Ezh2 by a small molecule inhibitor blocks tumor cells proliferation. *Proc Natl Acad Sci U S A*, **2012**. 109(52): p. 21360-21365.

[65] Knutson, S.K., Warholic, N.M., Wigle, T.J., Klaus, C.R., Allain, C.J., Raimondi, A., Porter Scott, M., Chesworth, R., Moyer, M.P., Copeland, R.A., Richon, V.M., Pollock, R.M., Kuntz, K.W., and Keilhack, H., Durable tumor regression in genetically altered malignant rhabdoid tumors by inhibition of methyltransferase EZH2. *Proc Natl Acad Sci U S A*, **2013**. 110(19): p. 7922-7927.

[66] Scourzic, L., Mouly, E., and Bernard, O.A., TET proteins and the control of cytosine demethylation in cancer. *Genome Med*, **2015**. 7(1): p. 9.

[67] Lian, C.G., Xu, Y., Ceol, C., Wu, F., Larson, A., Dresser, K., Xu, W., Tan, L., Hu, Y., Zhan, Q., Lee, C.W., Hu, D., Lian, B.Q., Kleffel, S., Yang, Y., Neiswender, J., Khorasani, A.J., Fang, R., Lezcano, C., Duncan, L.M., Scolyer, R.A., Thompson, J.F., Kakavand, H., Houvras, Y., Zon, L.I., Mihm, M.C., Jr., Kaiser, U.B., Schatton, T., Woda, B.A., Murphy, G.F., and Shi, Y.G., Loss of 5-hydroxymethylcytosine is an epigenetic hallmark of melanoma. *Cell*, **2012**. 150(6): p. 1135-1146.

[68] Stransky, N., Egloff, A.M., Tward, A.D., Kostic, A.D., Cibulskis, K., Sivachenko, A., Kryukov, G.V., Lawrence, M.S., Sougnez, C., McKenna, A., Shefler, E., Ramos, A.H., Stojanov, P., Carter, S.L., Voet, D., Cortes, M.L., Auclair, D., Berger, M.F., Saksena, G., Guiducci, C., Onofrio, R.C., Parkin, M., Romkes, M., Weissfeld, J.L., Seethala, R.R., Wang, L., Rangel-Escareno, C., Fernandez-Lopez, J.C., Hidalgo-Miranda, A., Melendez-Zajgla, J., Winckler, W., Ardlie, K., Gabriel, S.B., Meyerson, M., Lander, E.S., Getz, G., Golub, T.R., Garraway, L.A., and Grandis, J.R., The mutational landscape of head and neck squamous cell carcinoma. *Science*, **2011**. 333(6046): p. 1157-1160.

[69] Kan, Z., Jaiswal, B.S., Stinson, J., Janakiraman, V., Bhatt, D., Stern, H.M., Yue, P., Haverty, P.M., Bourgon, R., Zheng, J., Moorhead, M., Chaudhuri, S., Tomsho, L.P., Peters, B.A., Pujara, K., Cordes, S., Davis, D.P., Carlton, V.E., Yuan, W., Li, L., Wang, W., Eigenbrot, C., Kaminker, J.S., Eberhard, D.A., Waring, P., Schuster, S.C., Modrusan, Z., Zhang, Z., Stokoe, D., de Sauvage, F.J., Faham, M., and Seshagiri, S., Diverse somatic mutation patterns and pathway alterations in human cancers. *Nature*, **2010**. 466(7308): p. 869-873.

[70] Barth, T.K. and Imhof, A., Fast signals and slow marks: the dynamics of histone modifications. *Trends Biochem Sci*, **2010**. 35(11): p. 618-626.

[71] Zee, B.M., Levin, R.S., Xu, B., LeRoy, G., Wingreen, N.S., and Garcia, B.A., In vivo residue-specific histone methylation dynamics. *J Biol Chem*, **2010**. 285(5): p. 3341-3350.

[72] Shi, Y., Lan, F., Matson, C., Mulligan, P., Whetstine, J.R., Cole, P.A., Casero, R.A., and Shi, Y., Histone demethylation mediated by the nuclear amine oxidase homolog LSD1. *Cell*, **2004**. 119(7): p. 941-953.

[73] Tsukada, Y., Fang, J., Erdjument-Bromage, H., Warren, M.E., Borchers, C.H., Tempst, P., and Zhang, Y., Histone demethylation by a family of JmjC domain-containing proteins. *Nature*, **2006**. 439(7078): p. 811-816.

[74] Whetstine, J.R., Nottke, A., Lan, F., Huarte, M., Smolikov, S., Chen, Z., Spooner, E., Li, E., Zhang, G., Colaiacovo, M., and Shi, Y., Reversal of histone lysine trimethylation by the JMJD2 family of histone demethylases. *Cell*, **2006**. 125(3): p. 467-481.

[75] Fitzpatrick, P.F., Oxidation of amines by flavoproteins. *Arch Biochem Biophys*, **2010**. 493(1): p. 13-25.

[76] Kahl, P., Gullotti, L., Heukamp, L.C., Wolf, S., Friedrichs, N., Vorreuther, R., Solleder, G., Bastian, P.J., Ellinger, J., Metzger, E., Schule, R., and Buettner, R., Androgen receptor coactivators lysine-specific histone demethylase 1 and four and a half LIM domain protein 2 predict risk of prostate cancer recurrence. *Cancer Res*, **2006**. 66(23): p. 11341-11347.

[77] Hayami, S., Kelly, J.D., Cho, H.S., Yoshimatsu, M., Unoki, M., Tsunoda, T., Field, H.I., Neal, D.E., Yamaue, H., Ponder, B.A., Nakamura, Y., and Hamamoto, R., Overexpression of LSD1 contributes to human carcinogenesis through chromatin regulation in various cancers. *Int J Cancer*, **2011**. 128(3): p. 574-586.

[78] Kauffman, E.C., Robinson, B.D., Downes, M.J., Powell, L.G., Lee, M.M., Scherr, D.S., Gudas, L.J., and Mongan, N.P., Role of androgen receptor and associated lysine-demethylase coregulators, LSD1 and JMJD2A, in localized and advanced human bladder cancer. *Mol Carcinog*, **2011**. 50(12): p. 931-944.

[79] Lee, M.G., Wynder, C., Schmidt, D.M., McCafferty, D.G., and Shiekhattar, R., Histone H3 lysine 4 demethylation is a target of nonselective antidepressive medications. *Chem Biol*, **2006**. 13(6): p. 563-567.

[80] Schenk, T., Chen, W.C., Gollner, S., Howell, L., Jin, L., Hebestreit, K., Klein, H.U., Popescu, A.C., Burnett, A., Mills, K., Casero, R.A., Jr., Marton, L., Woster, P., Minden, M.D., Dugas, M., Wang, J.C., Dick, J.E., Muller-Tidow, C., Petrie, K., and Zelent, A., Inhibition of the LSD1 (KDM1A) demethylase reactivates the all-trans-retinoic acid differentiation pathway in acute myeloid leukemia. *Nat Med*, **2012**. 18(4): p. 605-611.

[81] Willmann, D., Lim, S., Wetzel, S., Metzger, E., Jandausch, A., Wilk, W., Jung, M., Forne, I., Imhof, A., Janzer, A., Kirfel, J., Waldmann, H., Schule, R., and Buettner, R., Impairment of prostate cancer cell growth by a selective and reversible lysine-specific demethylase 1 inhibitor. *Int J Cancer*, **2012**. 131(11): p. 2704-2709.

[82] Cloos, P.A., Christensen, J., Agger, K., Maiolica, A., Rappsilber, J., Antal, T., Hansen, K.H., and Helin, K., The putative oncogene GASC1 demethylates tri- and dimethylated lysine 9 on histone H3. *Nature*, **2006**. 442(7100): p. 307-311.

[83] Kruidenier, L., Chung, C.W., Cheng, Z., Liddle, J., Che, K., Joberty, G., Bantscheff, M., Bountra, C., Bridges, A., Diallo, H., Eberhard, D., Hutchinson, S., Jones, E., Katso, R., Leveridge, M., Mander, P.K., Mosley, J., Ramirez-Molina, C., Rowland, P., Schofield, C.J., Sheppard, R.J., Smith, J.E., Swales, C., Tanner, R., Thomas, P., Tumber, A., Drewes, G., Oppermann, U., Patel, D.J., Lee, K., and Wilson, D.M., A selective jumonji H3K27 demethylase inhibitor modulates the proinflammatory macrophage response. *Nature*, **2012**. 488(7411): p. 404-408.

[84] Haigis, M.C. and Sinclair, D.A., Mammalian sirtuins: biological insights and disease relevance. *Annu Rev Pathol*, **2010**. 5: p. 253-295.

[85] Hu, J., Jing, H., and Lin, H., Sirtuin inhibitors as anticancer agents. *Future Med Chem*, **2014**. 6(8): p. 945-966.

[86] Hu, J., He, B., Bhargava, S., and Lin, H., A fluorogenic assay for screening Sirt6 modulators. *Org Biomol Chem*, **2013**. 11(32): p. 5213-5216.

[87] Tervo, A.J., Kyrylenko, S., Niskanen, P., Salminen, A., Leppanen, J., Nyronen, T.H., Jarvinen, T., and Poso, A., An in silico approach to discovering novel inhibitors of human sirtuin type 2. *J Med Chem*, **2004**. 47(25): p. 6292-6298.

[88] Audrito, V., Vaisitti, T., Rossi, D., Gottardi, D., D'Arena, G., Laurenti, L., Gaidano, G., Malavasi, F., and Deaglio, S., Nicotinamide blocks proliferation and induces apoptosis of chronic lymphocytic leukemia cells through activation of the p53/miR-34a/SIRT1 tumor suppressor network. *Cancer Res*, **2011**. 71(13): p. 4473-4483.

[89] Jung-Hynes, B., Nihal, M., Zhong, W., and Ahmad, N., Role of sirtuin histone deacetylase SIRT1 in prostate cancer. A target for prostate cancer management via its inhibition? *J Biol Chem*, **2009**. 284(6): p. 3823-3832.

[90] Yuan, J., Minter-Dykhouse, K., and Lou, Z., A c-Myc-SIRT1 feedback loop regulates cell growth and transformation. *J Cell Biol*, **2009**. 185(2): p. 203-211.

[91] Luo, J., Su, F., Chen, D., Shiloh, A., and Gu, W., Deacetylation of p53 modulates its effect on cell growth and apoptosis. *Nature*, **2000**. 408(6810): p. 377-381.

[92] Ropero, S. and Esteller, M., The role of histone deacetylases (HDACs) in human cancer. *Mol Oncol*, **2007**. 1(1): p. 19-25.

[93] West, A.C., Smyth, M.J., and Johnstone, R.W., The anticancer effects of HDAC inhibitors require the immune system. *Oncoimmunology*, **2014**. 3(1): p. e27414.

[94] West, A.C. and Johnstone, R.W., New and emerging HDAC inhibitors for cancer treatment. *J Clin Invest*, **2014**. 124(1): p. 30-39.

[95] Bolden, J.E., Peart, M.J., and Johnstone, R.W., Anticancer activities of histone deacetylase inhibitors. *Nat Rev Drug Discov*, **2006**. 5(9): p. 769-784.

[96] Nebbioso, A., Clarke, N., Voltz, E., Germain, E., Ambrosino, C., Bontempo, P., Alvarez, R., Schiavone, E.M., Ferrara, F., Bresciani, F., Weisz, A., de Lera, A.R., Gronemeyer, H., and Altucci, L., Tumor-selective action of HDAC inhibitors involves TRAIL induction in acute myeloid leukemia cells. *Nat Med*, **2005**. 11(1): p. 77-84.

[97] Geng, L., Cuneo, K.C., Fu, A., Tu, T., Atadja, P.W., and Hallahan, D.E., Histone deacetylase (HDAC) inhibitor LBH589 increases duration of gamma-H2AX foci and confines HDAC4 to the cytoplasm in irradiated non-small cell lung cancer. *Cancer Res*, **2006**. 66(23): p. 11298-11304.

[98] Qian, D.Z., Kato, Y., Shabbeer, S., Wei, Y., Verheul, H.M., Salumbides, B., Sanni, T., Atadja, P., and Pili, R., Targeting tumor angiogenesis with histone deacetylase inhibitors: the hydroxamic acid derivative LBH589. *Clin Cancer Res*, **2006**. 12(2): p. 634-642.

[99] Piekarz, R.L., Frye, R., Turner, M., Wright, J.J., Allen, S.L., Kirschbaum, M.H., Zain, J., Prince, H.M., Leonard, J.P., Geskin, L.J., Reeder, C., Joske, D., Figg, W.D., Gardner, E.R., Steinberg, S.M., Jaffe, E.S., Stetler-Stevenson, M., Lade, S., Fojo, A.T., and Bates, S.E., Phase II multi-institutional trial of the histone deacetylase inhibitor romidepsin as monotherapy for patients with cutaneous T-cell lymphoma. *J Clin Oncol*, **2009**. 27(32): p. 5410-5417.

[100] Whittaker, S.J., Demierre, M.F., Kim, E.J., Rook, A.H., Lerner, A., Duvic, M., Scarisbrick, J., Reddy, S., Robak, T., Becker, J.C., Samtsov, A., McCulloch, W., and Kim, Y.H., Final results from a multicenter, international, pivotal study of romidepsin in refractory cutaneous T-cell lymphoma. *J Clin Oncol*, **2010**. 28(29): p. 4485-4491.

[101] Piekarz, R.L., Frye, R., Prince, H.M., Kirschbaum, M.H., Zain, J., Allen, S.L., Jaffe, E.S., Ling, A., Turner, M., Peer, C.J., Figg, W.D., Steinberg, S.M., Smith, S., Joske, D., Lewis, I., Hutchins, L., Craig, M., Fojo, A.T., Wright, J.J., and Bates, S.E., Phase 2 trial of romidepsin in patients with peripheral T-cell lymphoma. *Blood*, **2011**. 117(22): p. 5827-5834.

[102] Coiffier, B., Pro, B., Prince, H.M., Foss, F., Sokol, L., Greenwood, M., Caballero, D., Borchmann, P., Morschhauser, F., Wilhelm, M., Pinter-Brown, L., Padmanabhan, S., Shustov, A., Nichols, J., Carroll, S., Balser, J., Balser, B., and Horwitz, S., Results from a pivotal, open-label, phase II study of romidepsin in relapsed or refractory peripheral T-cell lymphoma after prior systemic therapy. *J Clin Oncol*, **2012**. 30(6): p. 631-636.

[103] Vickers, C.J., Olsen, C.A., Leman, L.J., and Ghadiri, M.R., Discovery of HDAC Inhibitors That Lack an Active Site Zn(2+)-Binding Functional Group. *ACS Med Chem Lett*, **2012**. 3(6): p. 505-508.

[104] Yoshida, K., Yamaguchi, K., Mizuno, A., Unno, Y., Asai, A., Sone, T., Yokosawa, H., Matsuda, A., Arisawa, M., and Shuto, S., Three-dimensional structure-activity relationship study of belactosin A and its stereo- and regioisomers: development of potent proteasome inhibitors by a stereochemical diversity-oriented strategy. *Org Biomol Chem*, **2009**. 7(9): p. 1868-1877.

[105] Hu, J. and Colburn, N.H., Histone deacetylase inhibition down-regulates cyclin D1 transcription by inhibiting nuclear factor-kappaB/p65 DNA binding. *Mol Cancer Res*, **2005**. 3(2): p. 100-109.

[106] Chan, S.T., Yang, N.C., Huang, C.S., Liao, J.W., and Yeh, S.L., Quercetin enhances the antitumor activity of trichostatin A through upregulation of p53 protein expression in vitro and in vivo. *PLoS One*, **2013**. 8(1): p. e54255.

[107] Mann, B.S., Johnson, J.R., Cohen, M.H., Justice, R., and Pazdur, R., FDA approval summary: vorinostat for treatment of advanced primary cutaneous T-cell lymphoma. *Oncologist*, **2007**. 12(10): p. 1247-1252.

[108] Marks, P.A., Discovery and development of SAHA as an anticancer agent. *Oncogene*, **2007**. 26(9): p. 1351-1356.

[109] Lee, H.Z., Kwitkowski, V.E., Del Valle, P.L., Ricci, M.S., Saber, H., Habtemariam, B.A., Bullock, J., Bloomquist, E., Shen, Y.L., Chen, X.H., Brown, J., Mehrotra, N., Dorff, S., Charlab, R., Kane, R.C., Kaminskas, E., Justice, R., Farrell, A.T., and Pazdur, R., FDA Approval: Belinostat for the Treatment of Patients with Relapsed or Refractory Peripheral T-cell Lymphoma. *Clin Cancer Res*, **2015**.

[110] Garnock-Jones, K.P., Panobinostat: first global approval. *Drugs*, **2015**. 75(6): p. 695-704.

[111] Surh, Y.J., Cancer chemoprevention with dietary phytochemicals. *Nat Rev Cancer*, **2003**. 3(10): p. 768-780.

[112] Kumar, B., Yadav, A., Hideg, K., Kuppusamy, P., Teknos, T.N., and Kumar, P., A novel curcumin analog (H-4073) enhances the therapeutic efficacy of cisplatin treatment in head and neck cancer. *PLoS One*, **2014**. 9(3): p. e93208.

[113] Malhotra, A., Nair, P., and Dhawan, D.K., Study to evaluate molecular mechanics behind synergistic chemo-preventive effects of curcumin and resveratrol during lung carcinogenesis. *PLoS One*, **2014**. 9(4): p. e93820.

[114] Guo, Y., Shu, L., Zhang, C., Su, Z.Y., and Kong, A.N., Curcumin inhibits anchorage-independent growth of HT29 human colon cancer cells by targeting epigenetic restoration of the tumor suppressor gene DLEC1. *Biochem Pharmacol*, **2015**.

[115] Sarkar, R., Mukherjee, A., Mukherjee, S., Biswas, R., Biswas, J., and Roy, M., Curcumin augments the efficacy of antitumor drugs used in leukemia by modulation of heat shock proteins via HDAC6. *J Environ Pathol Toxicol Oncol*, **2014**. 33(3): p. 247-263.

[116] Balasubramanyam, K., Varier, R.A., Altaf, M., Swaminathan, V., Siddappa, N.B., Ranga, U., and Kundu, T.K., Curcumin, a novel p300/CREB-binding protein-specific inhibitor of acetyltransferase, represses the acetylation of histone/nonhistone proteins and histone acetyltransferase-dependent chromatin transcription. *J Biol Chem*, **2004**. 279(49): p. 51163-51171.

[117] Kang, J., Chen, J., Shi, Y., Jia, J., and Zhang, Y., Curcumin-induced histone hypoacetylation: the role of reactive oxygen species. *Biochem Pharmacol*, **2005**. 69(8): p. 1205-1213.

[118] Connors, S.K., Chornokur, G., and Kumar, N.B., New insights into the mechanisms of green tea catechins in the chemoprevention of prostate cancer. *Nutr Cancer*, **2012**. 64(1): p. 4-22.

[119] Chung, M.Y., Lim, T.G., and Lee, K.W., Molecular mechanisms of chemopreventive phytochemicals against gastroenterological cancer development. *World J Gastroenterol*, **2013**. 19(7): p. 984-993.

[120] Thakur, V.S., Gupta, K., and Gupta, S., Green tea polyphenols increase p53 transcriptional activity and acetylation by suppressing class I histone deacetylases. *Int J Oncol*, **2012**. 41(1): p. 353-361.

[121] Thakur, V.S., Gupta, K., and Gupta, S., Green tea polyphenols causes cell cycle arrest and apoptosis in prostate cancer cells by suppressing class I histone deacetylases. *Carcinogenesis*, **2012**. 33(2): p. 377-384.

[122] Choi, K.C., Jung, M.G., Lee, Y.H., Yoon, J.C., Kwon, S.H., Kang, H.B., Kim, M.J., Cha, J.H., Kim, Y.J., Jun, W.J., Lee, J.M., and Yoon, H.G., Epigallocatechin-3-gallate, a histone acetyltransferase inhibitor, inhibits EBV-induced B lymphocyte transformation via suppression of RelA acetylation. *Cancer Res*, **2009**. 69(2): p. 583-592.

[123] Nandakumar, V., Vaid, M., and Katiyar, S.K., (-)-Epigallocatechin-3-gallate reactivates silenced tumor suppressor genes, Cip1/p21 and p16INK4a, by reducing DNA methylation and increasing histones acetylation in human skin cancer cells. *Carcinogenesis*, **2011**. 32(4): p. 537-544.

[124] Li, Y., Yuan, Y.Y., Meeran, S.M., and Tollefsbol, T.O., Synergistic epigenetic reactivation of estrogen receptor-alpha (ERalpha) by combined green tea polyphenol and histone deacetylase inhibitor in ERalpha-negative breast cancer cells. *Mol Cancer*, **2010**. 9: p. 274.

[125] Zhang, Y., Wang, X., Han, L., Zhou, Y., and Sun, S., Green tea polyphenol EGCG reverse cisplatin resistance of A549/DDP cell line through candidate genes demethylation. *Biomed Pharmacother*, **2015**. 69: p. 285-290.

[126] Khan, M.A., Hussain, A., Sundaram, M.K., Alalami, U., Gunasekera, D., Ramesh, L., Hamza, A., and Quraishi, U., (-)-Epigallocatechin-3-gallate reverses the expression of various tumor-suppressor genes by inhibiting DNA methyltransferases and histone deacetylases in human cervical cancer cells. *Oncol Rep*, **2015**. 33(4): p. 1976-1984.

[127] Balasubramanian, S., Adhikary, G., and Eckert, R.L., The Bmi-1 polycomb protein antagonizes the (-)-epigallocatechin-3-gallate-dependent suppression of skin cancer cell survival. *Carcinogenesis*, **2010**. 31(3): p. 496-503.

[128] Choudhury, S.R., Balasubramanian, S., Chew, Y.C., Han, B., Marquez, V.E., and Eckert, R.L., (-)-Epigallocatechin-3-gallate and DZNep reduce polycomb protein level via a proteasome-dependent mechanism in skin cancer cells. *Carcinogenesis*, **2011**. 32(10): p. 1525-1532.

[129] Deb, G., Thakur, V.S., Limaye, A.M., and Gupta, S., Epigenetic induction of tissue inhibitor of matrix metalloproteinase-3 by green tea polyphenols in breast cancer cells. *Mol Carcinog*, **2015**. 54(6): p. 485-499.

[130] Balasubramanian, S., Scharadin, T.M., Han, B., Xu, W., and Eckert, R.L., The Bmi-1 helix-turn and ring finger domains are required for Bmi-1

antagonism of (-) epigallocatechin-3-gallate suppression of skin cancer cell survival. *Cell Signal*, **2015**. 27(7): p. 1336-1344.

[131] Basak, S., Pookot, D., Noonan, E.J., and Dahiya, R., Genistein down-regulates androgen receptor by modulating HDAC6-Hsp90 chaperone function. *Mol Cancer Ther*, **2008**. 7(10): p. 3195-3202.

[132] Ruiz, P.A., Braune, A., Holzlwimmer, G., Quintanilla-Fend, L., and Haller, D., Quercetin inhibits TNF-induced NF-kappaB transcription factor recruitment to proinflammatory gene promoters in murine intestinal epithelial cells. *J Nutr*, **2007**. 137(5): p. 1208-1215.

[133] Priyadarsini, R.V., Vinothini, G., Murugan, R.S., Manikandan, P., and Nagini, S., The flavonoid quercetin modulates the hallmark capabilities of hamster buccal pouch tumors. *Nutr Cancer*, **2011**. 63(2): p. 218-226.

[134] Roy, S.K., Chen, Q., Fu, J., Shankar, S., and Srivastava, R.K., Resveratrol inhibits growth of orthotopic pancreatic tumors through activation of FOXO transcription factors. *PLoS One*, **2011**. 6(9): p. e25166.

[135] Yang, Q., Wang, B., Zang, W., Wang, X., Liu, Z., Li, W., and Jia, J., Resveratrol inhibits the growth of gastric cancer by inducing G1 phase arrest and senescence in a Sirt1-dependent manner. *PLoS One*, **2013**. 8(11): p. e70627.

[136] Venturelli, S., Berger, A., Bocker, A., Busch, C., Weiland, T., Noor, S., Leischner, C., Schleicher, S., Mayer, M., Weiss, T.S., Bischoff, S.C., Lauer, U.M., and Bitzer, M., Resveratrol as a pan-HDAC inhibitor alters the acetylation status of histone [corrected] proteins in human-derived hepatoblastoma cells. *PLoS One*, **2013**. 8(8): p. e73097.

[137] Dhar, S., Kumar, A., Li, K., Tzivion, G., and Levenson, A.S., Resveratrol regulates PTEN/Akt pathway through inhibition of MTA1/HDAC unit of the NuRD complex in prostate cancer. *Biochim Biophys Acta*, **2015**. 1853(2): p. 265-275.

[138] Schneider-Stock, R., Ghantous, A., Bajbouj, K., Saikali, M., and Darwiche, N., Epigenetic mechanisms of plant-derived anticancer drugs. *Front Biosci (Landmark Ed)*, **2012**. 17: p. 129-173.

[139] Hsu, A., Wong, C.P., Yu, Z., Williams, D.E., Dashwood, R.H., and Ho, E., Promoter de-methylation of cyclin D2 by sulforaphane in prostate cancer cells. *Clin Epigenetics*, **2011**. 3: p. 3.

[140] Su, Z.Y., Zhang, C., Lee, J.H., Shu, L., Wu, T.Y., Khor, T.O., Conney, A.H., Lu, Y.P., and Kong, A.N., Requirement and epigenetics reprogramming of Nrf2 in suppression of tumor promoter TPA-induced mouse skin cell transformation by sulforaphane. *Cancer Prev Res (Phila)*, **2014**. 7(3): p. 319-329.

[141] Tortorella, S.M., Royce, S.G., Licciardi, P.V., and Karagiannis, T.C., Dietary Sulforaphane in Cancer Chemoprevention: The Role of Epigenetic Regulation and HDAC Inhibition. *Antioxid Redox Signal*, **2014**.

[142] Li, Q., Eades, G., Yao, Y., Zhang, Y., and Zhou, Q., Characterization of a stem-like subpopulation in basal-like ductal carcinoma in situ (DCIS) lesions. *J Biol Chem*, **2014**. 289(3): p. 1303-1312.

[143] Cang, S., Ma, Y., Chiao, J.W., and Liu, D., Phenethyl isothiocyanate and paclitaxel synergistically enhanced apoptosis and alpha-tubulin hyperacetylation in breast cancer cells. *Exp Hematol Oncol*, **2014**. 3(1): p. 5.

[144] Liu, K., Cang, S., Ma, Y., and Chiao, J.W., Synergistic effect of paclitaxel and epigenetic agent phenethyl isothiocyanate on growth inhibition, cell cycle arrest and apoptosis in breast cancer cells. *Cancer Cell Int*, **2013**. 13(1): p. 10.

[145] Wang, L.G. and Chiao, J.W., Prostate cancer chemopreventive activity of phenethyl isothiocyanate through epigenetic regulation (review). *Int J Oncol*, **2010**. 37(3): p. 533-539.

[146] Druesne-Pecollo, N. and Latino-Martel, P., Modulation of histone acetylation by garlic sulfur compounds. *Anticancer Agents Med Chem*, **2011**. 11(3): p. 254-259.

[147] Lee, J.H., Kim, K.A., Kwon, K.B., Kim, E.K., Lee, Y.R., Song, M.Y., Koo, J.H., Ka, S.O., Park, J.W., and Park, B.H., Diallyl disulfide accelerates adipogenesis in 3T3-L1 cells. *Int J Mol Med*, **2007**. 20(1): p. 59-64.

[148] Fimognari, C., Lenzi, M., and Hrelia, P., Chemoprevention of cancer by isothiocyanates and anthocyanins: mechanisms of action and structure-activity relationship. *Curr Med Chem*, **2008**. 15(5): p. 440-447.

[149] Ho, E., Clarke, J.D., and Dashwood, R.H., Dietary sulforaphane, a histone deacetylase inhibitor for cancer prevention. *J Nutr*, **2009**. 139(12): p. 2393-2396.

[150] Dashwood, R.H. and Ho, E., Dietary agents as histone deacetylase inhibitors: sulforaphane and structurally related isothiocyanates. *Nutr Rev*, **2008**. 66 Suppl 1: p. S36-38.

[151] Telang, U., Brazeau, D.A., and Morris, M.E., Comparison of the effects of phenethyl isothiocyanate and sulforaphane on gene expression in breast cancer and normal mammary epithelial cells. *Exp Biol Med (Maywood)*, **2009**. 234(3): p. 287-295.

[152] Myzak, M.C., Karplus, P.A., Chung, F.L., and Dashwood, R.H., A novel mechanism of chemoprotection by sulforaphane: inhibition of histone deacetylase. *Cancer Res*, **2004**. 64(16): p. 5767-5774.

[153] Myzak, M.C., Tong, P., Dashwood, W.M., Dashwood, R.H., and Ho, E., Sulforaphane retards the growth of human PC-3 xenografts and inhibits HDAC activity in human subjects. *Exp Biol Med (Maywood)*, **2007**. 232(2): p. 227-234.

[154] Meeran, S.M., Patel, S.N., and Tollefsbol, T.O., Sulforaphane causes epigenetic repression of hTERT expression in human breast cancer cell lines. *PLoS One*, **2010**. 5(7): p. e11457.

[155] Fan, H., Zhang, R., Tesfaye, D., Tholen, E., Looft, C., Holker, M., Schellander, K., and Cinar, M.U., Sulforaphane causes a major epigenetic repression of myostatin in porcine satellite cells. *Epigenetics*, **2012**. 7(12): p. 1379-1390.

[156] Kar, S., Sengupta, D., Deb, M., Shilpi, A., Parbin, S., Rath, S.K., Pradhan, N., Rakshit, M., and Patra, S.K., Expression profiling of DNA methylation-mediated epigenetic gene-silencing factors in breast cancer. *Clin Epigenetics*, **2014**. 6(1): p. 20.

[157] Gerhauser, C., Epigenetic impact of dietary isothiocyanates in cancer chemoprevention. *Curr Opin Clin Nutr Metab Care*, **2013**. 16(4): p. 405-410.

[158] Chorley, B.N., Campbell, M.R., Wang, X., Karaca, M., Sambandan, D., Bangura, F., Xue, P., Pi, J., Kleeberger, S.R., and Bell, D.A., Identification of novel NRF2-regulated genes by ChIP-Seq: influence on retinoid X receptor alpha. *Nucleic Acids Res*, **2012**. 40(15): p. 7416-7429.

[159] Wang, L.G., Liu, X.M., Fang, Y., Dai, W., Chiao, F.B., Puccio, G.M., Feng, J., Liu, D., and Chiao, J.W., De-repression of the p21 promoter in prostate cancer cells by an isothiocyanate via inhibition of HDACs and c-Myc. *Int J Oncol*, **2008**. 33(2): p. 375-380.

[160] Wang, L.G., Beklemisheva, A., Liu, X.M., Ferrari, A.C., Feng, J., and Chiao, J.W., Dual action on promoter demethylation and chromatin by an isothiocyanate restored GSTP1 silenced in prostate cancer. *Mol Carcinog*, **2007**. 46(1): p. 24-31.

[161] Finnin, M.S., Donigian, J.R., Cohen, A., Richon, V.M., Rifkind, R.A., Marks, P.A., Breslow, R., and Pavletich, N.P., Structures of a histone deacetylase homologue bound to the TSA and SAHA inhibitors. *Nature*, **1999**. 401(6749): p. 188-193.

[162] Guyonnet, D., Berges, R., Siess, M.H., Pinnert, M.F., Chagnon, M.C., Suschetet, M., and Le Bon, A.M., Post-initiation modulating effects of allyl sulfides in rat hepatocarcinogenesis. *Food Chem Toxicol*, **2004**. 42(9): p. 1479-1485.

[163] Nian, H., Delage, B., Ho, E., and Dashwood, R.H., Modulation of histone deacetylase activity by dietary isothiocyanates and allyl sulfides: studies with sulforaphane and garlic organosulfur compounds. *Environ Mol Mutagen*, **2009**. 50(3): p. 213-221.

[164] Lea, M.A., Randolph, V.M., and Patel, M., Increased acetylation of histones induced by diallyl disulfide and structurally related molecules. *Int J Oncol*, **1999**. 15(2): p. 347-352.

[165] Nian, H., Delage, B., Pinto, J.T., and Dashwood, R.H., Allyl mercaptan, a garlic-derived organosulfur compound, inhibits histone deacetylase and enhances Sp3 binding on the P21WAF1 promoter. *Carcinogenesis*, **2008**. 29(9): p. 1816-1824.

[166] Druesne-Pecollo, N., Chaumontet, C., and Latino-Martel, P., Diallyl disulfide increases histone acetylation in colon cells in vitro and in vivo. *Nutr Rev*, **2008**. 66 Suppl 1: p. S39-41.

[167] Druesne, N., Pagniez, A., Mayeur, C., Thomas, M., Cherbuy, C., Duee, P.H., Martel, P., and Chaumontet, C., Diallyl disulfide (DADS) increases histone acetylation and p21(waf1/cip1) expression in human colon tumor cell lines. *Carcinogenesis*, **2004**. 25(7): p. 1227-1236.

[168] Druesne-Pecollo, N., Chaumontet, C., Pagniez, A., Vaugelade, P., Bruneau, A., Thomas, M., Cherbuy, C., Duee, P.H., and Martel, P., In vivo treatment by diallyl disulfide increases histone acetylation in rat colonocytes. *Biochem Biophys Res Commun*, **2007**. 354(1): p. 140-147.

[169] Bishayee, A., Ahmed, S., Brankov, N., and Perloff, M., Triterpenoids as potential agents for the chemoprevention and therapy of breast cancer. *Front Biosci (Landmark Ed)*, **2011**. 16: p. 980-996.

[170] Yadav, V.R., Prasad, S., Sung, B., Kannappan, R., and Aggarwal, B.B., Targeting inflammatory pathways by triterpenoids for prevention and treatment of cancer. *Toxins (Basel)*, **2010**. 2(10): p. 2428-2466.

[171] Dzubak, P., Hajduch, M., Vydra, D., Hustova, A., Kvasnica, M., Biedermann, D., Markova, L., Urban, M., and Sarek, J., Pharmacological activities of natural triterpenoids and their therapeutic implications. *Nat Prod Rep*, **2006**. 23(3): p. 394-411.

[172] Salminen, A., Lehtonen, M., Suuronen, T., Kaarniranta, K., and Huuskonen, J., Terpenoids: natural inhibitors of NF-kappaB signaling with anti-inflammatory and anticancer potential. *Cell Mol Life Sci*, **2008**. 65(19): p. 2979-2999.

[173] Shanmugam, M.K., Dai, X., Kumar, A.P., Tan, B.K., Sethi, G., and Bishayee, A., Oleanolic acid and its synthetic derivatives for the prevention and therapy of cancer: preclinical and clinical evidence. *Cancer Lett*, **2014**. 346(2): p. 206-216.

[174] Pollier, J. and Goossens, A., Oleanolic acid. *Phytochemistry*, **2012**. 77: p. 10-15.

[175] Ndlovu, B.C., Daniels, W.M., and Mabandla, M.V., Oleanolic Acid enhances the beneficial effects of preconditioning on PC12 cells. *Parkinsons Dis*, **2014**. 2014: p. 929854.

[176] Zhao, X., Liu, M., and Li, D., Oleanolic acid suppresses the proliferation of lung carcinoma cells by miR-122/Cyclin G1/MEF2D axis. *Mol Cell Biochem*, **2015**. 400(1-2): p. 1-7.

[177] Nakao, K., Miyaaki, H., and Ichikawa, T., Antitumor function of microRNA-122 against hepatocellular carcinoma. *J Gastroenterol*, **2014**. 49(4): p. 589-593.

[178] Jung, C.J., Iyengar, S., Blahnik, K.R., Ajuha, T.P., Jiang, J.X., Farnham, P.J., and Zern, M., Epigenetic modulation of miR-122 facilitates human

embryonic stem cell self-renewal and hepatocellular carcinoma proliferation. *PLoS One*, **2011**. 6(11): p. e27740.

[179] Castellano, J.M., Guinda, A., Delgado, T., Rada, M., and Cayuela, J.A., Biochemical basis of the antidiabetic activity of oleanolic acid and related pentacyclic triterpenes. *Diabetes*, **2013**. 62(6): p. 1791-1799.

[180] Zhou, X., Zeng, X.Y., Wang, H., Li, S., Jo, E., Xue, C.C., Tan, M., Molero, J.C., and Ye, J.M., Hepatic FoxO1 acetylation is involved in oleanolic acid-induced memory of glycemic control: novel findings from Study 2. *PLoS One*, **2014**. 9(9): p. e107231.

[181] Ikeda, Y., Murakami, A., and Ohigashi, H., Ursolic acid: an anti- and pro-inflammatory triterpenoid. *Mol Nutr Food Res*, **2008**. 52(1): p. 26-42.

[182] Gupta, M.B., Bhalla, T.N., Gupta, G.P., Mitra, C.R., and Bhargava, K.P., Anti-inflammatory activity of natural products. I. Triterpenoids. *Eur J Pharmacol*, **1969**. 6(1): p. 67-70.

[183] Liu, J., Pharmacology of oleanolic acid and ursolic acid. *J Ethnopharmacol*, **1995**. 49(2): p. 57-68.

[184] Zang, L.L., Wu, B.N., Lin, Y., Wang, J., Fu, L., and Tang, Z.Y., Research progress of ursolic acid's anti-tumor actions. *Chin J Integr Med*, **2014**. 20(1): p. 72-79.

[185] Chen, I.H., Lu, M.C., Du, Y.C., Yen, M.H., Wu, C.C., Chen, Y.H., Hung, C.S., Chen, S.L., Chang, F.R., and Wu, Y.C., Cytotoxic triterpenoids from the stems of Microtropis japonica. *J Nat Prod*, **2009**. 72(7): p. 1231-1236.

[186] Wang, J., Li, Y., Wang, X., and Jiang, C., Ursolic acid inhibits proliferation and induces apoptosis in human glioblastoma cell lines U251 by suppressing TGF-beta1/miR-21/PDCD4 pathway. *Basic Clin Pharmacol Toxicol*, **2012**. 111(2): p. 106-112.

[187] Singh, P.K. and Campbell, M.J., The Interactions of microRNA and Epigenetic Modifications in Prostate Cancer. *Cancers (Basel)*, **2013**. 5(3): p. 998-1019.

[188] Liby, K.T., Yore, M.M., and Sporn, M.B., Triterpenoids and rexinoids as multifunctional agents for the prevention and treatment of cancer. *Nat Rev Cancer*, **2007**. 7(5): p. 357-369.

[189] Liby, K.T. and Sporn, M.B., Synthetic oleanane triterpenoids: multifunctional drugs with a broad range of applications for prevention and treatment of chronic disease. *Pharmacol Rev*, **2012**. 64(4): p. 972-1003.

[190] Yore, M.M., Kettenbach, A.N., Sporn, M.B., Gerber, S.A., and Liby, K.T., Proteomic analysis shows synthetic oleanane triterpenoid binds to mTOR. *PLoS One*, **2011**. 6(7): p. e22862.

[191] Wang, Y.Y., Zhe, H., and Zhao, R., Preclinical evidences toward the use of triterpenoid CDDO-Me for solid cancer prevention and treatment. *Mol Cancer*, **2014**. 13: p. 30.

[192] Tabe, Y., Konopleva, M., Kondo, Y., Contractor, R., Tsao, T., Konoplev, S., Shi, Y., Ling, X., Watt, J.C., Tsutsumi-Ishii, Y., Ohsaka, A., Nagaoka, I., Issa, J.P., Kogan, S.C., and Andreeff, M., PPARgamma-active triterpenoid CDDO enhances ATRA-induced differentiation in APL. *Cancer Biol Ther*, **2007**. 6(12): p. 1967-1977.

[193] Wang, Y.Y., Yang, Y.X., Zhe, H., He, Z.X., and Zhou, S.F., Bardoxolone methyl (CDDO-Me) as a therapeutic agent: an update on its pharmacokinetic and pharmacodynamic properties. *Drug Des Devel Ther*, **2014**. 8: p. 2075-2088.

[194] Deeb, D., Brigolin, C., Gao, X., Liu, Y., Pindolia, K.R., and Gautam, S.C., Induction of Apoptosis in Pancreatic Cancer Cells by CDDO-Me Involves Repression of Telomerase through Epigenetic Pathways. *J Carcinog Mutagen*, **2014**. 5: p. 177.

[195] Hartmann, R.M., Morgan Martins, M.I., Tieppo, J., Fillmann, H.S., and Marroni, N.P., Effect of Boswellia serrata on antioxidant status in an experimental model of colitis rats induced by acetic acid. *Dig Dis Sci*, **2012**. 57(8): p. 2038-2044.

[196] Kruger, P., Daneshfar, R., Eckert, G.P., Klein, J., Volmer, D.A., Bahr, U., Muller, W.E., Karas, M., Schubert-Zsilavecz, M., and Abdel-Tawab, M., Metabolism of boswellic acids in vitro and in vivo. *Drug Metab Dispos*, **2008**. 36(6): p. 1135-1142.

[197] Abdel-Tawab, M., Werz, O., and Schubert-Zsilavecz, M., Boswellia serrata: an overall assessment of in vitro, preclinical, pharmacokinetic and clinical data. *Clin Pharmacokinet*, **2011**. 50(6): p. 349-369.

[198] Chaturvedi, D., Dwivedi, P., Chaturvedi, A., Mishra, N., Siddiqui, H.H., and Mishra, V., Semisynthetic hybrids of boswellic acids: a novel class of potential anti-inflammatory and anti-arthritic agents. *Medicinal Chemistry Research*, **2015**: p. 1-14.

[199] Park, B., Prasad, S., Yadav, V., Sung, B., and Aggarwal, B.B., Boswellic acid suppresses growth and metastasis of human pancreatic tumors in an orthotopic nude mouse model through modulation of multiple targets. *PLoS One*, **2011**. 6(10): p. e26943.

[200] Yadav, V.R., Prasad, S., Sung, B., Gelovani, J.G., Guha, S., Krishnan, S., and Aggarwal, B.B., Boswellic acid inhibits growth and metastasis of human colorectal cancer in orthotopic mouse model by downregulating inflammatory, proliferative, invasive and angiogenic biomarkers. *Int J Cancer*, **2012**. 130(9): p. 2176-2184.

[201] Shen, Y., Takahashi, M., Byun, H.M., Link, A., Sharma, N., Balaguer, F., Leung, H.C., Boland, C.R., and Goel, A., Boswellic acid induces epigenetic alterations by modulating DNA methylation in colorectal cancer cells. *Cancer Biol Ther*, **2012**. 13(7): p. 542-552.

[202] Takahashi, M., Sung, B., Shen, Y., Hur, K., Link, A., Boland, C.R., Aggarwal, B.B., and Goel, A., Boswellic acid exerts antitumor effects in colorectal cancer cells by modulating expression of the let-7 and miR-200 microRNA family. *Carcinogenesis*, **2012**. 33(12): p. 2441-2449.

[203] Rastogi, V., Santiago-Moreno, J., and Dore, S., Ginseng: a promising neuroprotective strategy in stroke. *Front Cell Neurosci*, **2014**. 8: p. 457.

[204] Choi, J.S., Chun, K.S., Kundu, J., and Kundu, J.K., Biochemical basis of cancer chemoprevention and/or chemotherapy with ginsenosides (Review). *Int J Mol Med*, **2013**. 32(6): p. 1227-1238.

[205] Murthy, H.N., Georgiev, M.I., Kim, Y.S., Jeong, C.S., Kim, S.J., Park, S.Y., and Paek, K.Y., Ginsenosides: prospective for sustainable biotechnological production. *Appl Microbiol Biotechnol*, **2014**. 98(14): p. 6243-6254.

[206] Shi, Q., Li, J., Feng, Z., Zhao, L., Luo, L., You, Z., Li, D., Xia, J., Zuo, G., and Chen, D., Effect of ginsenoside Rh2 on the migratory ability of HepG2 liver carcinoma cells: recruiting histone deacetylase and inhibiting activator protein 1 transcription factors. *Mol Med Rep*, **2014**. 10(4): p. 1779-1785.

[207] An, I.S., An, S., Kwon, K.J., Kim, Y.J., and Bae, S., Ginsenoside Rh2 mediates changes in the microRNA expression profile of human non-small cell lung cancer A549 cells. *Oncol Rep*, **2013**. 29(2): p. 523-528.

[208] Wu, N., Wu, G.C., Hu, R., Li, M., and Feng, H., Ginsenoside Rh2 inhibits glioma cell proliferation by targeting microRNA-128. *Acta Pharmacol Sin*, **2011**. 32(3): p. 345-353.

[209] Sato, F., Tsuchiya, S., Meltzer, S.J., and Shimizu, K., MicroRNAs and epigenetics. *FEBS J*, **2011**. 278(10): p. 1598-1609.

[210] Chan, L.S., Yue, P.Y., Mak, N.K., and Wong, R.N., Role of microRNA-214 in ginsenoside-Rg1-induced angiogenesis. *Eur J Pharm Sci*, **2009**. 38(4): p. 370-377.

[211] Suzuki, H., Maruyama, R., Yamamoto, E., and Kai, M., Epigenetic alteration and microRNA dysregulation in cancer. *Front Genet*, **2013**. 4: p. 258.

[212] Lv, X., Jiang, H., Liu, Y., Lei, X., and Jiao, J., MicroRNA-15b promotes neurogenesis and inhibits neural progenitor proliferation by directly repressing TET3 during early neocortical development. *EMBO Rep*, **2014**. 15(12): p. 1305-1314.

[213] Jin, S.G., Jiang, Y., Qiu, R., Rauch, T.A., Wang, Y., Schackert, G., Krex, D., Lu, Q., and Pfeifer, G.P., 5-Hydroxymethylcytosine is strongly depleted in human cancers but its levels do not correlate with IDH1 mutations. *Cancer Res*, **2011**. 71(24): p. 7360-7365.

[214] Liu, C., Liu, L., Chen, X., Shen, J., Shan, J., Xu, Y., Yang, Z., Wu, L., Xia, F., Bie, P., Cui, Y., Bian, X.W., and Qian, C., Decrease of 5-hydroxymethylcytosine is associated with progression of hepatocellular

carcinoma through downregulation of TET1. *PLoS One*, **2013**. 8(5): p. e62828.

[215] Liu, W.R., Tian, M.X., Jin, L., Yang, L.X., Ding, Z.B., Shen, Y.H., Peng, Y.F., Zhou, J., Qiu, S.J., Dai, Z., Fan, J., and Shi, Y.H., High expression of 5-hydroxymethylcytosine and isocitrate dehydrogenase 2 is associated with favorable prognosis after curative resection of hepatocellular carcinoma. *J Exp Clin Cancer Res*, **2014**. 33: p. 32.

[216] Orr, B.A., Haffner, M.C., Nelson, W.G., Yegnasubramanian, S., and Eberhart, C.G., Decreased 5-hydroxymethylcytosine is associated with neural progenitor phenotype in normal brain and shorter survival in malignant glioma. *PLoS One*, **2012**. 7(7): p. e41036.

[217] Chan, L.S., Yue, P.Y., Wong, Y.Y., and Wong, R.N., MicroRNA-15b contributes to ginsenoside-Rg1-induced angiogenesis through increased expression of VEGFR-2. *Biochem Pharmacol*, **2013**. 86(3): p. 392-400.

[218] Kang, K.A., Piao, M.J., Kim, K.C., Zheng, J., Yao, C.W., Cha, J.W., Kim, H.S., Kim, D.H., Bae, S.C., and Hyun, J.W., Compound K, a metabolite of ginseng saponin, inhibits colorectal cancer cell growth and induces apoptosis through inhibition of histone deacetylase activity. *Int J Oncol*, **2013**. 43(6): p. 1907-1914.

[219] Park, E.H., Kim, Y.J., Yamabe, N., Park, S.H., Kim, H.K., Jang, H.J., Kim, J.H., Cheon, G.J., Ham, J., and Kang, K.S., Stereospecific anticancer effects of ginsenoside Rg3 epimers isolated from heat-processed American ginseng on human gastric cancer cell. *J Ginseng Res*, **2014**. 38(1): p. 22-27.

[220] Shan, X., Fu, Y.S., Aziz, F., Wang, X.Q., Yan, Q., and Liu, J.W., Ginsenoside Rg3 inhibits melanoma cell proliferation through down-regulation of histone deacetylase 3 (HDAC3) and increase of p53 acetylation. *PLoS One*, **2014**. 9(12): p. e115401.

[221] Rogan, E.G., The natural chemopreventive compound indole-3-carbinol: state of the science. *In Vivo*, **2006**. 20(2): p. 221-228.

[222] Li, Y., Li, X., and Guo, B., Chemopreventive agent 3,3'-diindolylmethane selectively induces proteasomal degradation of class I histone deacetylases. *Cancer Res*, **2010**. 70(2): p. 646-654.

[223] Busbee, P.B., Nagarkatti, M., and Nagarkatti, P.S., Natural indoles, indole-3-carbinol and 3,3'-diindolymethane, inhibit T cell activation by staphylococcal enterotoxin B through epigenetic regulation involving HDAC expression. *Toxicol Appl Pharmacol*, **2014**. 274(1): p. 7-16.

[224] Beaver, L.M., Yu, T.W., Sokolowski, E.I., Williams, D.E., Dashwood, R.H., and Ho, E., 3,3'-Diindolylmethane, but not indole-3-carbinol, inhibits histone deacetylase activity in prostate cancer cells. *Toxicol Appl Pharmacol*, **2012**. 263(3): p. 345-351.

[225] Wong, C.P., Hsu, A., Buchanan, A., Palomera-Sanchez, Z., Beaver, L.M., Houseman, E.A., Williams, D.E., Dashwood, R.H., and Ho, E., Effects of

sulforaphane and 3,3'-diindolylmethane on genome-wide promoter methylation in normal prostate epithelial cells and prostate cancer cells. *PLoS One*, **2014**. 9(1): p. e86787.

[226] Wong, J.M., de Souza, R., Kendall, C.W., Emam, A., and Jenkins, D.J., Colonic health: fermentation and short chain fatty acids. *J Clin Gastroenterol*, **2006**. 40(3): p. 235-243.

[227] Ryningen, A., Stapnes, C., Lassalle, P., Corbascio, M., Gjertsen, B.T., and Bruserud, O., A subset of patients with high-risk acute myelogenous leukemia shows improved peripheral blood cell counts when treated with the combination of valproic acid, theophylline and all-trans retinoic acid. *Leuk Res*, **2009**. 33(6): p. 779-787.

[228] Fredly, H., Gjertsen, B.T., and Bruserud, O., Histone deacetylase inhibition in the treatment of acute myeloid leukemia: the effects of valproic acid on leukemic cells, and the clinical and experimental evidence for combining valproic acid with other antileukemic agents. *Clin Epigenetics*, **2013**. 5(1): p. 12.

[229] Coronel, J., Cetina, L., Pacheco, I., Trejo-Becerril, C., Gonzalez-Fierro, A., de la Cruz-Hernandez, E., Perez-Cardenas, E., Taja-Chayeb, L., Arias-Bofill, D., Candelaria, M., Vidal, S., and Duenas-Gonzalez, A., A double-blind, placebo-controlled, randomized phase III trial of chemotherapy plus epigenetic therapy with hydralazine valproate for advanced cervical cancer. Preliminary results. *Med Oncol*, **2011**. 28 Suppl 1: p. S540-546.

[230] Kang, S.H., Seok, Y.M., Song, M.J., Lee, H.A., Kurz, T., and Kim, I., Histone Deacetylase Inhibition Attenuates Cardiac Hypertrophy and Fibrosis through Acetylation of Mineralocorticoid Receptor in Spontaneously Hypertensive Rats. *Mol Pharmacol*, **2015**.

[231] Isoherranen, N., Yagen, B., and Bialer, M., New CNS-active drugs which are second-generation valproic acid: can they lead to the development of a magic bullet? *Curr Opin Neurol*, **2003**. 16(2): p. 203-211.

[232] Trojnar, M.K., Wierzchowska-Cioch, E., Krzyzanowski, M., Jargiello, M., and Czuczwar, S.J., New generation of valproic acid. *Pol J Pharmacol*, **2004**. 56(3): p. 283-288.

[233] Hemshekhar, M., Sebastin Santhosh, M., Kemparaju, K., and Girish, K.S., Emerging roles of anacardic acid and its derivatives: a pharmacological overview. *Basic Clin Pharmacol Toxicol*, **2012**. 110(2): p. 122-132.

[234] Eliseeva, E.D., Valkov, V., Jung, M., and Jung, M.O., Characterization of novel inhibitors of histone acetyltransferases. *Mol Cancer Ther*, **2007**. 6(9): p. 2391-2398.

[235] Balasubramanyam, K., Altaf, M., Varier, R.A., Swaminathan, V., Ravindran, A., Sadhale, P.P., and Kundu, T.K., Polyisoprenylated benzophenone, garcinol, a natural histone acetyltransferase inhibitor, represses chromatin

transcription and alters global gene expression. *J Biol Chem*, **2004**. 279(32): p. 33716-33726.

[236] Mantelingu, K., Reddy, B.A., Swaminathan, V., Kishore, A.H., Siddappa, N.B., Kumar, G.V., Nagashankar, G., Natesh, N., Roy, S., Sadhale, P.P., Ranga, U., Narayana, C., and Kundu, T.K., Specific inhibition of p300-HAT alters global gene expression and represses HIV replication. *Chem Biol*, **2007**. 14(6): p. 645-657.

[237] Delage, B. and Dashwood, R.H., Dietary manipulation of histone structure and function. *Annu Rev Nutr*, **2008**. 28: p. 347-366.

[238] Stronach, E.A., Alfraidi, A., Rama, N., Datler, C., Studd, J.B., Agarwal, R., Guney, T.G., Gourley, C., Hennessy, B.T., Mills, G.B., Mai, A., Brown, R., Dina, R., and Gabra, H., HDAC4-regulated STAT1 activation mediates platinum resistance in ovarian cancer. *Cancer Res*, **2011**. 71(13): p. 4412-4422.

[239] Milenkovic, D., Deval, C., Gouranton, E., Landrier, J.F., Scalbert, A., Morand, C., and Mazur, A., Modulation of miRNA expression by dietary polyphenols in apoE deficient mice: a new mechanism of the action of polyphenols. *PLoS One*, **2012**. 7(1): p. e29837.

[240] Sethi, R., Sethi, R., Redmond, A., and Lavik, E., Olfactory ensheathing cells promote differentiation of neural stem cells and robust neurite extension. *Stem Cell Rev*, **2014**. 10(6): p. 772-785.

[241] Hu, R., Saw, C.L., Yu, R., and Kong, A.N., Regulation of NF-E2-related factor 2 signaling for cancer chemoprevention: antioxidant coupled with antiinflammatory. *Antioxid Redox Signal*, **2010**. 13(11): p. 1679-1698.

[242] Shen, G. and Kong, A.N., Nrf2 plays an important role in coordinated regulation of Phase II drug metabolism enzymes and Phase III drug transporters. *Biopharm Drug Dispos*, **2009**. 30(7): p. 345-355.

[243] Talalay, P., Fahey, J.W., Holtzclaw, W.D., Prestera, T., and Zhang, Y., Chemoprotection against cancer by phase 2 enzyme induction. *Toxicol Lett*, **1995**. 82-83: p. 173-179.

[244] Slocum, S.L. and Kensler, T.W., Nrf2: control of sensitivity to carcinogens. *Arch Toxicol*, **2011**. 85(4): p. 273-284.

[245] Peng, J., Yuan, J.P., and Wang, J.H., Effect of diets supplemented with different sources of astaxanthin on the gonad of the sea urchin Anthocidaris crassispina. *Nutrients*, **2012**. 4(8): p. 922-934.

[246] Iwamoto, T., Hosoda, K., Hirano, R., Kurata, H., Matsumoto, A., Miki, W., Kamiyama, M., Itakura, H., Yamamoto, S., and Kondo, K., Inhibition of low-density lipoprotein oxidation by astaxanthin. *J Atheroscler Thromb*, **2000**. 7(4): p. 216-222.

[247] Aoi, W., Naito, Y., Sakuma, K., Kuchide, M., Tokuda, H., Maoka, T., Toyokuni, S., Oka, S., Yasuhara, M., and Yoshikawa, T., Astaxanthin limits

exercise-induced skeletal and cardiac muscle damage in mice. *Antioxid Redox Signal*, **2003**. 5(1): p. 139-144.

[248] Kobayashi, M., In vivo antioxidant role of astaxanthin under oxidative stress in the green alga Haematococcus pluvialis. *Appl Microbiol Biotechnol*, **2000**. 54(4): p. 550-555.

[249] Jyonouchi, H., Sun, S., Iijima, K., and Gross, M.D., Antitumor activity of astaxanthin and its mode of action. *Nutr Cancer*, **2000**. 36(1): p. 59-65.

[250] Yasui, Y., Hosokawa, M., Mikami, N., Miyashita, K., and Tanaka, T., Dietary astaxanthin inhibits colitis and colitis-associated colon carcinogenesis in mice via modulation of the inflammatory cytokines. *Chem Biol Interact*, **2011**. 193(1): p. 79-87.

[251] Nagendraprabhu, P. and Sudhandiran, G., Astaxanthin inhibits tumor invasion by decreasing extracellular matrix production and induces apoptosis in experimental rat colon carcinogenesis by modulating the expressions of ERK-2, NFkB and COX-2. *Invest New Drugs*, **2011**. 29(2): p. 207-224.

[252] Kang, J.O., Kim, S.J., and Kim, H., Effect of astaxanthin on the hepatotoxicity, lipid peroxidation and antioxidative enzymes in the liver of CCl4-treated rats. *Methods Find Exp Clin Pharmacol*, **2001**. 23(2): p. 79-84.

[253] Uchiyama, K., Naito, Y., Hasegawa, G., Nakamura, N., Takahashi, J., and Yoshikawa, T., Astaxanthin protects beta-cells against glucose toxicity in diabetic db/db mice. *Redox Rep*, **2002**. 7(5): p. 290-293.

[254] Ohgami, K., Shiratori, K., Kotake, S., Nishida, T., Mizuki, N., Yazawa, K., and Ohno, S., Effects of astaxanthin on lipopolysaccharide-induced inflammation in vitro and in vivo. *Invest Ophthalmol Vis Sci*, **2003**. 44(6): p. 2694-2701.

[255] Yuan, J.P., Peng, J., Yin, K., and Wang, J.H., Potential health-promoting effects of astaxanthin: a high-value carotenoid mostly from microalgae. *Mol Nutr Food Res*, **2011**. 55(1): p. 150-165.

[256] Lee, D.H., Kim, C.S., and Lee, Y.J., Astaxanthin protects against MPTP/MPP+-induced mitochondrial dysfunction and ROS production in vivo and in vitro. *Food Chem Toxicol*, **2011**. 49(1): p. 271-280.

[257] Tripathi, D.N. and Jena, G.B., Astaxanthin intervention ameliorates cyclophosphamide-induced oxidative stress, DNA damage and early hepatocarcinogenesis in rat: role of Nrf2, p53, p38 and phase-II enzymes. *Mutat Res*, **2010**. 696(1): p. 69-80.

[258] Zhang, X., Zhao, W.E., Hu, L., Zhao, L., and Huang, J., Carotenoids inhibit proliferation and regulate expression of peroxisome proliferators-activated receptor gamma (PPARgamma) in K562 cancer cells. *Arch Biochem Biophys*, **2011**. 512(1): p. 96-106.

[259] Choi, H.D., Kim, J.H., Chang, M.J., Kyu-Youn, Y., and Shin, W.G., Effects of astaxanthin on oxidative stress in overweight and obese adults. *Phytother Res*, **2011**. 25(12): p. 1813-1818.

[260] Maeda, H., Hosokawa, M., Sashima, T., and Miyashita, K., Dietary combination of fucoxanthin and fish oil attenuates the weight gain of white adipose tissue and decreases blood glucose in obese/diabetic KK-Ay mice. *J Agric Food Chem*, **2007**. 55(19): p. 7701-7706.

[261] Barros, M.P., Marin, D.P., Bolin, A.P., de Cassia Santos Macedo, R., Campoio, T.R., Fineto, C., Jr., Guerra, B.A., Polotow, T.G., Vardaris, C., Mattei, R., and Otton, R., Combined astaxanthin and fish oil supplementation improves glutathione-based redox balance in rat plasma and neutrophils. *Chem Biol Interact*, **2012**. 197(1): p. 58-67.

[262] Manerba, A., Vizzardi, E., Metra, M., and Dei Cas, L., n-3 PUFAs and cardiovascular disease prevention. *Future Cardiol*, **2010**. 6(3): p. 343-350.

[263] Adkins, Y. and Kelley, D.S., Mechanisms underlying the cardioprotective effects of omega-3 polyunsaturated fatty acids. *J Nutr Biochem*, **2010**. 21(9): p. 781-792.

[264] Saw, C.L., Huang, Y., and Kong, A.N., Synergistic anti-inflammatory effects of low doses of curcumin in combination with polyunsaturated fatty acids: docosahexaenoic acid or eicosapentaenoic acid. *Biochem Pharmacol*, **2010**. 79(3): p. 421-430.

[265] Wang, H., Khor, T.O., Saw, C.L., Lin, W., Wu, T., Huang, Y., and Kong, A.N., Role of Nrf2 in suppressing LPS-induced inflammation in mouse peritoneal macrophages by polyunsaturated fatty acids docosahexaenoic acid and eicosapentaenoic acid. *Mol Pharm*, **2010**. 7(6): p. 2185-2193.

[266] Calder, P.C., n-3 polyunsaturated fatty acids, inflammation, and inflammatory diseases. *Am J Clin Nutr*, **2006**. 83(6 Suppl): p. 1505S-1519S.

[267] Finocchiaro, C., Segre, O., Fadda, M., Monge, T., Scigliano, M., Schena, M., Tinivella, M., Tiozzo, E., Catalano, M.G., Pugliese, M., Fortunati, N., Aragno, M., Muzio, G., Maggiora, M., Oraldi, M., and Canuto, R.A., Effect of n-3 fatty acids on patients with advanced lung cancer: a double-blind, placebo-controlled study. *Br J Nutr*, **2012**. 108(2): p. 327-333.

[268] Silva Jde, A., Trindade, E.B., Fabre, M.E., Menegotto, V.M., Gevaerd, S., Buss Zda, S., and Frode, T.S., Fish oil supplement alters markers of inflammatory and nutritional status in colorectal cancer patients. *Nutr Cancer*, **2012**. 64(2): p. 267-273.

[269] Khor, T.O., Yu, S., and Kong, A.N., Dietary cancer chemopreventive agents - targeting inflammation and Nrf2 signaling pathway. *Planta Med*, **2008**. 74(13): p. 1540-1547.

[270] Saw, C.L. and Kong, A.N., Nuclear factor-erythroid 2-related factor 2 as a chemopreventive target in colorectal cancer. *Expert Opin Ther Targets*, **2011**. 15(3): p. 281-295.

[271] Yu, R., Mandlekar, S., Lei, W., Fahl, W.E., Tan, T.H., and Kong, A.N., p38 mitogen-activated protein kinase negatively regulates the induction of phase

II drug-metabolizing enzymes that detoxify carcinogens. *J Biol Chem*, **2000**. 275(4): p. 2322-2327.

[272] Yu, R., Lei, W., Mandlekar, S., Weber, M.J., Der, C.J., Wu, J., and Kong, A.N., Role of a mitogen-activated protein kinase pathway in the induction of phase II detoxifying enzymes by chemicals. *J Biol Chem*, **1999**. 274(39): p. 27545-27552.

[273] Kim, B.R., Hu, R., Keum, Y.S., Hebbar, V., Shen, G., Nair, S.S., and Kong, A.N., Effects of glutathione on antioxidant response element-mediated gene expression and apoptosis elicited by sulforaphane. *Cancer Res*, **2003**. 63(21): p. 7520-7525.

[274] Chen, C., Yu, R., Owuor, E.D., and Kong, A.N., Activation of antioxidant-response element (ARE), mitogen-activated protein kinases (MAPKs) and caspases by major green tea polyphenol components during cell survival and death. *Arch Pharm Res*, **2000**. 23(6): p. 605-612.

[275] Chan, L.W., Cheah, E.L., Saw, C.L., Weng, W., and Heng, P.W., Antimicrobial and antioxidant activities of Cortex Magnoliae Officinalis and some other medicinal plants commonly used in South-East Asia. *Chin Med*, **2008**. 3: p. 15.

[276] Chou, T.C., Drug combination studies and their synergy quantification using the Chou-Talalay method. *Cancer Res*, **2010**. 70(2): p. 440-446.

[277] Lee, J.J., Kong, M., Ayers, G.D., and Lotan, R., Interaction index and different methods for determining drug interaction in combination therapy. *J Biopharm Stat*, **2007**. 17(3): p. 461-480.

[278] Saw, C.L., Cintron, M., Wu, T.Y., Guo, Y., Huang, Y., Jeong, W.S., and Kong, A.N., Pharmacodynamics of dietary phytochemical indoles I3C and DIM: Induction of Nrf2-mediated phase II drug metabolizing and antioxidant genes and synergism with isothiocyanates. *Biopharm Drug Dispos*, **2011**. 32(5): p. 289-300.

[279] Rusca, A., Di Stefano, A.F., Doig, M.V., Scarsi, C., and Perucca, E., Relative bioavailability and pharmacokinetics of two oral formulations of docosahexaenoic acid/eicosapentaenoic acid after multiple-dose administration in healthy volunteers. *Eur J Clin Pharmacol*, **2009**. 65(5): p. 503-510.

[280] Aruoma, O.I., Methodological considerations for characterizing potential antioxidant actions of bioactive components in plant foods. *Mutat Res*, **2003**. 523-524: p. 9-20.

[281] Miller, K.D., Siegel, R.L., Lin, C.C., Mariotto, A.B., Kramer, J.L., Rowland, J.H., Stein, K.D., Alteri, R., and Jemal, A., Cancer treatment and survivorship statistics, 2016. *CA Cancer J Clin*, **2016**. 66(4): p. 271-289.

[282] Miyake, T., Nakayama, T., Naoi, Y., Yamamoto, N., Otani, Y., Kim, S.J., Shimazu, K., Shimomura, A., Maruyama, N., Tamaki, Y., and Noguchi, S., GSTP1 expression predicts poor pathological complete response to

neoadjuvant chemotherapy in ER-negative breast cancer. *Cancer Sci*, **2012**. 103(5): p. 913-920.

[283] Jhaveri, M.S. and Morrow, C.S., Methylation-mediated regulation of the glutathione S-transferase P1 gene in human breast cancer cells. *Gene*, **1998**. 210(1): p. 1-7.

[284] Esteller, M., Corn, P.G., Urena, J.M., Gabrielson, E., Baylin, S.B., and Herman, J.G., Inactivation of glutathione S-transferase P1 gene by promoter hypermethylation in human neoplasia. *Cancer Res*, **1998**. 58(20): p. 4515-4518.

[285] Saxena, A., Dhillon, V.S., Shahid, M., Khalil, H.S., Rani, M., Prasad, D.T., Hedau, S., Hussain, A., Naqvi, R.A., Deo, S.V., Shukla, N.K., Das, B.C., and Husain, S.A., GSTP1 methylation and polymorphism increase the risk of breast cancer and the effects of diet and lifestyle in breast cancer patients. *Exp Ther Med*, **2012**. 4(6): p. 1097-1103.

[286] Arai, T., Miyoshi, Y., Kim, S.J., Taguchi, T., Tamaki, Y., and Noguchi, S., Association of GSTP1 CpG islands hypermethylation with poor prognosis in human breast cancers. *Breast Cancer Res Treat*, **2006**. 100(2): p. 169-176.

[287] Krassenstein, R., Sauter, E., Dulaimi, E., Battagli, C., Ehya, H., Klein-Szanto, A., and Cairns, P., Detection of breast cancer in nipple aspirate fluid by CpG island hypermethylation. *Clin Cancer Res*, **2004**. 10(1 Pt 1): p. 28-32.

[288] Pongtheerat, T., Pakdeethai, S., Purisa, W., Chariyalertsak, S., and Petmitr, S., Promoter methylation and genetic polymorphism of glutathione S-transferase P1 gene (GSTP1) in Thai breast- cancer patients. *Asian Pac J Cancer Prev*, **2011**. 12(10): p. 2731-2734.

[289] Singal, R., van Wert, J., and Bashambu, M., Cytosine methylation represses glutathione S-transferase P1 (GSTP1) gene expression in human prostate cancer cells. *Cancer Res*, **2001**. 61(12): p. 4820-4826.

[290] Lee, W.H., Morton, R.A., Epstein, J.I., Brooks, J.D., Campbell, P.A., Bova, G.S., Hsieh, W.S., Isaacs, W.B., and Nelson, W.G., Cytidine methylation of regulatory sequences near the pi-class glutathione S-transferase gene accompanies human prostatic carcinogenesis. *Proc Natl Acad Sci U S A*, **1994**. 91(24): p. 11733-11737.

[291] Kong, A.N., Yu, R., Lei, W., Mandlekar, S., Tan, T.H., and Ucker, D.S., Differential activation of MAPK and ICE/Ced-3 protease in chemical-induced apoptosis. The role of oxidative stress in the regulation of mitogen-activated protein kinases (MAPKs) leading to gene expression and survival or activation of caspases leading to apoptosis. *Restor Neurol Neurosci*, **1998**. 12(2-3): p. 63-70.

[292] Lee, J.H., Khor, T.O., Shu, L., Su, Z.Y., Fuentes, F., and Kong, A.N., Dietary phytochemicals and cancer prevention: Nrf2 signaling, epigenetics,

and cell death mechanisms in blocking cancer initiation and progression. *Pharmacol Ther*, **2013**. 137(2): p. 153-171.

[293] Suzuki, T., Motohashi, H., and Yamamoto, M., Toward clinical application of the Keap1-Nrf2 pathway. *Trends Pharmacol Sci*, **2013**. 34(6): p. 340-346.

[294] Khor, T.O., Huang, M.T., Prawan, A., Liu, Y., Hao, X., Yu, S., Cheung, W.K., Chan, J.Y., Reddy, B.S., Yang, C.S., and Kong, A.N., Increased susceptibility of Nrf2 knockout mice to colitis-associated colorectal cancer. *Cancer Prev Res (Phila)*, **2008**. 1(3): p. 187-191.

[295] Saw, C.L., Yang, A.Y., Huang, M.T., Liu, Y., Lee, J.H., Khor, T.O., Su, Z.Y., Shu, L., Lu, Y., Conney, A.H., and Kong, A.N., Nrf2 null enhances UVB-induced skin inflammation and extracellular matrix damages. *Cell Biosci*, **2014**. 4: p. 39.

[296] Saw, C.L., Huang, M.T., Liu, Y., Khor, T.O., Conney, A.H., and Kong, A.N., Impact of Nrf2 on UVB-induced skin inflammation/photoprotection and photoprotective effect of sulforaphane. *Mol Carcinog*, **2011**. 50(6): p. 479-486.

[297] Xu, C., Huang, M.T., Shen, G., Yuan, X., Lin, W., Khor, T.O., Conney, A.H., and Kong, A.N., Inhibition of 7,12-dimethylbenz(a)anthracene-induced skin tumorigenesis in C57BL/6 mice by sulforaphane is mediated by nuclear factor E2-related factor 2. *Cancer Res*, **2006**. 66(16): p. 8293-8296.

[298] Gills, J.J., Jeffery, E.H., Matusheski, N.V., Moon, R.C., Lantvit, D.D., and Pezzuto, J.M., Sulforaphane prevents mouse skin tumorigenesis during the stage of promotion. *Cancer Lett*, **2006**. 236(1): p. 72-79.

[299] Frohlich, D.A., McCabe, M.T., Arnold, R.S., and Day, M.L., The role of Nrf2 in increased reactive oxygen species and DNA damage in prostate tumorigenesis. *Oncogene*, **2008**. 27(31): p. 4353-4362.

[300] Nakayama, M., Gonzalgo, M.L., Yegnasubramanian, S., Lin, X., De Marzo, A.M., and Nelson, W.G., GSTP1 CpG island hypermethylation as a molecular biomarker for prostate cancer. *J Cell Biochem*, **2004**. 91(3): p. 540-552.

[301] Van Neste, L., Herman, J.G., Otto, G., Bigley, J.W., Epstein, J.I., and Van Criekinge, W., The epigenetic promise for prostate cancer diagnosis. *Prostate*, **2012**. 72(11): p. 1248-1261.

[302] Tokumaru, Y., Harden, S.V., Sun, D.I., Yamashita, K., Epstein, J.I., and Sidransky, D., Optimal use of a panel of methylation markers with GSTP1 hypermethylation in the diagnosis of prostate adenocarcinoma. *Clin Cancer Res*, **2004**. 10(16): p. 5518-5522.

[303] Stewart, G.D., Van Neste, L., Delvenne, P., Delree, P., Delga, A., McNeill, S.A., O'Donnell, M., Clark, J., Van Criekinge, W., Bigley, J., and Harrison, D.J., Clinical utility of an epigenetic assay to detect occult prostate cancer in

histopathologically negative biopsies: results of the MATLOC study. *J Urol*, **2013**. 189(3): p. 1110-1116.

[304] Saw, C.L., Yang, A.Y., Guo, Y., and Kong, A.N., Astaxanthin and omega-3 fatty acids individually and in combination protect against oxidative stress via the Nrf2-ARE pathway. *Food Chem Toxicol*, **2013**. 62: p. 869-875.

[305] Li, R., Wu, H., Zhuo, W.W., Mao, Q.F., Lan, H., Zhang, Y., and Hua, S., Astaxanthin Normalizes Epigenetic Modifications of Bovine Somatic Cell Cloned Embryos and Decreases the Generation of Lipid Peroxidation. *Reprod Domest Anim*, **2015**. 50(5): p. 793-799.

[306] Yu, S., Khor, T.O., Cheung, K.L., Li, W., Wu, T.Y., Huang, Y., Foster, B.A., Kan, Y.W., and Kong, A.N., Nrf2 expression is regulated by epigenetic mechanisms in prostate cancer of TRAMP mice. *PLoS One*, **2010**. 5(1): p. e8579.

[307] Khor, T.O., Fuentes, F., Shu, L., Paredes-Gonzalez, X., Yang, A.Y., Liu, Y., Smiraglia, D.J., Yegnasubramanian, S., Nelson, W.G., and Kong, A.N., Epigenetic DNA methylation of antioxidative stress regulator NRF2 in human prostate cancer. *Cancer Prev Res (Phila)*, **2014**. 7(12): p. 1186-1197.

[308] Li, L.C. and Dahiya, R., MethPrimer: designing primers for methylation PCRs. *Bioinformatics*, **2002**. 18(11): p. 1427-1431.

[309] Hun Lee, J., Shu, L., Fuentes, F., Su, Z.Y., and Tony Kong, A.N., Cancer chemoprevention by traditional chinese herbal medicine and dietary phytochemicals: targeting nrf2-mediated oxidative stress/anti-inflammatory responses, epigenetics, and cancer stem cells. *J Tradit Complement Med*, **2013**. 3(1): p. 69-79.

[310] Hermann, A., Gowher, H., and Jeltsch, A., Biochemistry and biology of mammalian DNA methyltransferases. *Cell Mol Life Sci*, **2004**. 61(19-20): p. 2571-2587.

[311] Wang, H., Cao, R., Xia, L., Erdjument-Bromage, H., Borchers, C., Tempst, P., and Zhang, Y., Purification and functional characterization of a histone H3-lysine 4-specific methyltransferase. *Mol Cell*, **2001**. 8(6): p. 1207-1217.

[312] Esteve, P.O., Chin, H.G., Benner, J., Feehery, G.R., Samaranayake, M., Horwitz, G.A., Jacobsen, S.E., and Pradhan, S., Regulation of DNMT1 stability through SET7-mediated lysine methylation in mammalian cells. *Proc Natl Acad Sci U S A*, **2009**. 106(13): p. 5076-5081.

[313] Ellis, L., Atadja, P.W., and Johnstone, R.W., Epigenetics in cancer: targeting chromatin modifications. *Mol Cancer Ther*, **2009**. 8(6): p. 1409-1420.

[314] Shin, J.W., Ohnishi, K., Murakami, A., Lee, J.S., Kundu, J.K., Na, H.K., Ohigashi, H., and Surh, Y.J., Zerumbone induces heme oxygenase-1 expression in mouse skin and cultured murine epidermal cells through activation of Nrf2. *Cancer Prev Res (Phila)*, **2011**. 4(6): p. 860-870.

[315] Mavis, C.K., Morey Kinney, S.R., Foster, B.A., and Karpf, A.R., Expression level and DNA methylation status of glutathione-S-transferase genes in

normal murine prostate and TRAMP tumors. *Prostate*, **2009**. 69(12): p. 1312-1324.

[316] Chen, Y., Inoyama, D., Kong, A.N., Beamer, L.J., and Hu, L., Kinetic analyses of Keap1-Nrf2 interaction and determination of the minimal Nrf2 peptide sequence required for Keap1 binding using surface plasmon resonance. *Chem Biol Drug Des*, **2011**. 78(6): p. 1014-1021.

[317] Khor, T.O., Huang, Y., Wu, T.Y., Shu, L., Lee, J., and Kong, A.N., Pharmacodynamics of curcumin as DNA hypomethylation agent in restoring the expression of Nrf2 via promoter CpGs demethylation. *Biochem Pharmacol*, **2011**. 82(9): p. 1073-1078.

[318] Majid, S., Dar, A.A., Ahmad, A.E., Hirata, H., Kawakami, K., Shahryari, V., Saini, S., Tanaka, Y., Dahiya, A.V., Khatri, G., and Dahiya, R., BTG3 tumor suppressor gene promoter demethylation, histone modification and cell cycle arrest by genistein in renal cancer. *Carcinogenesis*, **2009**. 30(4): p. 662-670.

[319] Rennie, P.S. and Nelson, C.C., Epigenetic mechanisms for progression of prostate cancer. *Cancer Metastasis Rev*, **1998**. 17(4): p. 401-409.

[320] Stern, R.S., Prevalence of a history of skin cancer in 2007: results of an incidence-based model. *Arch Dermatol*, **2010**. 146(3): p. 279-282.

[321] Diepgen, T.L. and Mahler, V., The epidemiology of skin cancer. *Br J Dermatol*, **2002**. 146 Suppl 61: p. 1-6.

[322] Brash, D.E., Ziegler, A., Jonason, A.S., Simon, J.A., Kunala, S., and Leffell, D.J., Sunlight and sunburn in human skin cancer: p53, apoptosis, and tumor promotion. *J Investig Dermatol Symp Proc*, **1996**. 1(2): p. 136-142.

[323] Brenneisen, P., Sies, H., and Scharffetter-Kochanek, K., *Ultraviolet-B irradiation and matrix metalloproteinases - From induction via signaling to initial events*, in *Cell Signaling, Transcription, and Translation as Therapeutic Targets*, M. Diederich, Editor. 2002, New York Acad Sciences: New York. p. 31-43.

[324] Hansson, J., Vasan, R.S., Ärnlöv, J., Ingelsson, E., Lind, L., Larsson, A., Michaëlsson, K., and Sundström, J., Biomarkers of Extracellular Matrix Metabolism (MMP-9 and TIMP-1) and Risk of Stroke, Myocardial Infarction, and Cause-Specific Mortality: Cohort Study. *PLoS ONE*, **2011**. 6(1): p. e16185.

[325] Afaq, F., Adhami, V.M., and Mukhtar, H., Photochemoprevention of ultraviolet B signaling and photocarcinogenesis. *Mutation Research-Fundamental and Molecular Mechanisms of Mutagenesis*, **2005**. 571(1-2): p. 153-173.

[326] Schafer, M., Dutsch, S., auf dem Keller, U., Navid, F., Schwarz, A., Johnson, D.A., Johnson, J.A., and Werner, S., Nrf2 establishes a glutathione-mediated gradient of UVB cytoprotection in the epidermis. *Genes Dev*, **2010**. 24(10): p. 1045-1058.

[327] Gozzelino, R., Jeney, V., and Soares, M.P., *Mechanisms of Cell Protection by Heme Oxygenase-1*, in *Annual Review of Pharmacology and Toxicology*. 2010, Annual Reviews: Palo Alto. p. 323-354.

[328] Black, A.T., Gordon, M.K., Heck, D.E., Gallo, M.A., Laskin, D.L., and Laskin, J.D., UVB light regulates expression of antioxidants and inflammatory mediators in human corneal epithelial cells. *Biochemical Pharmacology*, **2011**. 81(7): p. 873-880.

[329] Coussens, L.M., Tinkle, C.L., Hanahan, D., and Werb, Z., MMP-9 supplied by bone marrow-derived cells contributes to skin carcinogenesis. *Cell*, **2000**. 103(3): p. 481-490.

[330] Mao, L., Wang, H., Qiao, L., and Wang, X., Disruption of Nrf2 enhances the upregulation of nuclear factor-kappaB activity, tumor necrosis factor-alpha, and matrix metalloproteinase-9 after spinal cord injury in mice. *Mediators Inflamm*, **2010**.

[331] Wang, H.Q. and Smart, R.C., Overexpression of protein kinase C-alpha in the epidermis of transgenic mice results in striking alterations in phorbol ester-induced inflammation and COX-2, MIP-2 and TNF-alpha expression but not tumor promotion. *Journal of Cell Science*, **1999**. 112(20): p. 3497-3506.

[332] Nelson, W.G. and Kastan, M.B., DNA strand breaks: the DNA template alterations that trigger p53-dependent DNA damage response pathways. *Mol Cell Biol*, **1994**. 14(3): p. 1815-1823.

[333] van Kranen, H.J., de Laat, A., van de Ven, J., Wester, P.W., de Vries, A., Berg, R.J., van Kreijl, C.F., and de Gruijl, F.R., Low incidence of p53 mutations in UVA (365-nm)-induced skin tumors in hairless mice. *Cancer Res*, **1997**. 57(7): p. 1238-1240.

[334] Han, E.S., Muller, F.L., Perez, V.I., Qi, W., Liang, H., Xi, L., Fu, C., Doyle, E., Hickey, M., Cornell, J., Epstein, C.J., Roberts, L.J., Van Remmen, H., and Richardson, A., The in vivo gene expression signature of oxidative stress. *Physiol Genomics*, **2008**. 34(1): p. 112-126.

[335] Ak, P. and Levine, A.J., p53 and NF-kappaB: different strategies for responding to stress lead to a functional antagonism. *Faseb J*, **2010**. 24(10): p. 3643-3652.

[336] Reuter, S., Gupta, S.C., Chaturvedi, M.M., and Aggarwal, B.B., Oxidative stress, inflammation, and cancer: how are they linked? *Free Radic Biol Med*, **2010**. 49(11): p. 1603-1616.

[337] Marrot, L., Jones, C., Perez, P., and Meunier, J.R., The significance of Nrf2 pathway in (photo)-oxidative stress response in melanocytes and keratinocytes of the human epidermis. *Pigment Cell Melanoma Res*, **2008**. 21(1): p. 79-88.

[338] auf dem Keller, U., Huber, M., Beyer, T.A., Kumin, A., Siemes, C., Braun, S., Bugnon, P., Mitropoulos, V., Johnson, D.A., Johnson, J.A., Hohl, D., and

Werner, S., Nrf transcription factors in keratinocytes are essential for skin tumor prevention but not for wound healing. *Mol Cell Biol*, **2006**. 26(10): p. 3773-3784.

[339] Wondrak, G.T., Cabello, C.M., Villeneuve, N.F., Zhang, S., Ley, S., Li, Y., Sun, Z., and Zhang, D.D., Cinnamoyl-based Nrf2-activators targeting human skin cell photo-oxidative stress. *Free Radic Biol Med*, **2008**. 45(4): p. 385-395.

[340] MacLeod, A.K., McMahon, M., Plummer, S.M., Higgins, L.G., Penning, T.M., Igarashi, K., and Hayes, J.D., Characterization of the cancer chemopreventive NRF2-dependent gene battery in human keratinocytes: demonstration that the KEAP1-NRF2 pathway, and not the BACH1-NRF2 pathway, controls cytoprotection against electrophiles as well as redox-cycling compounds. *Carcinogenesis*, **2009**. 30(9): p. 1571-1580.

[341] Lu, Y.P., Lou, Y.R., Yen, P., Mitchell, D., Huang, M.T., and Conney, A.H., Time course for early adaptive responses to ultraviolet B light in the epidermis of SKH-1 mice. *Cancer Res*, **1999**. 59(18): p. 4591-4602.

[342] Eaglstein, W.H., Sakai, M., and Mizuno, N., Ultraviolet radiation-induced inflammation and leukocytes. *J Invest Dermatol*, **1979**. 72(2): p. 59-63.

[343] Cole, C., Sambuco, C., Forbes, P., and Davies, R., Response to ultraviolet radiation: ear swelling in hairless mice. *Photodermatol*, **1984**. 1(3): p. 114-118.

[344] Huang, M.-T., Liu, Y., Ramji, D., Lo, C.-Y., Ghai, G., Dushenkov, S., and Ho, C.-T., Inhibitory effects of black tea theaflavin derivatives on 12-O-tetradecanoylphorbol-13-acetate-induced inflammation and arachidonic acid metabolism in mouse ears. *Molecular Nutrition & Food Research*, **2006**. 50(2): p. 115-122.

[345] Fisher, G.J., Wang, Z.Q., Datta, S.C., Varani, J., Kang, S., and Voorhees, J.J., Pathophysiology of premature skin aging induced by ultraviolet light. *N Engl J Med*, **1997**. 337(20): p. 1419-1428.

[346] Komatsu, J., Koyama, H., Maeda, N., and Aratani, Y., Earlier onset of neutrophil-mediated inflammation in the ultraviolet-exposed skin of mice deficient in myeloperoxidase and NADPH oxidase. *Inflamm Res*, **2006**. 55(5): p. 200-206.

[347] Gonzalez, S., Moran, M., and Kochevar, I.E., Chronic photodamage in skin of mast cell-deficient mice. *Photochem Photobiol*, **1999**. 70(2): p. 248-253.

[348] Lu, P., Takai, K., Weaver, V.M., and Werb, Z., Extracellular matrix degradation and remodeling in development and disease. *Cold Spring Harb Perspect Biol*, **2011**. 3(12).

[349] Mott, J.D. and Werb, Z., Regulation of matrix biology by matrix metalloproteinases. *Curr Opin Cell Biol*, **2004**. 16(5): p. 558-564.

[350] Marrot, L., Planel, E., Ginestet, A.C., Belaidi, J.P., Jones, C., and Meunier, J.R., In vitro tools for photobiological testing: molecular responses to

simulated solar UV of keratinocytes growing as monolayers or as part of reconstructed skin. *Photochem Photobiol Sci*, **2010**. 9(4): p. 448-458.

[351] Esteller, M., Epigenetics in cancer. *N Engl J Med*, **2008**. 358(11): p. 1148-1159.

[352] Momparler, R.L. and Bovenzi, V., DNA methylation and cancer. *J Cell Physiol*, **2000**. 183(2): p. 145-154.

[353] Zingg, J.M. and Jones, P.A., Genetic and epigenetic aspects of DNA methylation on genome expression, evolution, mutation and carcinogenesis. *Carcinogenesis*, **1997**. 18(5): p. 869-882.

[354] Baylin, S.B., Belinsky, S.A., and Herman, J.G., Aberrant methylation of gene promoters in cancer---concepts, misconcepts, and promise. *J Natl Cancer Inst*, **2000**. 92(18): p. 1460-1461.

[355] Laird, P.W. and Jaenisch, R., The role of DNA methylation in cancer genetic and epigenetics. *Annu Rev Genet*, **1996**. 30: p. 441-464.

[356] Chen, W.Y., Zeng, X., Carter, M.G., Morrell, C.N., Chiu Yen, R.W., Esteller, M., Watkins, D.N., Herman, J.G., Mankowski, J.L., and Baylin, S.B., Heterozygous disruption of Hic1 predisposes mice to a gender-dependent spectrum of malignant tumors. *Nat Genet*, **2003**. 33(2): p. 197-202.

[357] Tommasi, S., Dammann, R., Zhang, Z., Wang, Y., Liu, L., Tsark, W.M., Wilczynski, S.P., Li, J., You, M., and Pfeifer, G.P., Tumor susceptibility of Rassf1a knockout mice. *Cancer Res*, **2005**. 65(1): p. 92-98.

[358] Nandakumar, V., Vaid, M., Tollefsbol, T.O., and Katiyar, S.K., Aberrant DNA hypermethylation patterns lead to transcriptional silencing of tumor suppressor genes in UVB-exposed skin and UVB-induced skin tumors of mice. *Carcinogenesis*, **2011**. 32(4): p. 597-604.

[359] Koga, Y., Pelizzola, M., Cheng, E., Krauthammer, M., Sznol, M., Ariyan, S., Narayan, D., Molinaro, A.M., Halaban, R., and Weissman, S.M., Genome-wide screen of promoter methylation identifies novel markers in melanoma. *Genome Res*, **2009**. 19(8): p. 1462-1470.

[360] Kanavy, H.E. and Gerstenblith, M.R., Ultraviolet radiation and melanoma. *Semin Cutan Med Surg*, **2011**. 30(4): p. 222-228.

[361] Hocker, T. and Tsao, H., Ultraviolet radiation and melanoma: a systematic review and analysis of reported sequence variants. *Hum Mutat*, **2007**. 28(6): p. 578-588.

[362] Ballestar, E. and Esteller, M., Epigenetic gene regulation in cancer. *Adv Genet*, **2008**. 61: p. 247-267.

[363] Jaenisch, R. and Bird, A., Epigenetic regulation of gene expression: how the genome integrates intrinsic and environmental signals. *Nat Genet*, **2003**. 33 Suppl: p. 245-254.

[364] Wilkey, J.F., Buchberger, G., Saucier, K., Patel, S.M., Eisenberg, E., Nakagawa, H., Michaylira, C.Z., Rustgi, A.K., and Mallya, S.M., Cyclin D1

overexpression increases susceptibility to 4-nitroquinoline-1-oxide-induced dysplasia and neoplasia in murine squamous oral epithelium. *Mol Carcinog*, **2009**. 48(9): p. 853-861.

[365] Saab, R., Rodriguez-Galindo, C., Matmati, K., Rehg, J.E., Baumer, S.H., Khoury, J.D., Billups, C., Neale, G., Helton, K.J., and Skapek, S.X., p18Ink4c and p53 Act as tumor suppressors in cyclin D1-driven primitive neuroectodermal tumor. *Cancer Res*, **2009**. 69(2): p. 440-448.

[366] Nishijo, K., Chen, Q.R., Zhang, L., McCleish, A.T., Rodriguez, A., Cho, M.J., Prajapati, S.I., Gelfond, J.A., Chisholm, G.B., Michalek, J.E., Aronow, B.J., Barr, F.G., Randall, R.L., Ladanyi, M., Qualman, S.J., Rubin, B.P., LeGallo, R.D., Wang, C., Khan, J., and Keller, C., Credentialing a preclinical mouse model of alveolar rhabdomyosarcoma. *Cancer Res*, **2009**. 69(7): p. 2902-2911.

[367] Zheng, H., Ying, H., Yan, H., Kimmelman, A.C., Hiller, D.J., Chen, A.J., Perry, S.R., Tonon, G., Chu, G.C., Ding, Z., Stommel, J.M., Dunn, K.L., Wiedemeyer, R., You, M.J., Brennan, C., Wang, Y.A., Ligon, K.L., Wong, W.H., Chin, L., and DePinho, R.A., p53 and Pten control neural and glioma stem/progenitor cell renewal and differentiation. *Nature*, **2008**. 455(7216): p. 1129-1133.

[368] Trapnell, C., Roberts, A., Goff, L., Pertea, G., Kim, D., Kelley, D.R., Pimentel, H., Salzberg, S.L., Rinn, J.L., and Pachter, L., Differential gene and transcript expression analysis of RNA-seq experiments with TopHat and Cufflinks. *Nat Protoc*, **2012**. 7(3): p. 562-578.

[369] Zhu, L.J., Gazin, C., Lawson, N.D., Pages, H., Lin, S.M., Lapointe, D.S., and Green, M.R., ChIPpeakAnno: a Bioconductor package to annotate ChIP-seq and ChIP-chip data. *BMC Bioinformatics*, **2010**. 11: p. 237.

[370] Vaid, M., Sharma, S.D., and Katiyar, S.K., Honokiol, a phytochemical from the Magnolia plant, inhibits photocarcinogenesis by targeting UVB-induced inflammatory mediators and cell cycle regulators: development of topical formulation. *Carcinogenesis*, **2010**. 31(11): p. 2004-2011.

[371] Jhappan, C., Noonan, F.P., and Merlino, G., Ultraviolet radiation and cutaneous malignant melanoma. *Oncogene*, **2003**. 22(20): p. 3099-3112.

[372] Leiter, U. and Garbe, C., Epidemiology of melanoma and nonmelanoma skin cancer--the role of sunlight. *Adv Exp Med Biol*, **2008**. 624: p. 89-103.

[373] Moan, J., Porojnicu, A.C., and Dahlback, A., Ultraviolet radiation and malignant melanoma. *Adv Exp Med Biol*, **2008**. 624: p. 104-116.

[374] Nile, C.J., Read, R.C., Akil, M., Duff, G.W., and Wilson, A.G., Methylation status of a single CpG site in the IL6 promoter is related to IL6 messenger RNA levels and rheumatoid arthritis. *Arthritis Rheum*, **2008**. 58(9): p. 2686-2693.

[375] Tekpli, X., Landvik, N.E., Anmarkud, K.H., Skaug, V., Haugen, A., and Zienolddiny, S., DNA methylation at promoter regions of interleukin 1B,

interleukin 6, and interleukin 8 in non-small cell lung cancer. *Cancer Immunol Immunother*, **2013**. 62(2): p. 337-345.

[376] Gasche, J.A., Hoffmann, J., Boland, C.R., and Goel, A., Interleukin-6 promotes tumorigenesis by altering DNA methylation in oral cancer cells. *Int J Cancer*, **2011**. 129(5): p. 1053-1063.

[377] Mukhtar, H. and Elmets, C.A., Photocarcinogenesis: mechanisms, models and human health implications. *Photochem Photobiol*, **1996**. 63(4): p. 356-357.

[378] Tron, V.A., Rosenthal, D., and Sauder, D.N., Epidermal interleukin-1 is increased in cutaneous T-cell lymphoma. *J Invest Dermatol*, **1988**. 90(3): p. 378-381.

[379] Suiqing, C., Min, Z., and Lirong, C., Overexpression of phosphorylated-STAT3 correlated with the invasion and metastasis of cutaneous squamous cell carcinoma. *J Dermatol*, **2005**. 32(5): p. 354-360.

[380] Chan, K.S., Sano, S., Kataoka, K., Abel, E., Carbajal, S., Beltran, L., Clifford, J., Peavey, M., Shen, J., and Digiovanni, J., Forced expression of a constitutively active form of Stat3 in mouse epidermis enhances malignant progression of skin tumors induced by two-stage carcinogenesis. *Oncogene*, **2008**. 27(8): p. 1087-1094.

[381] Cancer Genome Atlas, N., Comprehensive molecular characterization of human colon and rectal cancer. *Nature*, **2012**. 487(7407): p. 330-337.

[382] Sengupta, N., Yau, C., Sakthianandeswaren, A., Mouradov, D., Gibbs, P., Suraweera, N., Cazier, J.B., Polanco-Echeverry, G., Ghosh, A., Thaha, M., Ahmed, S., Feakins, R., Propper, D., Dorudi, S., Sieber, O., Silver, A., and Lai, C., Analysis of colorectal cancers in British Bangladeshi identifies early onset, frequent mucinous histotype and a high prevalence of RBFOX1 deletion. *Mol Cancer*, **2013**. 12: p. 1.

[383] Chang, G., Xu, S., Dhir, R., Chandran, U., O'Keefe, D.S., Greenberg, N.M., and Gingrich, J.R., Hypoexpression and epigenetic regulation of candidate tumor suppressor gene CADM-2 in human prostate cancer. *Clin Cancer Res*, **2010**. 16(22): p. 5390-5401.

[384] Yang, S., Yan, H.L., Tao, Q.F., Yuan, S.X., Tang, G.N., Yang, Y., Wang, L.L., Zhang, Y.L., Sun, S.H., and Zhou, W.P., Low CADM2 expression predicts high recurrence risk of hepatocellular carcinoma patients after hepatectomy. *J Cancer Res Clin Oncol*, **2014**. 140(1): p. 109-116.

[385] He, W., Li, X., Xu, S., Ai, J., Gong, Y., Gregg, J.L., Guan, R., Qiu, W., Xin, D., Gingrich, J.R., Guo, Y., and Chang, G., Aberrant methylation and loss of CADM2 tumor suppressor expression is associated with human renal cell carcinoma tumor progression. *Biochem Biophys Res Commun*, **2013**. 435(4): p. 526-532.

[386] Katiyar, S.K., Matsui, M.S., and Mukhtar, H., Kinetics of UV light-induced cyclobutane pyrimidine dimers in human skin in vivo: an

immunohistochemical analysis of both epidermis and dermis. *Photochem Photobiol*, **2000**. 72(6): p. 788-793.

[387] Singh, S., Vrishni, S., Singh, B.K., Rahman, I., and Kakkar, P., Nrf2-ARE stress response mechanism: a control point in oxidative stress-mediated dysfunctions and chronic inflammatory diseases. *Free Radic Res*, **2010**. 44(11): p. 1267-1288.

[388] Chun, K.S., Kundu, J., Kundu, J.K., and Surh, Y.J., Targeting Nrf2-Keap1 signaling for chemoprevention of skin carcinogenesis with bioactive phytochemicals. *Toxicol Lett*, **2014**. 229(1): p. 73-84.

[389] Jeronimo, C. and Henrique, R., Epigenetic biomarkers in urological tumors: A systematic review. *Cancer Lett*, **2014**. 342(2): p. 264-274.

[390] Wang, F., Zhang, N., Wang, J., Wu, H., and Zheng, X., Tumor purity and differential methylation in cancer epigenomics. *Brief Funct Genomics*, **2016**. 15(6): p. 408-419.

[391] Fenaux, P. and Ades, L., Review of azacitidine trials in Intermediate-2-and High-risk myelodysplastic syndromes. *Leuk Res*, **2009**. 33 Suppl 2: p. S7-11.

[392] Golabek, K., Strzelczyk, J.K., Wiczkowski, A., and Michalski, M., Potential use of histone deacetylase inhibitors in cancer therapy. *Contemp Oncol (Pozn)*, **2015**. 19(6): p. 436-440.

[393] van Doorn, R., Gruis, N.A., Willemze, R., van der Velden, P.A., and Tensen, C.P., Aberrant DNA methylation in cutaneous malignancies. *Semin Oncol*, **2005**. 32(5): p. 479-487.

[394] Bachman, A.N., Curtin, G.M., Doolittle, D.J., and Goodman, J.I., Altered methylation in gene-specific and GC-rich regions of DNA is progressive and nonrandom during promotion of skin tumorigenesis. *Toxicol Sci*, **2006**. 91(2): p. 406-418.

[395] Schinke, C., Mo, Y., Yu, Y., Amiri, K., Sosman, J., Greally, J., and Verma, A., Aberrant DNA methylation in malignant melanoma. *Melanoma Res*, **2010**. 20(4): p. 253-265.

[396] Yang, A.Y., Lee, J.H., Shu, L., Zhang, C., Su, Z.Y., Lu, Y., Huang, M.T., Ramirez, C., Pung, D., Huang, Y., Verzi, M., Hart, R.P., and Kong, A.N., Genome-wide analysis of DNA methylation in UVB- and DMBA/TPA-induced mouse skin cancer models. *Life Sci*, **2014**. 113(1-2): p. 45-54.

[397] Yang, A.Y., Kim, H., Li, W., and Kong, A.N., Natural compound-derived epigenetic regulators targeting epigenetic readers, writers and erasers. *Curr Top Med Chem*, **2016**. 16(7): p. 697-713.

[398] Lee, Y.H., Wang, E., Kumar, N., and Glickman, R.D., Ursolic acid differentially modulates apoptosis in skin melanoma and retinal pigment epithelial cells exposed to UV-VIS broadband radiation. *Apoptosis*, **2014**. 19(5): p. 816-828.

[399] Tokuda, H., Ohigashi, H., Koshimizu, K., and Ito, Y., Inhibitory effects of ursolic and oleanolic acid on skin tumor promotion by 12-O-tetradecanoylphorbol-13-acetate. *Cancer Lett*, **1986**. 33(3): p. 279-285.

[400] Cho, J., Rho, O., Junco, J., Carbajal, S., Siegel, D., Slaga, T.J., and DiGiovanni, J., Effect of Combined Treatment with Ursolic Acid and Resveratrol on Skin Tumor Promotion by 12-O-Tetradecanoylphorbol-13-Acetate. *Cancer Prev Res (Phila)*, **2015**. 8(9): p. 817-825.

[401] Dinkova-Kostova, A.T., Liby, K.T., Stephenson, K.K., Holtzclaw, W.D., Gao, X., Suh, N., Williams, C., Risingsong, R., Honda, T., Gribble, G.W., Sporn, M.B., and Talalay, P., Extremely potent triterpenoid inducers of the phase 2 response: correlations of protection against oxidant and inflammatory stress. *Proc Natl Acad Sci U S A*, **2005**. 102(12): p. 4584-4589.

[402] Kim, H., Ramirez, C.N., Su, Z.Y., and Kong, A.N., Epigenetic modifications of triterpenoid ursolic acid in activating Nrf2 and blocking cellular transformation of mouse epidermal cells. *J Nutr Biochem*, **2016**. 33: p. 54-62.

[403] Balasubramanian, S., Chew, Y.C., and Eckert, R.L., Sulforaphane suppresses polycomb group protein level via a proteasome-dependent mechanism in skin cancer cells. *Mol Pharmacol*, **2011**. 80(5): p. 870-878.

[404] Saha, K., Hornyak, T.J., and Eckert, R.L., Epigenetic cancer prevention mechanisms in skin cancer. *AAPS J*, **2013**. 15(4): p. 1064-1071.

[405] Fisher, M.L., Adhikary, G., Grun, D., Kaetzel, D.M., and Eckert, R.L., The Ezh2 polycomb group protein drives an aggressive phenotype in melanoma cancer stem cells and is a target of diet derived sulforaphane. *Mol Carcinog*, **2016**. 55(12): p. 2024-2036.

[406] Fortes, C., Mastroeni, S., Melchi, F., Pilla, M.A., Antonelli, G., Camaioni, D., Alotto, M., and Pasquini, P., A protective effect of the Mediterranean diet for cutaneous melanoma. *Int J Epidemiol*, **2008**. 37(5): p. 1018-1029.

[407] Kune, G.A., Bannerman, S., Field, B., Watson, L.F., Cleland, H., Merenstein, D., and Vitetta, L., Diet, alcohol, smoking, serum beta-carotene, and vitamin A in male nonmelanocytic skin cancer patients and controls. *Nutr Cancer*, **1992**. 18(3): p. 237-244.

[408] Lu, Y.P., Lou, Y.R., Peng, Q.Y., Nghiem, P., and Conney, A.H., Caffeine decreases phospho-Chk1 (Ser317) and increases mitotic cells with cyclin B1 and caspase 3 in tumors from UVB-treated mice. *Cancer Prev Res (Phila)*, **2011**. 4(7): p. 1118-1125.

[409] Lou, Y.R., Peng, Q.Y., Li, T., Medvecky, C.M., Lin, Y., Shih, W.J., Conney, A.H., Shapses, S., Wagner, G.C., and Lu, Y.P., Effects of high-fat diets rich in either omega-3 or omega-6 fatty acids on UVB-induced skin carcinogenesis in SKH-1 mice. *Carcinogenesis*, **2011**. 32(7): p. 1078-1084.

[410] Ananthaswamy, H.N. and Pierceall, W.E., Molecular mechanisms of ultraviolet radiation carcinogenesis. *Photochem Photobiol*, **1990**. 52(6): p. 1119-1136.

[411] Chiba, H., Clifford, J., Metzger, D., and Chambon, P., Specific and redundant functions of retinoid X Receptor/Retinoic acid receptor heterodimers in differentiation, proliferation, and apoptosis of F9 embryonal carcinoma cells. *J Cell Biol*, **1997**. 139(3): p. 735-747.

[412] Tufaro, A.P., Azoury, S.C., Crompton, J.G., Straughan, D.M., Reddy, S., Prasad, N.B., Shi, G., and Fischer, A.C., Rising incidence and aggressive nature of cutaneous malignancies after transplantation: An update on epidemiology, risk factors, management and surveillance. *Surg Oncol*, **2015**. 24(4): p. 345-352.